

THE
American Journal of
ANATOMY

MANAGING EDITOR
DONALD DUNCAN
THE UNIVERSITY OF TEXAS
MEDICAL BRANCH
GALVESTON TEXAS

ASSOCIATE EDITORS

BURTON L. BAKER
UNIVERSITY OF MICHIGAN

SAM L. CLARK, JR.
WASHINGTON UNIVERSITY

C. P. LEBLOND
McGILL UNIVERSITY

RICHARD J. BLANDAU
UNIVERSITY OF WASHINGTON

DON W. FAWCETT
HARVARD UNIVERSITY

HARLAND W. MOSSMAN
UNIVERSITY OF WISCONSIN

VOLUME 117
JULY SEPTEMBER, NOVEMBER 1963

PUBLISHED BY
THE WISTAR INSTITUTE OF ANATOMY AND BIOLOGY
PHILADELPHIA PA

CONTENTS

No 1 JULY 1965

F O SIMPSON The Transverse Tubular System in Mammalian Myocardial Cells	1
AVERILL A. LIEBOW Patterns of Origin and Distribution of the Major Bronchial Arteries in Man	19
KJELL FUXE, TOMAS HÖKFELT AND OVE NILSSON A Fluorescence and Electronmicroscopic Study on Certain Brain Regions Rich in Monoamine Terminals	33
LUIS BIERPICA AND LEOPOLDO F MONTES Secretory Epithellum of the Large Axillary Sweat Glands. A Cytochemical and Electron Microscopic Study	47
J P MARQUES-PEREIRA AND C. P. LEBLOND. Mitosis and Differentiation in the Stratified Squamous Epithellum of the Rat Esophagus	73
N J NADLER. APPENDIX I. Theory Concerning the Transfer of Cells Out of the Basal Layer of the Epithellum of the Esophagus.	87
HELEN WENDLER DEANE AND SARAH WURZELMANN Electron Microscopic Observations on the Postnatal Differentiation of the Seminal Vesicle Epithellum of the Laboratory Mouse	91
DANIEL S. FRIEND AND MICHAEL J MURRAY Osmium Impregnation of the Golgi Apparatus	135
J T IRVING AND S A. MIGLIORZ. Connective Tissue Responses to Altered Collagen and Bone Implants	151

No. 2 SEPTEMBER 1965

J B. GAVIN A Comparison of the Incisor Teeth of Intact, Hypophysectomized and Thyroparathyroidectomized Rats	159
RUTH ELLEN BULGER The Fine Structure of the Aglomerular Nephron of the Toadfish <i>Opsanus tau</i>	171

MILTON W BRIGHTMAN The Distribution Within the Brain of Ferritin Injected into Cerebrospinal Fluid Compartments. II Parenchymal Distribution	193
DAVID J SIMMONS AND RUDOLPH F NUNZEMACHER Growth of the Rat Epiphyseal Cartilage Plate Following Partial Amputation	221
DENNIS WEBER Phase Microscopic Observations of Rat Incisor Enamel	233
P E DUFFY AND M MENEVEZ Electron Microscopic Observations of Neurosecretory Granules Nerve and Glial Fibers and Blood Vessels in the Median Eminence of the Rabbit	251
F BOHATIRCHUK The Study of Calcification of Mammalian Cartilage in Norm and Pathology by Stain Historadiography	287

No 3 NOVEMBER 1965

SERGEI PITIRIMOVITCH SOROKIN On the Cytology and Cytochemistry of the Opossum's Bronchial Glands	311
GURMEET K DHALIWAL AND M R N PRASAD Cytology and Histochemistry of the Pituitary Gland of the Five-striped Palm Squirrel, <i>Funambulus pennanti</i> (Wroughton)	339
GURMEET K DHALIWAL AND M R N PRASAD Effects of Gonadectomy Androgen Administration and Thyroidectomy on the Cytology of the Pituitary Gland of the Five-striped Palm Squirrel, <i>Funambulus pennanti</i> (Wroughton)	353
MARY W STALEY AND JERRY S TRIER Morphologic Heterogeneity of Mouse Paneth Cell Granules before and after Secretory Stimulation	365
ILHAN BUTUKOZER, KAMILE SEVKI MUTLU AND FRANK A PEPE Antigen (Ferritin) and Antibody Distribution in the Rat Lymph Node after Primary and Secondary Responses and after Prolonged Stimulation	385
JOSEPH H KRONMAN AND JOSEPH J SPINALE A Histochemical Study of Testosterone-induced Changes in the Submandibular and Sublingual Gland of Mice	417
G DALLENBACH HELLWEG J V BATTISTA AND F D DALLENBACH Immunohistological and Histochemical Localization of Relaxin in the Metrial Gland of the Pregnant Rat	433
INDEX TO VOLUME 117	451

The Transverse Tubular System in Mammalian Myocardial Cells

F O SIMPSON

Wellcome Medical Research Institute University of Otago Medical School,
Dunedin, New Zealand

ABSTRACT The fine structure of ox myocardial cells, as seen in transverse sections, is described. The presence of an extensive system of transverse tubules at Z region levels has been confirmed, the walls of the tubules being continuous with the sarcolemma.

Preliminary observations in smaller animals indicate that similar tubules are readily seen in guinea-pig myocardial cells and are present, but are more difficult to find, in the rat; communication between the tubules and the exterior is readily demonstrated in the guinea-pig but less readily in the rat.

Contact between the transverse tubules and the Z regions was not particularly close, and thin delicate circumferential Z tubule was noted to lie round the myofibrils at most Z regions.

The Z regions, on cross section, shows tightly packed square array of filaments, double in number compared with the thin filaments seen elsewhere in the sarcomere; the appearances probably confirm for heart muscle the Z region structure which has been described for skeletal muscle.

Continuity of the sarcolemma with the walls of the transverse tubules in mammalian cardiac muscle was first recognized by Lindner ('57) and this relationship was demonstrated in more detail by Simpson and Oertels ('61-'62) and by Nelson and Benson ('63). A similar relationship had also been noted in cockroach myocardium by Edwards and Challice ('60) in insect flight muscle by Smith ('61) and in the myocardium of the snail by North ('62).

Since then it has been shown that the transverse tubules communicate with the extracellular space in several types of striated muscle (Franzini-Armstrong, '64; Franzini-Armstrong and Porter '64a) and recently Huxley ('64) has shown that ferritin molecules can readily enter the transverse tubular system even in vertebrate skeletal muscle.

It appears therefore that failure to find communication between transverse tubules and the extracellular space has been largely due to fixation artefact, cardiac muscle of larger mammals being evidently less vulnerable in this regard. However it is still of interest to extend the observations in mammalian cardiac muscle by means of transverse sections as in the present paper

and thus to study the relationship of the tubules to the Z regions of the myofibrils.

METHODS

Small portions of cardiac muscle of ox, sheep guinea pig and rat were fixed in buffered 1% osmium tetroxide for one and one-half hours, dehydrated in acetones and embedded in Vestopal W. The ox and sheep specimens were obtained at the abattoir and there was thus a delay of about ten minutes between the time of death and the start of fixation. The specimens of guinea pig and rat were obtained under ether anaesthesia, and in the case of the rat the heart was first perfused with 5% for maldehyde in phosphate buffer (pH 7.2-7.4) (Sabatini et al., '63). Thin sections were cut with a Porter Blum microtome stained with 1% uranyl acetate in 50% ethanol, and examined in a Philips 100 B electron microscope.

This paper is concerned mainly with the findings in ox cardiac muscle.

OBSERVATIONS

The main features of the myocardial cells, as seen in cross section, were the

The author is working under grant from the Medical Research Council of New Zealand.

sarcolemma, myofibrils mitochondria a variety of tubules and a variable amount of space (possibly partly artefact) slightly more opaque than the extracellular space and containing often faintly granular material. A nucleus golgi apparatus and pigment granules were also sometimes seen.

Myofibrils

The size and shape of the myofibrils varied greatly in some cases the profiles were evidently those of wide flat myofibrils (e.g. $0.6 \times 6 \mu$) arrayed perpendicular to a cell surface (fig. 3). The larger myofibrils sometimes had curious "U" or "C" shapes and could even be ring-shaped with a core containing a small mitochondrion and small tubules (figs 4-6). In other parts of a cell the myofibrils were often smaller in cross section, and some cells seemed to contain only these smaller myofibrils with no regularity of their array.

The plane of section was never perfectly transverse over a whole cell and therefore the successive parts of the sarcomeres could be recognized across a cell, as

figure 3 where a Z region is seen just above center and A regions above and below. This tissue was mainly fully contracted and therefore there was in most cases no gap between the Z regions and the thick filaments. An exception to this is shown in figure 1 where the plane of section has passed through areas where only thin filaments are present.

The array of thick filaments was regular and hexagonal at the centers of the sarcomeres (fig. 3) and became less regular on approaching the Z regions. Where thin filaments were present between the thick ones the ratio of thin to thick was approximately 2:1. In the Z region itself a close-packed tetragonal array of dots could be seen. With serial sections at fairly high power it was possible to compare the numbers of thin filaments with the number of points seen in the Z region by marking off a square or rectangle in the latter calculating the number of points present and then counting the number of filaments seen in the corresponding area of another section of the same myofibril. It turned out that there were twice as many points in the Z array as there were thin filaments in the A band in this contracted tissue. If

as appears probable the structure of the Z region in heart muscle is similar to that described by Knappels and Carlsen ('62) and Franzini Armstrong and Porter ('64) then it is evident that the Z array as seen in the present sections is made up of the ends of both sets of thin filaments meeting at the Z region. The sections were moderately thick and this probably explains why both sets of filament ends were present together.

Transverse tubules

These were a prominent feature with walls composed of plasma membrane and basement membrane. They were seen almost exclusively in relation to the Z regions starting as invaginations of the sarcolemma at the edge of the cell and extending into the interior with a certain amount of ramification. Occasionally as in figure 2, a "tubule" was clearly lying at a level other than at a Z region. It is possible that such a structure might be a cleft in the cell rather than a tubule but serial sections would be needed to clarify this.

As already mentioned it proved to be difficult to obtain true cross-sections of a cell at Z region level and the full extent of the transverse tubule system could not be demonstrated in single sections although the complexity of parts of the system could be well seen (figs. 1 and 10).

The continuity of the walls of these tubules with the sarcolemma could be clearly seen (figs. 1 3 4 6) so that there is no doubt that the lumen of the tubules communicates with the extracellular space. Even the single sections could hardly be interpreted in any other way although similar appearances might be made by clefts rather than tubules however serial sections (figs. 4-7) show clearly that an invagination of sarcolemma can be traced as a tubule in succeeding sections into the interior of the cell. Quite often as in this case the lumen of the tubule was smallest at the sarcolemma and widened out inside the cell the minimum width was 600-700 Å and the maximum up to 4 000 Å the most usual width being about 1 500-2,500 Å.

In some cells and in some regions of other cells the transverse tubules were numerous and there appeared to be one

tubule between each neighboring pair of subsarcolemmal myofibrils. This particularly occurred where as in figures 1 and 3 the myofibril arrangement was very regular. Where the myofibrils were smaller there did not appear to be a tubule at each possible site for a tubule.

Relationship of transverse tubules to sarcoplasmic reticulum

The relationship of the transverse tubules to the sarcoplasmic reticulum or longitudinal sarcotubular system is not yet clear and in the present material is partly obscured by artefact. There appear to be two distinct types of delicate tubules in relation to the transverse tubules and Z band. In the first place, there is evidently a network of fine tubules above and below each transverse tubule as shown in the serial sections (figs. 4-7) this network probably corresponds to flattened tubule or vesicle profiles seen lying against the transverse tubules in longitudinal sections (fig. 11 and also Simpson and Oertels, '62) and not seen lying beside a transverse tubule unless the latter occurs (as in figs. 2 and 12) a little above or below a Z band level.

The other type of fine tubule appears to run horizontally round the myofibril at each Z band (figs. 8, 9, 10, 11, 12). It can usually be discerned wherever the typical Z band appearances are present, and examples of serial sections have not indicated that more than one such tubule is present at a given Z region. This circumferential tubule is about 220 Å in diameter with slightly dilated points on it, suggesting that it is joined by longitudinally-running tubules, (figs. 8 and 9 and fig. 13). Thus, if in fact there is only one circumferential tubule at each Z region then this would indicate that the longitudinal tubule systems of neighboring sarcomeres are continuous across the Z region.

No particularly close contact was observed between the transverse tubules and the Z regions of the myofibrils. Admittedly the gap between them was probably exaggerated by the swelling of the cells but the thin circumferential tubules seemed to intervene between the Z region and the transverse tubule.

Longitudinal connections between transverse tubules

Evidence was sometimes seen in longitudinal sections (fig. 14) that longitudinal communication occurred between adjacent sets of transverse tubules and this was also noted in smaller animals such as the rat (fig. 13) and the guinea-pig (fig. 15).

Findings in rat and guinea pig

Of these smaller animals, the guinea-pig heart resembles that of the larger animals such as the ox and sheep in that the transverse tubules were prominent and communication between the tubules and the extracellular space could be readily seen. In the rat, on the other hand while characteristic tubules could be seen within the cell (fig. 13) communication between the tubules and extracellular space was much more difficult to demonstrate even after initial formaldehyde fixation; invaginations of the sarcolemma were seen at Z band levels but they did not seem to penetrate so far into the interior of the cell as in the ox or sheep or guinea-pig. However further serial sections would be needed to clarify this point.

DISCUSSION

It is usually not difficult in longitudinal sections of mammalian cardiac muscle to differentiate between true transverse tubules and the spurious invaginations which are seen in swollen and overcontracted cells with their well-known "scalloped" cell membrane. Nevertheless, it was clearly desirable to exclude any possibility of this particular artefact by making observations on transverse sections. The question of course arises as to whether any other artefact in the transverse sections could produce the appearances of invaginations of the cell membrane. Longitudinal clefts in the cell may certainly be seen on transverse sections but they seem to be characterized by a mouth wider than that of the true tubules. In any case any possibility of confusion is refuted by serial sections (examples of which are shown in figs. 4-7).

The present findings therefore confirm the interpretation previously made (Lindner '57; Simpson and Oertels '61 and '62

Nelson and Benson '63) that the transverse tubules communicate with the extracellular space.

The evidence in favor of the transverse tubules acting as a pathway for the spread of the activating impulse into the interior of a muscle cell has been fully discussed in many of the papers cited and it will not be further discussed here.

It is evident that the transverse tubules are more readily seen in certain mammalian hearts than in others: the difficulty in demonstrating them in the rat could be due either to a relative sparseness of the tubules or to some physical characteristic of the tubules in the rat rendering them more vulnerable to fixation artefact, so that—as in skeletal muscle—their connection with the exterior tends to become lost.

The three-dimensional diagram of Nelson and Benson ('63) illustrates also the present author's concept of the transverse tubular system in the myocardium of larger mammals. The depiction of the longitudinal elements of the sarcoplasmic reticulum as thin round tubules which communicate with flattened vesicles lying against the transverse tubules is also in agreement with the author's views. However the present findings indicate that there is an additional element of the sarcoplasmic reticulum present at each Z level namely the round thin walled tubule about 220 Å in diameter lying in a circumferential fashion round the myofibril at the Z region and closely applied to it. This circumferential Z tubule thus intervenes between the Z region and any transverse tubule which may be present. Further investigation is clearly needed to determine how constantly such a circumferential Z tubule is present, both in the ox and in other species and also to determine its exact relationship to the longitudinal elements of sarcoplasmic reticulum.

The Z region structure in ox myocardium appears to be similar to that described by Knappels and Carlsen ('62) and Franzini-Armstrong and Porter ('64) as there are twice as many points in the Z array as there are thin filaments in the neighboring contracted A region. It is evident that the Z array in the present

sections is made up of the ends of both sets of thin filaments meeting at the Z region. The sections were moderately thick and this probably explains why both sets of filament ends were always present together.

ACKNOWLEDGMENTS

The author wishes to express his gratitude to Miss J. M. Ledingham and Mr. M. K. Reynolds for their technical assistance. The Philips 100 B Electron Microscope belongs to the Electron Microscope Unit of the Medical Research Council of New Zealand.

LITERATURE CITED

- Edwards, G. A., and C. E. Challice 1960 The ultrastructure of the heart of the cockroach, *Blattella germanica*. *Ann. Entomol. Soc. Am.*, 53: 360-383.
- Franzini-Armstrong, C. 1964 Fine structure of sarcoplasmic reticulum and transverse tubular system in muscle fibers. *Fed. Proc.*, 23: 827-836.
- Franzini-Armstrong, C., and K. R. Porter 1961 Sarcoplasmic invaginations constituting the T system in fish muscle fibers. *J. Cell Biol.*, 22: 678-690.
- 1964b The Z disc of skeletal muscle fibers. *Z. Zellforsch.* 61: 661-672.
- Huxley, H. E. 1964 Evidence for continuity between the central elements of the triads and extracellular space in frog sartorius muscle. *Nature* 202: 1067-1071.
- Knappels, G. G., and F. Carlsen 1962 The ultrastructure of the Z disc in skeletal muscle. *J. Cell Biol.*, 13: 323-335.
- Lindner, E. 1957 Die submikroskopische Morphologie des Herzmuskels. *Z. Zellforsch.*, 45: 703-748.
- Nelson, D. A., and E. S. Benson 1963 On the structural continuities of the transverse tubular system of rabbit and human myocardial cells. *J. Cell Biol.*, 18: 297-313.
- North, R. J. 1963 The fine structure of the myofiber in the heart of the snail *Helix aspersa*. *J. Ultrastr. Res.*, 8: 205-218.
- Sbatini, D. D., K. Benach and R. J. Barroett 1963 Cytochemistry and electron microscopy. *J. Cell Biol.*, 17: 18-58.
- Simpson, F. O., and S. J. Oertels 1961 Relationship of the sarcoplasmic reticulum to ryanodine in sheep cardiac muscle. *Nature*, 189: 758-759.
- 1962 The fine structure of sheep myocardial cells; sarcoplasmic invaginations and the transverse tubular system. *J. Cell Biol.*, 12: 91-100.
- Smith, D. E. 1961 The structure of insect fibrillar flight muscle. *J. Cell Biol.*, 10 (suppl.): 123-158.

PLATES

Abbreviations

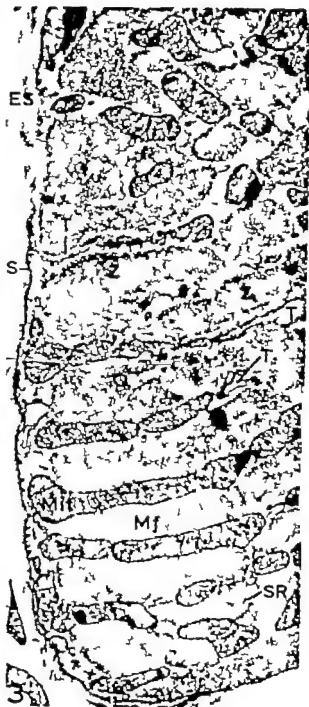
A, A region of myofibril	M, M region of myofibril
BM, basement membrane	Mf myofibril
CSR, circumferential tubule of sarcoplasmic reticulum at Z region	Mit, mitochondrion
ES extracellular space	PM plasma membrane
F5R, flattened tubule of sarcoplasmic reticulum	PV pinocytotic vesicles
I I region of myofibril	S sarcolemma
Long longitudinal connection between transverse tubules	SR, sarcoplasmic reticulum
LSR, longitudinal tubule of sarcoplasmic reticulum	T transverse tubule
	W widening on CSR
	Z, Z region of myofibril

PLATE 1

EXPLANATION OF FIGURES

Figures 1-12 are transverse sections of ox myocardial cells.

- 1 Transverse section through edge of a partly relaxed cell showing Z, I and A regions of myofibrils and also parts of the transverse tubular system (T) $\times 12,500$.
- 2 Transverse section, not a Z region level but nevertheless showing a deep invagination or transverse tubule (T) Flattened tubules of sarcoplasmic reticulum (F5R) are seen lying against the sides of the transverse tubules. $\times 12,500$.
- 3 Slightly oblique but mainly transverse section through edge of a full-contracted cell, showing wide flat myofibrils and other bizarre-shaped myofibrils. The section has passed through Z region just above center and here parts of the transverse tubular system are seen (T) The array of thick and thin filaments in the A regions is less regular near the Z regions. The dark shadows are staining artefact. $\times 16,000$



Abbreviations

A, A region of myofibril	M, M region of myofibril
BM, basement membrane	Mf myofibril
CSR, circumferential tubule of sarcoplasmic reticulum at Z region	Mlt, mitochondrion
ES, extracellular space	PM, plasma membrane
FTR, flattened tubule of sarcoplasmic reticulum	PV pinocytotic vesicles
I, I region of myofibril	S sarcolemma
Long, longitudinal connection between transverse tubules	SR, sarcoplasmic reticulum
LSR, longitudinal tubule of sarcoplasmic reticulum	T transverse tubule
	W widening on CSR
	Z, Z region of myofibril

PLATE 1

EXPLANATION OF FIGURES

Figures 1-12 are transverse sections of ox myocardial cells.

- 1 Transverse section through edge of a partly relaxed cell, showing Z, I, and A regions of myofibrils and also parts of the transverse tubular system (T) $\times 12,500$.
- 2 Transverse section, not Z region level but nevertheless showing deep invagination or transverse tubule (T). Flattened tubules of sarcoplasmic reticulum (FTR) are seen lying against the sides of the transverse tubules. $\times 12,500$.
- 3 Slightly oblique, but mainly transverse, section through edge of full-contracted cell showing wide flat myofibrils and other bizarre-shaped myofibrils. The section has passed through Z region just above center and here parts of the transverse tubular system are seen (T). The array of thick and thin filaments in the A regions is less regular near the Z regions. The dark shadows are staining artefact. $\times 16,000$.



PLATE 3

EXPLANATION OF FIGURES

- 4-7 Figure 4 is an enlargement of part of figure 3, and figures 5, 6, and 7 are serial sections of the same area. A transverse tubule (T) which is readily identified by the curiously-shaped myofibril beside it, is cut at different levels as it penetrates into the cell. Another tubule (T) becomes evident also.

Intricate branching tubules of the sarcoplasmic reticulum (SR) can be discerned in figures 4 and 7 evidently lying close up against the transverse tubule (T) — (i.e. lying above and below the transverse tubule if it were seen in longitudinal section).

Note small mitochondria and some tubules of sarcoplasmic reticulum lying in the center of one myofibril (Mf) $\times 34,500$

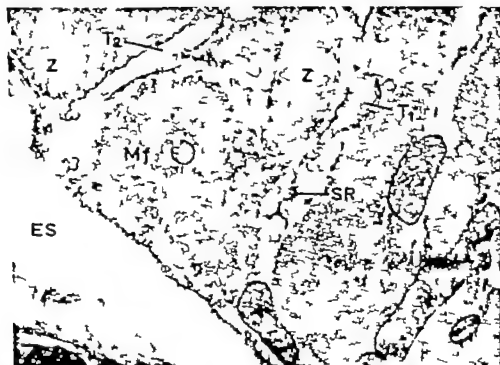


PLATE 4

EXPLANATION OF FIGURES

- 8-9 Higher power views of parts of figures 6 and 7 respectively showing consecutive sections through the Z region of myofibril. Note square array of filaments in the Z region.

At the Z level, a fine tubule can be seen at some places lying circumferentially (CSR) round the myofibril; these tubules show local widenings (W) which appear to correspond to small longitudinal tubules (LSR) seen in cross-section in the neighboring photograph. There appears therefore to be communication between the circumferential and longitudinal tubules. $\times 53,000$.

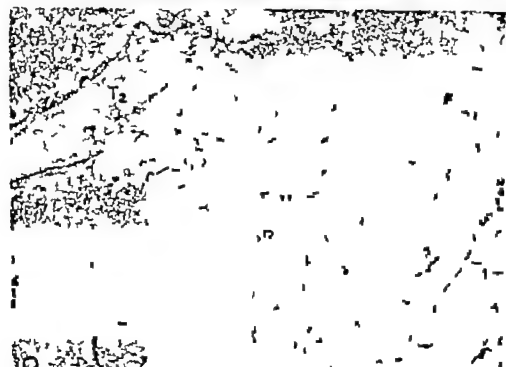
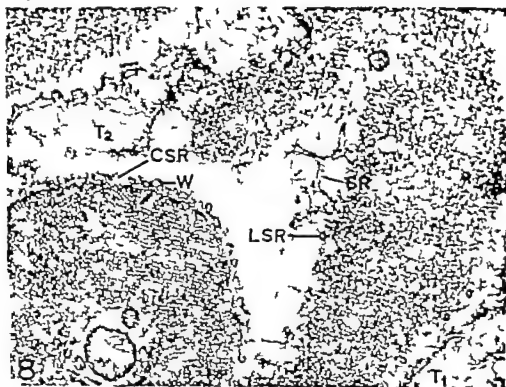


PLATE 5

EXPLANATION OF FIGURES

- 10 Transverse section, partly at Z level, showing ramifying transverse tubule (T). Elements of sarcoplasmic reticulum (LSR) are seen beside it, including — at Z region only — parts of circumferential fine tubules (CSR) $\times 25,500$.
- 11 Myofibril cut mainly at Z level, showing parts of the fine circumferential tubule (CSR) and its longitudinal connections (LSR). Part of transverse tubule is also seen (T) $\times 47,000$.
- 12 Transverse section at edge of cell, showing transverse tubule (T), myofibrils cut at Z level and others cut at A level. One flattened tubule (FSR) of sarcoplasmic reticulum is present beside the transverse tubule on the side where the myofibril is cut at A level. Elements of the fine circumferential tubule (CSR) are present round the myofibrils cut at Z level. The "stretched" appearance of some connecting tubules of the SR may well be artefact. $\times 43,000$.

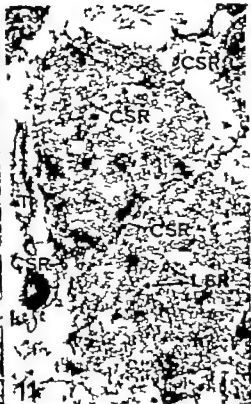
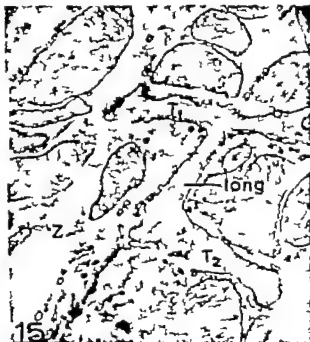


PLATE 6

EXPLANATION OF FIGURES

Figures 13 14 and 15 show longitudinal sections of myocardial cells of different animals.

- 13 Rat papillary muscle fixed by initial perfusion with 4% buffered formaldehyde, and subsequent osmic acid fixation. Parts of transverse tubular system are seen (T T T) with longitudinal connection (Long.) between T and T $\times 12,000$.
- 14 Ox ventricular muscle; slightly oblique longitudinal section showing tubule similar to the transverse tubules but running longitudinally between two Z levels. Flattened tubules (FTR) of sarcoplasmic reticulum lie against the larger tubule. $\times 37,000$
- 15 Guinea-pig ventricular muscle; longitudinal section showing two transverse tubules (T T) and a longitudinal connection (Long.) between them. $\times 34,000$



Patterns of Origin and Distribution of the Major Bronchial Arteries in Man¹

AVERILL A. LIEBOW

Department of Pathology Yale University School of Medicine
New Haven, Connecticut

ABSTRACT In 50 lungs prepared as casts, the most common pattern of arrangement of the bronchial arteries, occurring in 30% of all lungs, was that of two posterior bronchial trunks to each side; next in frequency was the pattern of two trunks to the left and one to the right lung. In more than three-fourths of all cases there were not more than two bronchial arteries on each side. In two-thirds of the specimens various bronchial arteries arose both directly from the aorta and indirectly from an intercosto-bronchial trunk. At least one intercosto-bronchial trunk was present in 37 of the 50 specimens. All such trunks, even those supplying the left lung, took origin from the right side of the aorta, almost always from the first or second posterior segmental aortic branches, i.e., at the level of the fifth or sixth thoracic vertebra. Almost all intercosto-bronchial trunks yielded right bronchial artery. Approximately 64% of the left bronchial arteries spring directly from the aorta. In 22% single trunk was the source of all bronchial arteries to both lungs, and in 14% this trunk arose directly from the aorta. In 64% also there was at least one bronchial artery that supplied bronchi of both lungs.

Arteries arising high on the anterior or right lateral surface of the aorta were found in more than one-half of the casts more than three times as frequently as in previously reported dissections.

It is surprising that while much has been written on the distribution of the bronchial vessels within the lung (Miller '25) and their interrelationships with the pulmonary arteries especially in disease (Wood and Miller '38 Liebow '39 '62) there is little information concerning the modes and levels of origin from the aorta. This subject has assumed some practical importance since expanded bronchial arteries constitute the blood supply of pulmonary neoplasms and these vessels can be catheterized (Viamonte '64) and used as a route for direct introduction of chemotherapeutic agents in high concentration (Clifton and Mahajan, '63 Soderberg et al. '64). The larger monographs on the anatomy of the lung (Hovelacque et al., '36 Hayek, '60) deal with these vessels in the most general terms. Only two detailed descriptions have appeared, one by Nakamura in 1934 and the other by Cauldwell and co-workers in 1948. Each is founded on dissections of some 150 cadavers. The present observations are based largely on the detailed analysis of the structures in 50 corrosion casts. These offer the advantage of preserving certain vessels that are difficult to trace even in the most care-

ful dissections. The casts also facilitate the accurate illustration of the various patterns of origin and distribution of the bronchial arteries (figs. 1-11).

MATERIALS AND METHODS

The 50 lungs subjected to detailed analysis were from adults who came to necropsy as a result of injury or disease not primarily related to the lungs. The aorta and its branches were washed, and then injected *in situ* with vinyl plastic by a method described elsewhere (Liebow et al., '47). After partial hardening of the plastic the lungs and posterior mediastinal structures were removed for inflation, injection of the pulmonary vessels and bronchial tree and finally corrosion in concentrated hydrochloric acid. Another 100 casts similarly prepared were also examined principally for identification of the less prominent accessory bronchial arteries.

Posterior and accessory bronchial arteries

The main bronchial arterial supply usually springs from the aorta directly or by

¹Supported by grant from the NIH, USPHS (RR-07177).

mediation of an intercosto-bronchial artery. These two types of vessels will be referred to as the posterior bronchial arteries. An intercosto-bronchial artery is a segmental posterior aortic branch the distribution of which is indicated by its name.

The term accessory bronchial arteries will be employed for vessels reaching the bronchi from branches of the aorta other than the aortic intercostals. These are discussed more fully below. There are abundant free connections with mediastinal and even coronary vessels of small size. Only those with a diameter exceeding 100 μ can be considered in the accessory group.

Classification of bronchial arterial patterns

In the description to follow the major classification will be based on the number of posterior bronchial arteries as defined above to each lung. In this classification the branches of an artery distributed solely to one lung are not counted as separate bronchial arteries even though they may proceed to separate lobes (fig. 8 R). When a trunk is distributed to both lungs the successive branches are given separate designations for example left superior right and left inferior in figure 8.

The terms superior middle and inferior are used to denote the major bronchial arteries the reference being to the relative levels of origin from the aorta and not the ultimate level of distribution within the

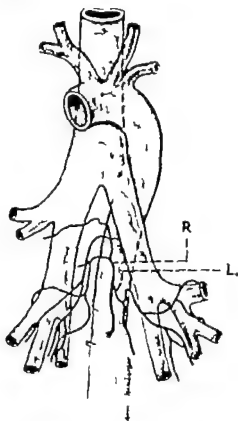


Fig. 1 Group II. A single common aortic trunk springing from the anterior surface of the aorta divides into one right and one left bronchial artery. An esophageal branch can be seen at its origin from the left bronchial artery. Specimen A7841. Key R, Right bronchial artery; L, Left bronchial artery.

TABLE 1
Distribution of posterior bronchial arteries to each lung

Type	Numbers of bronchial arteries		Present series		Series of Cawdwell et al.	
	Left	Right	Number	%	Number	%
I	2	1	10	20	61	40.67
II	1	1	5	10	32	21.33
III	2	2	15	30	31	20.67
IV	1	2	8	16	14	9.33
V	3	1	1	2	6	4.00
VI	3	2	8	16	3	2.00
VII	2	3	1	2	1	0.67
VIII	4	1			1	0.67
IX	1	4			1	0.67
X	1	3	1	2		
XI	3	3	1	2		
XII	2	3	2	4		
XIII	4	2	1	2		
Totals	-	-	50	100	150	100.1

bronchial tree. This designation serves except for the few instances where there are more than three separate bronchial arteries to one lung. In this circumstance, superior middle and inferior middle are the terms employed for the two central branches.

Analysis of major patterns of posterior bronchial arteries

A comparison of observations made upon the 50 casts in the present series, with the results of 150 dissections described by Cauldwell and co-workers is presented in table 1. The first nine groups

listed are the same as those of Cauldwell et al (48) although examples of their groups VIII and IX are lacking in the present series and it has been necessary to add four additional groups. Certain of the variations in pattern are indicated in figures 1-9. The chief difference in the two series is that more bronchial arteries have been found for each pair of lungs in the casts than in the dissections. Most of the additional arteries found in the casts arose from the right lateral surface of the arch of the aorta (see table 4 and fig. 6).

In our experience the most common arrangement, accounting for 30% of all

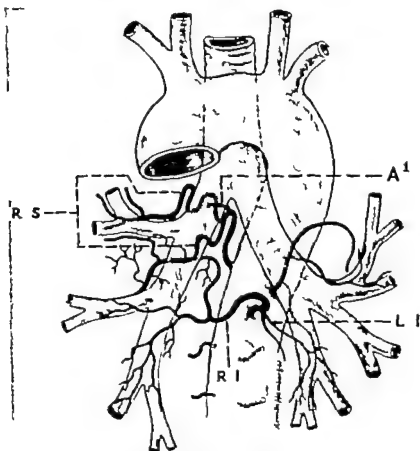


Fig. 2. Group III. One intercosto-bronchial trunk yields both A_1 and the right superior bronchial artery. Note that the right superior has branches both to the upper and middle lobe. A left superior bronchial artery arises directly from the aorta. There is one common aortic trunk also derived from anterior surface of the aorta which yields both right inferior and left inferior bronchial artery. This common trunk is source also of small esophageal branch. Specimen no. 43. Key: S, Superior; I, Inferior. A = First aortic intercostal artery. Other symbols as in key to figure 1.

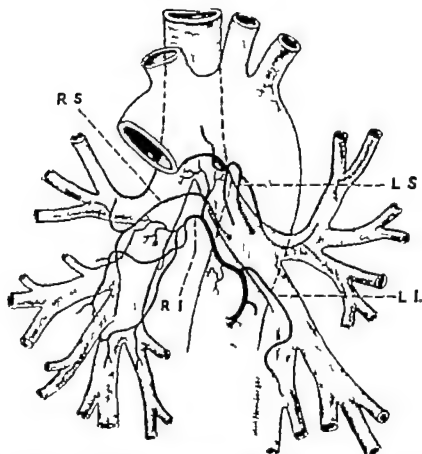


Fig. 3 Group III. All of the bronchial arteries have direct aortic origin, with no intercosto-bronchial trunk. One common trunk yields both right inferior and left inferior artery. This trunk is the source also of small vessel to the esophagus. The apparently sub-carinal branch of R.I. is mediastinal rather than bronchial artery. Specimen no. 45. Key as in preceding figures.

specimens is that of group III where two posterior bronchial arteries are distributed to each lung (figs. 2, 3 and 4). Meckel (1831-32) concurs in this statement. Next in order of incidence (20%) is the arrangement commonly presented as the classical by many including Caudwell et al. of two left and one right bronchial arteries (group I). The inverse arrangement (group IV fig. 5) is almost as common in our series as the classical, while it is only one-fourth as frequent in the Caudwell series. In this we are in agreement with Hovelacque et al. (37) (see page 137 of their monograph) although they maintain that the arrangement two on one side, one on the opposite is the most prevalent. Fourth in order of incidence in our mate-

rial is the condition of distribution of a single main trunk to each bronchus (group II). A glance at table 1 shows that the first four groups account for 76% of the specimens in our series and for 92% of those in the Caudwell series.

Modes of origin of the bronchial arteries

As defined, a posterior bronchial artery may take origin directly from the aorta, or from a branch that also yields an intercostal artery (intercosto-bronchial trunk). Thirty-three of the 50 specimens exhibited bronchial arteries of both modes of origin. In 13 there was aortic origin only and in four all bronchial arteries were mediated by an intercosto-bronchial trunk. The re-

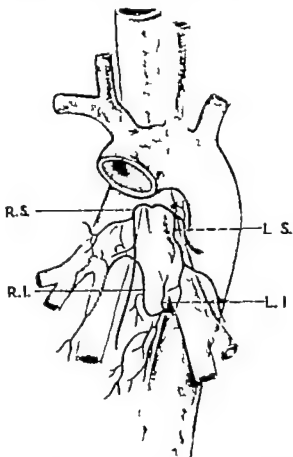


Fig. 4 Group III. Two common aortic trunks are present. Several esophageal and mediastinal branches are seen, the largest being derived from the right superior and right inferior bronchial arteries. Specimen no. 5. Key as in preceding figures.

spective percentages in the Nakamura series were 79.8, 17.8 and 2.4. It is interesting to note that in the 13 where there was aortic origin only seven presented as a single trunk that gave origin to all of the bronchial arteries of both lungs (Fig. 1). A similar instance is presented by Boyden (45).

Origin from intercosto-bronchial trunks

At least one intercosto-bronchial trunk was present in 37 of the 50 specimens (74%). The percentage in Cauldwell's group was 88.7 and in Nakamura's 81.2. This was predominantly the vessel that yielded the first aortic intercostal artery

(table 2, Figs. 2, 5, 7 and 9). In 31 of the 37 specimens only a single intercosto-bronchial trunk existed, but in the other six there occurred two intercosto-bronchial trunks (Fig. 7). These usually comprised the first and second posterior segmental aortic branches, but in one instance the first and third (Fig. 7) and in another the first and fourth respectively were involved (table 2).

All of the intercosto-bronchial trunks took origin from the right side of the aorta, even those that supplied a bronchial artery to the left bronchial tree. A left bronchial artery was derived in this fashion in 15 specimens (30%). In common with the branch to the right in all but two in-

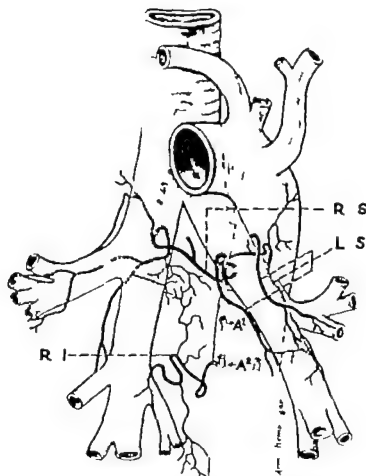


Fig 3 Group IV There is one intercosto-bronchial trunk giving rise to A_1 and R_1 and one common aortic trunk for the superior arteries of both sides. Mediastinal and oesophageal branches can be seen to originate chiefly from the right superior and inferior arteries. Specimen no 34 Key as in preceding figures.

TABLE 2
Levels of origin of intercosto-bronchial arteries

	A	A	A	A	A + 2
A. Single intercosto-bronchial (31 specimens)	22	8			1
B. Double intercosto-bronchial (6 specimens)	6	4	1	1	
C. Total (37 specimens)	28	12	1	1	1

In this instance (specimen 30) single arterial trunk came off the aorta at the level of A and, proceeding cephalad, yielded successively A and A and then the right superior bronchial artery

stances. In both of these there was a double intercosto-bronchial trunk one of which the caudad, yielded a solitary left inferior bronchial artery. Thus it is apparent that 41 of the 43 intercosto-bronchial trunks listed in table 2 yielded a right bronchial artery

Forty-three per cent of all right bronchial arteries were of intercosto-bronchial origin while 84.3% of the left bronchial arteries sprung directly from the aorta.

Common trunks

A bronchial vessel supplying both lungs will be termed a common trunk.

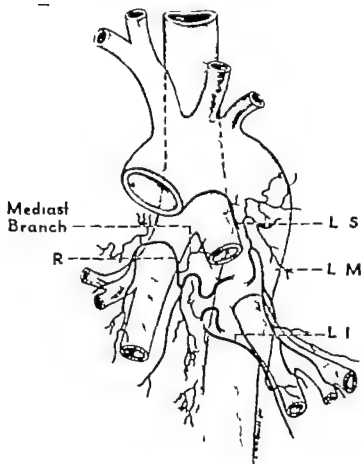


Fig 6 Group V All of the bronchial arteries have separate and unmediated origins from the aorta. There is a small left superior bronchial artery arising just below the arch where the right side of the aorta is in contact with the left main bronchus. Several esophageal and mediastinal branches are derived from all of these vessels. Specimen no 1 Key M, Middle. Other symbols as in preceding figures.

TABLE 3
Origins of common bronchial arterial trunks

1	All B.A. from single common trunk	11
	a. Intercoasto-bronchial origin	4
	b. Aortic origin	7
2	One common trunk, other B.A. of separate origins	21
	a. C.T. of intercoasto-bronchial origin	4
	b. C.T. of aortic origin	17
3	Double common trunks	10
	a. Including one of intercoasto-bronchial origin	6
	b. Aortic origin of C.T. only	4
	Total specimen with C.T.	42

In only eight of the 50 specimens did all of the bronchial arteries arise separately from the aorta, or from an intercosto-bronchial trunk (fig 6). In the vast majority (84%) there was at least one bronchial artery which ultimately supplied the bronchi of both lungs (table 3). It is remarkable that common trunks were noted in only 26% of Cauldwell's dissections.

In 11 lungs a solitary common trunk was the source of all bronchial arteries of both sides (fig 1). Four of these were intercosto-bronchial trunks (all derived from A) and seven sprang directly from the aorta as described in the preceding section.

One common trunk, associated with additional separately derived bronchial ar

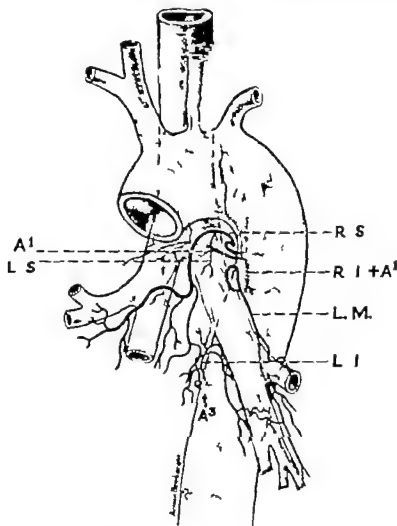


Fig. 7 Group VI. Two intercosto-bronchial trunks, and one common aortic trunk are seen. The former yield A₁ and A₂ respectively. The common intercosto-bronchial trunk is the origin of R.I. and L.M. This is an example of an intercosto-bronchial trunk that gives origin to left bronchial artery as well as right. The inferior intercosto-bronchial trunk also supplies the left lung via L.I. A common aortic trunk is the origin of R.S. and L.S. The right superior bronchial artery is in anterior transit, and passes from its source in the common aortic trunk, between the arch of the aorta and the left main bronchus over which it is looped to cross, anteriorly of the carina, to the right lung. Several mediastinal and esophageal branches are also in evidence. Specimen no 24. Key as in preceding figures.

teries was found in 21 of the 50 specimens. Four of these were of intercosto-bronchial origin while the other 17 took origin from the aorta.

Double common trunks were found in ten specimens (fig. 4) and in six of these at least one common trunk had an intercosto-bronchial origin.

Branches from the lateral or anterior surfaces of the concavity of the arch of the aorta above the first aortic intercostal

The presence of arteries arising high on the anterior or right lateral surface of the aorta above the first aortic intercostal

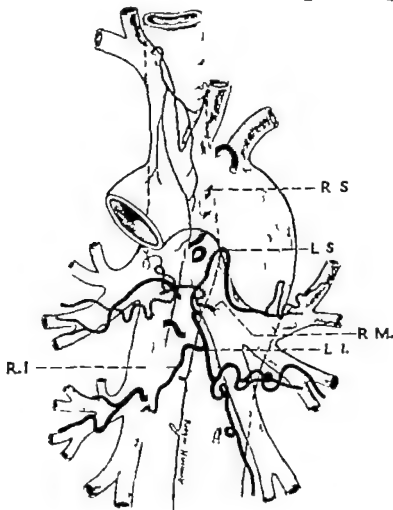


Fig. 8 Group VI. There is one common aortic trunk that yields, in succession, L.S., and then R.I. and L.I. R.S. originates in remarkable position from the aorta at the base of the left subclavian artery then passes in anterior transit over the left main bronchus to yield branches to the right upper and middle lobes. The bronchial arteries in this specimen are enlarged in association with the bronchiectasis and organizing pneumonia from which this patient suffered. There is also an accessory branch which originates from the innominate artery just proximal to the bifurcation of the latter. This supplies the trachea and the region of the aorta, and small branches are distributed to both main bronchi. Such vessels have been called superior bronchial arteries by some. Specimen no. A5222. Key in preceding figures.

TABLE 4

Branches from right lateral or anterior face of arch of aorta		face of arch of aorta
1. Left + Right	16	
2. Left superior alone	8	
3. Right alone	5	

(figs. 4 and 6) has been mentioned but not stressed by previous observers. Such arteries were found in 54% of the specimens in the present series but in only 14.7% of Cauldwell's dissections. The observed arrangement of the vessels is indicated in table 4. In two of the 16 in the first group of that table two separate trunks took origin in this position. In one of these

the arrangement was left superior plus right inferior and left middle and in the other the arrangement was left superior and right superior plus left inferior.

Anterior transit of posterior bronchial arteries

In many instances a bronchial artery supplying the right bronchial tree looped over the left main bronchus in halpin fashion and then passed anteriorly of the trachea at the level of the carina to be distributed within the right lung (figs. 4, 7 and 8). This circuitous arrangement was observed in 23 of the 50 casts but it was noted in only 8.7% of Cauldwell's dissec-

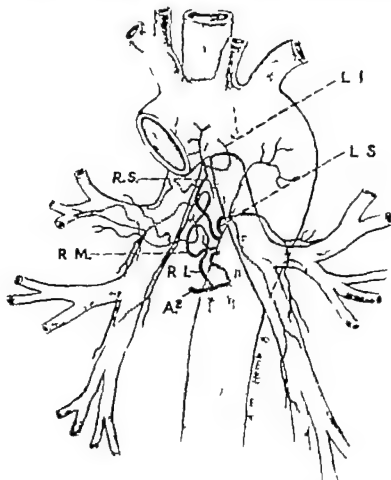


Fig. 9 Group XII. There is one intercosto-bronchial trunk (yielding A_2) and one common aortic trunk that is the source of R.S. and L. 1. Note that L.L. supplies the upper portion of the left main bronchus. It is given the designation L.L. nevertheless, since the trunk of its origin is caudad to that of the L.S. trunk. Specimen no. 2. Key as in preceding figures.

tions. In instances where the aorta arched over the right main bronchus rather than in its usual position, the left bronchial artery sometimes pursued an analogous course (fig. 10). The position of this frequently large branch of the aorta anteriorly of the carina is of surgical interest.

Invariably the bronchial arteries following this course took origin directly from the anterior or right lateral aspect of the aorta, or from the base of a subclavian artery (fig. 8); they were never of the intercosto-bronchial type. Usually the right superior bronchial artery was the vessel in anterior transit (19 instances) but in four it was the right inferior. Such right bronchial arteries usually (in 17 of 23 instances) arose as common trunks that yielded also a branch, most commonly the superior to the left side. Of the six arising as single right bronchial arteries, two were right inferior bronchial arteries.

Accessory bronchial arteries

Only occasionally do the accessory bronchial arteries represent the major bronchial arterial inflow. To discover these vessels in normal specimens, special detailed and systematic study is necessary. Their usual small size precludes their easy demonstration by dissection. In the preparation of the casts in the present investigation, injection of the costo-cervical trunk was accomplished routinely but the technique was not designed to inject more than the first few millimeters of the other primary branches of the subclavian artery. Had this been done doubtless additional accessory bronchial arteries would have been found.

In approximately 150 casts sizable accessory bronchial arteries were demonstrated in four instances (fig. 8). In certain other specimens (fig. 10) a bronchial

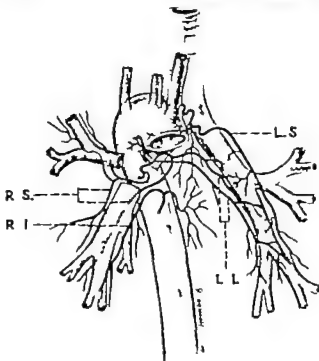


Fig. 10 Group III. An instance of right aorta in patient with tetralogy of Fallot. There is no fundamental change in the bronchial pattern and right middle lobe is present. There is one common aortic trunk that yields R.S. and L.I. L.S. has an unusual origin, being derived from the aorta at the base of the innominate artery which in this case is distributed to the left side. This artery is in anterior transit as in figure 8. Esophageal arteries take origin from L.S. and R.I. Specimen no. A8206. Key as in preceding figures.

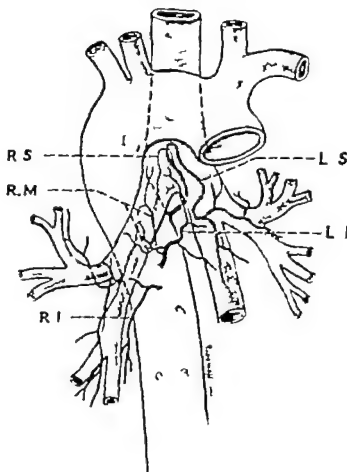


Fig 11 From patient with situs inversus. In this instance the bronchial pattern is the reverse of normal and the classification is that of Group VI in mirror image. There is one common aortic trunk that yields vessels to both sides. Specimen no. A8177 Key as in preceding figures.

artery arising from the aorta at the base of the subclavian was discovered, but such aortic vessels were classified as "posterior" bronchial arteries. This incidence of accessory bronchial arteries of between 2 and 3% is approximately the same as is given by Cauldwell, but probably represents a bare minimum.

Topographic relations of origins of the bronchial arteries to the vertebral column

In the present series at least 75% of all major bronchial arterial trunks arose at the level of the first or second aortic intercostal arteries that is at the level of the fifth or sixth thoracic vertebrae. In Cauld-

well's observations, 70.1% of all left bronchial arteries of aortic origin emerged from a segment limited by the cranial margin of T5 and the caudad margin of T6. Eighty-three per cent of right aortic bronchial arteries arose between these limits.

DISCUSSION

In the present series the average number of bronchial vessels for the right side was 1.90 while in Cauldwell's it was 1.78 the respective average numbers for the left side were 1.78 and 1.37. The discrepancy is even greater in relation to the observations presented by Nakamura. In part this may be a matter of definition, since major branches of a bronchial arterial

trunk to the side other than that of its major distribution have been counted in the present series.

A major factor in the discrepancy is that branches arising from the right lateral portion of the arch of the aorta especially have been missed. Here the aorta crosses the left main bronchus and these frequently small vessels are buried in the areolar tissue between these two intimately associated structures (fig. 8) and would be difficult to discover even in the most careful dissection.

The frequency of accessory bronchial arteries encountered in the present series 2.7% is much higher than one would expect from the statement of O'Rahilly et al. (30) that only 12 examples of subclavian origin of bronchial arteries had been reported up to 1950. The idea of their rarity however is contravened by such descriptions as that of Meckel (1831-32) or of Haller (1747). O'Rahilly reports the origin of major right and left bronchial arteries from a single stem which arose in common with the left superior intercostal arteries from the subclavian. It was not possible to state whether posterior bronchial arteries were also present, since the dissection of this anatomical subject had progressed too far.

Bronchial arteries of subclavian or innominate origin represent the most frequently encountered of the accessory bronchial arteries in man. Usually the left subclavian is the vessel of origin (O'Rahilly '50). Vessels to the bronchi derived from the subclavian have been termed superior bronchial arteries by Meckel (1831-32) who contrasted them with the "inferior bronchial arteries of aortic origin. Confusion in this usage however has been introduced by Rauber Kopsch ('29) who employed the same term for bronchial arteries derived from the concavity of the aortic arch. "Accessory" has, therefore, been used as the more inclusive designation in the present description.

The internal mammary arteries have also been cited as sources of bronchial vessels (called by some anterior). The large bronchial branches of the internal mammary are usually derived close to the origin in the subclavian. Both the trachea

and hilar portions of the bronchi are supplied. Hovelacque, Monod and Evrard ('37) review the published description of these and other rare sources of accessory bronchial arteries including the superior intercostal and inferior thyroid. As judged from expanded vessels in fibrotic lungs minute arterial branches may also normally be distributed to the bronchi via the pulmonary ligaments and retropleural tissues from the pericardiophrenic esophageal and other mediastinal vessels. Rarely accessory bronchial arteries take origin in common with a major coronary artery or from a persistent ductus arteriosus. Isolated instances have been described of bronchial arterial supply derived from the aorta below the diaphragm.

LITERATURE CITED

- Boyden, E. A. 1945 The intrahilar and related segmental anatomy of the lung. *Surgery* 18: 706-731.
- Cauldwell, E. W., R. G. Sleight, R. E. Lindner and B. J. Anson 1948 The bronchial arteries. *Surg. Gynec. Obstet.*, 86: 305-412.
- Chilton, E. E., and D. R. Mahajan 1963 Technique for visualization and perfusion of bronchial arteries: Suggested clinical and diagnostic applications. *Cancer*, 16: 444-453.
- Haller, A. 1747 *Iconum anatomicarum partium corporis humani. Fasc. III. Arteriae capitis, menterii, thoracis, renum.* Goettingen, A. Vandenhoeck, 31-40.
- Hayek, H. 1900 *The Human Lung.* Translated by V. E. Krahl. Hafner Publishing Co., Inc., New York.
- Hovelacque, P. G. Monod and H. Evrard 1937 *Le Thorax.* Paris, Maloine.
- 1936 *Notes u Sujet des Arteries Bronchiques.* *Ann. Anat. Path.*, 13: 129-141.
- Hudson, C. L., A. R. Moritz and J. T. Westm 1932 The extracardiac anastomoses of the coronary arteries. *J. Exp. Med.*, 56: 919-925.
- Liebow, A. A. 1952 Recent observations on pulmonary collateral circulation. *Med. Thorac.*, 19: 609-622.
- Liebow, A. A., M. R. Hales, G. E. Lindskog and W. E. Bloomer 1947 Plastic demonstrations of pulmonary pathology. *Bull. Internat. Assn. Med. Museums*, 37: 110-129.
- Liebow, A. A., M. R. Hales and W. E. Bloomer 1959 Relation of bronchial to pulmonary vascular tree. In: 1956 *Pulmonary Circulation.* An International Symposium, Grune and Stratton, New York, 79-98.
- Meckel, J. F. 1831-32 *Manual of General, Descriptive and Pathological Anatomy* Translated from the German into French, with additions and notes by A. J. L. Jourdan and G. Breschet, and from the French by A. S. Doane. Vol. 2, Celline, Hanny and H. C. Sleight, New York, 237-252.

- Miller W. S. 1925 The vascular supply of the bronchial tree. *Am. Rev. Tuberc.*, 12 87-93
- Nakamura, N. 1924 Zur Anatomie der Bronchialarterien. *Anat. Anz.*, 58 508-517
- O'Rahilly R., H. Debeon and T. S. King 1950 Subclavian origin of bronchial arteries. *Anat. Rec.*, 106 227-238
- Rauber A., and F. Kopsch 1929-34 *Lehrbuch und Atlas der Anatomie des Menschen*. Vol. 3 Leipzig, G. Thieme 313-314
- Soderberg, C. H., M. P. Colbert and L. A. Leese 1964 Bronchial artery infusion therapy of lung neoplasms with nitrogen mustard. *Surgery* 58 897-904
- Vlamonte, M., J. 1964 Selective bronchial arteriography in man. *Radiology* 83 830-839
- Wood, D. A., and M. Miller 1938 The role of the dual circulation in various pathologic conditions of the lungs. *J. Thorac. Surg.*, 7 642-670.

A Fluorescence and Electronmicroscopic Study on Certain Brain Regions Rich in Monoamine Terminals

KJELL FUXE, TOMAS HÖKFELT AND OVE NILSSON

Department of Histology, Karolinska Institute, Stockholm, Sweden

ABSTRACT With the use of both the sensitive fluorescence method of Falck and Hillarp for the histochemical demonstration of monoamines at the cellular level and electron microscopy the synaptic terminals were studied in nucleus caudatus putamen, nucleus tractus solitarius and the substantia grisea periventricularis of the fourth ventricle. In all three regions numerous boutons of size similar to the varicosities of the monoamine terminal exist. They form mostly synapses with dendrites. The boutons more or less filled with either small (about 300–350 Å) medium sized (about 450 Å) or — but less commonly — large (about 550–600 Å) agranular vesicles. Larger (about 800–1,000 Å) granular vesicles are found in all three regions studied. In comparison to the agranular vesicles, however, they are practically always few. In animals treated with large dose of reserpine or nialamide none of the different types of vesicles showed any obvious changes. It is concluded that the monoamine storage granules are not identical with the large granular vesicles, but that they with the method used, appear as small, agranular vesicles.

Specific monoamine neurons exist in the central nervous system and there is little doubt that they are monoaminergic (cf Dahlström and Fuxe '64a, b; Fuxe '65a). The terminals belonging to these neurons are present in a vast number of areas and nuclei. The noradrenaline (NA) terminals in the hypothalamus were the first to be demonstrated (Carlsson, Falck and Hillarp '62). Three different types of monoamine terminals have been found forming and storing dopamine (DA) NA and 5-hydroxytryptamine (5-HT) respectively. These terminals are often concentrated to certain nuclei and regions. DA terminals are accumulated e.g. in the nucleus caudatus putamen (neostriatum) (Andén, Carlsson, Dahlström, Fuxe, Hillarp and Larsson, '64; Andén, Dahlström, Fuxe and Larsson, '65). NA terminals in e.g. the nucleus tractus solitarius and 5-HT terminals in e.g. the cranial, ventricular part of the substantia grisea periventricularis of the fourth ventricle (Fuxe, '65b).

In this paper the three above-mentioned areas have been studied both with the sensitive and specific histochemical fluorescence method of Falck and Hillarp (Falck, Hillarp, Thilme and Torp '62; Falck, '62) and with electron microscopy with a view to determining the ultrastructure of the

monoamine terminal, establishing whether or not there exists any morphological differences between the three types of monoamine terminals at the ultrastructural level, and finding out with which cell structures they make the synaptic contacts.

MATERIAL AND METHODS

About 150 male albino rats (Sprague-Dawley b. wt 200 to 250 g) were used. A large dose of the potent monoamine oxidase inhibitor nialamide (500 mg/kg i.p., 5 to 6 hours before killing) was administered to 18 animals. This treatment produces a very marked increase in the 5-HT content of the 5-HT neurons and the terminals of these neurons are thus more easily visualized (Dahlström and Fuxe '64a). To deplete the monoamine stores in the brain (cf Carlsson, '65) reserpine (10 mg/kg i.p. 24 hours before killing) was administered to 18 animals. Forty normal rats and 3 and 5 rats treated with nialamide and reserpine respectively were sacrificed for electron microscopy. The rest of the animals were taken for fluorescence microscopy.

Fluorescence microscopy The animals were killed by decapitation under light ether anaesthesia. The neostriatum, pons and medulla oblongata were freeze-dried

treated with formaldehyde gas for one hour at +80°C embedded in paraffin, sectioned (mainly cross-sections) and mounted as previously described in detail (Dahlström and Fuxe '64a). During the formaldehyde treatment, primary catecholamines—such as DA and NA—and 5-HT are converted into strongly fluorescent 6,7-dihydroxy-3,4-dihydroisoquinolines and 6-hydroxy-3,4-dihydro- β -carboline with a green and yellow fluorescence respectively (Corrodi and Hillarp '63 '64).

Electron microscopy The brain of the animals was fixed by perfusion under sodium pentobarbital anaesthesia (35 mg/kg i.p.) with a glutaraldehyde-bichromate solution (5% glutaraldehyde and 2% potassium bichromate in a phosphate buffer pH = 8.4) (Sabatini, Benesch and Barnett, '63) for about 10–15 minutes according to the technique of Bodian and Taylor ('63). Small pieces of the caput of the caudate nucleus and pieces containing respectively the nucleus tractus solitarius and the substantia grisea periventricularis were dissected out and refixed for 2 to 4 hours in a buffered solution of 1% osmic acid tetroxide solution buffered at pH 7.4 with veronal acetate rinsed dehydrated in ethyl alcohol and embedded in Epon (Luft, '61).

The two latter pieces were cut for light microscopy with glass knives in an LKB-ultramicrotome and stained with toluidine blue (pH = 8–9). On the basis of these light microscopical sections the nucleus tractus solitarius (fig. 3) and the substantia grisea periventricularis were identified and these nuclei were trimmed for electron microscopy. The sections approximately 600–700 Å thick, were stained with uranyl acetate followed by lead staining (Reynolds, '63). An RCA EMU-3a electron microscope was used.

RESULTS

The synaptic terminals of the central monoamine neurons—like the peripheral adrenergic terminals—are terminal branches which show abundant and characteristic varicosities along their entire length (Carlsson, Falck, Fuxe and Hillarp '64; Fuxe, '65a). The varicosities exhibit a strong specific fluorescence due to the presence of very high concentrations of the respective monoamines.

Fluorescence microscopy

Nucleus caudatus putamen. A strong, diffuse green fluorescence is present between the nerve cells. The fluorescence is seen under optimal reaction conditions to originate from abundant very fine DA terminals (Fuxe Hökfelt and Nilsson '64). A small to medium increase in fluorescence intensity was observed after nialamide.

Nucleus tractus solitarius. A dense plexus of fine green fluorescent NA (and possibly some DA) terminals the varicosities of which are mainly 0.5 to 2.0 μ thick and 0.8 to 3 μ long, is present between the nerve cells (fig. 2). Some terminals however were observed to make close contacts with the cell bodies. There is a marked decrease in their number at the border towards the nucleus hypoglossus. The fine yellow fluorescent 5-HT terminals in the nucleus tractus solitarius were difficult to observe in normal animals since they have a lower fluorescence intensity and are much less frequent than the green-fluorescent terminals. After nialamide treatment, however they developed a fairly strong fluorescence and could be seen distinctly. No obvious increase in the fluorescence of the CA terminals was observed after this treatment.

The substantia grisea periventricularis of the fourth ventricle (the area in the midline just under the ependyma). A dense mass of fine yellow fluorescent dots (0.3 to 1 μ thick) of weak fluorescence is seen in this region (fig. 1). The dots in all probability represent the varicosities of very fine 5-HT terminals (Fuxe '65a, b). The intensity of the fluorescence is strongly increased on treatment with nialamide. The yellow fluorescent varicosities in this region have not been observed to make any close contacts with nerve cell bodies. Very few green-fluorescent CA terminals are present.

Reserpine was found completely to abolish the fluorescence of the terminals in all the regions studied.

Electron microscopy

Boutons (presynaptic bags containing synaptic vesicles) were present in all the regions studied. In the neostriatum many of them had a diameter below 0.4 μ (figs. 4 and 5) while in the nucleus tractus soli-

taril the diameter varied mainly between 0.6 to 2 μ and in the substantia grisea periventricularis mainly between 0.3 to 1.5 μ .

Most of the boutons in the three regions studied contained vesicles which were predominantly of fairly uniform size and appearance. The vesicles were agranular and most of them had diameters ranging between 300 and 600 Å. The vesicles present in one and the same bouton were of a fairly uniform size. It was found that the boutons could be divided into three groups containing small (of about 300–350 Å size) medium sized (of about 450 Å size) and large (of about 550–600 Å size) vesicles respectively (figs. 8, 9 and 11). The majority of the boutons contained small or medium sized vesicles while only a small proportion of boutons were observed to contain vesicles of the large size.

The vesicles within a bouton varied widely in number. Some boutons contained only few vesicles, but it cannot be excluded that this was due to postmortem changes. Other boutons were densely packed, sometimes showing an almost crystalline pattern of vesicles.

Boutons were also found that contained not only vesicles of the small agranular type but in addition a varying number of much larger vesicles (on the average about 800–1,000 Å in diameter) with a central core of variable size and density (figs. 7 and 8). Such boutons were present in all the regions studied. Granular vesicles of the same type were found also comparatively often in fine axons of a diameter of 0.15–0.3 μ (figs. 7 and 8) together with a few agranular vesicles or none at all. Granular vesicles were rare in the neostriatum but fairly common in the two other regions where approximately 60% of the total number of boutons contained at least one granular vesicle. The number of granular vesicles within each bouton varied greatly (from 1 to 15 granular vesicles were found per square micron of sectioned bouton) but was practically always small in comparison with the number of agranular vesicles in the same bouton.

The synaptic junctions of the vast majority of axon terminals in the regions studied seemed to be axo-dendritic and of type I according to Gray ('56, '61a,b) (figs.

6, 10 and 11). The post-synaptic components appeared mostly to be dendritic trunks and spines but no typical spine apparatus was observed.

In the substantia grisea periventricularis axo-dendritic junctions that more closely resemble type II were sometimes seen. Axo-somatic junctions of type II were observed occasionally in the nucleus tractus solitarius and the neostriatum. No synaptic junctions between boutons were found in the regions studied.

DISCUSSION

There is little doubt that the abundant varicosities occurring along the entire length of peripheral adrenergic and central monoamine terminals are presynaptic structures specialized for the synthesis, storage and release of the respective monoamines (Dahlström and Fuxe, '64a, Fuxe '65a, Malmfors '65; Norberg and Hamberger '64). A dense plexus of such terminals is present in each of the three regions of the brain studied in the present paper. It therefore seems reasonable to assume that a certain percentage of the observed boutons containing synaptic vesicles should be identical with the varicosities of the monoamine terminals.

As regards size, the fluorescence and electron microscopic observations are in agreement. The neostriatum contains a number of very fine (probably partly sublightmicroscopic) DA terminals with small varicosities. The nucleus tractus solitarius has numerous NA terminals with large varicosities (mainly 0.5 to 2 μ thick). The varicosities of the 5-HT terminals in the substantia grisea periventricularis are smaller (0.3 to 1 μ). In the neostriatum numerous boutons were found to be smaller than 0.4 μ , and in the two other regions the boutons showed a size range covering that of the varicosities.

Boutons with agranular vesicles of three main size ranges could be seen in the regions studied. In spite of the fact that preparative procedures may influence the size and structure of the vesicles true differences may exist since boutons with well preserved vesicles of different sizes could be seen lying close together (figs. 9 and 11).

The granular vesicles found had a more or less dense central core and were about

800 to 1000 Å in diameter i.e. of type I according to Grillo and Palay ('63). Granular vesicles of different types have been found both in the peripheral nervous system, e.g. in the autonomic ganglia and in nerve endings in smooth muscle (Taxi, '61a, b; Richardson '62, '64) and in the central nervous system, e.g. in the anterior hypothalamus (Pellegrino de Iraldi, Farini Duggan and De Robertis '63). In the peripheral nervous system the granular vesicles, mainly of types II and III (Wolfe et al. '62; Richardson '64) and in the central nervous system the granular vesicles of type I (Pellegrino de Iraldi, Farini Duggan and De Robertis, '63) have been assumed to be identical with the NA storage granules. In the three regions studied the large granular vesicles were always few in comparison with the agranular vesicles. The microphotos in the paper by Pellegrino de Iraldi, Farini Duggan and De Robertis ('63) show that this is true also of the boutons in the anterior hypothalamus of rat. The varicosities of the NA terminals however store very high concentrations of the amine (probably in the order of 10 000 µg/g wet weight) and there is little doubt that most of the NA is kept in specific storage granules (see Dahlström and Fuxe '64a; Fuxe '65a; Hamberger, Malmfors, Norberg and Sachs, '64; Norberg and Hamberger '64). It can be calculated that the transmitter granules must therefore occupy a large proportion of the volume of a varicosity even if they have the same extraordinarily high capacity to store amines as the granules of the adrenal medullary cell (Hillarp personal communication). It therefore seems quite improbable that the large granular vesicles observed in the hypothalamus and in the three regions studied in the present paper should be identical with CA storage granules. No obvious changes in their appearance were observed in animals treated with a very large dose of nialamide (cf. Pellegrino de Iraldi and De Robertis '63) which produces strongly increased levels of 5-HT in the brain. Of much greater significance however is the fact that reserpine which depletes the stores of monoamines in the synaptic terminals (see Dahlström and Fuxe '64a) seemed likewise to induce no changes in the appear-

ance of the granular vesicles in spite of the very large dose used. No clear reduction in the number of vesicles was observed but such a reduction cannot be excluded.

The conclusion seems inescapable that the large granular vesicles observed in these three regions of the brain are not identical with monoamine storage granules. Furthermore, this conclusion is supported by the fact that the large granular vesicles were observed to about the same extent in the nucleus vestibularis medialis (Hökfelt, unpublished data) which contains practically no monoamine terminals (Dahlström and Fuxe '64). Therefore it may be that, with the methods used, the latter appear as small agranular vesicles. In the rat iris for instance, the varicosities of both adrenergic and cholinergic terminals have been found to be filled with agranular vesicles of the same appearance (Nilsson, '64; Hökfelt and Nilsson, '65).

The vast majority of boutons in the regions studied form axo-dendritic junctions and very few axo-somatic synapses seem to exist. Therefore it may be that most of the monoamine terminals in these regions also form synapses with dendrites. The observations made with the fluorescent microscope strongly support this view. Most of the fluorescent terminals are found between the nerve cell bodies and not in close contact with them. Also most of the CA terminals in certain zones of the hippocampal formation seem to form axo-dendritic junctions (Blackstad, '63; Fuxe, '65a). Thus, data are now available which indicate that the monoamine terminals in the central nervous system may in certain areas form mainly axo-dendritic junctions. No axo-axonal synapses have so far been observed (cf. Gray '62). The monoamine terminals therefore probably form few — if any — such junctions, indicating that presynaptic inhibition — if present — is not commonly involved in monoaminergic transmission in the regions studied.

ACKNOWLEDGMENTS

For generous supplies of drugs we are indebted to the following companies: Swedish Ciba, Stockholm, Sweden (reserpine); Swedish Pfizer, Stockholm, Sweden (nialamide).

This study has been supported by research grants (12X 715-07 and Y 247) from the Swedish Medical Research Council, the Knut and Alice Wallenberg Foundation, and by a Public Health Service Research Grant (NB 05236-01) from the National Institute of Neurological Diseases and Blindness.

LITERATURE CITED

- Andén, N.-E., A. Carlsson, A. Dahlström, K. Fuxe, N.-A. Hillarp and K. Larsson 1964 Demonstration and mapping out of nigro-neostriatal dopamine neurons. *Lif Sci.*, 3 823-830
- Andén, N.-E., A. Dahlström, K. Fuxe and K. Larsson 1965 Further evidence for the presence of nigro-neostriatal dopamine neurons in the rat. *Amer J Anat.*, 116 329-334.
- Blackstad, T W 1963 Ultrastructural studies on the hippocampal region. *Progr Brain Res.*, 3: 123-148.
- Bodian, D and N T ylor 1963 Synapses arising at central nodes of Ranvier and note on fixation of the central nervous system. *Pharmacol. Rev.* 11 490-493.
- Carlsson, A. 1965 Drugs which block the storage of 5-hydroxytryptamine and related amines. In: *Handbuch der Exp. Pharmacol.* Ed., V. Eppner Springer-Verlag, Berlin-Göttingen-Heidelberg (in press)
- Carlsson, A., B. Falck, K. Fuxe and N.-A. Hillarp 1964 Cellular localization of monoamines in the spinal cord. *Acta Physiol. Scand.*, 60 113-119
- Carlsson, A., B. Falck and N.-A. Hillarp 1962 Cellular localization of brain monoamines. *Acta Physiol. Scand.*, 86 Suppl. 196, 1-23.
- Cocroft, H., and N.-A. Hillarp 1963 Fluoreszenzmethoden zur histochemischen Nachbarschabung von Monoaminen. I. Identifizierung der fluoreszierenden Produkte aus Modellversuchen mit 6,7-Dimethoxytryptamin-derivaten und Formaldehyd. *Helv Chim. Acta*, 46 2425-2430.
- 1964 Fluoreszenzmethoden zur histochemischen Nachbarschabung von Monoaminen. 2. Identifizierung des fluoreszierenden Produktes aus Dopamin und Formaldehyd. *Helv Chim. Acta*, 47 911-918.
- Dahlström, A., and K. Fux 1964a Evidence for the existence of monoamine-containing neurons in the central nervous system. I. Demonstration of monoamines in the cell bodies of brain stem neurons. *Acta Physiol. Scand.*, 62: Suppl. 232, 1-53.
- 1964b Localization of monoamines in the lower brain stem. *Experientia*, 20 368-369.
- Falck, B 1962 Observations on the possibilities of the cellular localization of monoamines by fluorescence method. *Acta Physiol. Scand.*, 86 Suppl. 197 1-25.
- Falck, B., N.-A. Hillarp, G. Thiesse and A. Torp 1962 Fluorescence of catecholamines and related compounds condensed with formaldehyde *J Histochem. Cytochem.*, 10 348-354
- Fuxe, K. 1965a Evidence for the existence of monoamine neurons in the central nervous system. III: The monoamine nerve terminals. *Z. Zellforsch.*, 65 573-590.
- 1965b The distribution of monoamine terminals in the central nervous system of the rat. *Acta Physiol. Scand.*, 84 Suppl. 247
- Fuxe, K., T Hökfelt and O. Nilsson 1964 Observations on the cellular localization of dopamine in the caudate nucleus of the rat. *Z. Zellforsch.*, 63: 701-706.
- Gray E. G. 1959 Axo-somatic and axo-dendritic synapses in the cerebral cortex: an electromicroscope study *J Anat. (Lond.)* 93 420-433.
- 1961 The granule cells, mossy synapses and Purkinje spine synapses of the cerebellum: light and electron microscope observations. *J Anat. (Lond.)* 95 345-356.
- 1961b Ultrastructure of synapses of the cerebral cortex and of certain specializations of the neuroglial membranes. In *Electron Microscopy in Anatomy* Eds. J. D. Boyd, F. R. Johnson, and J. D. Lever Edward Arnold, London, pp. 54-73
- 1962 A morphological basis for presynaptic inhibition. *Nature (Lond.)* 193 82-83.
- Grillo, M., and S. L. Palay 1963 Granule-containing vesicles in the uterine nervous system. *Electron Microscopy* Ed. S. S. Broese, Jr., Academic Press, New York, 2: U-1
- Hamberger B T Malmfors, K.-A. Norberg and Ch. Sachs 1964 Uptake and accumulation of catecholamines in peripheral adrenergic neurons of reserpinized animals, studied with histochemical method. *Biochem. Pharmacol.*, 13 841-849
- Hökfelt, T and O Nilsson 1965 The relationship between nerves and smooth muscle cells in the rat iris. II. The sphincter muscle. *Z. Zellforsch.*, (in press)
- Luft, J. H. 1961 Improvements in epoxy resin embedding methods. *J Biophysic. and Biochem. Cytol.* 9 400-414
- Malmfors, T 1965 Release and depletion of the transmitter in adrenergic terminals produced by nerve impulses after inhibition of noradrenaline synthesis or reabsorption. *Life Sci.*, 3 1367-1402.
- Nilsson, O 1964 The relationship between nerves and smooth muscle cells in the rat iris. I. The dilator muscle. *Z. Zellforsch.*, 64 166-171.
- Norberg, K.-A., and B. Hamberger 1964 The sympathetic adrenergic neuron. Some characteristics of the peripheral adrenergic neuron revealed by histochemical studies on the intraneuronal distribution of the transmitter *Acta Physiol. Scand.*, 63 Suppl. 232.
- Pellegrino de Iraldi, A., and E. de Robertis 1963 Action of reserpine, iproizid and pyrogallol on nerve endings of the pineal gland. *Int. J. Neuropharmacol.*, 2 231-239
- Pellegrino de Iraldi, A., H. Farini Duggan and E. de Robertis 1963 Adrenergic synaptic vesicles in the anterior hypothalamus of the rat. *Anat. Rec.*, 143 521-531

- Reynolds, E. S. 1963 The use of lead citrate at high pH as an electron-opaque stain in electron microscopy. *J. Cell Biol.*, 17: 206-212.
- Richardson, K. C. 1962 The fine structure of autonomic nerve endings in smooth muscle of the rat vas deferens. *J. Anat. (Lond.)* 96: 427-442.
- 1964 The fine structure of the albino rabbit iris with special reference to the identification of adrenergic and cholinergic nerves and nerve endings in its intrinsic muscles. *Amer. J. Anat.*, 114: 173-206.
- Sabatini, D. D., K. Benesh and R. J. Barnett 1963 The preservation of cellular ultrastructure and enzymatic activity by aldehyde fixation. *J. Cell. Biol.*, 17: 19-33.
- Taxi, J. 1961 Étude de l'ultrastructure des zones synaptiques dans les ganglions sympathiques de la Grenouille. *C. R. Acad. Sci.*, 251: 174-176.
- 1961b Sur l'innervation des fibres musculaires lisses de l'intestin de Souris. *C. R. Acad. Sci.*, 252: 331-333.
- Wolfe, D. E., L. T. Potter, K. C. Richardson and J. Axelrod 1962 Localizing tritiated norepinephrine in sympathetic axons by electron microscopic autoradiography. *Science*, 138: 440-442.

PLATE 1

EXPLANATION OF FIGURES

- 1 Superficial zone of the substantia grisea periventricularis of nialamide treated rat. Transverse section. The very fine 5-HT terminals are so closely packed that they appear as a mass of yellow-fluorescent dots (G) lying just under the ependyma (E) of the fourth ventricle (V) $\times 210$.
- 2 Nucleus tractus solitarii and nucleus motorius dorsalis n. vagi of normal rat. Transverse section. A very dense plexus of CA terminals is present within the nucleus tractus solitarii (S) and nucleus motorius dorsalis nervi vagi (D) while far fewer terminals are observed within the nucleus hypoglossus (H). The fourth ventricle is present at V $\times 170$.
- 3 Transverse section of an Epon embedded section stained with toluidine blue. Nucleus tractus solitarii (S) nucleus motorius dorsalis nervi vagi (D) and nucleus hypoglossus (H) are observed lying under the fourth ventricle (V) $\times 170$.

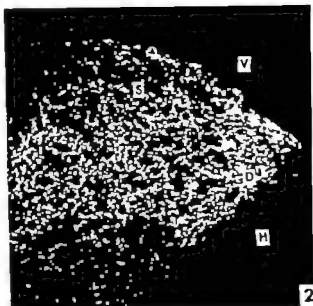
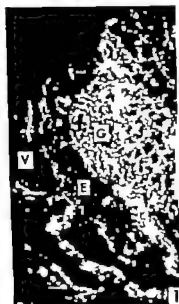


PLATE 2

EXPLANATION OF FIGURES

- 4 Nucleus caudatus putamen of normal rat. A dense plexus of very fine axons, and many boutons containing agranular vesicles. Two large granular vesicles can be seen (→) $\times 36,000$.
- 5 Nucleus caudatus putamen of normal rat. A large number of small boutons (b) about 0.3 to 0.4 μ in size (i.e., around the limit of the resolving power of the fluorescence microscope). $\times 29,000$.
- 6 Nucleus caudatus putamen of normal rat. Many large boutons containing agranular vesicles. Some synapses of type I can be observed () $\times 24,000$.



PLATE 3

EXPLANATION OF FIGURES

- 7 Nucleus tractus solitarius of normal rat. Two large boutons (b) with high content of agranular vesicles. Large granular vesicles (→) can be seen in boutons and in fine axons. $\times 32,000$
- 8 Nucleus tractus solitarius of normal rat. A large dendrite (d) surrounded by five boutons (b) all making synaptic contacts (s) with the dendrite. Medium sized agranular vesicles are found in two of these (→) while the others contain small agranular vesicles. Granular vesicles are present in some boutons and in fine axons (→) $\times 23,000$



PLATE 4

EXPLANATION OF FIGURES

- 9 Substantia grisea paraventricularis of normal rat. Two boutons packed with agranular vesicles of different size ranges. One bouton (b_1) contains vesicles of about 550 to 600 Å in diameter and the other (b_2) vesicles of about 350 Å in diameter. $\times 25,000$.
- 10 Substantia grisea paraventricularis of normal rat. Two boutons (b) with agranular vesicles. One bouton makes synaptic contact of type I () with spine of dendrite. $\times 44,000$.
- 11 Substantia grisea paraventricularis of normal rat. Three boutons each containing granular vesicles of certain sizes: b_1 vesicles of about 550–600 Å, b_2 vesicles of about 450 Å and b_3 of about 350 Å in diameter. b_2 and b_3 make synaptic contacts of type I with the same dendrite (d). $\times 34,000$.



Secretory Epithelium of the Large Axillary Sweat Glands

A CYTOCHEMICAL AND ELECTRON MICROSCOPIC STUDY¹

LUIS BIEAFICA AND LEOPOLDO F. MONTES

*Instituto de Biología y Medicina Experimental, Buenos Aires, Argentina
and Department of Dermatology Baylor University College of Medicine
Houston, Texas*

ABSTRACT The secretory cells of large axillary sweat glands from 12 normal adults were studied at the light and electron microscope levels, using techniques for localization of enzyme reaction product. The morphological and cytochemical characteristics of the plasma membrane and cell organelles (Golgi apparatus, lysosomes, mitochondria, endoplasmic reticulum, secretory granules) were observed. An interpretation of the secretory process was attempted. Most of the evidence spoke against the existence of an apocrine mechanism. Possibly some of the methods employed also could be used for the demonstration of hormone action on the LASG.

The existence of an apocrine mechanism of secretion in the large axillary sweat glands (LASG) of humans has never been conclusively proved. Contrary to early histologic observations (Krompecher '19, Loeschke '25, Kilar '26, Herzenberg '27, Karrenberg, '28, Richter '32) more recent cytologic studies (Minamitani, '41, Montagna, '59, Montes et al. '60) have cast serious doubts regarding its existence. Furthermore electron microscopic reports (Charles '59, Kurosumi et al. '59, Hibbs '62, Yasuda and Ellis; Montagna, '62) seem to indicate that a severe disturbance of the cellular integrity does not take place during the release of the secretion.

Little is known about the formation of secretion granules, their chemical nature or ultimate fate. The precise ultrastructural and cytochemical characteristics of the endoplasmic reticulum, mitochondria, Golgi apparatus and lysosomes are not well established either. Finally the enzymatic activity of the lateral membranes have to our knowledge not been investigated.

In an attempt to further understanding of these problems we have studied several cytochemical aspects of these glands. The main approach has been the electron microscopic localization of sites of enzyme reaction product, employing newer methods of fixation and embedding.

MATERIALS AND METHODS

This study was performed using axillary skin from 12 normal volunteer young adults (9 males and 3 females) ranging in age from 16 to 36 years 11 white and one Negro. Biopsy specimens were obtained surgically removing a 2 x 1 cm piece of whole skin after administering local anesthesia (2% xylocaine without epinephrine).

Cytochemical procedures

One-half of each specimen was fixed overnight at 4 C in cold formal calcium (Baker '46) with addition of 5% sucrose (Holt and Hicks '61). Sections were obtained on a Leitz freezing microtome after removing the epidermis.

For evaluation of plasma membrane and its specialized areas the activity for apparent adenosinetriphosphatase (ATPase) was investigated using the method of

This investigation was supported by research grants from the Upjohn Company from the Consejo Nacional de Investigaciones Científicas y Técnicas (Argentina) and from the American Cancer Society (International Research Grant ACS 14,777).

Present address: Department of Pathology, Albert Einstein College of Medicine, New York 61, N. Y.
Abbreviations: ATP, adenosine-5'-triphosphate; ATPase, adenosinetriphosphatase; AMP, adenosine-5'-monophosphate; APase, acid phosphatase; IDP, inosinediphosphate; TFP, thiaminepyrophosphate; TFPase, thiaminepyrophosphatase; DPNH, reduced diphosphopyridine nucleotide; DPNH, reduced triphosphopyridine nucleotide; NBT, nitroblue tetrazolium; NADPase, ...

Wachstein and Meisel ('57); lysosomes were marked by their acid phosphatase (APase) activity (DeDuve '59 Novikoff '61) using the Gomori medium ('52) the Golgi apparatus was identified by its ability to split nucleosidediphosphatase (Novikoff and Goldfischer '61 Ibid, '61) with inosine-diphosphate (IDP) or thiaminepyrophosphate (TPP) as substrates. For mitochondria sodium succinate, reduced diphosphopyridine nucleotide (DPNH) and reduced triphosphopyridine nucleotide (TPNH) were used as substrates in the tetrazolium procedure (NBT) (Novikoff et al. '61 Nachlas et al. '57).

A. For *light microscopy* 10 μ sections were cut into cold distilled water and incubated at 37° for 10 to 30 minutes for ATPase 5 to 30 minutes for acid phosphatase 10 to 30 minutes for nucleosidediphosphatase 10 to 30 minutes for DPNH—tetrazolium reductase and 20 to 60 minutes for TPNH—tetrazolium reductase. Unfixed 6 μ cryostat sections were used for demonstration of succinic dehydrogenase activity. The incubation time for this enzyme was 30 minutes. After incubation, sections were rinsed in distilled water. The sections incubated in the different media with phosphates were examined after immersing them in dilute yellow ammonium sulfide for 1 to 2 minutes, and then washed. All sections were mounted in Kaiser's glycerogel (Lillie '54). Occasionally cryostat sections were also used for demonstration of oxidative enzyme activity.

B. For *cytochemical studies at the electron microscope level* the skin was fixed in formal calcium overnight or in glutaraldehyde for two hours then washed in cacodylate buffer (Sabatini et al. '63). Sections 25 to 40 μ thick were cut into cold 5% sucrose incubated in the phosphate medium with sucrose in the same concentration at 37° C with shaking of the dishes to avoid precipitation. The optimal incubation time was determined by visualization of the sections in light ammonium sulfide and checking them with the light microscope. Sections incubated in the APase and TPPase media without visualization in the sulfide solution were washed in the sucrose solution, fixed in osmium and processed in the manner described for un-

incubated tissue. When the sections were in absolute ethanol the glands were dissected under the binocular stereomicroscope, cut in small pieces and embedded in Epon.

Control sections were incubated in the same media but without substrates and processed in the same way as above.

Electron microscopy

The other portion of each biopsy was rapidly immersed in cold buffered 1% osmium tetroxide containing 45 mg of sucrose per ml (Caulfield '57). The epidermis was excised the remaining tissue cut in about 2 mm cubes and fixed for two hours at 2–5° C. After a brief rinsing in buffer tissues were dehydrated in graded ethyl alcohols. While in absolute ethanol, the LAGS were dissected under the binocular stereomicroscope and trimmed in tiny pieces. These were transferred to propylene oxide and finally embedded in Epon, according to the method of Luft ('61). An average of nine glands per biopsy was isolated, making the total number of glands available for study more than one hundred.

Sections were cut using glass knives on a Porter Blum microtome and mounted on copper grids covered by a thin layer of collodion. Some specimens were mounted on bars grids. Some sections were studied directly after mounting whereas most were stained afterwards with uranyl acetate and lead hydroxide or lead citrate (Karnovsky '61; Reynolds, '63).

A Siemens Elmiskop I electron microscope with an accelerating voltage of 60 KV was used. Micrographs were taken at original magnifications of 2000 to 35000 diameters and enlarged or reduced as desired.

OBSERVATIONS

Because of different stages in the secretory cycle the appearance of secretory cells of LAGS changes from one cell to another. Within the same tubule a cell may also vary remarkably from its neighboring cell.

Using the binocular stereomicroscope, the dissection and individual isolation of the LAGS becomes an easy task. As pointed out by Hurley and Smiley ('60) they are visualized as small glomerular masses, approximately 1 mm in diameter. They were previously an interesting problem in cell fractionation studies, to our knowledge still to be performed with these glands.

Furthermore the cell appearance differs according to the section angle. This makes the interpretation of each observation difficult (Montes et al. '60). The main features pertaining to the cytoplasmic organelles are summarized in the following paragraphs.

1 The *Cell Membrane* presented many specializations. The luminal surface was linear with scattered microvilli of various sizes and orientations (fig. 12). These had either a single or multiple implantation as observed by Hibbs ('62). Some presented a wide base and appeared to be fading, while others appeared to be in the process of being formed. These latter seemed to be composed of a single membrane and to contain no material within them. This microvilli showed no ATPase activity.

At the lateral or intercellular spaces the arrangement of the membrane was simple. However there were some reinforcements: a terminal bar near the cell surface and one or two desmosomes at the lower half of the cell (fig. 14). As already shown by Montagna ('62) the cell membrane became complex at the bottom of the cell where uniformly arranged folds were seen. These folds were clearly seen between the myoepithelial cells where wide intercellular spaces were formed (figs. 14 and 15). At this level the cell membrane showed peculiar ATPase activity (figs. 1 and 2).

In contrast, the luminal border and the lateral portion did not split ATP (figs. 1 and 2). Thus ATPase activity was present only in the folded specialization of the basal part of the membrane namely in those portions which contact the interne milieu. The much-folded membrane also was able to split other phosphates such as TPP and IDP. AMP was tried once and gave a light stain reaction at pH 7.2 and pH 9.4. The splitting activity increased from nucleosidemonomosphate to nucleosidetriphosphate.

2. The *Golgi Apparatus* was an impressive organelle in this cell. It spread over a very wide area between the nucleus and the lumen. The morphology was quite complex and the most prevalent images were packed smooth membranes forming arrays, saccules or cisternae of different sizes and shapes but with the same circular disposition (fig. 16). There was an abun-

dance of vesicles 0.02 to 0.04 μ in diameter which in favorable sections resembled an irregular crown. In the mesh other organelles were enclosed — ribosomes, secretion granules and mitochondria. The Golgi apparatus stained well when TPP was used as substrate, showing clear supranuclear threads (figs. 3, 4, 5 and 21). In cross sections through the organelle it resembled a delicate network (fig. 4). IDP also was split but the stain reaction was less apparent because it was obscured by the reaction of the endoplasmic reticulum.

3. *Lysosomes* were quite visible with optical microscopy (figs. 6, 7 and 8). With short incubation times they appeared to have a clear peripheral ring of APase activity. They were almost perfectly round and located in the Golgi area and the apical portion of the cell but far from the luminal surface. Occasionally they were seen in the bottom of the cell. In high columnar cells loaded with granules the APase activity was so strong that even with short incubation times all the apical portion of the cell stained intensely black. In medium-sized cells they were clearly distinguishable from the mature secretion granules. In dilated tubules with flat epithelium, the cells had only few lysosomes.

When the APase reaction was examined under the electron microscope the electron dense precipitate was observed in granules close to the Golgi lamella or Golgi vesicles (fig. 20). In favorable sections and incubation times it was mainly at the periphery of the granules (fig. 20). In some granules the reaction was uniform throughout. In larger granules near the apex of the cell, the reaction was absent or very weak, suggesting a decrease in the amount or in the intensity of enzymatic activity (fig. 19).

4. Succinic dehydrogenase DPNH tetrazolium reductase and TPNH tetrazolium reductase activities were also demonstrable in these glands. Dark formazan particles of mitochondrial size and shape were abundant in the basal part of the cells (figs. 9, 10, 11) and absent from the apical zone. Such a distribution for Mitochondria has also been described in several cytologic studies (Minamitani, 41; Montes '60; Montagna, '61). The DPNH tetrazolium reductase activity was particularly strong around the nucleus (figs. 10 and 11).

The electron microscope revealed that rounded or oval mitochondria with a dense matrix and occasional osmophilic dots, were also numerous in the base of the cell (fig. 13). Many of them were close to the folded portion of the basal cell membrane (fig. 15A) thus resembling other tissues with this type of arrangement (Rhodin, '58; Rutberg '61). In the supranuclear region close to the Golgi area mitochondria were more dense with more osmophilic dots, distortion and even disappearance of cristae (figs. 17B, 17C, 18).

5. The *endoplasmic reticulum* was distributed among the mitochondria as rough surfaced membranes (fig. 13). There also was a wide distribution of free ribosomes (fig. 15A) many of them in clusters. They lacked the regular arrangement observed in other tissues (pancreatic acinar cell, thyroid cell, etc.) but were fairly well developed.

6. *Secretion granules* were a prominent finding in these cells (fig. 12A). Scarce and small in the resting cell, they varied in size from 0.5 to 6 μ . Those closer to the Golgi region (fig. 16) were small, heavily osmophilic dots with a minute precipitate at the periphery. These granules were associated with a dense matrix resembling altered mitochondria described in the Golgi area (fig. 17).

Granules closer to the lumen seemed lighter and bigger (fig. 12) having sometimes a light, squared or rectangular area in the center. Some of them seemed to be disintegrating.

7. The *apical cytoplasm* showed two different submicroscopic elements in the zone below the luminal border: (1) many vacuoles of various sizes and shapes and (2) fine electron dense granules (fig. 12B). Similar granular material was often found in the lumen of the glands. Cellular debris, secretion granules or characteristic organelles were never observed in the lumen.

DISCUSSION

The secretory cells of the LAG proved to be good material for cytochemical, electron microscopic and electron histochemical studies. The absence of the secretion granules from both the apical cytoplasm and the lumen supports earlier thoughts (Montes, '60) that they are not the end

product of the secretory process. Our observations provided an opportunity to study the plasma membrane in its basal portion. Its infoldings are in relation to intercellular spaces connecting the cell with the "interne milieu" from which the precursor of the secretion could be obtained. This basal portion but not the lateral and luminal surfaces stains darkly when ATP is used as substrate. This agrees with Novikoff's ('60) findings of the same activity in the distal convoluted and the thick limbs of kidney ultrastructural observations of Rutberg ('61) in the striated duct of the rat parotid gland, and those of Rhodin ('58) in the kidney tubule. Perhaps these deep intrusions of the plasma membrane into the cytoplasm could be directed to increase the absorption surface or to interlock neighbor cells in the manner suggested by Rhodin. Mitochondria, abundant in the basal part of the cell (Montes, '60) may provide a system of high oxidative rate, apt for transport of water and cations (Rutberg, '61; Novikoff '60; Rouiller '60; Taggart, '58). The special feature of intramitochondrial dense granules seems to support this idea (Rouiller '60). We were unable to detect a significant number of small vesicles in the basal cytoplasm, as pointed out by Kurosomi ('59). The few we observed seemed to represent cross sections of the invaginated infoldings.

The mitochondrial localization was similar to that described in cytologic studies (Minamitani, 41; Montes et al. '60; Montagna '62) and the characteristics of the organelle to those reported in previous electron microscopic studies (Charles, '59; Kurosomi et al. '59; Hibbs '62).

Our observations do not agree with previous reports (Kurosomi, '59; Hibbs '62) on the scarcity of the ergastoplasm in LAG. A system of rough surfaced membranes exists mainly around the mitochondria in different parts of the cell (fig. 13). Also free ribosomes are present particularly at the base (fig. 15A). These rough surfaced membranes lack the peculiar pattern observed in other tissues such as the exocrine pancreas but they must relate to the cytoplasmic basophilia observed prom-

The "secretion" granules have been described histochemically as PAS-positive — diastase-resistant bodies containing β -proteoglycan and 1,3-glycol groups.

nently in light microscopy of LASG (Montes et al., '60). The ability of this ergastoplasm to split nucleosidediphosphates, observed in many types of cells (Essner and Novikoff '62) speaks in favor of its participation in the early stages of synthesis of the secretory materials on their way to the Golgi area. This function of the endoplasmic reticulum in the LASG had been suggested by Montes et al. ('60) following earlier thoughts of Minamitani ('41) and Montagna ('62).

The role of the Golgi apparatus is now better understood. New methods coupling autoradiography and electron microscopy (Caro, '61; Caro and Palade '61) have shown in the acinar pancreas, a concentration of elaborated product in the vacuoles of the Golgi apparatus and further detection in the mature granules. Biochemical assays agree with such sequences (Sleke vitz and Palade, '58a, '58b '59 '60). The process seems similar in many types of cells ranging from protein secretory (Palay '58) to neurosecretory products (Scharrer and Brown, '61) and would also apply to the LASG. Many vacuoles were observed in the Golgi area and this was the same zone where the light microscopy showed accumulation of lysosomes. Cytochemical methods at the electron microscope level revealed a close relation between the Golgi lamellae stained with the TPP reaction and the lysosomes with the acid phosphatase (fig. 20).

It is interesting that the identity of PAS positive granules, a prominent feature of the LASG (Montes et al. '60; Montagna, '62; Goltz et al., '58) and lysosomes has been demonstrated with the electron microscope in the Kupffer cells (Novikoff, '61). Lipofuscin granules have acid phosphatase activity and therefore a derivation from lysosomal material was suspected (Essner and Novikoff '60). Furthermore the auto-fluorescence of lysosomes in different cells recently has been demonstrated (Koenig '63). This is interesting in relation to the classic demonstration by Hurley and Shelley ('60) of lipofuscin and fluorescence in some of the granules in the LASG.

The fact that many granules seemed to be altered mitochondria would agree with recent reports which described mitochon-

drial transformation into granules (Bernhard et al., '55; Wallace '60; Novikoff '61).

The difference in staining reaction for APase from one cell to another could mean that every cell is in a different secretory state, and therefore the synthesis of the secretion is to some extent independent among them. When the APase activity was checked under the electron microscope the large granules stained weaker than the small ones whose lead precipitate was more dense. In fact, some regions of the large granules remained unstained. This could be explained by a decrease in the total amount of the enzyme or a relative diminution produced by the granule enlargement due to its increased water content.

An interpretation for the large size of many granules is lacking at the present time. The observation of fine granular material throughout the apical cytoplasm would indicate that granules may dissolve as has been suggested by others (Montes, et al., '60; Montagna, '62) (fig. 12B). Furthermore we failed to observe any secretory granules or cellular debris in the lumen of the glands, which confirms Hibbs ('62) and Charles ('59) observations. A disruption of the apical membrane (Charles, '59) was never seen. If this is true the passage of material into the lumen must be accomplished by some other mechanism. The absence of granules in the apical portion speaks against the extrusion of them by an apocrine process. The "apocrine secretory processes in the sense pointed out by Kurosumi et al ('59) were never detected either. The abundance of large vacuoles arranged beneath the luminal surface may have significance in the exit of the secretion. The material which has passed through the apical cytoplasm following disintegration of the large granules could conceivably be enclosed in smooth membranes and transported to the luminal surface. The possibility of a coalescence of these membranes with the apical cell membrane was suggested by many of our high magnification electron micrographs. It seems possible that a further breakdown of the cell membrane would occur for the extrusion of the material, following which a reconstitution of the membrane could take place.

Our observations lead us to suggest the following hypothesis (fig. 22) to explain the sequence of mechanisms in the production of the secretion.

(1) The absorbed material, mainly ions and water passes through the numerous infoldings of the basal cell membrane rich in nucleosidetriphosphate splitting activity.

(2) Mitochondria, present in large numbers in the basal portion of the cell, supply important oxidative enzymes necessary for the early synthesis of the secretion.

(3) This is accomplished by a clearly developed ergastoplasm (endoplasmic reticulum).

(4) A further elaboration takes place in the Golgi apparatus where the preformed secretion is enclosed in smooth surfaced membranes containing high TPPase levels and possibly other hydrolytic enzymes.

(5) The lysosomes or immature granules located in the Golgi area gain size and electron microscopic density by incorporation of other substances.

(6) Mitochondrial changes suggest the possibility that some of the granules arise from mitochondria.

(7) The lysosomal enzymatic pool carries out its digestive process upon the incorporated materials, as granules become bigger and denser.

(8) Mature granules decrease their density lose the APase activity and finally break up spreading their content on the apical cytoplasm. Dense small droplets and dark particles are visible in that region.

The next step although not detected by us, was suggested by the presence of vacuoles beneath the luminal surfaces. A mechanism of exocytosis the reverse directional process of pinocytosis (Moore and Ruska '57) could likely carry the material into the lumen. If this latter point is definitely proved it will mean that these glands are not really apocrine.

Another question to be clarified is the nature of the small dark particles in the apical zone. Histochemical (Montagna, '62) and electron microscopic studies (Hibbs '62, Montagna, '62) have emphasized the presence of iron in the glands. In addition ferric iron has been detected by Hurley and Shelley performing chemical

tests of the apocrine sweat ('60). One electron micrograph by Montagna ('62) suggests that the large mature granules may contain ferritin. We think that perhaps the iron could be provided by mitochondrial transformation since this organelle possesses iron in its enzymatic system.

An interesting application of some of these methods will be their use for the study of possible hormone action on the LASG. The existence of an endocrine control of the secretion has been considered for many years (Hurley and Shelley '60) but never proved (Shelley and Cahn, '55). Steroid hormones are potent inhibitors of enzymes involved in the oxidation of DPNH (Hayano et al. '60 Yelding and Tomkins '59). Corticosterone inhibits oxidation of DPNH and cortisol acts similarly but is less potent (Jensen, '59). Cortisol seems to increase the permeability of the mitochondrial membrane which results in leaching of DPN from mitochondria (Gallagher '58). It seems possible that similar changes could be demonstrated in the LASG following steroid therapy. It is also interesting to mention thoughts (DeDure, '59 Novikoff '61) that lysosomes could be target organelles for hormones, and to point out that steroids may modify lysosomal stability (Weissmann and Thomas, '62). It will be interesting to look for lysosomes changes induced by hormones in the LASG also.

ACKNOWLEDGMENTS

We are indebted to Drs. A. C. Curtis and B. A. Houssay for their interest in this project, and to Drs. B. L. Baker, R. G. Freeman, J. M. Knox, R. A. Liebelt and A. B. Novikoff for critical reading of the manuscript. Also we wish to thank Dr. A. B. Novikoff for provision of many substrates we used.

The technical assistance of Miss Amalia Casco and Miss Susana Camocardi, and the valuable cooperation of Mr. Luis Millara in the preparation of the photographs are acknowledged.

Parts of this theory have already been elaborated by other investigators (Montagna, '61 Montes, '62, Hibbs, '62, Montagna, '62).

LITERATURE CITED

- Baker J. R. 1946 The histochemical recognition of Hyaline. *Quart. J. Microsc. Sci.*, 87 441.
- Bernhard, W. F. Hagopian and R. Lepus 1955 Coupes ultrafines d'éléments sanguins et de ganglions lymphatiques étudiés au microscope électronique. *Rev. Hematol.*, 10 287.
- Caro, L. G. 1961 Electron microscopic radioautography of thin sections: The Golgi zone as site of protein concentration in pancreatic acinar cells. *J. Biophys. Biochem. Cytol.*, 10 37.
- Caro, L. G., and C. E. Palade 1961 Le rôle de l'appareil de Golgi dans le processus sécrétoire. *Etude autoradiographique*. C. R. Soc. Biol. (Paris) 155 1750.
- Caulfield, J. B. 1957 Effects of varying the vehicle for OsO₄ in tissue fixation. *J. Biophys. Biochem. Cytol.*, 3: 827.
- Charles A. 1959 An electron microscopic study of the human axillary apocrine gland. *J. Anat.*, 93 225.
- DeDova, C. 1956 Lysosomes, new group of cytoplasmic particles. In *Subcellular Particles*, T. H. yashi, ed. Ronald Press, New York, pp. 123-159.
- Easner E., and A. B. Novikoff 1960 Human hepatocellular pigments and lysosomes. *J. Ultrastruct. Res.*, 3 374.
- 1963 Cytological studies on two functional hepatomas. Interrelations of endoplasmic reticulum, Golgi apparatus and lysosomes. *J. Cell Biol.*, 15 289.
- Gallagher C. H. 1958 Effect of hydrocortisone on mitochondrial membrane permeability. *N. turn*, 152: 1315.
- Goltz, R. W. R. M. Fusaro and J. Jarvis 1958 The demonstration of acid substances in normal skin by alcian blue. *J. Invest. Dermat.*, 31 183.
- Gomori, G. 1952 *Microscopic Histochemistry: Principles and Practice*. University of Chicago Press, Chicago, p. 272.
- H. yano, M., R. I. Drefman and E. Y. Yamada 1950 The inhibition of d-amino oxidase by desoxycorticosterone. *J. Biol. Chem.*, 186 603.
- Herzenberg, H. 1927 Neue beiträge zur lehre von den apokrinen schweißdrüsen. *Virch. Arch. f. path. Anat. u. Physiol.*, 206 422.
- Hibbs, R. G. 1962 Electron microscopy of human apocrine sweat glands. *J. Invest. Dermat.*, 38 77.
- Holt, S. J. and R. M. Hicks 1961 Studies on formalin fixation for electron microscopy and cytochemical staining purposes. *J. Biophys. Biochem. Cytol.* 11 47.
- Hurley H. J. and W. B. Shalley 1960 The Human Apocrine Sweat Gland in Health and Disease. Charles C. Thomas, Springfield, Ill.
- Jensen, P. K. 1956 Corticosterone inhibition of pyridine nucleotide oxidase from heart sarcomeres. *N. turn* 184 (Suppl. 7) 451.
- Karnovsky M. J. 1961 Simple methods for staining with lead t high pH in electron microscopy. *J. Cell Biol.*, 11 79.
- Karzenberg, C. L. 1928 Histologische untersuchungen vom schweißhauthaut bei beiden geschlechtern und in verschiedenen lebensaltes. *Dermat. Wchnschr.* 87 1273.
- Klaar J. 1926 Zur kenntnis des weiblichen axillargangens beim menschen. *Wien. klin. Wchnschr.* 39 127.
- Koenig, H. 1963 The autofluorescence of lysosomes. *J. Histochem. and Cytochem.*, 11 555.
- Krompacher E. 1919 Zur kenntnis der geschwülste und hypertrophien der schweißdrüsen. *Arch. Dermat. & Syph.*, 126 755.
- Kurosaki, K., T. Kitamura and T. Tjima 1959 Electron microscopic studies on the human axillary apocrine sweat glands. *Arch. Histo. J. p.*, 16 533-560.
- Lillie R. D. 1954 *Histopathologic Technique and Practical Histochemistry* 2nd ed., McGraw-Hill Book Co., New York.
- Loeschcke H. 1925 Über zyklische vorgänge in den drüsen des schweißhählenorgans und ihre abhängigkeit vom sexualzyklus des weibes. *Virchows. Arch. f. path. Anat.*, 235 253.
- Luft, J. M. 1961 Improvements in epoxy resin embedding methods. *J. Biophys. Biochem. Cytol.* 9 406.
- Minamitani, K. 1941 Zytologische und histologische untersuchungen der schweißdrüsen in menschlicher schweißhaut. *Okaj. Folia Anat. Jap.* 21 81.
- Montagna, W. 1950 *Histology and cytochemistry of human skin. XIX. The development and fate of the axillary organ.* *J. Invest. Dermat.*, 33 151.
- 1962 *Structure and function of the skin. Chapter 7. The Apocrine Sweat Glands*, 2nd ed., Academic Press.
- Montes, L. F. B. L. Baker and A. C. Curtis 1960 The cytology of the large axillary sweat glands in man. *J. Invest. Dermat.*, 35 273-291.
- Moore D. H., and H. Ruska 1957 The fine structure of capillaries and small arteries. *J. Biophys. Biochem. Cytol.*, 3 457.
- Nachlas, M. M., K. C. Tsou, E. DeGuzza, C. B. Cheng and A. M. Seligman 1957 Cytochemical demonstration of succinic dehydrogenase by the use of new p-nitrophenyl substituted ditrazoles. *J. Histochem. Cytochem.*, 5 420.
- Novikoff, A. B. 1960 The rat kidney cytochemical and electron microscopic studies. In *Biology of Pyelonephritis*, E. Qutran and E. Kass, eds. Little, Brown and Co., Boston, pp. 113-144.
- 1961 Mitochondria (Chondriosomes). In *The Cell*, Vol. II, J. Brachet and A. E. Mirsky eds., Academic Press, New York, p. 330.
- 1961 Lysosomes and Related Particles. In *The Cell*, Vol. II, J. Brachet and A. E. Mirsky eds., Academic Press, New York, pp. 423-488.
- Novikoff A. B., and A. Goldfischer 1961 Nucleosidediphosphatase activity in the Golgi apparatus. *Proceed. Vth Intl. Congress Biochemistry Moscow* p. 184 Pergamon Press, Ltd., Oxford.
- 1961 Nucleosidediphosphatase activity of the Golgi apparatus and its usefulness for cytological studies. *Proc. Natl. Acad. Sci.*, 47 802.
- Novikoff A. B., E. Easner S. Goldfischer and M. Hens 1962 Nucleosidediphosphatase activities of cytoplasmic membranes. *Symp. Intl. Soc. Cell Biol.*, 1 149.

- Novikoff, A. B., W. Y. Shin and J. Drucker 1961 Mitochondrial localization of oxidative enzymes: staining results with two tetrazolium salts. *J. Biophys. Biochem. Cytol.*, 9: 47.
- Novikoff, A. B., J. Drucker, W. Y. Shin and S. Goldfischer 1961 Further studies of the apparent adenosinetriphosphatase activity of cell membranes in formal-calcium fixed tissues. *J. Histochem. Cytochem.*, 9: 434.
- Palay S. L. 1955 The morphology of secretion. In *Frontiers in Cytology* S. L. Palay ed., Yale University Press, New Haven.
- Reynolds, E. S. 1963 The use of lead citrate at high pH as an electron-opaque stain in electron microscopy. *J. Cell Biol.*, 17: 208.
- Rhodin, J. 1958 Anatomy of kidney tubules. *Int'l. Rev. Cytol.*, 7: 483.
- Richter, W. 1933 Beiträge zur normalen und pathologischen anatomie der pfortnen hautdrüsen des menschen mit besonderer berücksichtigung des schalenhohlorgane. *Virchows. Arch. f. path. Anat.*, 287: 277.
- Rouffier C. 1960 Physiological and pathological changes in mitochondrial morphology. *Int'l. Rev. Cytol.*, 9: 227.
- Rutberg, U. 1961 Ultrastructure and secretory mechanism of the parotid gland. *Acta Odont. Scand.*, 19 Suppl. 30.
- Sabathin, D. D. K. Benesh and R. J. Barnett 1963 Cytochemistry and electron microscopy. The preservation of cellular ultrastructure and enzymatic activity by aldehyde fixation. *J. Cell Biol.*, 17: 19.
- Scharrer, E., and S. Brown 1961 Neurosecretion. XII. The formation of neurosecretory granules in the earthworm, *Lumbricus terrestris*. *Z. Zellforsch.*, 54: 830.
- Ivey W. B. and M. M. Cahn 1955 Experimental studies on the effect of hormones on the human skin with reference to the axillary apocrine sweat gland. *J. Invest. Dermat.*, 25: 187.
- Slavovitz, P., and G. E. Palade 1958a A cytochemical study on the pancreas of the guinea pig. II. Functional variations in the enzymatic activity of microsomes. *J. Biophys. Biochem. Cytol.*, 4: 309.
- 1958b A cytochemical study on the pancreas of the guinea pig. III. In vivo incorporation of leucine-1- C^{14} into the proteins of cell fractions. *J. Biophys. Biochem. Cytol.*, 4: 337.
- 1959 A cytochemical study on the pancreas of the guinea pig. V. In vivo incorporation of leucine-1- C^{14} into the chymotrypsinogen of various cell fractions. *J. Biophys. Biochem. Cytol.*, 7: 619.
- Taggart, J. V. 1958 Mechanisms of renal tubular transport. *Am. J. Med.*, 24: 774.
- Wachstein, M., and E. Meisel 1957 Histochemistry of hepatic phosphatases: a physiological pH with special reference to the demonstration of bile canaliculi. *Am. J. Clin. Path.*, 17: 13.
- Walker, D. W., and A. M. Salzman 1961 Formalin fixation in the cytochemical demonstration of succinic dehydrogenase of mitochondria. *J. Biophys. Biochem. Cytol.*, 9: 415.
- Wallace, B. J. 1960 The relation of mitochondrial morphology to succinoxidase activity as observed in the rat kidney after protein injection. *J. Histochem. and Cytochem.*, 80: 105.
- Weisman, G., and L. J. Thomas 1963 Stains on lysosomes. *Exp. Med.*, 116: 443-450.
- Yasuda, K., and R. A. Ellis 1963 Electron microscopy of human apocrine sweat glands. Personal communication to W. Montagna.
- Yielding, K. L., and C. M. Tomkins 1959 Inhibition of the enzymic oxidation of DPNH by steroid hormones. *Proc. N. t. Acad. Sci.*, 45: 1730.

PLATE 1

EXPLANATION OF FIGURES

Figures 1 to 11 are light micrographs; figures 12 to 21 electron micrographs.

- 1 Human LAG tubule incubated in ATP medium at pH 7.2 for 15 minutes at 37°C. Arrows indicate the basal portion of the plasma membrane which stains strongly. The luminal border and the lateral part of the cell membrane show no activity. $\times 400$.
- 2 Same section as in figure 1. Enlarged view to show the infoldings of the basal portion of the plasma membrane encircling the myoepithelial cells. $\times 1,600$.

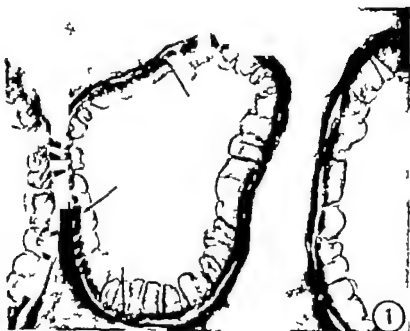
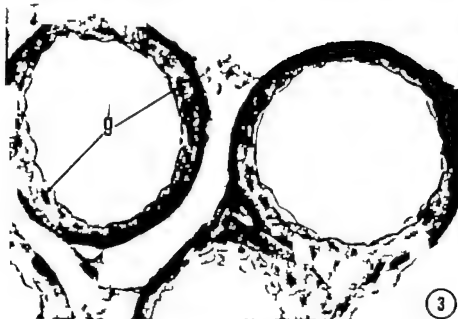


PLATE 2

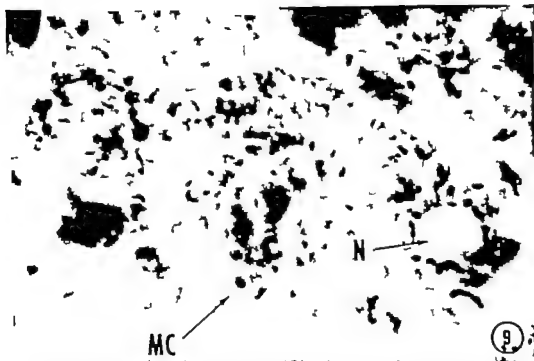
EXPLANATION OF FIGURES

- 3 LASC tubules incubated in TPP medium at pH 7.2 for 30 minutes at 37°C. Some cells with staining of the Golgi apparatus (g) are shown. $\times 400$.
- 4 Same section as in figure 3. A cross section of various cells illustrating the network of the Golgi apparatus (arrows) $\times 1,600$.
- 5 Same section as in figures 3 and 4. A longitudinal section showing the picture of the Golgi apparatus (arrows) $\times 1,600$.





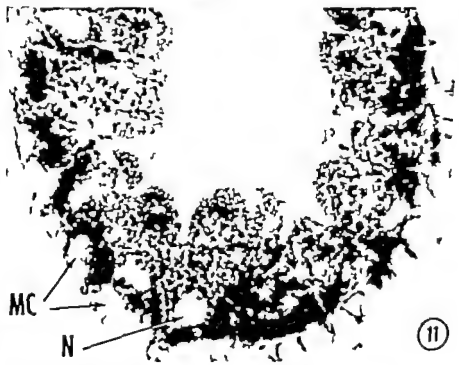
- 6 LASC tubule incubated in APase medium at pH 5.2 for 15 minutes at 37°C. Lysosomal population varies from one cell to another. In some cells the strong reaction obscures the details, in others lysosomes (1) are clearly visible as individual dots. Lysosomes are concentrated in the supranuclear region. The cells have no lysosomes in the apical portion beneath the brush border. $\times 400$.
- 7 Same section as in figure 6. Lysosomes are accumulated in the supranuclear zone. The stain is so strong in some cells that individuality of lysosomes is lost. $\times 1,600$.
- 8 Same section as in figures 6 and 7. Lysosomes appear as individual dots in their usual supranuclear location of the Golgi area. $\times 1,600$.



- 9 Succinic dehydrogenase activity in LAGL. N trofoemazan particles having the size and shape of mitochondria are shown. Many of them are concentrated around the nucleus (N). The cytoplasmic ground substance is weakly stained. Myoepithelial cells (MC) are practically un stained (cryostat section) $\times 2,400$.

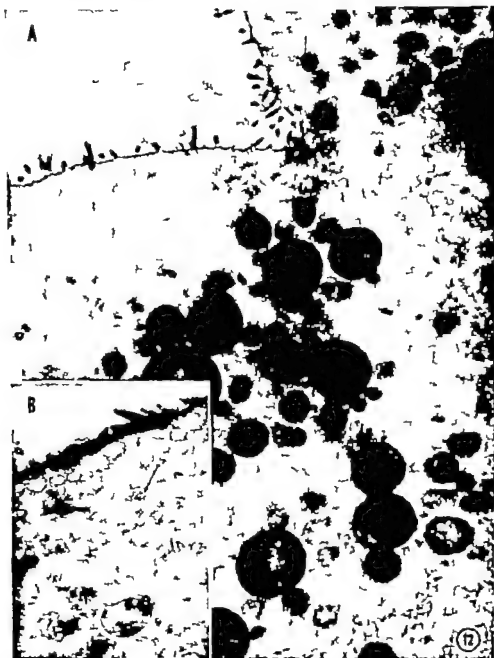


10

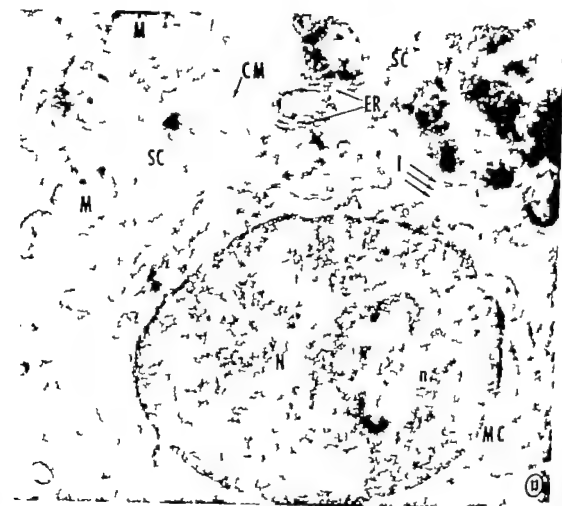


11

- 10 LAG tubules incubated in the DPNH-NBT medium for ten minutes at 37°C. The stain predominates around the nucleus $\times 400$.
- 11 Same procedure as in figure 10. Enzymatic activity is concentrated in the basal and perinuclear regions of the cells. There is no reaction in the nucleus (N). Myoepithelial cells (MC) show very little activity (cryostat section) $\times 1,600$.



- 12 A Luminal portion of two adjacent secretory cells with free linear surface showing irregular microvilli. There are no granules beneath the free border. Granules show different electron densities. $\times 12,500$.
 B Free border of secretory cell showing microvilli and many vacuoles. Arrow points to cluster of minute dense particles quite abundant in the peral portion $\times 19,000$.



13 Basal portion of two secretory cells (SC) and their lateral membrane (CM) with undulations and infoldings (I). The secretory cells show many rounded mitochondria (N) with dense cores. The endoplasmic reticulum (ER) appears around mitochondria. A myoepithelial cell (MC) with large nucleus (N) and ucleol (n) also seen $\times 42,000$.

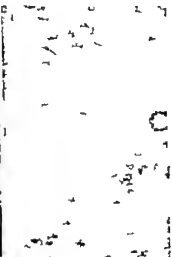


- 14 Two myoepithelial cells (MC) and the lower portion of secretory cell (SC) with differentiation of its plasma membrane desmosome (D) and infoldings (I) which contact the large intercellular spaces (IS). The basement membrane with arrays of collagen fibrils (F) is also seen. $\times 27,000$.

PLATE 9

EXPLANATION OF FIGURE

- 15 A Basal part of two adjacent secretory cells showing mitochondria (m) ribosomes () the complex system of plasma membrane with many infoldings and the large intercellular spaces (IS) $\times 20,000$.
B Detail of the infoldings of the basal portion of the plasma membrane $\times 140,000$.





16 Demonstration of the Golgi apparatus of secretory cell showing smooth membranes (m) and vesicles () of different sizes. In the mesh of the Golgi apparatus dense mitochondria (M) is seen. Outside the Golgi area there are many granules with variable electron densities. $\times 33,500$



- 17 A Granules with dense rounded dots of different sizes and myelinic figures (mf) $\times 80,000$.
 B Altered mitochondria (1) among normal ones (2) showing increased density on the cristae and peripheral deposits. $\times 40,000$.
 C Other image suggesting mitochondrial transformation. Persistence of the double membrane (arrow) in granule with round dots of different size and electron density $\times 40,000$.



- 12 Many mitochondria (M) with clear cristae. There are many granules (G) (immature?) of different density crowded by dense round dots. Some are about the same size and shape as mitochondria. The arrows point to deposits in membranes which resemble the mitochondrial double membrane. The deposits seem to start in the internal mitochondrial membrane. Golgi apparatus (g) $\times 53,000$.



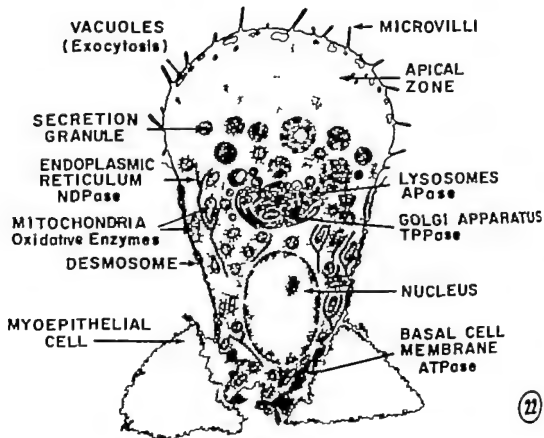
19 Section incubated in APase medium for five minutes at 37°C and processed afterwards for electron microscopy. Granules with different degree of precipitation are seen. The reaction is weaker in the large granule (G) $\times 37,000$

PLATE 14

EXPLANATION OF FIGURES

- 20 Section processed in the same way as in figure 19. Several lysosomes (L) observed in the Golgi region are shown. The precipitate is mainly at the periphery of lysosomes. $\times 51,000$.
- 21 Section incubated in TPP medium for 15 minutes at 37°C. The TPPase activity is concentrated in the Golgi apparatus (g) $\times 25,500$.





22 Diagram illustrating submicroscopic features in secretory cell of large axillary sweat gland

Mitosis and Differentiation in the Stratified Squamous Epithelium of the Rat Esophagus

J. P. MARQUES-PEREIRA AND C. P. LEBLOND

Department of Anatomy McGill University Montreal, Canada

ABSTRACT The fate of the cells of the stratified squamous epithelium of the esophagus was investigated radioautographically in young adult rats \pm various time intervals after single injection of thymidine- H^3 .

Soon after injection, labeled cells appeared in the basal layer of the epithelium (stratum basale). During the following 12 hours the labeled cells completed DNA synthesis and mitosis, and mostly remained in the basal layer. After 12 hours, however the labeled cells arising from the mitoses were transferred to the spinous layer (stratum spinosum) \pm the rate of 1.2% per hour.

The respective fates of the two daughter cells of mitosis were then examined using two-dimensional maps showing the location of the labeled nuclei at 24 and 48 hours after injection. It was assumed that any two nuclei located side by side and overlaid by similar number of grains are the two daughter cells of mitosis. Such pairs of labeled daughter cells fell into three categories: (1) Basal pairs composed of two basal cells; (2) Outgoing pairs, composed of two spinous (or granular) cells; and (3) Mixed pairs composed of one basal and one spinous (or granular) cell. Since three possibilities were encountered \pm the two time intervals, the mitoses could not be differential (in which case the pairs of daughter cells would consist of cell remaining in the basal layer and another migrating to the spinous layer; that is, all pairs would be "mixed"). Instead, the frequency of the three types of pairs was such as to indicate that the transfer of basal cell to the spinous layer is chance event which can affect any basal cell (except those undergoing DNA synthesis or mitosis). Accordingly the transfer of either or both daughter cells of mitosis would also be due to chance.

The transfer of cell out of the basal layer is critical step in the life of the cell, since it precludes further division and appears to trigger differentiation.

The cells of stratified squamous epithelia are renewed continuously as the production of new cells in the deeper layers of these epithelia is balanced by the loss of cells from the surface (Leblond and Walker '56).

A popular explanation for this renewal is based on the postulate that mitotic divisions of epithelial cells are differential, that is yield two different daughter cells one which remains in the deeper layers to divide again and another which migrates towards the surface to differentiate and eventually be sloughed off (Cowdry '50; Rolshoven, '51; Mercor '62). Since each dividing cell would have one daughter cell capable of division the number of mitotable cells would remain constant even though differentiated cells are being produced and lost. A steady state of the renewing cells would thus normally result from differential mitoses.

Unfortunately there is no evidence for the existence of differential mitoses in re-

newal systems. In fact, it has been shown that spermatogonial mitoses are not differential in the testis of monkeys (Clermont and Leblond, '59) and rats (Clermont, '62). Preliminary work on the epithelium of the rat esophagus failed to detect such mitoses either (Leblond, Greulich and Pereira '64). The present work was undertaken not only to confirm this conclusion but also to seek for evidence that the two daughter cells arising from each epithelial mitosis of the esophagus have equal potentialities or in other words that the mitoses are equivalent.

In a preliminary experiment, rats were sacrificed at various time intervals after injection of thymidine- H^3 and sections of the esophagus were radioautographed. The preparations made at the early time intervals were used to find out which cells of

Present address: Departamento de Histologia Embriologica, Faculdade de Medicina de Porto Alegre, Universidade de Rio Grande do Sul, Brasil. Dr. Pereira was the recipient of Rockefeller F. Research Fellowship. Differential mitoses have also been named asymmetric unequal and bivalent.

the epithellum synthesize DNA and under go mitosis. The preparations obtained at later times served to gain some idea of the fate of the cells arising from those mitoses. In another experiment the two daughter cells arising from a mitosis were traced in detail in animals sacrificed 24 and 48 hours respectively after thymidine- H^3 injection. The method used was based on the observation that when a thymidine H^3 labeled cell divides the daughter cells are also labeled and each one contains half or very nearly half the radioactivity of the mother cell (Taylor et al. '57). Hence in radioautographs the two daughter cells of a mitosis should be overlaid by approximately the same number of silver grains. The actual work consisted of mapping the labeled cells of the esophageal epithellum. Any two juxtaposed cells showing the same number of silver grains were taken to arise from the same mitosis. It was then possible to determine whether or not these two daughter cells had the different fates postulated by the differential mitosis hypothesis.

MATERIALS AND METHODS

Preliminary experiment

Twenty four young adult male Sherman bino rats with a body weight of about 100 g received a subcutaneous injection of $1\mu\text{C}$ of thymidine H^3 (360 mc/mM) per g body weight at some time between 9:00 A.M. and 11:00 A.M. The animals were then sacrificed at 20 and 30 minutes, 1 2 3 6 12 24 48 and 72 hours after thymidine- H^3 injection. Each time group included two animals except the six-hour one which had four and the 20-minute group which had one animal only.

The esophagus was fixed in Boulin and embedded in paraffin. Transverse sections were cut at 3 μ , stained with hematoxylin-eosin and covered with NTB2 emulsion according to the coating technique of radioautography described by Kopriwa and Leblond ('62). Exposure time was 30 days.

The number of labeled cells in the basal and other layers of the esophageal epithellum was counted in several cross sections of esophagus up to a total of 400-500 labeled cells per animal. After correction by Abercrombie's method ('46) the results were expressed as number of labeled cells

per cross section and as per cent of labeled cells out of the basal layer (table 1)

Mapping experiment

It was assumed that the two daughter nuclei arising from a labeled mitosis would not only be equally labeled (Taylor et al. '57) but would also be located side by side, with no other nucleus in-between. Obviously the selection of such nuclei could only be done in serial sections. It was therefore decided to prepare serially cut radioautographs and work out two-dimensional maps of the labeled nuclei.

Serial cross sections were cut of the esophagus of two 200-g rats which, in an experiment of Messier and Leblond ('60) had been sacrificed at 24 and 48 hours respectively after thymidine- H^3 injection. Thirty serial radioautographs were prepared for each animal.

The mapping technique was similar to that used by Clermont and Leblond ('59) to identify and pair spermatogonia arising from the same mitosis and is shown diagrammatically in figure 1. The portion of the esophageal epithellum selected for mapping is depicted as a cylinder cut open and the serial sections as successive strips drawn on the wall. (The height of each strip corresponds to the thickness of the histological section.) It may be imagined that for mapping the strips are applied to a flat surface as done in the upper part of the diagram. The labeled nuclei located in the basal layer are transferred with the strips onto the flat surface (fig. 1 solid line circles). As for the labeled nuclei present in the spinous and granular layers, they are drawn in as if projected on the basal layer (broken line circles).

For the actual work of mapping each serial section of the region selected was photographed at 500 \times . Silver grains were then counted over all the labeled nuclei visible in the serial sections and each count was written in on the photographic picture of the corresponding nucleus.

A preliminary map was then drawn on tracing paper. First each serial section was depicted as a row (referred to by a number as shown in fig. 2 top left). Next, a landmark parallel to the long axis of the esophagus (e.g. a blood vessel) was selected in the sections and drawn in on the

TABLE 1

Distribution of labeled cells in the Malpighian layer of the esophageal epithelium
(Corrected by Abercrombie's method)

Time after thymidine- H^3 injection	Mean number of labeled cells per cross section			Average % of labeled cells out of the basal layer	Presence of labeled metaphases
	Total	Basal layer	Spinous and granular layers		
Hours					
0.3	25	25	0.0	0.0	—
0.6	40	40	0.1	0.2	—
	28	28	0.1		
1	54	54	0.0	0.3	—
	35	35	0.3		
2	70	70	0.0	0.0	+
	47	47	0.0		
3	61	61	0.3	0.5	+
	83	82	0.5		
6	88	83	1.4	1.9	+
	84	83	1.1		
	80	78	1.5		
	100	97	2.7		
12	99	97	2.1	3.0	—
	103	99	3.9		
24	60	67	13.0	18.5	—
	83	65	17.0		
48	75	44	31.0	43.2	+
	113	59	54.0		
72	120	67	53.0	41.5	+
	114	69	45.0		

map as a vertical line crossing the rows. Then, the photograph of the first section was placed on a horizontal x-ray viewing box and the tracing paper was superimposed in such a way that the vertical line coincided with the landmark. The paper was then shifted repeatedly so as to make the line above the first row follow the basement membrane as faithfully as possible. Hence when a labeled nucleus was encountered in the photograph it could be drawn on the tracing paper at the exact distance from the landmark. In the same manner the labeled nuclei on each photograph were transferred to the corresponding row on the paper.

In the 3- μ serial sections used, portions of the same nucleus could be found in two three or even four consecutive sections. Therefore the successive portions of each labeled nucleus appeared next to one another in the map. They were then

drawn together as a single nucleus in which the grain counts of each portion were recorded (fig. 2, top). These counts were added and the total number of silver grains per nucleus, recorded on a simplified version of the map (fig. 2, base). Incidentally the map was also divided into a series of columns which were referred to by letters (fig. 2 top line) so that a given cell could be identified by two coordinates.

With the help of the maps, it was found possible to arrange the cells into pairs (referred to as presumed pairs) which are characterized by close proximity and by a similar number of overlying silver grains. Close proximity implied that the two members of a presumed pair were in physical contact at some point and no cells were found between them. This rule was rigidly observed in the 24-hour

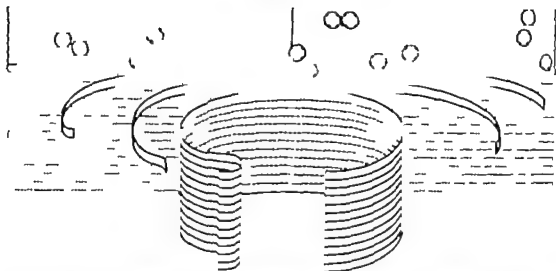


Fig 1 The lower portion of the diagram represents the esophagus cut open. The lines drawn on the wall depict the serial sections as a series of consecutive strips. (The width of the strips is related to the thickness of the sections in proportion to the magnification used.)

It may be imagined that each strip is cut open and spilled on a flat surface as shown at the top of the diagram. The map thus obtained represents the esophageal epithelium viewed from the lumen. Labeled nuclei are transferred to the flat surface with the portion of the strip in which they are located. The labeled nuclei of the basal layer are drawn as solid line circles and those from the other layers as broken line circles.

Care is taken to keep each labeled nucleus at an exact distance from a landmark in each section. The landmark is depicted in the diagram by the vertical solid line in the center.

TABLE 3
Frequency of P values of the difference between the grain counts of the two cells of presumed pairs

	10	$0.99 > P > 0.70$	$0.09 > P > 0.40$	$0.39 > P > 0.10$
24-hour map				
Basal pairs	10	37	22	19
Mixed pairs	3	13	8	9
Outgoing pairs	1	4	0	2
48-hour map				
Basal pairs	1	4	5	1
Mixed pairs	5	3	4	4
Outgoing pairs	2	2	6	2

map (although this is not apparent for all pairs in fig 7). In the 48-hour map (fig 8) basal cells were again paired only if in contact at some point but there was not always contact between two paired spinous cells nor between presumed pairs composed of a basal and a spinous cell. The difficulty was that spinous cells enlarged and their limits were often indistinct. In these cases, a fairly close proximity rather than contact was used as a criterion in selecting presumed pairs.

When the two members of a presumed pair did not show the same grain count, statistical analysis was used to test whether the difference could be accounted for by random variation. It was assumed that the sum of the grain counts found over the two nuclei of a presumed pair is close to the theoretical grain count over the mother cell. The Chi-square test was then applied to compare this theoretical value with the observed grain counts of the two individual cells (table 2).

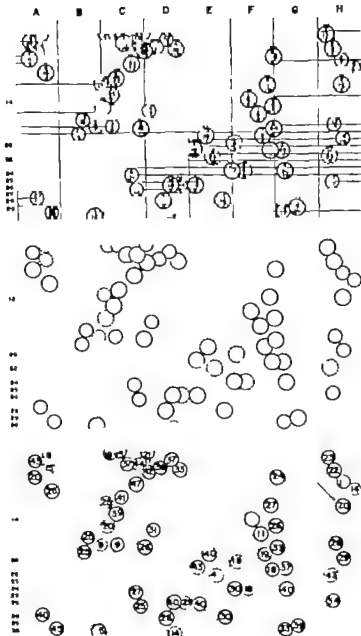


Fig. 3 The three parts of this diagram show steps in reconstructing and mapping the labeled nuclei in a segment of the esophageal epithelium.

The top diagram shows horizontal lines overlapped by solid circles (basal cell nuclei) and broken circles (spinosus cell nuclei). The strip between any two horizontal lines corresponds to the portion of the esophageal wall present within one section, that is, the thickness of each histological section. Each section is referred to by a number (from 1-30) as shown to the left. Each circle shows the numbers recorded in the successive sections of the corresponding nucleus.

When working with the map the individual nuclei are identified by using two sets of coordinates. Horizontal rows are referred to by the numbers of individual sections (left) and vertical columns, by letters (top).

The middle diagram represents the same area as the upper diagram, but drawn without lines to emphasize the clusters of labeled reconstructed nuclei.

The lower diagram represents the same labeled nuclei, but with the total number of silver grains written in each one of them. Thin dotted lines outline the presumed pairs of daughter cells.

RESULTS

The esophageal epithelium of the rat is composed of (1) the *Malpighian region* which includes the *basal layer* (stratum basale) composed of a single layer of cells which line the basement membrane (fig 3) and frequently show mitotic figures (figs. 12-16) the *spinous layer* (stratum spinosum) composed not only of typical spinous cells, but also of cells which are intermediate between them and the basal cells and are referred to as transitional cells (fig. 3) and the *granular layer* (stratum granulosum; figs. 4-5); (2) the *keratinized region* with the *glassy* (stratum lucidum) *horny* (stratum corneum) and *desquamating* (stratum disjunctum) layers (fig 5)

Preliminary experiment

The total number of labeled cells per cross section of esophagus (table 1) was about 50 at one and two hours after thymidine-H³ injection increased with time to about twice that number by 12 hours and seemed to remain unchanged until 72 hours

When the distribution of labeled cells was examined in the various layers of the

Malpighian region (table 1; fig. 6) it appeared that at 20 minutes and up to three hours after injection virtually all labeled cells were in the basal layer. Silver grains were not seen at that time over typical spinous cells and only exceptionally over those cells that are transitional between basal and typical spinous cells. At six and 12 hours only a few spinous cells, mostly transitional ones were labeled. At 24 hours many labeled cells were found in the deeper portion of the spinous layer. By 48 hours many were scattered throughout spinous and granular layers. The number of labeled spinous and granular cells seemed to reach a plateau by 48 hours (fig 6)

Mapping experiment

Twenty-four hour map The map made from radioautographs of the esophagus of a rat sacrificed 24 hours after thymidine-H³ injection contained 305 labeled nuclei. Of these 81.6% were located in the basal layer while the remaining 18.4% were in the spinous layer though close to the basal layer. Most of the map is represented in figure 7 which shows 251 of the 305 nuclei investigated.

Fig 3 Esophageal epithelium of rat in cross section. H. and E. $\times 800$.

The Malpighian region is composed of the usual basal, spinous and granular layers. The basal layer (B) is distinct and consists of a single layer of crowded, low columnar cells in contact with the basement membrane of the epithelium. The nuclei occupy major part of the cell. They tend to be ovoid, with their long axis perpendicular to the surface. The cytoplasm is scanty but densely basophilic. The upper and lower ends of the cells are often rounded (oblique arrow)

The "spinous layer" or stratum spinosum (S) is composed of cells which tend to spread out parallel to the surface. They have large, light nucleus and a particularly large cytoplasm, so that nuclei seem to be far from one another. Those cells which are found along the hypothetical line separating basal from spinous layer show moderately basophilic cytoplasm and nuclear features intermediate between those of basal nuclei and typical spinous cell nuclei (T). They are referred to as transitional cells and often appear to be squeezed between basal cells, but they are considered to be part of the spinous layer.

Above the spinous layer lies the "granular layer" or stratum granulosum (G) the cells of which exhibit small, round, deeply basophilic keratohyalin granules, which are largest and most numerous in the outermost cell row.

Finally the keratinized region may be seen (K)

Fig 4 Same as figure 3. The single file arrangement of basal layer cells is particularly clear. The granular layer shows two stages in the degeneration of nuclei, indicated by two horizontal arrows. $\times 800$

Fig 5 Granular layer and keratinized region. $\times 1,800$

The cells of the granular layer (g and g') have large often degenerating nuclei, well outlined cytoplasm and keratohyalin granules.

The keratinized region includes a thin, acidophilic and homogeneous band, the *glassy layer* (stratum lucidum, GL) followed by several rows of keratinized cells making up the *"horny layer"* (stratum corneum, H) and finally the loose plates of the *desquamating layer* (stratum disjunctum, D)



Figures 3 to 5

% of labeled cells
out of the basal layer

60

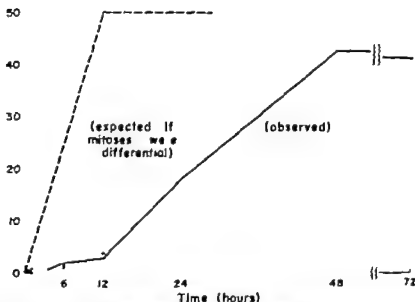


Fig. 6 The fraction of labeled cell nuclei observed outside the basal layer is plotted against time as freely drawn solid line. The broken line indicates the result expected if the transfer of cells out of the basal layer were an immediate result of differential mitoses. The solid line indicates that by 12 hours only about 3% labeled cells are outside the basal layer. By 24 hours and 48 hours, the number of labeled cells in the spinous and granular layers increases rapidly. A plateau is reached at about 48 hours.

Presumed pairs of daughter cells were detected by using the criteria outlined in the method section (equal number of grains and proximity). Of the 305 nuclei mapped a total of 256 could be matched in this manner giving 128 presumed pairs (fig. 7). When the total number of grains over the two cells of each presumed pair were compared by the Chi-square test, the label content of the two members did not differ significantly since the P value was usually high and always greater than 0.10 (table 2). Hence the 128 presumed pairs are likely to be composed of cells with an equal content of radioactivity that is to be true pairs of daughter cells.

The presumed pairs fall into three categories: (1) those composed of two basal cells — *basal pairs* — of which there were 88 that is 69% of the paired cells; (2) those composed of one basal and one spinous (or granular) cell — *mixed pairs* — of which there were 33 that is 26%

and (3) those composed of two spinous (or granular) cells — *outgoing pairs* of which there were seven that is 5% of the paired cells. The averages of the total number of grains per nucleus in the three categories of paired cells (table 3) were not significantly different.

Of the 49 labeled nuclei which could not be paired 46 were located near the edges of the map and therefore the other member of the pair may well have been out of the mapped area. Three, that is about 1% of the cells were centrally located.

Forty-eight hour map. In the serial sections of the esophagus of a rat sacrificed 48 hours after thymidine H injection, 101 labeled nuclei were investigated. About half of the labeled cells were located in the basal layer and the other half in the spinous and granular layers. A few labeled cells at the limit between granular and keratinized region showed nuclear disintegration and were overlaid by rare after

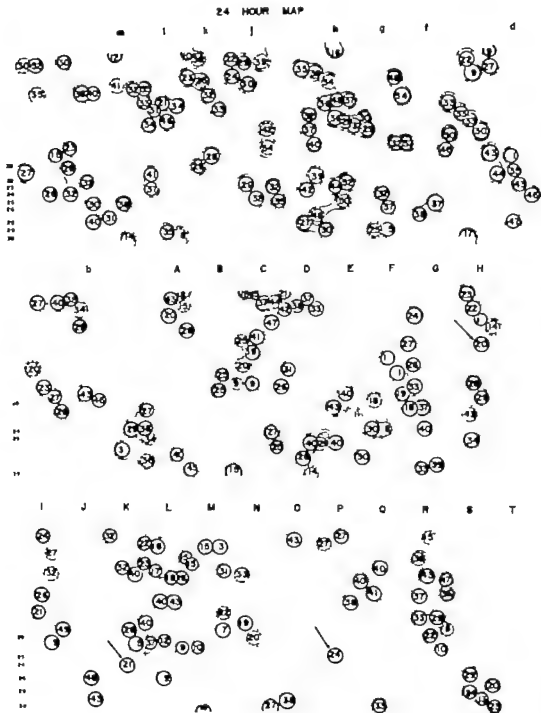


Fig. 7 Three consecutive portions of map of labeled nuclei in esophageal epithelium 24 hours after thymidine-H injection. The labeled nuclei of the basal layer are drawn in solid lines and those out of the basal layer in broken lines. Thin dotted lines outline the presumed pairs. If we disregard the nuclei located near the upper and lower portion of each map only three nuclei could not be paired (arrows)

grains. No silver grains were seen over the keratin (nor were there any in the animals of the first experiment sacrificed at 48 or 72 hours)

In the map (presented in full in fig. 8), 101 labeled cells were found of which 78 were identified as presumed pairs (fig. 8). Statistical analysis showed that the bld

TABLE 3

Frequency of pairs of the three types and mean grain count per cell in the 24 hour map

Type of pair	Frequency	Mean grain count per cell \pm S.E.
Basal	69	31.5 ± 0.23
Mixed	26	31.4 ± 1.8 (basal partner) 31.6 ± 1.7 (partner out of basal layer)
Outgoing	5	34.6 ± 3.2

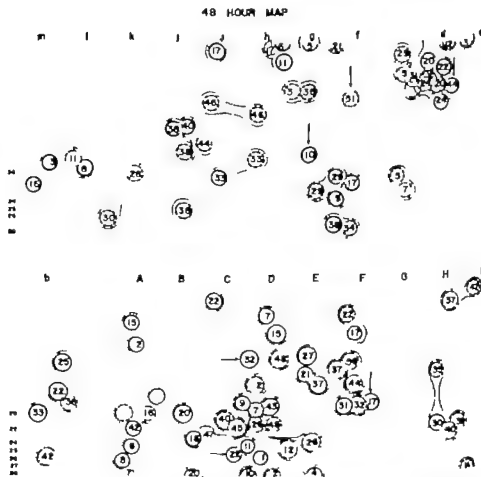


Fig. 8 Two consecutive maps of labeled nuclei in esophageal epithelium 48 hours after thymidine- H^3 injection. The labeled nuclei of the basal layer are drawn in solid lines, those of the spinous layer in broken lines while those of the granular layer are drawn with alternate lines and dots. Presumed pairs are outlined by thin dotted lines. The arrows indicate the unpaired nuclei.



Figs. 9, 10 and 11. Radioisotographs of esophageal epithelium of 200 g male rat sacrificed 48 hours after injection of 1 μ c of thymidine- H^3 per g of body weight. $\times 875$.

Fig. 9 Basal pair

Fig. 10 Mixed pair

Fig. 11 Differentiating pair

TABLE 4

Frequency of pairs of the three type and mean grain count per cell in the 48-hour map

Types of pairs	Frequency	Mean grain count per cell \pm S.E.
	%	
Basal	29	15.9 ± 1.22
Mixed	42	29.2 ± 2.8 (basal partner) 30.6 ± 2.7 (partner out of basal layer)
Outgoing	29	25.1 ± 2.6

content of the two members of the presumed pairs did not differ significantly (table 2). The presumed pairs would then be composed of cells with an equal content of radioactivity that is, would be true pairs of daughter cells.

As in the 24-hour group the presumed pairs fell into three categories: (1) basal pairs 29% (fig. 9), (2) mixed pairs 42% (fig. 10) and (3) outgoing pairs 29% (fig. 11). The mean total number of grains per nucleus did not differ significantly in mixed and outgoing pairs, but was about half as small in basal pairs (table 4). The mean grain count over basal cells at 48 hours was also half that over any cell type at 24 hours (table 3).

The remaining 25 labeled nuclei could not be paired. Eighteen of these because of proximity to the edge of the map may have a partner outside. A tentative explanation for the seven centrally located unpaired cells will be proposed below.

DISCUSSION

Sequence of events in the esophageal epithelium

Up to one hour after thymidine- H^3 administration labeled nuclei were numerous in the basal layer of the esophageal epithelium (table 1) but were so rarely seen in the spinous layer (0.2%) that their presence was attributed to basal cells located along

a fold of the basement membrane and cut at such an angle as to appear to be outside the basal layer. As for mitotic figures they were always restricted to the basal layer. It was concluded that only the cells of the basal layer can synthesize DNA and undergo mitosis. When thymidine-H was injected repeatedly every cell of the basal layer became labeled (Leblond et al. '64) so that all the cells of this layer can synthesize DNA and presumably divide. Hence all basal cells and only these cells can function as stem cells of the stratified epithelium of the esophagus. The basal layer would thus be the germinal layer (stratum germinativum) of this epithelium.

By six and 12 hours after thymidine-H³ injection (table 1) a small but significant number of labeled cells appeared in the spinous layer mainly as transitional cells. By 24 hours labeling was seen in many typical spinous cells and by 48 hours in many granular cells. Since thymidine-H³ mostly disappears from the circulation within two hours after injection (Messier '60) the labeled spinous and granular cells seen at later time intervals could only come from the transformation of labeled basal cells. Therefore cells of the basal layer must have transferred to the spinous and to the granular layer while acquiring features of the cells in these layers. Finally at 48 hours some of the lightly labeled granular cells showed a disintegrating nucleus. Presumably these cells were losing their label prior to keratinization. Indeed, no label was seen over the keratinized region at any time.

The outward migration of differentiating cells observed in radioautographs was in accord with classical views on the renewal of stratified squamous epithelia. Furthermore the timing indicated that it takes less than 48 hours for cells to progress from basal to granular layer and beyond.

After the 48-hour interval the labeled cells present in the spinous and granular layer presumably continued their outward migration, eventually undergoing keratinization and losing their label. And yet, the number of labeled cells in the epithelium had not decreased by 72 hours (table 1, fig. 6 and unpublished experiment). Were new labeled cells produced in the meantime to balance the loss? For an

answer to this question, let us first point out that the cells which were labeled by an injection of thymidine H³ underwent division soon after the injection, as shown by the doubling of the number of labeled cells between one and 12 hours (table 1) and the presence of labeled metaphases in the basal layer at three and six hours (last column of table 1). At 12 and 24 hours, no metaphase was labeled so that the labeled cells were no longer in the mitotic phase of their life cycle. The reappearance of labeled metaphases at 48 hours indicated that a second wave of mitotic division was adding new labeled cells. Presumably this further addition of labeled cells approximately balanced the loss taking place at the limit between granular layer and keratinized region. As a result, the total number of labeled cells in the epithelium remained about the same at 48 and 72 hours (table 1).

Identification of the pairs of daughter cells arising from mitosis

The two criteria used to pair labeled cells, that is equal grain count and contact or at least close proximity were those expected from any two sister cells arising from a labeled mitosis. Indeed the label should be equally divided between the DNA of these two cells (Taylor et al., '57) and, therefore, both should have a similar grain count. Furthermore attachment of the cells to one another by desmosomes should minimize their relative displacements at least in the basal layer. It was therefore concluded that the presumed pairs identified by our two criteria (figs. 7 and 8) consisted of sister cells.

One difficulty was that some of the nuclei in the map could not be paired. At nearly all of these were located along the upper and lower edges of the maps. It was not possible to decide whether they had a partner outside. Therefore these nuclei were not considered further. There were however a few "single" labeled nuclei so far from the edges to be explained in this manner. This was the case with three of them in the 24-hour map (that is about 1%). The first thought that came to mind was that the partner had degenerated and been removed. However by 24 hours, none of the nuclei had reached the granular

layer—the only place where signs of degeneration were ever seen. Another explanation was that the three single nuclei had synthesized DNA but had not undergone mitosis, thus remaining at the post duplication stage G_2 (as suggested by Gel'fant '62) in his work on the epidermis although the grain counts over the three "single" nuclei were not as high as would be expected in such a case). As for the seven single centrally located nuclei in the 48-hour map they may be tentatively explained as follows. First if the basal partner of a mixed pair or one of the two partners of a basal pair had divided again just before the 48-hour interval, the sum of the grain counts over the two new cells should equal that over the non-dividing spinous or basal partner (which would then be single). This would seem to be the case for the single nuclei indicated by horizontal arrows in figure 8. Secondly if a labeled cell had progressed beyond the granular layer and keratinized, it would no longer be recognized and the remaining partner would appear to be single as may be the case for the cells indicated by vertical arrows in figure 8.

The other central cells—256 in the 24-hour map and 152 in the 48-hour map—were taken to consist of pairs of daughter cells arising from the same mitosis.

Differentiation as a result of differential mitosis

Let us first recall that some authors proposed that the stem cells of renewal systems (Cowdry '50 Rolaboven, '51) and particularly those of stratified epithelia (Mercer '62) proliferate by means of differential mitosis. The two daughter cells of such mitoses would receive different amounts of genetic material and thus be led to different fates, that is one cell would divide again as stem cell and the other would differentiate. In the esophagus in particular the cell fated to differentiate would move out of the basal layer and undergo the changes culminating in keratinization, while the other cell would remain in the basal layer and divide again as stem cell. It might be expected that the differentiating cell would transfer out of the basal layer soon after mitosis, so that by about 12 hours after injection of thymidine- H^3

50% of the labeled cells should appear in the spinous layer. Instead, only 3.0% were found in this layer (fig. 6). This observation indicated that no more than 3% of the cells might arise from differential mitoses unless, however there were a delay in the transfer of differentiating cells out of the basal layer. Even so each pair would eventually become a mixed pair (composed of a basal and a spinous or granular cell) while there would not be any outgoing pair (composed of two spinous or granular cells). However outgoing pairs were seen in both maps and their number increased from 5% at 24 hours to 29% at 48 hours after injection. At least, the cells of these pairs did not come from differential mitoses!

Are mitoses of the esophageal epithelium equivalent?

An equivalent mitosis is one that yields two daughter cells which are identical and therefore have similar potentialities. If this were the case for the mitoses of the esophageal epithelium, the probability of transfer to the spinous layer would be the same for the two daughter cells.

A priori, it might be thought that the probability of transfer is the same for any cell of the basal layer. In such a case basal cells would be transferable at any stage of their mitotic cycle. However the absence of mitotic figures in transitional and spinous cells showed that transfer does not take place during mitosis. Similarly labeled cells were hardly ever seen out of the basal layer during the first three hours and seldom between three and 12 hours after thymidine- H^3 injection. Hence cells are little or not transferable during DNA synthesis and mitosis. On the other hand, after 12 hours that is after the first wave of mitosis was completed the rate of trans-

Incidentally when the various types of mitosis figures found in the basal layer were examined (unpublished) 96% of those were oriented in parallel to the basement membrane (figs. 13 and 14) or obliquely (figs. 2 and 14) and therefore, the two daughter cells would be expected to remain in the basal layer. A small number of mitoses are oriented perpendicularly to the basement membrane, so that one of their daughter cells seems to be directly in the spinous layer, as suggested by figure 14. The percentage of this type of mitoses (4%) is about the same as that of the labeled cells found out of the basal layer at completion of mitosis (3%) by 12 hours after thymidine- H^3 (table 1). Hence, the mitotic figures perpendicular to the basement membrane may account for the rare cells released to the spinous layer during the first 12 hours.

fer out of the basal layer became rapid. Thus, the number of labeled cells found out of this layer increased with regularity from 3.0% at 12 hours to 18.5% at 24 hours and 45.2% at 48 hours (fig. 6) that is cells were transferred at the rate of 1.2% per hour. Briefly then basal cells appeared to be readily transferable from the time they arise out of mitosis until they start synthesizing DNA prior to the next mitosis.

The problem is then whether the two cells arising from a mitosis or in fact, all cells arising from mitosis over a given period have the same probability of leaving the basal layer. In such a case the labeled cells in let us say the 24-hour map (which arose from mitosis during the 12 hours following injection) should be randomly distributed as basal mixed and outgoing pairs. The occurrence of the three types of pairs would then follow definite statistical laws. In Appendix I the distribution of the three types of pairs as observed at 24 and 48 hours was compared with the distribution expected on the basis of random transfer. The results of the analysis (table 5) showed no significant difference between observed and expected data. It was therefore concluded that the numbers of pairs observed at 24 and 48 hours were consistent

with the concept that all the labeled cells had the same probability of being transferred out of the basal layer. Accordingly the two daughter cells of each labeled mitosis would be equally liable to transfer. It is concluded that either one or both or none of the two daughter cells of any mitosis can be transferred (whereas any cell remaining in the basal layer will divide again).

Cell transfer and differentiation

The lack of evidence in favor of differential mitosis implied that neither daughter cell was fated to undergo differentiation. Instead both daughter cells of mitosis would be equivalent at least with regard to their transferability to the spinous layer. Furthermore signs of differentiation were not found in basal cells whereas in transitional cells that is in cells already out of the basal layer there were indications that differentiation was underway: enlargement of the nucleus, decreased basophilia,

It therefore seemed that differentiation started after the cells left the basal layer. Leaving the basal layer must have caused changes in the microenvironment, such as loss of contact with connective tissue, reduced availability of metabolites and so on. Presumably such changes trigger the sequence of events in differentiation.

What then causes the transfer of cells out of the basal layer? It may be assumed that the addition of new cells by mitosis in this layer tends to increase population pressure. It is indeed clear that, on the average at least, any cell added by mitosis can be accommodated only if another cell is forced out of the basal layer. Thus, population pressure may well be the random acting factor which causes transfer.

ACKNOWLEDGMENTS

This work was supported by a Blott Term grant of the Medical Research Council of Canada.

The authors are grateful to Dr. N. J. Nadler for advice in the interpretation and analysis of the data and to Dr. D. Bray for assistance in statistics. Valuable and unstinting collaboration has been received from Mrs. N. Neumarkt.

LITERATURE CITED

- Abercrombie M. 1946 Estimation of nuclear population from microtome sections. *Anat. Rec.* 94: 233-248.
- Amano, M., B. Messler and C. P. Leblond 1959 Specificity of labeled thymidine as DNA precursor in radioautography. *J. Histochem. Cytochem.* 7: 153-155.
- Clermont Y. and C. P. Leblond 1950 Differentiation and renewal of spermatogonia in the monkey *Macaca rhesus*. *Am. J. Anat.* 54: 237-274.
- Cowdry E. V. 1950 A Textbook of Histology (14th Edition) Lea and Febiger Philadelphia.
- Gelfant, R. 1962 Initiation of mitosis in relation to the cell division cycle. *Exp. Cell Res.* 26: 395-403.
- Kopriwa, B. M. and C. P. Leblond 1962 Is improvement in the coating technique of radio-

Results are consistent with the concept that transfer of basal cells to the spinous layer occurs randomly except during DNA synthesis and so on. Yet, there may be other non-random factors influencing the egress of cells. Thus the different grade curves of the two types of basal cells in table 4 suggest that the presence of a spinous partner in a pair may delay the onset of mitosis of the basal partner. Such an observation, however, does not detract from the equivalence of the two daughter cells if they arise from mitosis.

- utography J Histochem. Cytochem 10 259-254.
- Leblond, C. P. and B. E. Walker 1956 Renewal of cell populations. *Physiol. Rev.* 36 235-275.
- Leblond, C. P., R. Greenbach and J. P. Marques-Pereira 1964 Relationship of cell formation and cell migration in the stratified squamous epithelia. In: *Advances in Biology of Skin*. (Ed. Adlard & Son Ltd., Bartholomew Press, Dorking) Vol. 5, p. 39-67.
- Mercer E. H. 1952 The Cancer Cell. *Brit. Med. Bull.* 18 187-192.
- Messier B. 1960 Radioautographic localization of newly formed DNA after injection of thymidine- H^3 into rats and mice. Ph.D. thesis. McGill University.
- Messier B., and C. P. Leblond 1960 Cell proliferation and migration as revealed by radioautography after injection of thymidine- H^3 into male rats and mice. *Am. J. Anat.* 106 247-285.
- Reischoffen, E. 1851 Ueber die Reifungsstufen bei der Spermatogenese mit einer Kritik des bisherigen Begriffs der Zellreihungen. *Verh. d. Anat. Ges.* 49 189-197.
- Taylor J. H. P. & Woods and W. L. Hughes 1957 The organization and duplication of chromosomes as revealed by autoradiographic studies using tritium-labeled thymidine. *Proc. Nat. Acad. Sci.* 43 122-125.
- Verne J. 1960 *Précis d'Histologie. La Cellule* — les Thèmes — les Organes. (5th edition) Masson et Cie Paris.

APPENDIX I

THEORY CONCERNING THE TRANSFER OF CELLS OUT OF THE BASAL LAYER OF THE EPITHELIUM OF THE ESOPHAGUS

N. J. NADLER

Department of Anatomy McGill University

Following injection of an appropriate radioactive DNA precursor suppose that after mitosis of the labeled cells in the basal layer of the esophagus there are N pairs of labeled daughter cells or $2N$ labeled cells. Suppose further that at a

certain time, a proportion, p of the $2N$ labeled cells has transferred out of the basal layer. If the transfer of the labeled cells is a random event then the probability that such a cell will transfer is p and the probability that it will not is $1 - p$.

TABLE 5

Comparison of expected and observed numbers of pairs of the three types at 24 and 48 hours after injection of thymidine- H^3 (with χ^2 -square testing of the differences)

	Expected	Observed	square test (Observed-expected) expected
24-hour map			
Basal pairs	$(1-p)2N = 85.3$	88	0.06
Mixed pairs	$2p(1-p)N = 34.4$	33	0.73
Outgoing pairs	$p^2N = 4.4$	7	1.61
Total	$N = 128$	126	2.44
48-hour map			
Basal pairs	$(1-p)2N = 19$	22	0.47
Mixed pairs	$2p(1-p)N = 33$	33	0.95
Outgoing pairs	$p^2N = 19$	23	0.47
Total	$N = 76$	78	1.80

With one degree of freedom, the χ^2 -square for the 24-hour map 2.44, and for the 48-hour map, 1.80, give P values between 0.50 ($P = 1.44$) and 0.10 ($P = 3.78$). Hence the differences between observed and expected numbers of pairs are not significant.

For any pair of labeled daughter cells there are four possibilities

1 Both cells will transfer (outgoing pairs) The probability of this occurrence is $p \times p$ or p^2 . Of the N pairs the number so affected is p^2N

2 The first cell will transfer and the second not (mixed pairs) The probability of this occurrence is $p(1-p)$. Of the N pairs the number so affected is $p(1-p)N$

3 The first cell will not transfer and the second will (mixed pairs) Of the N pairs the number so affected is the same as in the previous case that is $p(1-p)N$

4 Neither cell will transfer (basal pairs) The probability of this occurrence is $(1-p)(1-p)$. Of the N pairs the number so affected is $(1-p)^2N$

Therefore, at the time under consideration, the number of outgoing pairs is p^2N the number of mixed pairs is two times $p(1-p)N$ and the number of basal pairs is $(1-p)^2N$

The value of p is determined by observation as it is the proportion of all the paired cells which are found outside the basal layer at the time under consideration, that is $33 + (2 \times 7)/256 = 0.184$ in the 24-hour map and $32 + (2 \times 22)/152 = 0.5$ in the 48-hour map. From these values of p we can calculate what numbers of pairs of the

three types are expected at the two time intervals. These expected values may then be compared to the numbers of pairs of the three types which were actually observed in the maps. If the distribution is similar for expected and observed numbers, then the transfer of labeled cells must have been a random event.

The results (table 5) demonstrated that the differences between the distribution of expected and observed numbers of pairs is not significant whether the 24-hour or 48-hour data are considered. Hence the observed numbers of pairs may be explained by a random distribution, which in turn implies a random transfer of cells out of the basal layer

The reason for the use of 1 rather than 2 degrees of freedom in the statistical analysis is that the data from which p (and therefore the expected values) was calculated were the same data as those from which the numbers of the three types of pairs were obtained.

In order to be able to work with 2 degrees of freedom, the statistical calculations were repeated using data from another experiment (summarized in table 1) in which the proportion of labeled cells out of the basal layer, p , averaged 0.185 at 24 hours and 0.51 at 48 hours. The expected figures were calculated from these values of p as done in table 5. The squares were found to be 2.45 and 3.55 for the 24-hour and 48-hour data respectively. In this case, they are 2 degrees of freedom. Again, the differences between expected and observed were not significant. (At 24 hours, the P value was close to 0.30, while at 48 hours, it was $0.10 > P > 0.10$.)

This approach confirms the conclusion that the observed data are not significantly different from those expected on the basis of random transfer of labeled cells.

PLATE 1

EXPLANATION OF FIGURES

Figures 12-15 Stratified squamous epithelium of rat. H. and E. 1100.

- 12 The basal layer shows an obliquely oriented metaphase (M)
- 13 Anaphase (A) oriented parallel to the basement membrane
- 14 Obliquely oriented telophase (T)
- 15 Parallel telophase (T)
- 16 Telophase perpendicular to the basement membrane (T). One of the daughter cells is retained in the basal layer (B) while the other is in the spinous layer (S)



Electron Microscopic Observations on the Postnatal Differentiation of the Seminal Vesicle Epithelium of the Laboratory Mouse¹

HELEN WENDLER DEANE AND SARAH WURZELMANN

Departments of Anatomy and Pathology Albert Einstein College of Medicine Bronx 61 New York

ABSTRACT The cytological changes occurring in the epithelium of the mouse seminal vesicle between 5 and 49 days of postnatal life have been traced by electron microscopy.

Initially the epithelium was composed of typical immature columnar cells. During the second week of life, the principal changes were: rapid cell proliferation, followed by increases in the amounts of organized ergastoplasm and Golgi material. During the third week, dense secretory material appeared in Golgi cisternae and then in the lumen of the gland.

The parallelism between these changes and those found in maturing pancreatic acinar tissue has been assessed. Comment is made on the attachment of ribosomes to endoplasmic reticulum in the initiation of protein-secretory activity and the importance of the subsequent proliferation of ergastoplasmic and Golgi membranes. The evidence for relating these cytological and secretory alterations in the seminal vesicle to rising titer of androgen during the prepubertal period has been cited.

Other observations included: () Evidence for considerable amount of cellular slowing and reabsorption during the first two postnatal weeks; (b) an association of mitochondria with developing desmosomes, and () the appearance of basal cells first during the second week of postnatal life, thus suggesting that they arise by dedifferentiation of columnar cells.

The available evidence indicates that epithelium of the seminal vesicle, as of several other male accessory glands require androgens for its morphogenesis, fetal development and for its progressive differentiation thereafter. The observations establishing these generalizations have been reviewed by numerous

(Moore, '39 '51; Price '47 Jost, '48 '53 '57 Parkes '55; Dorfman '51 Shipley '56 Turner '60 Burns, '61 Price and Williams-Ashman, '61 Szirmai Wells, '62) A similar dependence on androgen has been demonstrated *in vitro* (Demuth, '41; Jost, '53; Price and Pannaschek '56 '59 Lasnitzki, '58; Burns, '61)

For the initial development and for complete maintenance, testosterone (usually of testicular origin) seems to be the prime factor. There may be some auxiliary support by weaker androgens of adrenal origin once the organ anlagen have been established and the initial tissue differentiation has occurred and the adrenal androgen appears able to prevent complete regression after postnatal castration (How-

ard, '46 Ponse '50 Price and Ingle '57 Deanealy '58 '60 Price and Williams-Ashman '61 Howard and Migeon, '62) In addition, there may be some synergism between androgens and either somatotrophin or luteotrophin (e.g., Chase Geschwind and Bern '57 Antiloff Prasad and Meyer '60 Lostro, '62)

In the mouse and rat, the degree of organ development that is reached prenatally involves hardly more than the evagination of a sacculle from near the caudal end of each Wolffian duct. A slight flexure develops at the tip of this diverticulum before birth, but no internal folding of the mucosa is evident (Wiesner '34 Price '38 '47 Clegg, '59 Burns, '61) Certainly no signs of secretory activity have appeared in the epithelial cells at the birth. This fact makes possible organs from postnatal animals cytological maturation of

This investigation was supported by National Service Research Grants CG219 from the National Institutes of Health. A preliminary report was presented at the 1964 Regional Conference on "Development '64).

which is representative of a protein-secreting epithelium dependent on hormone stimulation.

This paper presents a description of the cytodifferentiation of the epithelium of the seminal vesicle of the mouse tracing its maturation from the first postnatal week until sexual maturity which is attained in males of this species by about six weeks of age (Snell, 41 Baillie, '61). Previous descriptions of this maturation as observable at the light microscopic level were provided for the laboratory mouse by Howard ('39) and for the very similar organ of the rat by Price ('36) and Clegg ('59). With a hormone-dependent tissue such examinations provide a fundamental approach to the analysis of how hormones affect cellular functions of their target organs.

MATERIAL AND METHODS

Male mice of Swiss albino stock, born in our own laboratory were killed on days 5 7 8 9 11 12, 13 14 15 18 20 22, 29 38 42, 45 and 49 after birth. A total of 41 young animals was studied. Glands from six-month-old mice were used as representative of the fully mature state. All animals were killed between 9 and 10 A.M. / From the mice below four weeks of age, the bladder urethra and terminal portions of the ureters and vasa deferentia, with the attached accessory glands were removed *in toto* and immersed in a pool of chilled fixative. With the aid of a dissecting microscope the seminal vesicles could then be cut free, diced and transferred to a container of cold fixative. The glands of older animals were cut out individually, gently drained of as much secretory fluid as possible, and then cut into smaller blocks while immersed in fixative.

The usual fixative for the glands from immature animals was selected after experimentation. It contained 2% OsO₄, made up in 0.1 M phosphate buffer pH 7.8 to which was added 5% (0.15 M) sucrose. (The final pH of this mixture was 7.4.) In a few instances the material was fixed in solutions containing no additive whatsoever or 10% sucrose or 0.9% NaCl. The glands of adults were customarily fixed in a mixture containing 10% su-

crose, to minimize distention of the extracellular channels (Deane, '63).

Fixation was continued at 4°C for two and one-half to three hours. Thereafter, the tissue blocks were thoroughly rinsed in a chilled solution of 0.1 M buffer and cut into still smaller pieces then dehydrated through successively stronger concentrations of chilled ethanol, cleared in propylene oxide and imbedded in an epoxy resin mixture adapted from a formula devised by Luft ('61) containing Shell Epon 812, the hardening anhydrides DDSA and NMA, and the polymerizer DMP-30 (for details see Deane '63).

Sections were cut at approximately 75 μ m and mounted without support, on 200-mesh copper grids. They were stained with either an alcoholic solution of uranyl acetate or with aqueous lead citrate (Reynolds, '63) followed by alcoholic uranyl acetate. The preparations were studied in RCA EMU 3E or 3G electron microscope operated at 100 kV. Micrographs were taken on Ilford N60 or Kodak Contrast lantern slide plates at initial magnifications of from about 1,800 to about 12,000 times; these pictures were enlarged photographically 2 to 4-fold as desired.

In addition 1- μ sections of the bladders were stained with methylene blue plus azure II (Richardson, Jarett and Field, '60) for study under the light microscope.

OBSERVATIONS

Light micrographs of 1- μ sections of the epoxy-embedded material have been used to supplement the electron micrographs, in particular to reveal the over-all organization of tissues within the seminal vesicle. Sections of material fixed in OsO₄ and stained with methylene blue plus azure II have the merit that the secretory material when present, appears blue-black and hence readily distinguishable from the faintly staining cytoplasm.

The results will be described by type rather than by the age of the specimen to avoid repetition. Thus we will deal, for example, with the form and arrangement of the epithelial cells later with the material then with the cytoplasmic organelles, etc. However it is well to point out at the beginning that the material took

organize itself into three, or at the most four age groups according to the degree of differentiation of the seminal vesicle epithelium, as follows: (a) In mice 5-9 days of age the epithelial cells remain immature in appearance seeming to be involved in cell multiplication and consequent glandular growth (figs. 1-6) (b) In mice 11-14 days of age the epithelium shows initial signs of becoming a proteinaceous glandular tissue and basal cells become apparent (figs. 7-13) (c) In mice more than 15 days old, the formation of dense proteinaceous secretory granules assumes dominance with the secretory cells becoming indistinguishable from those of an adult by about six weeks (figs. 14-20) Thereafter there is some hypertrophy of the epithelial cells perhaps, but major change is that secretory material begins to accumulate in the lumen of the seminal vesicle, resulting in a further distention of the organ (figs. 21-23)

Over-all structure of the gland

In the youngest animals studied here (five-day postnatal animals) each seminal vesicle consists of a slightly curved tube, lined by a simple lining epithelium on a lamina propria surrounded by the prospective muscularis. During the subsequent few days, there is no change in the appearance of the cells but there is a slow growth of the seminal vesicle as a whole, principally as a result of epithelial multiplication, which results in an extension in the length of the organ and internal folding of the mucosa. This is a beginning corrugation of the external aspect of the gland. This differentiation continues steadily so that by three weeks the gland appears like a small replica of the adult organ, with its characteristic highly folded mucosa.

With both the light and electron microscopical sections through the mucosa of the youngest animals show a narrow, generally collapsed lumen, surrounded by a moderately high pseudostratified epithelium (figs. 1, 2, 5). The delicate basement (boundary) lamina of the epithelium itself rests on a thin interstitial space composed of sparse collagenous fibrils. This in turn is surrounded by closely packed con-

nective tissue cells primitive smooth muscle cells (fig. 3) and occasional small blood vessels (fig. 15). No further description of these underlying tissues will be given here. Suffice it to say that during the second week of postnatal life the smooth muscle cells show clear signs of elongation, hypertrophy and maturation, with the development of broad zones of myofilaments. Organs in the male reproductive tract provide excellent objects in which to study maturation of smooth muscle cells in postnatal material.

During subsequent weeks, as the epithelial cells multiply and the secretory function emerges sections of the gland reveal a branching of the epithelium and a distention of the lumen with the result that the epithelial cells adopt a simple columnar rather than a pseudostratified arrangement (figs. 11, 14, 22).

Organization of the epithelium

In the youngest animals, all the epithelial cells are tall and very narrow on the average about 20 μ high and 3-5 μ wide (figs. 1, 2, 5, 7). As a result, the nuclei are greatly elongated crowded and pushed to different levels. So far as can be determined all cells in the youngest group reach from the basement lamina to the luminal border no short, stellate basal cells have been found in animals less than 11 days old.

During subsequent weeks, the most important change to take place in the shape of the columnar epithelial cells is that they gradually become broader reaching a width of about 5 μ at 18 days (figs. 14, 15) and 6-7 μ in the adult (figs. 22, 23). Associated with this enlargement, the nuclei steadily become more rounded and come to lie pretty much in a row rather than at several levels.

While the columnar cells are increasing in width there is also some fluctuation in height. In the third week, the cells appear on the average shorter than at younger ages (figs. 14, 15) being only about 15 μ high instead of 20 μ . In subsequent periods, they exhibit considerable variation in height in different parts of the gland, with cells lying near the bases of the clefts being often taller than those on the sides of the folds. However in the

adult, the average cell height is again 20 μ (figs 22, 23). This enlargement in width and height of cells no doubt contributes somewhat to the over-all growth of the organ during the prepuberal and puberal periods.

The columnar cells typically bulge somewhat into the lumen, with the apical membrane being thrown into crowded, short, irregularly spaced microvilli (figs 2, 4, 6, 7-10, 12, 13, 15-17, 23). The lateral margins of the cells show relatively slight undulations except at the corners where three or four cells come together — here there may be considerable vertical interdigitation or fluting (figs. 10, 12, 13, 18). Occasional stud-like attachments may be seen in the upper half of the epithelial layer (figs. 2, 10, 18). There is considerable folding, both vertical and lateral of adjoining cell surfaces near the base of the epithellum; this feature is more easily appreciated in cross or oblique sections through the epithellum (fig 10). However the cells present a fairly smooth foot to the basement lamina (figs. 3, 15, 23).

In cross section the cells exhibit 4 to 6 sides (fig 10). They are generally closely apposed throughout their length, but small pockets of intercellular space are occasionally found, especially in the lower half of the epithellum, during the first two weeks of life (figs. 2, 6, 12). Thereafter such gaps are rare.

The apical portions of the cells are tightly bound together by broad dense junctional complexes (figs. 2, 4, 6 *et seq.*) that are entirely typical of those found in most mammalian columnar epithelia (Farquhar and Palade, '63). That is, there is first a belt in which the membranes of the adjacent cells are actually fused (zonula occludens) followed by an underlying belt in which the membranes are firmly adherent but not fused (zonula adherens). In both segments of the terminal bar each plasma membrane is greatly thickened on its inner aspect by electron-dense material. Below the terminal bar proper there are rings of fairly closely spaced desmosomes (figs. 4, 9). In the most immature specimens here studied additional desmosomes have not been found attaching cells below the uppermost part of the epithellum but they occur deeper in the layer at widely

spaced intervals by the end of the second week (e.g. figs. 12, 15, 18).

The form and appearance of undifferentiated basal cells, the other element of the epithellum found in the older specimens, will be described in a later section (p. 98). Now we will give a cytological description of the columnar cells.

Cytology of the columnar cells

In the youngest animals the cytological features are quite simple and uniform (figs. 2-4). Over-all, the electron density of the cytoplasm is low as compared with that in the older animals. Not only are there fewer electron-dense structures, but the readiness with which electron-opaque stains are taken up appears to be lower. Similarly the stainability of the osmium fixed, epoxy imbedded sections with fast dyes is slight in the one- to two-week specimens in comparison with older glands.

Nuclei. The nuclei are large and oval to spherical, depending on the age of the mouse. They present a relatively smooth outline. In the youngest animals there is margination of dense chromatin in some but not all of the cells (figs. 2, 3). This characteristic becomes more prevalent with age (figs. 7, 10, 15, 23). In all specimens the nucleus exhibits one or more complex nucleoli when cut in the appropriate plane. The number and conspicuousness of nuclear pores tend to increase with age. The nuclear envelope is double at all times, but in the youngest mice the outer element does not appear to be studded with ribosomes (fig 4). Only in the older animals when the ergastoplasm is relatively well organized, do ribosomes regularly cover this membrane (e.g., figs. 16, 17, 21).

Mitotic figures are detected most frequently in glands from animals during the second week of life but to some extent also at the end of the first week and during the third and fourth weeks (figs 5, 11) they have not been observed in older mice. In this material mitoses have been encountered only in columnar cells, not in basal ones.

A fortunate section showing to our advantage one of the centrioles and its condensed chromosomes of a dividing cell is shown in figure 6. Note that the cell retains tight junctions with its neighbor.

A small Golgi apparatus is present. The stage of division is probably anaphase since segments of prospective nuclear envelope (arrows) appear to be accumulating near the chromosomes (e.g., Moses '64 Robbins and Gonatas, '64). Also the lower margins of the cell appear ruffled. It should be pointed out that the kind of preparation employed on this material has failed to preserve the tubular aspect of the spindle fibrils; the spindle zone appears composed of structureless streaks emanating from the centriole.

Mitochondria. The cells exhibit fairly abundant mitochondria. These are slender, one-quarter to one-half μ in diameter and quite long, clearly exceeding 2μ in length (e.g., figs. 2, 12, 16, 23). (Indeed, observations made with the light microscope on thicker sections, in which more mitochondria may be seen in their total length suggest that they may reach more than 5μ (Macklin and Macklin '32).) The cristae are moderate in number and tend to traverse most of the width of the organelle but they are sometimes short (fig. 20); in general, they are of simple form but they occasionally loop or branch (fig. 16). The mitochondrial matrix is very dense. Opaque granules within the mitochondria are uncommon in the youngest specimens, more common in over two weeks old (e.g., figs. 16, 18, 23). However granules are more common in the younger glands, where they are much less dense (e.g., figs. 2, 4).

In many of the youngest specimens and in this particular series of glands 20 days of age we have repeatedly found a pair of mitochondria flanking a desmosome whether this be one lying just below the terminal bar or deeper in the epithelium. Examples are shown in figures 4, 9, 15, 18-20. In figures 7 and 13 a single mitochondrion lies adjacent to a desmosome. We term this association a mitochondrial-desmosome complex. In many examples there appears to be dense material perhaps fibrous or tubular between the outer mitochondrial membrane and the dense component of the plasma membrane at the desmosome (figs. 4, 18-20).

Polyribosomes and ergastoplasm. In the youngest mice studied (5-9 days of age)

most of the cytoplasm consists of an endoplasm containing clusters and rosettes of ribosomes such clusters now being termed polyribosomes (Warner Rich and Hall '62 Watson, '63 Grobstein, '64). Only scattered, short lengths of membranous endoplasmic reticulum with associated ribosomes (ergastoplasm) are found in the sections from these youngest animals (figs. 2-4). Such membrane systems must occupy a very small proportion of the cell volume. No smooth-surfaced endoplasmic reticulum is certainly identifiable in this cell type.

During the interval between 11 and 14 days, there is some increase in the number of segments of ergastoplasm (figs. 7, 9, 13). This proliferation occurs especially in the infranuclear portion of the cell. There also appears to be some overall increase in the concentration of ribosomes per cell, which may account in part for the greater electron density of the cytoplasm at this age in comparison with the younger group.

In the third week the amount of organized ergastoplasm increases steadily (figs. 15, 16). Now there are several layers of ergastoplasmic cisternae below and along side the nucleus as well as some enclosing the Golgi zone in the upper half of the cell. By the end of the fourth week, the ergastoplasmic system is even more concentrated. Below the nucleus there is a progressive increase in the number of cisternae which eventually become closely organized into a tight whorl (figs. 21, 23). The increasing amount of this membranous system is illustrated for the apical portion of the columnar cells in figures 17-20 and 23. In general, the cisternae appear somewhat distended in these older specimens in comparison with the youngest mice (cf. figs. 3, 9, 12). An exceptional picture for these older animals is shown in figure 17 in which the ergastoplasm seems tightly shut; this specimen was fixed in a solution containing 10% rather than 5% sucrose.

Older specimens show that most ribosomes are attached to membranes relatively few particles seem to lie free between the lamellae. In some favorable instances it is possible to see that some ribosomes are however grouped in ro-

settes or rows, both near the nucleus and near the edge of the cell (fig 21)

Golgi apparatus secretory granules
The evolution of the Golgi apparatus follows a similar time course. In the young est animals studied, there lie in the supra nuclear zones of the cells stacked lamellae of collapsed Golgi saccules and a few associated vesicles all of which are small (figs. 2-4-6). During the latter half of the second week, as the ergastoplasm begins to proliferate there is a tendency for the Golgi saccules to proliferate too and, more strikingly to become distended (figs. 7-9-10-12). As a result, the supranuclear region of the cells assumes a clear appearance in light-microscope preparations (e.g., fig 11) as is typical of these cells in an active secretory state (Price '36 Howard '39 Howard and Migeon, '62)

In a very few cells of all preparations of mice aged 11-14 days, dense granules of what looks like secretory material have been found within distended vacuoles in the Golgi zone. As in more mature glands such granules are surrounded by a space that contains no electron-dense material. The granules are consistently small however generally being only 0.1 or 0.2 μ in diameter. Cells containing granules never become prevalent in this age group and none of the micrographs selected for this paper happens to contain one. A micrograph illustrating a secretory granule in an epithelial cell of a 14-day specimen has been published elsewhere (Deane '64)

During the third week and thereafter the Golgi apparatus comes to occupy a steadily larger portion of the supranuclear half of the cell (figs. 15-18-23). The cavities of the membrane system become increasingly distended. By the end of the fourth week, sections through the Golgi zone of most columnar cells show at least some large mature secretory granules within clear vacuoles bounded by a dense membrane presumably of Golgi origin (fig 17)

In the younger specimens, many such large vacuoles appear to contain no granule or one so small that it is regularly missed in section (fig 16). The dense secretory material evidently first condenses within the narrow saccules of the Golgi

system (fig 17) then enters small vesicles budded off from these. Above the zone of small vesicles are larger vacuoles containing large granules. Finally in occasional fields it has been possible to see vacuoles close to or fused with the apical plasma membrane apparently in the process of releasing their contents into the lumen (fig 17)

Structures associated with resorption.
Also found in all specimens but to a varying degree from cell to cell, are signs of active resorption by the columnar cells—micropinocytotic tubules and vesicles lying just under the apical surface of the cell plus small vacuoles with ill-defined contents multivesicular bodies and dense bodies of assorted sizes deeper in the cell in the Golgi zone or even below the nucleus (figs. 2-4-7-10-12-15-16-21-22). To some degree but only in the younger animals these structures seem to be associated with the presence of cellular debris in the lumen as described in the next paragraph.

In the glands from mice up to two-and-one-half weeks of age debris in the lumen sometimes consists of cell fragments or recognizable free organelles such as mitochondria but more often it consists of unidentifiable particles or a homogeneous dense material (e.g. fig 10). In figure 1 a long ribbon of cytoplasm is shown that appears so unstructured that it probably has been shed into the lumen certainly it is not bound to adjacent cells by a junctional complex. Moreover a few specimens of this young group exhibit what are interpreted as dying cells, filled with lipid droplets dense bodies and empty vesicles they bulge conspicuously into the lumen as though in process of being ejected from the epithelium. These happened to be seen particularly in specimens 7-9 and 10

Most remarkably areas of tissue were found in which there are large masses of protoplasm undergoing intracellular digestion and destruction. Particularly striking is the field shown in figure 13, which is representative of several areas in one 11-day and one 14-day specimen. Here, obviously healthy cells contain within large intracellular vacuoles intact portions of cells consisting not only of recognizable

mitochondria and stacks of Golgi saccules, but even of nuclear masses within nuclear envelopes. The vacuoles can be seen to have two membranes, one presumed to belong to the ingesting cell, the other to be the plasma membrane of the ingested cytoplasm. In the nuclear masses the chromatin exhibits the type of clumped density seen in pyknosis, probably attributable to the dissociation of deoxyribonucleic acid (DNA) and histones (Alfert, '55). Accumulations having the dense banded, crystalline pattern presented by degenerating protoplasm (Bellairs '61)—we think possibly chromatin—have also been found in occasional cells lying close to others with inclusion bodies containing identifiable bits of nucleus or cytoplasm. In some sections cut in the appropriate plane, it could be established that nuclear remains were contained in a cell with a normal nucleus thus indicating that these phenomena were not signs of autodigestion.

No indications of desquamation or of uptake of gross masses of cytoplasm have been seen after 18 days.

Cytoskeleton. No well defined structural organization of the cytoplasm exists, but there are what appear in most preparations from the first two weeks to be cytoplasmic streaks running roughly lengthwise in the cell. With the preparative procedure employed, we have usually been unable to detect any filamentous or substructure in these streaks, but arrangement plus the displacement of structures from the streaks suggest that they mark the presence of a fibrous composing a cytoskeleton. (We have observed such streaks even more commonly in the tall epithelial cells of the epididymidis in young mice (Deane and Friedel, '63).) In a few of the seminal vesicle preparations, in which there is no known difference in preparative technique, such streaks could be resolved into clusters of filaments (e.g. figs. 12, 13). They resemble the keratin filaments reported in stratified epithelium by K. (1961).

In addition, the peripheral layer of cytoplasm, not only at the apex of the cell, but also along the sides and at the base

appears largely free of structures except filaments—in addition to the tubules and vesicles interpreted as indicative of micropinocytosis (fig. 12). This layer thus resembles the terminal web of the columnar cells of the intestine or the ectoplasm of amoeboid cells. The specialization disappears from the seminal vesicle epithelium except at the apex, after about three weeks of age. Possibly the increase in numbers of membranous structures masks the conspicuousness of this feature.

Cilia. An oddity found in this material was several well developed intracellular cilia, an example of which is illustrated in figure 8. A related development has been seen in a 40-day-old specimen, in which the cilium occurred on a basal cell and protruded into the intercellular space. Not only has it been reported earlier that seminal vesicle cells may possess a single flagellum (Macklin and Macklin, '32) but we know that many cells develop cilia, especially during embryonic development (Sorokin, '62; Grillo and Palay '63). From our own experience we can say they are far less frequent in this derivative of the wolffian duct than in the epididymis (Deane and Friedel, '63).

Variability. A point that remains to be stressed is that the preceding descriptions represent the norm found in the samples examined. Particularly with the youngest group in which most cells were so immature it could readily be seen that some variability occurred in the degree of development of the ergastoplasm or Golgi apparatus in cells in different parts of one gland. It seems possible to us that cells close to the wolffian duct, for example might, at any one time be somewhat further differentiated than those near the growing tips, and that such difference might explain the range of images found. Establishing such a speculation would require that the samples be taken from known portions of the gland rather than in the haphazard fashion used here.

Another instance in which a phenomenon appeared highly restricted in location in the samples examined, concerned the instances of ingestion of nuclei (e.g., fig. 13). Here again, only one of five or six blocks sampled per gland showed images

of the types described. The portion of the gland in which these phenomena were taking place could not be determined.

Basal cells

As stated earlier no cells not reaching the lumen could be identified certainly in the youngest specimens. However in one 11-day mouse and in all animals of greater age there appear between the bases of the columnar cells, occasional unspecialized, stellate basal cells. Such cells in the adult, exhibit almost no polyribosomes and relatively few membranous structures in the cytoplasm aside from mitochondria and a small cluster of Golgi lamellae (figs. 21-23 also Deane, '63 fig. 6). The nucleus is pleomorphic, apparently adopting a form compatible with that of the cell as a whole.

Basal cells are relatively rare at first. For example the fields shown in figures 7 and 8 are the only areas in many grids examined in which basal cells were detectable in an 11-day-old specimen and even in these sections only portions of the processes of such cells could be found. The perikarya were not seen. And no stellate undifferentiated cells lacking an abundance of polyribosomes are evident in figure 10 a section of a 13-day gland cut in a plane favorable to their detection. However a pleomorphic nucleus in cytoplasm otherwise like that of neighboring cells is a suggestive image.

Basal cells appear gradually to become more prevalent, although we have made no attempt to determine their ratio to columnar cells at various ages.

In figure 15 is shown an example of a cell that seems somewhat intermediate between a basal cell and a columnar cell. It has less ergastoplasm than its columnar neighbors and it possesses a centriole lying at a low level in the epithelium. One possible interpretation is that this is a case in which a basal cell is differentiating and stretching upward to become a columnar cell. Alternatively it might be in the process of dedifferentiating from a columnar cell.

DISCUSSION

Several points that emerge from this description of the maturation of the epi-

thelial lining of the seminal vesicle of the mouse merit comment and evaluation. (a) Primary interest concerns the sequence of events observed during the growth and differentiation of the immature epithelial cells into secretory ones. (b) The dependence of these several phenomena on a rising titer of androgen will be discussed. Other points we will then consider briefly include (c) the question of the significance of resorptive activity by this developing epithelium (d) the question of the relationship of mitochondria to desmosomes and (e) the question of the nature of the basal cells.

(a) *Differentiation of the secretory epithelium* In broad outline, the maturation of the seminal vesicle epithelium follows closely the pattern exhibited by mammalian pancreatic acinar tissue (cf. Munger '58 Ferreira, '59 Pipen, '61 Kallman and Grobstein, '64). This resemblance is not surprising since the cytological characteristics of the active seminal vesicle cell indicate that its major activity is the secretion of protein (Macklin and Macklin '32; J. Porter and Melampy '52; Melampy and Cavazos, '53 Deane and Porter '60 Price and Williams-Ashma, '61; Szirmai, '62; Deane '63 Cavazos, Belt, Sheridan and Feagans, '64 Moss '64 Chap. 3).

During differentiation, a relatively unstructured immature columnar epithelial cell, containing an abundance of polyribosomes and mitochondria but only a less extended Golgi complex (see K. Porter '51) rapidly develops an extensive ergastoplasm and exhibits enlargement of the Golgi saccules. Subsequently dense proteinaceous material is detectable within Golgi saccules, is formed into granules within large Golgi vacuoles and is released into the lumen.

These associations are consistent with the current working hypothesis that proteins destined for export are synthesized in the ergastoplasm then somehow flow into the Golgi complex where they are condensed into granules, presumably by the withdrawal of water; vacuoles containing such products migrate to the surface and fuse with the plasmalemma to release the contained material from the cell (cf.

De Robertis Nowinski and Saez '60 Palade, Siekevitz and Caro '62 Palade, '64) Dynamic evidence for this hypothesis on pancreatic acinar cells has been adduced by Caro and Palade ('64) using an isotopically labeled amino acid and autoradiography of electron microscopic preparations. A corresponding study on chondroblasts was made by Revel and Hay ('63). In the present material, there are of course gaps in the morphological evidence for the hypothesis. For example we have never seen unequivocal examples of direct continuity between ergastoplasmic channels and Golgi saccules. Such fusion must be extremely transient.

Based on their discussion on the recently acquired evidence for the message-reading capacity of aggregated ribosomes or polyribosomes (e.g., Warner et al. '62; Watson, '63; Gierer '63; Malt and Speakman, '64; Hultin, '64) Grobstein ('64) and Kallman and Grobstein ('64) have stressed the importance of the occurrence of such ribosomal aggregates before secretory activity is initiated. This topic has also been considered extensively for a somewhat different protein-secreting cell by Ross and Benoit ('64). The immature seminal vesicle epithelium similarly exhibits polyribosomes before the ergastoplasm differentiates and secretion begins. They also occur in the secretory cells of the adult. Polyribosomes have been shown to persist in other adult cells — e.g. the pancreatic acinar cell (Palade Siekevitz and Caro '62) and the liver cell (Björkman, '64).

The increase in membranous components of the cytoplasm is of course the single most impressive development during cell maturation. For the differentiating neuroblast, the increase in the proportion of the cytoplasm occupied by ergastoplasmic membranes was quantified by Bellairs ('59). Other examples have been discussed by K. Porter ('61) and Moulé ('64). In comparison to the amount of effort applied to the investigation of the role of the nucleus and of RNA in differentiation and function, very little has yet been made to elucidate the role of phospholipid or lipoprotein membranes. However it is known that isolated ergastoplasmic membranes carry several important enzymes (Ernst Siekevitz and

Palade '62 Schneider and Kuff '64) and that there is considerable turnover of phospholipids during secretion (Hokin and Hokin '62). Recently Hörchner Kassenaar and Querido ('63) have demonstrated that testosterone stimulates the synthesis of phospholipids in the seminal vesicle.

So far we have emphasized the protein secretion by the seminal vesicle. It should be remembered, however that these cells form and release additional products, notably fructose, sorbitol, and citric acid (Price and Williams-Ashman, '61 Mann, '64 Chap. 10 Baillie '64). There is still no evidence as to which organelles if any might be concerned with the formation and transport of small organic molecules. It seems noteworthy however that the distention of the ergastoplasm in this tissue is inversely related to shifts in the osmolarity of the fixing solution (Deane '63). This relation suggests the possibility that the ergastoplasmic cisternae contain considerable amounts of small osmotically active substances. Moreover the mature Golgi vacuoles also exhibit a large perigranular space. This space, present even in the unfixed gland, may also contain a solution rich in hexoses, polyols and organic ions. In considering the quite comparable cytological features of the posterior lobe of the rabbit prostate gland, Schantz ('64) similarly concluded that such large vacuoles might contain a fructose solution in addition to the protein granule.

(b) *Androgen dependence of growth and differentiation.* For the seminal vesicle induction and subsequent differentiation of the organ are attributed to androgens (see Introduction). Differentiation of the cells a rising mitotic rate and signs of protein and other secretion have all been associated with a minimal or rising level of circulating androgen. It may be supposed that the primary effect of the androgen is to activate genes (e.g. Karlsson '61 Watson '63; Moses, '64 Williams-Ashman et al. '64). This topic has been tackled by Kidson and Kirby ('64) in relation to testosterone. However this influence is ordinarily the one least susceptible of evaluation by electron microscopy.

Price ('38 44 47) has demonstrated that growth and differentiation of the seminal vesicle epithelium slow down rapidly and then cease after castration of the neonatal or young rodent but can be restored readily with administration of small amounts of androgen. She based her conclusion on determinations of mitotic activity increases in cell height, development of light (Golgi) zones and appearance of secretory granules in Bouin fixed material. A repetition of these experiments using electron microscopy to evaluate cytological responsiveness at a higher level of resolution, should contribute even more information.

Our present observations suggest that an increase in hormonal activation must occur at about the end of the first postnatal week, when there is first a rise in mitotic rate then a maturation of ergastoplasm and Golgi apparatus. Some secretory granules have been seen as early as 11 days and they become prevalent by 15-18 days.

So far as mitosis in the epithelium of the seminal vesicle is concerned, Allen ('58) has shown that this reaches a peak 48-54 hours after the administration of a single small dose of testosterone to adult mice castrated 30 days earlier. Similar

its were obtained by Cavazos and Elampy ('54) with rats. It should be noted that castration of neonatal animals did not cause a complete cessation of cell division (Price 44). Whether this reflected the presence of extragonadal androgen or other stimuli has not been determined. Normally there is almost no mitosis in this epithelium in adult mice (Palc '64).

Using long-term castrated mice Kochakian and Harrison ('62) and Kassenaar, Kouwenhoven and Querido ('62) found that androgens increase the total and relative amounts of ribonucleic acid (RNA) in seminal vesicles as did Rabinovitch, Junqueira and Rothchild ('51) with rats and Kochakian ('64) with guinea pigs. Wicks and Kenny ('64) reported that the stimulus to RNA synthesis is demonstrable within 70 minutes after testosterone administration. The RNA may be presumed to be derived principally from the epithelial cells — from their nuclei, the ribo-

somes and the soluble RNAs. In histological preparations the expected changes in cytoplasmic basophilia that is attributable to RNA occur with castration and the administration of androgen. However for some still unexplained reason castration of the adult mouse (in contrast to other species) is not followed by any conspicuous decline in the population density of ribosomes in seminal vesicle cells (Dene and Porter '60 Szirmai, '63) although the total number per cell of course drops. A re-examination of such material prepared by the improved methods now available should be undertaken.

Protein secretion by the seminal vesicles has not yet been measured in such small animals as the mouse, although the steady rise in number and size of the secretory granules within the cells and in the glandular lumen of maturing mice is certainly suggestive. However for the rat, J. Porter and Melampy ('52) demonstrated shifts in the amount of the protein in castrated and testosterone-treated animals and Wilson ('61) demonstrated increased incorporation of isotopically labeled amino acids in the seminal vesicles of rats treated with testosterone. For the guinea pig, Kochakian, Hill and Costa ('64) have presented analytical data showing that the protein secretion is androgen-dependent. Kochakian ('64) has demonstrated a rise in amino acid incorporation into seminal vesicle protein when testosterone is given to gonadectomized guinea pigs. Other examples are reviewed by Mann ('64, Chap. 12). The relation between RNA synthesis and protein synthesis, as stimulated by testosterone has been discussed, *inter alia*, by Wilson ('61), Wicks and Kenny ('64), Kochakian ('64) and Williams-Ashman, Liao, Hancock, Jurkowitz and Silverman ('64).

So far as the secretion of smaller molecules is concerned, Baillie ('64) has recently compared the activity of steroid hormone synthesizing enzymes, such as Δ -3 β -hydroxysteroid dehydrogenases, in developing mouse testis with the quantity of fructose and citric acid secreted by the seminal vesicle. He found that fructose was already detectable in the fluid that could be withdrawn from the seminal vesicle at three weeks of age; thereafter

it rose steadily to a peak at eight weeks. This pattern resembled the change in steroid-synthesizing ability of testicular interstitial tissue. It has been demonstrated in maturing bulls that the rise in citrate and fructose secretion closely parallels the increase in testicular androgen (Lindner and Mann '60; Lindner and Mann, '61; Mann, '64; Chap. 12).

Finally it might be noted that for the rat ventral prostate and apparently for other accessory glands as well, Rosenkrantz, Castle and McLaughlin ('62) obtained data showing a marked rise in the level of dehydrogenase activity between 15 and 21 days of postnatal life, with peak activity reached by 28 days. Most such enzymes are generally considered to reside in mitochondria. No striking changes were evident in number or structure of the mitochondria in our material, so that it seems likely that the acquisition of enzymic activity need not necessarily be associated with morphological change.

(c) *Signs of cellular destruction and resorption.* Evidence for the sloughing of some epithelial cells, and then for the resorption of the debris or even of large fragments thereof, seemed conspicuous in the younger specimens before secretory activity became prominent.

A useful consideration, in this regard, concerns the hypothesis developed by Glöcksmann ('51-'64) viz. that during morphogenesis the remodeling of a tissue or organ requires that certain cells be discarded and destroyed even though they are perfectly healthy. Of particular interest is Glöcksmann's description of how the fragments of the discarded cells are ingested by their neighbors, their nuclei being completely digested within one to seven hours. This process is far faster than ordinary necrosis, and might easily be overlooked.

Using light microscopic techniques, Bengmark and Forsberg ('59) have remarked on the prevalence of such desquamation and resorption in the morphogenesis of the ducts and glands of the genital tracts in both sexes and more recently Bengmark and Nilsson ('62) have reported signs of cellular destruction and resorption during the formation of the human seminal vesicle. Evidence of nu-

clear destruction was located principally in the neck of the gland which was shrinking at the same time that the rest of the gland was enlarging rapidly. Similar conclusions were reached by Clegg ('69) for rat seminal vesicle though on the basis of fewer specimens. In our material, the location within the gland of the areas showing signs of cellular resorption is unknown (see p. 97).

A previous study with the electron microscope, showing such phenomena of cell death and resorption during normal embryogenesis has been reported by Belairs ('61) her pictures of ingested, pyknotic nuclei and of crystallized, protoplasmic debris in cells of chick blastoderm paralleled our own findings. Others have described signs of destruction of portions of cells during tissue differentiation but not the phagocytosis of one cell by another (e.g. Behnke, '63).

It is important to emphasize however that the apparatus for one form of resorptive activity — that involving micropinocytotic tubules and vesicles plus multivesicular bodies, coupled with the resulting dense bodies and residual bodies (Novikoff, '61-'63) — occur in seminal vesicle epithelium throughout life long after there is any evidence of cell sloughing. What do such signs indicate? One possibility seems to be that there is constant resorption of secreted materials by this epithelium. Even though these mice when mature were generally kept with females, and even though male mice are said to have small ejaculations in the absence of the opportunity for copulation, there may be steady pressure in the seminal vesicle, which induces some resorption of luminal contents. That this epithelium indefinitely retains the ability to resorb is underlined by the fact that almost all of the stored secretory material is taken up from the lumen within a week after castration, apparently through active ingestion by the columnar cells (Deane and Porter '60 and later observations). This type of activity namely absorption rather than secretion is of course dominant in many other epithelia derived from the wolffian duct, notably those in the ductuli efferentes and ductus epididymidis (e.g., Shaver '54; Nicander '57; Burgos '64).

(d) Mitochondrial-desmosome complexes

A striking association observed repeatedly in this material has been the flanking of desmosomes by mitochondria. The fact that no such associations were seen in animals more than a month old makes it possible that this relation is somehow concerned with the formation of desmosomal attachments between cells. Yet such associations have not previously been described or illustrated, to our knowledge—even in a study directly concerned with reformation of desmosomes after the dissociation of embryonic cells (Overton '62).

We cannot help but be impressed with the frequent accumulation of electron-dense material between the mitochondrion and the thickened plasma membrane. Is this material derived from the mitochondrion or is it formed under its influence? One possibility that comes to mind is that the material may contain a high concentration of divalent cations such as calcium ions. Sedar and Forte ('64) have demonstrated that calcium is an important factor governing the adherence of cells at desmosomes and zonulae adherentes. Since the dense granules in mitochondria seem to be repositories of divalent cations (Peschey '64; Lehninger '64) perhaps the mitochondria are the source of this constituent for desmosomes. We hope to pursue the study of this association.

(e) Basal cells A final topic that we find intriguing is the nature of the basal cells. These seem generally interpreted as reserve cells (Macklin and Macklin, '32; Bern '63; Lasnitzki, '63). Yet in our own experience mitotic figures occur in columnar cells and rarely if ever in basal ones. The presence of some cells intermediate in appearance between the undifferentiated basal cell and the highly specialized columnar cell has been noted here and similar images were seen (though not reported) in a previous study when testosterone had been administered to adult mice (Deane and Porter '60). The point remains however that there is no direct evidence of which we are aware to show that basal cells can in fact differentiate into secretory cells. Cell modulation might involve dedifferentiation as well as differentiation.

A pertinent reason for believing the basal cells are formed by dedifferentiation is their complete absence from the mouse seminal vesicle before ten days of age. Not surprisingly no hint of this fact seems to have previously been made for seminal vesicle since it is only by electron microscopy that the identification of basal cells can be made with any confidence. However it is interesting that Benoit ('6) found that basal cells are absent from mouse epididymis at birth and first become evident at five days. He too concluded that they represent columnar cells that have retracted from the lumen.

The cytological features of basal cells observed by electron microscopy do not suggest, however, that they are simply collapsed columnar cells. In addition to the marked differences in form of the cell and of its nucleus, the cytoplasm of a typical basal cell is far less differentiated than even that of an immature columnar cell. From all observations we have made thus far we can only conclude that the basal cell does indeed derive, by dedifferentiation, from the columnar cell. We certainly have never seen the slightest evidence of an invasion of the epithelium through the basement lamina. If dedifferentiation is indeed the origin of basal cells, however the significance of their occurrence and the nature of the stimulus causing the process remain completely unknown. Since basal cells are widely distributed in the male reproductive system but not common in other systems, their nature deserves renewed study.

ACKNOWLEDGMENTS

This paper was completed while the senior author was on sabbatical leave in part supported by a fellowship from the Commonwealth Fund. She wishes to express her appreciation to Professor J. Dixon Boyd, The Anatomy School University of Cambridge, England, for generous provision of facilities during this period.

LITERATURE CITED

- Alpert, M. 1955 Changes in the staining capacity of nuclear components during cell degeneration. *Biol. Bull.* 100: 1-12.
Allen, J. M. 1958 The influence of hormones on cell division. II. Time response of ac-

- seminal vesicle, coagulating gland and ventral prostate of castrate mice to single injection of testosterone propionate. *Exp. Cell Res.*, 14: 143-148.
- Artlitz, H. R., M. N. R. Prasad and R. K. Meyers 1960 Action of prolactin on seminal vesicles of guinea pigs. *Proc. Soc. Exp. Biol. Med.*, 103: 77-80.
- Baillie A. H. 1961 Observations on the growth and histochemistry of the Leydig tissue in the postnatal prepubertal mouse testis. *J. Anat. (Lond.)* 95: 357-370.
- 1964 Further observations on the growth and histochemistry of the Leydig tissue in the postnatal prepubertal mouse testis. *J. Anat. (Lond.)* 98: 403-419.
- Behnke O. 1963 Demonstration of acid phosphatase-containing granules and cytoplasmic bodies in the epithelium of foetal rat duodenum during certain stages of differentiation. *J. Cell Biol.*, 18: 251-255.
- Bellairs, R. 1959 The development of the nervous system in chick embryos. *J. Embryol. Exp. Morph.*, 7: 94-115.
- 1961 Cell death in chick embryos as studied by electron microscopy. *J. Anat. (Lond.)* 95: 54-60.
- Bergmark, S., and J. G. Forsberg 1960 Some remarks on degeneration granules in the genital sphere. *Z. Zellforsch.*, 49: 604-606.
- Bergmark, S., and S. Nilsson 1962 The human seminal vesicle. I. The morphogenesis of the seminal vesicle. *Acta Chir. Scand., Suppl.* 296: 7-31.
- Bernot, J. 1926 Recherches anatomiques, cytologiques et histophysiologiques sur les voies excrétrices du testicule, chez les mammifères. *Arch. Anat. Histol. Embryol.* 5: 173-418.
- Bern, H. A. 1963 Discussion. *Nat. Cancer Inst. Monogr.* 12: 105-106.
- Björkman, N. 1964 Aggregated ribosomes in liver cells. In: *Electron Microscopy* Ed. M. Tliffach. Prague, Czech. Acad. Sci. Vol. B., pp. 35-36.
- Burgos, M. H. 1964 Uptake of colloidal particles by cells of the caput epididymidia. *Anat. Rec.* 148: 517-523.
- Burnes, R. K. 1961 Role of hormones in the differentiation of sex. In: *Sex and Internal Secretions*, 3rd ed., Ed. W. C. Young. Baltimore: Williams and Wilkins. Vol. I, Chap. 2, pp. 78-158.
- Caro, L. G. and G. E. Palade 1964 Protein synthesis, storage and discharge in the pancreatic acinar cells. *J. Cell Biol.*, 20: 473-495.
- Cavazos, L. F. and R. M. Melampy 1954 Cytological effects of testosterone propionate on epithelium of rat seminal vesicles. *Endocrinology* 54: 840-848.
- Cavazos, L. F. W. D. Belt, M. N. Sheridan and W. M. Ferguson 1964 The fine structure of the hamster seminal vesicles with reference to pigment formation. *Z. Zellforsch.*, 63: 179-193.
- Chase, M. D. I. I. Geschwind and H. A. Bern 1957 Synergistic role of prolactin in response of male rat sex accessories to androgen. *Proc. Soc. Exp. Biol. Med.*, 94: 680-683.
- Clegg, E. J. 1959 Postnatal changes in the histology of the seminal vesicle and coagulating gland in the rat. *J. Anat. (Lond.)* 93: 361-367.
- Costa, G., C. D. Kochakian and J. Hill 1962 Effect of testosterone propionate on the incorporation of glycine-3-C¹⁴ in guinea pig tissues. *Endocrinology* 70: 175-181.
- Deane, H. W. 1963 Electron microscopic observations on the mouse seminal vesicle. *Nat. Cancer Inst. Monogr.* 12: 63-83.
- 1964 Maturation of seminal vesicle epithelium in the laboratory mouse. In: *Electron Microscopy* Ed. M. Tliffach. Prague, Czech. Acad. Sci. Vol. B., pp. 581-583.
- Deane H. W. and W. E. Friedel 1963 Electron microscopic observations on the maturation of the epithelium of the caput epididymidis of the laboratory mouse. Unpublished observations.
- Deane H. W. and K. R. Porter 1960 A comparative study of cytoplasmic basophilia and the population density of ribosomes in the secretory cells of mouse seminal vesicle. *Z. Zellforsch.*, 52: 667-711.
- Deanesly R. 1958 Secretion of androgens by the adrenal cortex of the mouse. *Nature (Lond.)* 182: 263-265.
- 1960 A test of androgen production by the rat adrenal. *J. Endocrin.*, 20: vii-viii.
- Demuth, F. 1941 Züchtung von Knochen-Samenblase in vitro und Testosteron. *Acta Brevia Neerl.*, 11: 116-123.
- De Robertis, E. D. P. W. Nowinski and F. A. Sax 1960 General Cytology 3rd ed. Philadelphia and London, Saunders. Chap. 6, pp. 131-168.
- Dorfman, R. L. and R. A. Shipley 1956 Androgens. New York, Wiley.
- Ernst, L., P. Siekevitz and G. E. Palade 1962 Enzyme-structure relationships in the endoplasmic reticulum of rat liver. *J. Cell Biol.*, 15: 541-562.
- Farquhar M. G., and G. E. Palade 1963 Junctional complexes in various epithelia. *J. Cell Biol.*, 17: 375-418.
- Ferreira, J. F. D. 1950 A diferenciação do condriome, aparelho de Golgi e ergastoplasma. Lisboa, Inst. de alta Cultura, 214 pp.
- Gierer A. 1963 Function of aggregated reticulocyte ribosomes in protein synthesis. *J. Mol. Biol.*, 6: 146-157.
- Glücksmann, A. 1951 Cell deaths in normal vertebrate ontogeny. *Biol. Rev.* 26: 59-86.
- 1964 Mitosis and degeneration in the morphogenesis of the human foetal lung in vitro. *Z. Zellforsch.*, 64: 101-110.
- Gelfo, M. A., and S. L. Palay 1963 Ciliated Schwann cells in the autonomic nervous system of the adult rat. *J. Cell Biol.*, 18: 430-438.
- Grobstein, C. 1964 Cytodifferentiation and its controls. *Science*, 143: 643-650.
- Hay M. F. H. R. Lindner and T. Mann 1961 Morphology of bull testes and seminal vesicles in relation to testicular androgens. *Proc. Roy. Soc., B*, 154: 433-449.
- Hokin, L. E., and M. R. Hokin 1962 The synthesis and secretion of digestive enzymes by

- pancreatic tissue *in vitro*. Ciba Founda. Symp., The Exocrine Pancreas. London, J and A. Churchill, pp. 188-207.
- Hörchner P. A. A. H. Kassehaar and A. Querido 1963 Influence of testosterone (propionate) on the phospholipid metabolism in the seminal vesicle of castrated male rats. *Acta Physiol. Pharmacol. Neerl.*, 12 163-164.
- Howard, E. 1959 Effects of castration on the seminal vesicles as influenced by age, considered in relation to the degree of development of the adrenal X zone. *Am. J. Anat.*, 65 205-249.
- 1948 The effect of adrenalectomy on the accessory reproductive glands of mice castrated for short periods. *Endocrinology* 38 186-194.
- Howard, E., and C. J. Milgrom 1962 Sex hormone secretion by the adrenal cortex. *Handb. Exp. Pharmacol.*, Erg W 14/1 Chap 5, pp. 670-687.
- Holtin, T. 1964 Ribosomal functions related to protein synthesis. *Internat. Rev. Cytol.*, 18 1-30.
- Jost, A. 1948 Le controle hormonal de la différenciation du sexe. *Biol. Rev.* 23 201-236.
- 1963 Problems of fetal endocrinology. The gonadal and hypophyseal hormones. *Recent Progr. Hormone Res.*, 8 379-418.
- 1957 La fonction endocrine d testicule foetal. In *La Fonction Endocrine du Testicule*. Paris, Masson.
- Kallman F and C. Grubstein 1964 Fine structure of differentiating mouse pancreatic endocrine cells in transfilter culture. *J. Cell Biol.*, 90 309-413.
- Karlson, P. 1961 Biochemische Wirkungsweise der Hormone. *Dtsch. Med. Wochr.* 86 668-674.
- Kassehaar A., A. Koorssenhoven and A. Querido 1962 On the metabolic action of testosterone and related compounds. V The effect of testosterone on the nucleic acid composition of seminal vesicles and kidneys of mice. *Acta Endocrinol. (Kbh.)* 39 223-233.
- Kidson, C., and E. S. Kirby 1964 Selective alteration of mammalian messenger-RNA synthesis: Evidence for differential action of hormones on gene transcription. *Nature*, 203 599-603.
- Kochakian, C. D. 1964 Effect of castration and testosterone on protein biosynthesis in guinea pig testis preparations. *Acta Endocrinol. (Kbh.) Symp.* 22 16 pp.
- Kochakian, C. D. and D. G. Harrison 1962 Regulation of nucleic acid synthesis by androgens. *Endocrinology* 70: 99-102.
- Kochakian, C. D. J. Hill and G. Costa 1964 Amino acid composition of the proteins of the muscles and organs of the normal, castrated and testosterone treated guinea pig. *Acta Endocrinol. (Kbh.)* 45: 813-822.
- Luzzatli, L. 1958 The effect of carcinogens, hormones and vitamins on organ cultures. *Internat. Rev. Cytol.*, 7 40-121.
- 1963 Growth pattern of the mouse prostate gland in organ culture and its response to sex hormones vitamin A, and 3-methylcholanthrene. *Nat. Cancer Inst. Monogr.* 12: 391-403.
- Kahniger A. L. 1964 The Mitochondria. New York and Amsterdam, Benjamin. Co. 8 pp 157-179.
- Lindner H. R., and T. Mann 1960 Relationship between the content of androgenic steroid in the testes and the secretory activity of its seminal vesicles of the bull. *J. Endocrine* 21 341-360.
- Lustroh, A. J. 1962 Effect of testosterone and growth hormone on muscle acid and protein in the sex accessory glands of Long-Evans and Sprague-Dawley rats. *Endocrinology* 70: 10-749.
- Laft, J. H. 1961 Improvement in epoxy resin embedding methods. *J. Microsc. Techn. Cytol.*, 9 408-414.
- Macklin, C. C., and M. T. Macklin 1933 The seminal vesicles, prostate, and bulbourethral glands. In *Special Cytology* 2nd ed. Ed. L. V. Cowdry. New York, Hoeber Vol. 2, p. 173-182.
- Malt, R. A., and P. T. Speakman 1964 The social aggregates associated with the production of collagen. *Lif. Sciences*, 3 81-84.
- Mann T. 1964 The Biochemistry of Testes and of the Male Reproductive Tract. London, Methuen.
- Melampy R. M., and L. F. Cavazos 1953 Effects of testosterone propionate on biochemical reactions of rat seminal vesicles. *Endocrinology* 52 173-187.
- Moore, C. R. 1959 Biology of the testes in Sex and Internal Secretions, 2nd ed. Ed. E. Allen, C. H. Deane and E. A. Dost. Baltimore, Williams and Wilkins. Chap. 7 p. 353-451.
- 1951 Experimental studies on the male reproductive system. *J. Urol.*, 65 497-502.
- Moses, M. J. 1964 The nucleus and chromosomes: A cytological perspective. In *Chromosomes and Cell Physiology* 2nd ed., Ed. G. H. Beatty. Oxford Univ. Press, pp. 493-566.
- Moula, Y. 1964 Endoplasmic reticulum and microsome of rat liver. In: *Cellular Mechanisms in Development*, Ed. M. Locke. New York and London, Academic Press, pp. 97-113.
- Munger B. L. 1958 A phase and electron microscopic study of cellular differentiation in pancreatic acinar cells of the mouse. *Am. J. Anat.*, 103 1-19.
- Niesender L. 1967 On the regional identity and cytochemistry of the ductal epithelium in rabbits. *Acta Morph. Neerl.-Scand.* 1 9-114.
- Northcutt, A. B. 1961 Lysosomes and related particles. In: *The Cell*, Ed. J. Brucher and J. E. Minsky. New York and London, Academic Press, Vol. II, pp 423-482.
- 1963 Lysosomes in the physiology and pathology of cells. Contributions of electron methods. (Ciba Found. Symp., Lysosomes Lecture, Churchill, pp. 25-77.
- Overton, J. 1962 Mesodermic development in normal and reassociating cells in the rat chick blastoderm. *Dev. Biol.*, 4 532-541.

- Palade G. E. 1964 The organization of living matter. *Proc. Nat. Acad. Sci. (U.S.)* 52: 613-634.
- Palade, G. E., P. Flakavitz and L. G. Caro 1962 Structure, chemistry and function of the pancreatic acinar cell. *Ciba Found. Symp., The Exocrine Pancreas*. London, Churchill, pp. 23-53.
- Parkes, A. S. 1953 Endocrinology of the testis. *Brit. Med. Bull.* 11 106-110.
- Peschay L. D. 1964 Electron microscopic observations on the accumulation of divalent cations in intramitochondrial granules. *J. Cell Biol.* 20: 95-109.
- Pale, E. R. 1964 Labelling of DNA and cell division in so called non-dividing tissues. *J. Cell Biol.* 22: 21-25.
- Papan, N. 1960 Licht und elektronenmikroskopische Untersuchungen über die Differenzierung des embryonalen Pankreas der Maus. *Z. Zellforsch.* 52: 291-314.
- Pomes, K. 1950 La fonction sexuelle de la cortico-surrénale. *J. Suisse Méd.* 7 170-180.
- Porter, J. C., and R. M. Melampy 1962 Effects of testosterone propionate on the seminal vesicle of the rat. *Endocrinology* 51 412-420.
- Porter K. R. 1961 The ground substance; observations from electron microscopy. In: *The Cell*. Ed. J. Brachet and A. E. Mirsky. New York and London, Academic Press. Vol. II, Chap. 9, pp. 621-675.
- Price, D. 1958 Normal development of the prostate and seminal vesicles of the rat, with study of experimental post-natal modifications. *Am. J. Anat.* 60 79-127.
- 1944 The development of reactivity in the accessory reproductive organs of castrated and spayed rats injected with testosterone propionate. *Physiol. Zool.* 17 377-391.
- 1947 An analysis of the factors influencing growth and development of the mammalian reproductive tract. *Physiol. Zool.* 20 213-247.
- Price, D., and D. J. Ingle 1957 Androgenic effects of autotransplants of adrenals in the accessory reproductive glands of adult castrated rats. *Rev. Suisse Zool.* 64 743-753.
- Price, D. and R. Farnbacher 1956 Organ culture studies of foetal rat reproductive tracts. *Ciba Found. Coll., Ageing*, 2: 3-12.
- 1950 Comparative responsiveness of homologous sex ducts and accessory glands of foetal rats in culture. *Arch. Anat. Micro. Morph. Exp.* 48 (Suppl.): 223-243.
- Price D. and H. G. Williams-Ashman 1961 The accessory reproductive glands of mammals. In: *Sex and Internal Secretions*, 3rd. ed. Ed. W. C. Young, Baltimore, Williams and Wilkins. Vol. I, Chap. 8, pp. 366-463.
- Rabinovitch, M., L. C. U. Junqueira and H. A. Rothchild 1951 Influence of testosterone on nucleic acid phosphorus of rat seminal vesicle. *Science*, 114 531-532.
- Ravel, J-P and E. D. Hay 1963 An autoradiographic and electron microscopic study of collagen synthesis in differentiating cartilage. *Z. Zellforsch.* 61 110-144.
- Reynolds, E. S. 1963 The use of lead citrate at high pH as an electron-opaque stain in electron microscopy. *J. Cell Biol.* 17 208-212.
- Richardson, K. C., L. Jarrett and E. H. Flinks 1960 Embedding in epoxy resins for ultrathin sectioning in electron microscopy. *Stain Technol.* 35: 313-323.
- Robbins, E., and M. E. Gonatas 1964 The ultrastructure of a mammalian cell during the mitotic cycle. *J. Cell Biol.* 21 429-463.
- Rosenkrantz, H., V. Castle and E. R. McLaughlin 1963 Influence of ablation, hormones and age on the enzyme systems in the tissues of the male rat. *Endocrinology* 71 307-313.
- Ross, R., and E. P. Benditt 1964 Wound healing and collagen formation. IV. Distortion of ribosomal patterns of fibroblasts in scurvy. *J. Cell Biol.* 22: 363-389.
- Schantz, B. 1964 Electron microscopy observations on the posterior lobe of the prostate gland in rabbits. *Acta A.* 56 54-60.
- Schneider W. C., and E. L. Kuff 1964 Centrifugal isolation of subcellular components. In: *Cytology and Cell Physiology* 3rd ed., Ed. G. H. Bourne. Oxford Univ. Press, pp. 19-89.
- Sedar, A. W. and J. G. Forte 1964 Effects of calcium depletion on the junctional complex between oxyntic cells of gastric glands. *J. Cell Biol.* 22: 173-188.
- Shaver, S. L. 1964 The role of starodilia in removing India ink particles from the lumen of the rat epididymis. *Anat. Rec.* 119 177-185.
- Snell, G. D. 1941 Biology of the Laboratory Mouse. Philadelphia, Blakiston. Chap. 2, Reproduction, pp. 53-88.
- Sorokin, E. 1962 Centrioles and the formation of rudimentary cilia by fibroblasts and smooth muscle cells. *J. Cell Biol.* 15 363-377.
- Sotomai, J. A. 1962 Histological aspects of the action of androgens and estrogens. *Ciba Symp., Protein Metabolism*. Berlin, Springer pp. 45-77.
- Turner C. D. 1960 General Endocrinology 3rd ed. Philadelphia, Saunders. Chap. 3, The biology of sex and reproduction, pp. 273-330.
- Warner, J. R., A. Rich and C. E. Hall 1962 Electron microscope studies of ribosomal clusters synthesizing hemoglobin. *Science*, 128 1299-1303.
- Watson, J. D. 1963 Involvement of RNA in the synthesis of proteins. *Science*, 140 17-26.
- Wells, L. J. 1963 Experimental studies of the role of the developing gonade in mammalian sex differentiation. In: *The Ovary* Ed. S. Zuckerman. New York and London, Academic Press. Vol. II, Chap. 14A, pp. 121 153.
- Wicks, W. D. and F. T. Kenny 1964 RNA synthesis in rat seminal vesicles. Stimulation by testosterone. *Science*, 144 1346-1347.

- Wiesner B. P. 1934 The post-natal development of the genital organs in the albino rat. *J Obstet. Gynaec. Brit. Exp.* 41 867-922.
- Williams-Ashman, H. G., S. Liao, R. L. Hancock, L. Jankowitz and D. A. Silverman 1964 Testicular hormones and the synthesis of ribonucleic acids and proteins in the prostate gland.

Rec. Progress Hormone Res., 20: 347-371.

Wilson, J. D. 1961 Localization of the biochemical site of action of testosterone on protein synthesis in the seminal vesicle of the rat. *J. Clin. Invest.*, 41 153-161.

Unless otherwise described, all electron micrographs are from seminal vesicles fixed in osmium tetroxide solution containing 5% sucrose. The sections were stained with a lead citrate-uranyl acetate sequence. The marker indicates 1 μ . The light micrographs are of thicker epoxy sections, stained with methylene blue and azure II and photographed with a yellow filter.

Abbreviations

BC, basal cell	JC junctional complex (terminal bar)
BL, basement lamina (membrane)	L, glandular lumen
BV blood vessel	M, mitochondrion
C, centriole	MP microplasmic tubules and vesicles
CD cellular debris in lumen	MV multivesicular body
Cl, cilium	NE, nuclear envelope
D, desmosome	NP nuclear pore
DB dense body (? lysosome)	Nu, nucleolus
Ec, ectoplasm	P polyribosomes; aggregated ribosomes
Er ergastoplasm; rough-surfaced endoplasmic reticulum	R, residual body
GZ, Golgi zone	S cytoplasmic streak, cytoskeleton
IG intercellular gap	SG secretory granules
IT interstitial tissue	SM, smooth muscle cell
	St, studlike attachment of cells

PLATE 1

EXPLANATION OF FIGURES

Figures 1 and 2 Seminal vesicle of a five-day-old mouse; vertical sections through mucosa.

- 1 A 1- μ section, $\times 720$. The epithelial cells appear tall and so narrow that the nuclei of adjacent cells lie at different levels between the base and the apex. The lumen is collapsed.
- 2 An ultrathin section, $\times 11,200$. The pseudostratified organization of the epithelium is evident. All cells are similar with the cytoplasm containing mainly mitochondria (M) and clusters of ribosomes (polyribosomes) together with compact stacks of Golgi saccules and associated small vesicles (GZ) in the supranuclear region. There are only scattered, short segments of ergastoplasm (rough-surfaced endoplasmic reticulum Er). Clear cytoplasmic streaks (S) presumably consisting of clusters of microfilaments, occur at all levels of the cell. The peripheral cytoplasm, or ectoplasm (Ec) along the sides and particularly at the apex of the cell, is relatively free of structures other than tubules and vesicles, which are suggestive of microplasmic activity (MP). The apical membrane exhibits some microvilli. What appears to be desquamated cellular debris (CD) occupies much of the lumen (L). The epithelial cells are closely packed, except for one intercellular gap (IG). The elongated nuclei are relatively pale, but they exhibit complex nucleoli (Nu) and some pores (NP). Additional labels: D desmosome; DB dense body IT interstitial tissue; JC, junctional complex (terminal bar); MV multivesicular body St, studlike attachment.



PLATE 2

EXPLANATION OF FIGURES

Figures 3 and 4 Seminal vesicle of a five-day-old mouse, same specimen as in figures 1 and 2.

- 3 The basal portion of the epithelium plus some of the underlying tissue, $\times 11,360$. The basal cytoplasm contains principally clusters of ribosomes (polyribosomes, P) scattered mitochondria (M) and few dense bodies (DB). Only occasional wisps of ergastoplasm (Er) occur. The cells appear to be quite extensively interdigitated along their bases (see fig. 10). The thin basement, or boundary lamina (BL) rests in turn on narrow interstitial space containing isolated collagenous fibrils, some attenuated cells (probably fibroblasts) and primitive smooth muscle cells (SM).
- 4 Apices of several columnar epithelial cells, $\times 15,400$. The supranuclear portion of the cell contains collapsed, clustered Golgi saccules (GZ) with their associated small vesicles, plus numerous mitochondria (M) an abundance of polyribosomes (P) and few segments of ergastoplasm (Er). Dense bodies (DB) and multivesicular bodies (MV) occur regularly. The apical surface is thrown into short microvilli, which fill the collapsed lumen (L). Adjacent cells are tightly joined by junctional complex (JC)-desmosome system. In two parts of the field, desmosome below junctional complex is closely flanked by mitochondria (arrows). The nuclear envelope (NE) appears double, but the outer membrane is not visibly studded with ribosomes. Ec, layer of apparently unstructured ectoplasm.

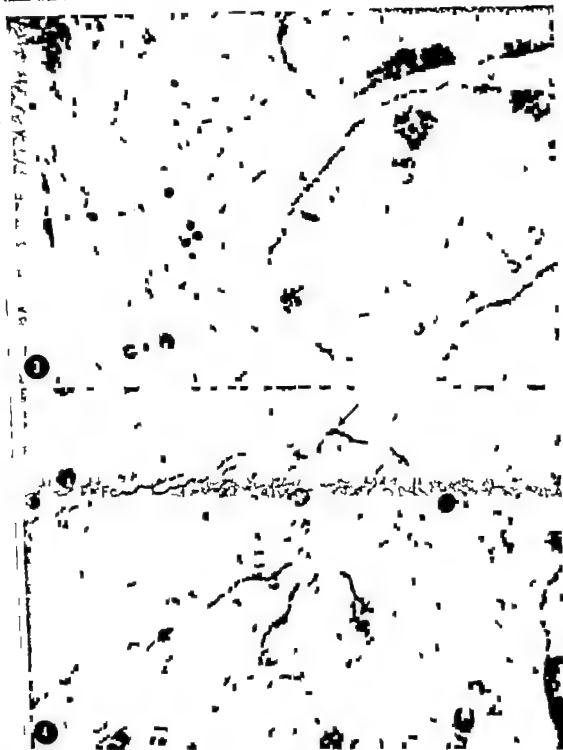


PLATE 3

EXPLANATION OF FIGURES

Figures 5 and 6 Seminal vesicle of an eight-day-old mouse. Especially during the second week, the epithelium of the seminal vesicle exhibits numerous mitotic figures.

- 5 A light micrograph $\times 720$. A late anaphase figure can be seen in the middle of the field; several other nuclei show the condensation of chromatin suggestive of early prophase.
- 6 An electron micrograph, $\times 9,940$. The mitotic figure shown is also probably in anaphase. A centriole (C) and part of the spindle lie to the left of the cluster of chromosomes. At several points around the chromosomes, short segments of endoplasmic reticulum (arrows) may be seen coalescing to produce the nuclear envelope. The nuclei of nearby cells show condensation of chromatin and active-appearing nucleoli (N). Additional labels: D desmosome; DB dense body; GZ, Golgi zone; IG intercellular space; JC junctional complex; L, lumen.



PLATE 4

EXPLANATION OF FIGURE

Electron micrograph of vertical section through the mucosa of the seminal vesicle of an 11-day-old mouse $\times 7,350$. The columnar cells average 20μ in height, 4μ in width. In this specimen, there appears to have been some increase in the amount of organized argyrophilous (Er) over that found earlier especially in the basal part of the cell. The Golgi saccules and vesicles (GZ) also show some distention. The nuclei of the columnar cells display increased density of the marginal chromatin, and possible increase in number of nucleoli (Nu). Evident around the bases of the columnar cells are some segments of basal cells (BC) whose cytoplasm contains far fewer organelles than even the immature columnar cells in the neonatal mouse. Additional labels. BL, basement lamina; D, desmosome; DB, dense body; L, lumen; arrow, mitochondrial-desmosome complex.

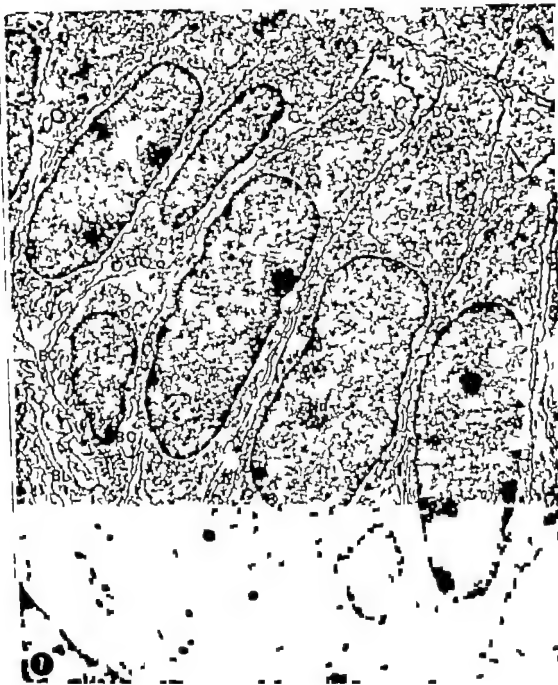


PLATE 5

EXPLANATION OF FIGURES

- 8 Oblique section through the epithelium of the seminal vesicle of an 11-day-old mouse $\times 8400$. An intracellular cilium (Ci) with its centriolar basal body Bc is in the apical cytoplasm of one cell. A nearby desmosome has single associated mitochondrion (arrow). The nucleus in the upper right shows chromosomal condensation, suggesting that it is entering prophase. Additional labels: BC, process of basal cell; L, lumen; MV, multivesicular body.
- 9 Oblique section through the pieces of several epithelial cells, $\times 13,830$. The Golgi zone (GZ) of one cell is mostly composed of distended saccules, plus associated small vesicles. N, dense contents are evident within the Golgi saccules at this age, however. Although free polyribosomes (P) are still predominant, there now seems to be more organized ergastoplasm (Er) than in the first week. Along the lines between arrows 1 and 2, and 3 and 4 run the membranes of adjoining cells, cut obliquely along which portions of several desmosomes (D) can be detected. Along the apical border of one cell are numerous micropinocytotic tubules and vesicles (MP). Additional labels: C, centriole; JC, junctional complex, with arrow pointing to mitochondrial-desmosome complex; L, lumen; MV, multivesicular body; S, cytoplasmic streak.



PLATE 6

EXPLANATION OF FIGURES

- 10 A low-power electron micrograph of an oblique section through the seminal vesicle epithelium of a 12-day-old mouse, $\times 8,800$. This picture reveals especially well the greater degree of cell interdigitation near their bases (bottom of picture) than near their apices. No unspecialized basal cells can be identified with certainty but the nucleus marked ? may belong to a cell destined to become one, since it lies in a plane parallel to the basement lamina (BL) and shows deep indentations. Additional labels: D, desmosomes; GZ, Golgi zones; L, lumen, containing some homogeneous dense debris; MV, multivesicular body; R, residual body presumably product of intracellular digestion; S, clear cytoplasmic streak.
- 11 A light micrograph of the seminal vesicle of a 15-day-old mouse, $\times 790$. This shows the increased branching of the mucosal lining, and also the greater differentiation of the Golgi region of the cells (clear zone) a feature that develops at the end of the second week of postnatal life. Compare with figures 1 and 2. Labels: m, mitotic figures; bc, basal cell distinguishable from its columnar neighbors.



PLATE 7

EXPLANATION OF FIGURE

- 12 Electron micrograph of the upper portions of several columnar cells, 13-day-old mouse $\times 17,000$. These cells exhibit numerous tubules, vesicles and multivesicular bodies in the most apical ectoplasm (MP) plus accumulations of multivesicular bodies (MV) and dense bodies (DB) deeper in the cytoplasm. This preparation reveals especially well the presence of longitudinal filaments along the lateral margins of the cell (Ec) as well as in the streaks (S) in the endoplasm. Additional labels: D desmosomes; Er ergastoplasm; GZ, Golgi complex; IG intercellular gap; L, lumen; M mitochondrion; P polyribosomes.

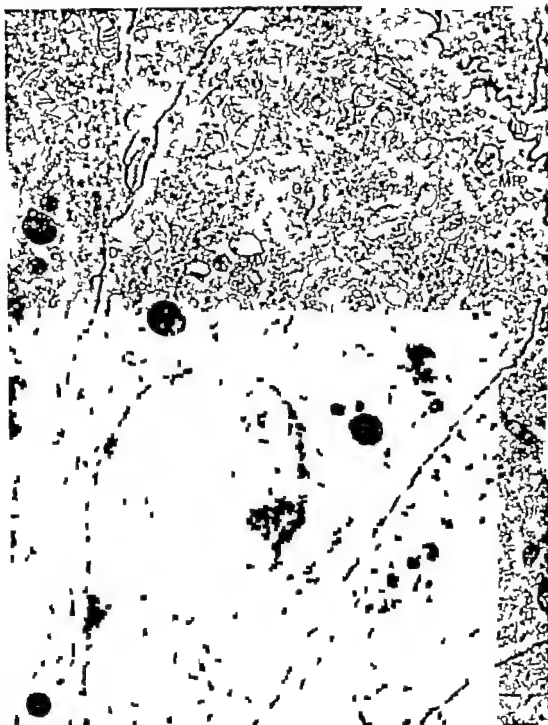


PLATE 8

EXPLANATION OF FIGURE

- 13 Electron micrograph of the seminal vesicle of 13-day-old mouse $\times 17,000$. In this area, the cells contain large vacuoles (V1-V5) enveloping portions of other cells which contain nuclear material (V1, V2) or other recognizable cytoplasmic organelles (V3-V5). The two enclosed nuclear bodies are evidently pyknotic, with the chromatin condensed in large masses against the persisting double nuclear envelope (NE). Additional labels: Er, ergastoplasm; GZ, Golgi zone; L, luminal aspects of cells; S, filamentous cytoplasmic streak.

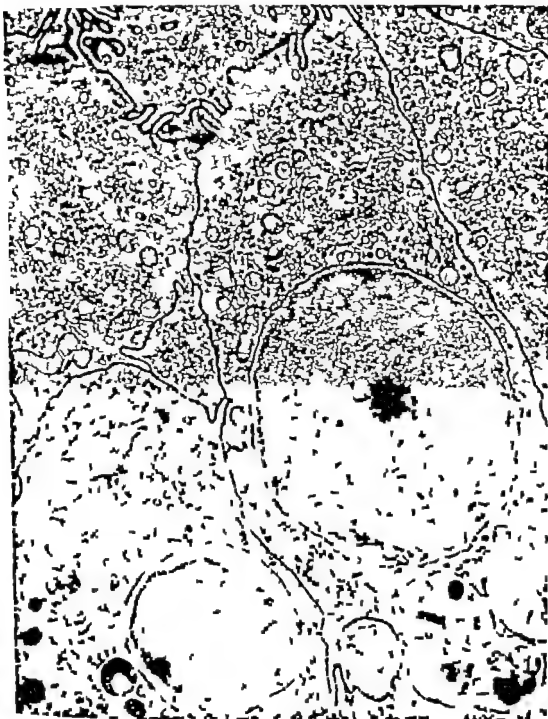


PLATE 9

EXPLANATION OF FIGURES

Figures 14 and 15. Seminal vesicle from an 18-day-old mouse; secretory material is clearly evident in Golgi vesicles and has also been released into the lumen.

- 14 Light micrograph, $\times 720$. The clear Golgi zones now often contain small, dark granules, some of which are evident near the top of the arrow.
- 15 Electron micrograph, $\times 11,800$. In this area, the columnar cells are about 12 μ tall, 5 μ wide. The chromatin appears more distinct, and ergastoplasm (Er) and the Golgi apparatus (GZ) are far more developed than at earlier ages. Small secretory granules (SG) up to 0.3 μ in diameter occur within Golgi vacuoles of many cells, as well as in the lumen (upper left). The cell marked 7BC has less developed ergastoplasm than its neighbors, plus a centriole (C) lying in the lower half of the epithelium — suggestive that this may be a cell intermediate in form between columnar secretory cell and typical basal cell. Additional labels: BV blood vessels (lumen to the right of the field shown); D desmosome; DB, dense body; MV multivesicular body; arrow mitochondrial-desmosome complex.



PLATE 10

EXPLANATION OF FIGURE

- 10 Electron micrograph of the gland of an 18-d y-old mouse, same specimen as in figures 14 and 15. Apical half of columnar cells, $\times 17,600$. The ergastoplasm (Er) and Golgi complex (GZ) are well developed; secretory granules (SG) are included in some distended Golgi cisternae and are also present in the lumen. The nuclear envelope (NE) shows particles studding its outer membrane. Sacs of ingestion are also present; MIP micropinocytotic inclusions and vesicles; MV multivesicular body. Also labeled C, centrioles; JC, junctional complex; P polyribosomes; St, stud-like attachment of two cells.



PLATE 11

EXPLANATION OF FIGURE

- 17 Electron micrograph of the apical portions of several columnar cells from the seminal vesicle of 29-day-old mouse, $\times 23,500$. This tissue was fixed in solution containing 10% rather than 5% sucrose; the section was stained with uranyl acetate only. This field illustrates that the secretory material first acquires sufficient density to be distinguished within the Golgi saccules (single arrow) then accumulates in larger and larger granules (SG) within Golgi saccules. At the double arrows, upper left, Golgi saccule appears to be opening into the lumen. Additional labels: D desmosome; Ec apical ectoplasm, having filamentous appearance; Er ergastoplasm, which is bound near the nucleus and also around the Golgi zone; JC, oblique section of junctional complex binding cells together; MP microplasmocytotic tubules and vesicles.



PLATE 12

EXPLANATION OF FIGURES

Figures 18-20 Details of the structure of mitochondrial-desmosome complexes, as seen in the gland of 29-day-old mouse

- 18 $\times 23,200$; 20, $\times 48,000$. In figure 18 are shown six desmosomes (arrows) that are each flanked, more or less clearly by two mitochondria. In several instances, dense material appears between mitochondria and cell membranes. In figure 20, four of these desmosomes are shown at higher power. The mitochondrion labeled M (figs. 18, 20) is associated with three desmosomes. Electron-dense somewhat fibrous or tubular material lies between the mitochondria and desmosomes. The ergastoplasmic cisterna labeled Er (figs. 18-20) seems to lose its ribosomes in the vicinity of the Golgi cisternae and vacuoles nearby. Also labeled GZ, Golgi zone cut in nearly cross section; JC junctional complex cut obliquely; MV multivesicular body; SG secretory granule within Golgi vacuole; St strand attaching to cells possible developing mitochondrial-desmosome complex.
- 19 Another section from the same block, $\times 33,000$. A mitochondrial-desmosome complex below the junctional complex (JC) shows an accumulation of electron-dense material between the outer mitochondrial membranes and the thick desmosome walls. Also identified GZ, Golgi zone; L, glandular lumen, at base of a microvillus

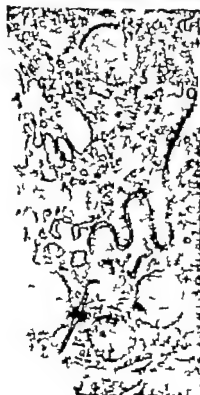


PLATE 13

EXPLANATION FIGURE

- 21 Electron micrograph of somewhat oblique section through the basal portion of the seminal vesicle epithelium of a 49-day-old mouse. 36,000. Most of the field is occupied by part of a columnar secretory cell, and it shows to good advantage the tight packing of the ergastoplasmic whorl. Along both the upper right and lower aspects of the nucleus may be seen nuclear pores cut in frontal section (NP). In the nearby cytoplasm as well as near the cell surface the ribosomes can be seen to be arranged in aggregates (P). At the lower right-hand portion of the picture there are portions of an undifferentiated basal cell (BC). DB dense bodies; M. mitochondrion.



PLATE 14

EXPLANATION OF FIGURES

- 22 and 23** Appearance of the seminal vesicle of an adult mouse six months old. This tissue was fixed in medium containing 10% rather than 5% sucrose. **22**, Light micrograph, $\times 720$; **23**, electron micrograph $\times 8,000$. The columnar cells now average 15-20 μ in height and 6-7 μ in width. An irregularly shaped basal cell (BC) is included in figure **23**, and similar cell (bc) may be seen in figure **22**. The cytological characteristics of protein-secreting glandular tissue predominate, with the cytoplasm overwhelmingly occupied by ergastoplasm (Er) and large supranuclear Golgi zone in which the vacuoles contain large secretory granules (SG) often exceeding 1 micron in diameter. Secretory material granular in appearance, also occupies the lumen (L). The mitochondria (M) of the columnar cells seem broader and less dense than those of the basal cell, as well as those of more immature glands (cf. figs. 2, 7); dense granules therein are more common. Additional labels: D desmosome; DB dense body; IT interstitial tissue; JC junctional complex; NP nuclear pore; Nu, nucleolus; R, residual body possibly lipoidal.



Osmium Impregnation of the Golgi Apparatus¹

DANIEL S. FRIEND AND MICHAEL J. MURRAY

Department of Anatomy Harvard Medical School, Boston, Massachusetts

ABSTRACT The Golgi complex consists of a heterogeneous assemblage of small vesicles, larger vacuoles, and characteristic packets of flattened cisternae morphologically distinct from other membranous organelles of the cytoplasm. It is polarized with respect to its position in the cell and also shows recognizable polarity in the arrangement of structural components within the complex. This polarity holds for cells in which the Golgi complex seems to have quite different functions, such as in the epithelial cells of mouse epididymis and of Brunner's gland, and plasma cells in the lamina propria of the intestine examined in this study. The present investigation employs a classical method for impregnation of the Golgi apparatus with the objective of more accurately localizing with the electron microscope the sites of osmium reduction within this heterogeneous organelle and of comparing the distribution of these sites with morphological indications of polarization within the Golgi lamellar systems. The osmium impregnation procedure generally used in this study consisted of fixing the tissues in 1.5% osmium tetroxide buffered with α -chloridine followed by osmication in 2% aqueous osmium tetroxide for 40 hours at 40°C. After osmication the three cell types studied consistently exhibited a selective localization of osmium to the cisternae and vesicles on one side of the Golgi complex. The observations that only the outer vesicles and cisternae contain osmium while other cytologically similar elements under the same conditions do not, emphasizes the heterogeneous, bipolar nature of the Golgi apparatus. The substances responsible for osmium reduction are quite dependent on the local environment provided are apparently formed during the prolonged phase of the exposure of the tissue to osmium and are most likely localized at the inner face of the membranes of the outer cisternae and vesicles.

Electron microscopic confirmation of the reality of the Golgi apparatus as a discrete cell organelle restimulated interest in investigation of its structure and function. After the initial fine structural observations in 1954 by Dalton and Felix ('54) numerous investigators rapidly established that the Golgi complex is morphologically distinct from other membranous organelles of the cytoplasm and consists of a heterogeneous assemblage of small vesicles, larger vacuoles, and characteristic packets of flattened saccules or cisternae (Grasse and Carasso '57; Hagenau and Bernhard '55; Pollister and Pollister '57; Sjostrand and Hanson, '54). It has since become increasingly apparent that the Golgi apparatus is not only polarized with respect to its position within the cell but also shows a recognizable polarity in the arrangement of structural components within the complex. The cisternae at the two surfaces of the same lamellar system of parallel profiles differ somewhat in their structure and in their relations to other components (Daniels, '64; Fawcett '64; Mollenhauer and Whaley '63; Smith '63; Novikoff

and Shin, '64). This asymmetry presumably holds some meaning for the function of the organelle but just what its significance may be remains to be elucidated.

The first suggestion of heterogeneity in the properties of the membranes comprising the Golgi apparatus of vertebrate cells though not stated was implicit in the conclusion of Dalton and Felix ('56) that the classical picture of a reticulum was the result of selective osmium reduction in certain parts of the apparatus. Slightly different distributions of heavy metal in other cells were reported by Pollister and Pollister ('57) but the existence of regional affinities for osmium within the Golgi complex was nonetheless confirmed. The impression gained however was simply that the sites of Golgi impregnation in the classical cytological methods differed in various cell types. Recent improvements in specimen preparation for electron microscopy as well as cytochemistry and radioautography at

Research supported by the U.S.P.H.S. National Institute of General Medical Sciences grant GM 10183-06.
Present address: University of California School of Medicine, Department of Pathology San Francisco, California 94122.

the submicroscopic level have provided evidence for structural and functional polarization within the ordered assemblages of cisternae themselves. For example electron micrographs of glandular cells often show accumulation of product in the lumens of the cisternae at one surface but not at the other (Fawcett '64, Novikoff and Shin, '64, Zeigel and Dalton, '62), and radioautographic studies confirm that concentration of the product does not occur uniformly throughout (Caro, '61, Revel and Hay '63). Cytochemical studies have revealed that specific mono- and di-phosphatases are often localized only in certain of the innermost cisternae while those at the outside of the stack have no demonstrable activity (Smith '63, Novikoff and Shin, '64). In the present investigation, a modified Kopsch Kolatchev method of impregnation (Dalton and Felix, '56; Owens and Bensley '29) is used for electron microscopic study of the Golgi apparatus. The object of this study is to localize more accurately the sites of osmium reduction within this heterogeneous organelle and to compare the distribution of these sites with morphological indications of polarization of function within the lamellar systems of the Golgi complex.

e epithelial cells of mouse epididymis d of Brunner's gland and plasma cells the lamina propria of the intestine consistently exhibited a selective localization of osmium reduction in the cisternae on one side of the complex. The possible significance of this polarity will be discussed.

MATERIALS AND METHODS

General procedure Mature adult male mice of the AKD-2 strain were used in this study. The animals were killed by cervical dislocation after light ether anesthesia. The abdomen and scrotum were rapidly incised the first portion of the duodenum and epididymis excised and minced into 1 to 2 mm blocks in a few drops of 1.3% osmium tetroxide buffered to pH 7.45 with α -collidine (Bennett and Luft '59). In several preparations the buffered fixative contained 0.045 gm of sucrose and approximately 0.03 mg of calcium chloride per cubic ml. The tissues were then transferred to vials containing fresh buffered fixative at 4 C or at room

temperature where they remained for 1 to 2 hours. Generally final osmium tetroxide reduction was more successful in tissues prepared in buffered fixative without the sucrose and calcium chloride and fixed at room temperature whereas the opposite was true for the control tissues prepared for routine electron microscopy. After fixation, the control tissues were quickly dehydrated in a graded series of cold alcohols and brought to room temperature in 100% ethanol. The dehydration was completed in propylene oxide and the tissues embedded in Epon (Luft, '61).

The buffered fixative was decanted from the tissues which were to be post-osmicated and the fixative replaced by unbuffered 2% aqueous osmium tetroxide, pH 6.5. The vials were then placed in a 40°C oven for 1 to 7 days. (The use of 4% unbuffered osmium tetroxide in place of the 2% solution gave similar results the use of less than 1% osmium tetroxide markedly decreased the number of impregnated Golgi areas. Aqueous osmium tetroxide buffered above pH 6.7 with α -collidine, phosphate, or veronal acetate did not yield significant impregnation even after seven days of post-osmification.) Forty to 48 hours of exposure to osmium at 40 C proved most suitable for electron microscopy.

After decanting the osmium tetroxide, the blocks were rapidly dehydrated in a series of increasing concentrations of ethanol and dehydration completed in propylene oxide. Embedding was in Epon. Sections were cut with glass knives on a Porter Blum microtome and those displaying gold interference colors were picked up on uncoated 150 mesh copper grids. The sections were examined unstained or lightly stained with lead salts (Allison '61). Electron micrographs were taken on an RCA EMU 3F microscope. Sections for light microscopy were cut at 1 μ and examined unstained or stained with 1% toluidine blue in borax or with 1% ethanolic solution of fast green.

Further modifications Additional blocks of epididymis were fixed in 2% glutaraldehyde buffered to pH 7.35 with cacodylate (Gordon et al. '63) or 6.5% glutaraldehyde and 2% acrolein (Sandborn et al.)

buffered to pH 7.5 with cacodylate, or in 1.3% osmium tetroxide as described above. After the glutaraldehyde glutaraldehyde and acrolein, or osmium tetroxide fixations, the Golgi apparatus of each group of tissues reduced osmium to comparable degrees after incubation with unbuffered osmium tetroxide for 48 hours at 40 C. Treatment for 30 minutes with 1% mercuric chloride prior to osmication of the glutaraldehyde-fixed tissue increased the amount of non-specific osmium tetroxide reduction in structures not impregnated by post-osmication alone. The additional impregnated structures are collagen and those generally considered Schiff-positive. The treatment of the osmium tetroxide-fixed tissue with mercuric chloride shifted osmium reduction almost exclusively to the fibrous components of connective tissue. After glutaraldehyde fixation and immersion in mercuric chloride subsequent treatment of the tissue with an aldehyde blocking agent, dimedone (6,6-dimethyl-cyclo-hexane 1:3 dione) decreased the osmium impregnation in Schiff positive structures outside the Golgi apparatus. Treatment of all of the fixed tissues with dimedone alone did not alter the usual results of post-osmication. Post-osmication with dimedone as the diluent, however, does prevent osmium impregnation of the Golgi apparatus, but the extent of reaction of OsO_4 with the aldehyde blocking agent is not yet clear and prohibits an assumption that the interference with the Golgi impregnation is due to the blockage of aldehyde groups.

OBSERVATIONS AND DISCUSSION

General configuration of the Golgi apparatus. The vesicles, cisternae and vacuoles of the Golgi apparatus vary in number, size and internal density in various vertebrate cells, but the location of the Golgi complex within the cell and its typical configuration can be described with some confidence. Visualized in three dimensions, the lamellar packets of the Golgi apparatus appear to outline a discontinuous cap adjacent to the nucleus. In cell types with an unusually large Golgi complex, packets of cisternae forming its wall have the shape of an indented hollow sphere with the curvature of the juxta-nu-

clear cisternae conforming to the contour of the nucleus (fig. 3). The Golgi vacuoles, frequently containing a substance of some density appear to arise from terminal expansions of the inner cisternae (fig. 2). In this inner region the secretory product assumes its final, membrane-bounded form (Dalton, '61; Fawcett, '64; Zeigel and Dalton '62). The inner cistern in this case thus corresponds to what other authors have called the emitting or vacuolar pole. Conversely the outer cistern corresponds to the forming face described in other animal (Novikoff and Shin, '64) and plant cells, (Mollenhauer and Whaley '63) or the smooth vesicle pole of the Golgi as described in amoebae (Daniels, '64). Smaller Golgi vesicles, 200 to 600 A in size cluster around the terminal expansions of all the cisternae and along the surface of the innermost and outermost cisternae of the lamellar packets (figs. 1-3). In close topographic association with the Golgi complex are centrioles, multivesicular bodies, and heterogeneous dense bodies, presumed to be lysosomes.

This general description holds for cells in which the Golgi complex seems to have quite different functions. In Brunner's gland, the dense secretory material appears to be concentrated and compacted into granules in the Golgi apparatus and is perhaps in part, formed by it. Whether the Golgi complex is involved in elaboration or release of immune globulins in plasma cells is uncertain. The secretory function, if any of the Golgi apparatus in the epididymal epithelial cell is not known. Nevertheless, the Golgi complexes of all three cell types depart little from the generalized description given above (figs. 1-3).

Osmium reduction. The distribution of metal deposits after post-osmication of the three cell types studied is similar and the epididymis, which has been more extensively studied, can be considered as representative. In the epididymis the Golgi complex forms an extensive supranuclear crown composed of a cylindrical band or wall of 8 to 10 cisternae, clear vacuoles and numerous vesicles (Dalton and Felix '64). From one surface of the packets of cisternae to the other there is an evident asymmetry characterized by a progressive decrease from outside to inside in cluster

nal length and a concomitant increasing thickness. After fixation and 40 hours of exposure to aqueous osmium tetroxide at 40 C deposits of reduced osmium are invariably localized within the lumen of the outer one to four cisternae in many of the vesicles at their ends, and in the vesicles aligned along the outer cistern (figs. 4 5 7 8). This localization is not entirely uniform in that all Golgi zones are not impregnated and the amounts of reduced osmium vary but in favorable preparations after any of the fixatives employed, the majority of Golgi complexes do reduce osmium to some degree and wherever the reduction does occur the localization is precisely similar. Most of the metallic deposits are totally electron opaque while a few others appear less dense. Less dense areas are often found in cisternae adjacent to the outer cisternae and seem to represent the last and weakest areas of osmium reduction (figs. 7-8).

The vesicles at the ends of the inner cisternae the vesicles within multivesicular bodies and the vacuoles associated with the complex remain entirely free of the metallic deposits in this cell type (figs. 4 and 5).

The cisternae of the plasma cell Golgi apparatus characteristically occur in packets of 4 to 6. Granules perhaps unrelated to the major secretory product of the cell, appear to arise from the inner cistern (fig. 3). In Brunner's gland cells, the cisternae number 6 to 11 to a packet and both the increasing cisternal density from the outer lamella inward and the increasing depth of lumen is somewhat more apparent than in the plasma cell (fig. 2). In this cell, the vacuoles with dense contents clearly arise from the innermost cisternae and go on to develop into the mature secretory granules (Friend, '65). The appearance of vacuoles with dense centers on the inner side while clear ones predominate on the outer side further accentuates the bipolarity. Osmium tetroxide reduction in both the plasma cell and in the cells of Brunner's gland is very similar to that described for the epididymis but in these two secretory cell types the reduction is more consistently found in the vesicles which surround the outermost cistern and is less uniform in the outer cisternae (fig.

6). In the cells which compose Brunner's gland osmium reduction was specifically looked for in transition zones and adjacent vesicles. Transition zones are the smooth areas of the rough-surfaced endoplasmic reticulum that form buds which give rise to the vesicles that are believed to transport quanta of the protein secretory product to the Golgi apparatus (Siekevitz and Palade, '60) (Zelger and Dahm, '62). The lack of reduced osmium in the buds and vesicles may support the view that the vesicles containing protein carry their contents directly to the inner regions of the Golgi cisternae and vacuoles. As illustrated by osmium reduction, these vesicles do not appear to be related to those associated with the outer osmium reducing vesicles and cisternae.

Outside the Golgi apparatus reduction of the osmium tetroxide also occurs in lysosomes and pigment bodies, but deposits of osmium in these dense bodies is less conspicuous than in the Golgi complex. In the small basal cells of the epididymal epithelium and in occasional smooth muscle cells of the tunic, the nuclear envelope and short segments of the rough surfaced endoplasmic reticulum immediately continuous with it sometimes contain reduced osmium. The granules of polymorphonuclear granulocytes and the vesicles of peripheral nerves also reduce osmium. After glutaraldehyde fixation and treatment of the tissues with mercuric chloride osmium reduction is much more marked in the cytoplasmic ground substance outside the Golgi apparatus and in the structures mentioned above as well as in the basement membrane. Whether the amount of reduction outside the Golgi is inversely proportional to the reduction within the Golgi apparatus as suggested by Owens and Bensley ('29) is uncertain.

Discussion of osmium localization. Osmium tetroxide reduction after 24 or 72 hours of impregnation varies quantitatively but not qualitatively from the optimal 40 to 48 hour results. Shorter contact with the osmium tetroxide yields smaller deposits in the outermost Golgi elements longer contact increases the amount of the deposit which then extends beyond the limits of the membrane limited cisternae and vesicles. Lighter deposits

inadequate for detection by light microscopy afford finer localization of the reduced osmium by electron microscopy and the reduction product, presumably by dried osmium dioxide or metallic osmium (Hanker et al., '64) first appears within the lumen and along the inner face of the smooth membranes of the cisternae and vesicles (Figs. 7 and 8). After prolonged exposure the metallic product appears outside the confines of the compartments, but only when the deposits are heavy and the lumens are filled. The substance responsible for osmium reduction or aggregation is therefore most likely localized at or near the inner face of the membrane of the outer cisternae and vesicles. If as seems likely the responsible agents reside within the membranes rather than in the lumens, this suggests that the membranes themselves differ in composition in different areas and that the inner and outer membranes of the same lamellar packet are different in their properties.

In the past, shortcomings in methodology have been invoked as reasons for the capriciousness of the reaction and the variations in density and localization of the osmium reduction (Dalton and Felix, '56; Pollister and Pollister '57). These variations, however, might well reflect the physiologic state of the Golgi apparatus at the time of fixation. It is plausible that the requisite reducing or aggregating substance may be present in sufficient concentration or proper form only during a certain phase of Golgi activity. Reducing aldehydes for example, might only be exposed during slow hydration of the unsaturated phospholipids of newly forming membranes or the necessary concentration of

inorganic ion may be dependent on a particular segregating activity of the outer vesicles and cisternae. These activities could then be necessary for the reaction to occur and it would be expected that the Golgi complexes of all cells in a tissue not be at the same stage of activity and therefore not react in the same fashion.

We do not know the chemical nature of the substances which react and are not that their presence results in microscopically visible osmium precipitation, but we do know that the factors responsible for the osmium localization are quite

dependent on the local environment provided and that the reducing substance is most likely formed during the prolonged phase of exposure of the tissue to osmium. At a pH greater than seven or at a temperature below 30° for example the reaction only occurs to negligible degrees even after seven days. Even at optimal pH and temperature 24 hours are necessary for sufficient concentrations of osmium black to be localized with certainty in the electron microscope. Generally small dust-like particles which are presumably reduced osmium are widely distributed in the sections (Figs. 7 and 8) but the simultaneous localization of dense deposits of osmium in the Golgi apparatus in tissues exposed for shorter than optimal times, strongly implies that the results are not due to the migration of reduced osmium alone. It is doubtful that the reducing substance is itself only incidental in the fine localization of the reaction although raising the pH, adding a variety of buffers, or adding chloride salts or using fixatives that alter the response in the Golgi apparatus could conceivably operate as well on osmium aggregation as on osmium reduction.

The range of substances in the tissue which can reduce osmium is wide. Thiol and aldehyde groups reduce osmium relatively rapidly; alkenes, alkynes, arylamines, and phenols reduce osmium more slowly (Hanker et al., '64). Blocking the pre-existing thiol groups with mercury in glutaraldehyde fixed tissues or blocking the pre-existing aldehyde groups with dimedone in the osmium tetroxide or glutaraldehyde fixed tissues does not alter the Golgi impregnation. Exposure of the fixed tissue to osmium dissolved in dimedone does prevent Golgi impregnation, but the aldehyde blocking agent itself precipitates osmium and presumably loses its blocking activity. The activity of the other possible OsO₄ reducing groups has not yet been studied in similarly fixed tissues. As methods for doing so become available, the investigation of such chemical groups capable of reducing osmium under the defined conditions, should reveal the responsible substance in the outer Golgi lamellae and vesicles. We do know that enzymes are not responsible for the osmium reduction since the reaction works

well in enzyme-killed osmium and acrolein fixed tissues.

Despite our uncertainty as to the mechanism of osmium deposition the observations that the outer vesicles and cisternae contain osmium while other cytologically similar elements under the same conditions do not, further emphasizes the heterogeneous nature of the Golgi apparatus. Since only the outer cisternae and vesicles reduce osmium under the prescribed conditions, the Golgi apparatus can certainly be said to be bipolar by this standard and the cytologic, cytochemical, and radioautographic observations of other investigators imply the same (Smith, '63; Daniels '64; Novikoff and Shin '64; Peterson and Leblond '64; Revel and Hay '63; Schneider and Kuff '64; Siekevitz and Palade '60; Zeigel and Dalton '62). Understanding the full nature of this asymmetry of the Golgi apparatus as well as discovery of the mechanism of osmium deposition may lead to more complete understanding of its function.

ACKNOWLEDGMENTS

The authors are grateful to Drs. Don Fawcett, Jean-Paul Revel, and Morris Kary for their helpful advice and encouragement during the course of this study and to Dr. Don Fawcett for reviewing the manuscript.

LITERATURE CITED

- Bennett, H. S., and J. H. Luft 1959 8-collidine as basis for buffering fixatives. *J. Biophys. and Biochem. Cytol.*, 6: 113.
- Care, L. G. 1961 Electron microscopic radioautography of thin sections: the Golgi zone as site of protein concentration in pancreatic acinar cells. *J. Biophys. and Biochem. Cytol.*, 10: 37.
- Dalton, A. J. 1961 Golgi apparatus and secretion granules. In *The Cell* Vol. II (J. Brachet and A. E. Mirsky eds.) New York, Academic Press, p. 603.
- Dalton, A. J. and M. D. Felix 1954 Cytological and cytochemical characteristics of the Golgi substance of epithelial cells of the epidermis in situ, in homozygotes, and after isolation. *Am. J. Anat.*, 94: 171.
- 1956 A comparative study of the Golgi complex. *J. Biophys. and Biochem. Cytol.*, 2: 79.
- Daniels, E. 1964 Origin of the Golgi system in amoebae. *Zeit. f. Zellforsch.*, 64: 38.
- Fawcett, D. W. 1964 In histology and cytology. In: *Modern Developments in Electron Microscopy* (B. M. Siegal, editor). New York, Academic Press. Page 257.
- Friend, D. S. 1963 The fine structure of Brunner's gland in the mouse. *J. Cell Biol.* 25: 563.
- Gordon, G. B., L. R. Miller and K. G. Beach 1963 Fixation of tissue culture cells for ultrastructural cytochemistry. *Exp. Cell Res.* 21: 440.
- Grasse, P. P. and N. Carrasco 1957 Ultrastructure of the Golgi apparatus in protozoa and metazoa. *Nature (London)* 174: 31.
- Hagenan, F., and W. Bernhard 1953 L'appareil de Golgi dans les cellules normales et cancéreuses de vertébrés. *Arch. Anat. Mic.* 44: 27.
- Hanker, J. S., A. R. Seaman, L. P. Weiss, H. Vos R. A. Bergman, and A. M. Seligman 1964 Osmiophilic reagents: new cytochemical principles for light and electron microscopy. *Science* 146: 1039.
- Kuff, E. L., and A. J. Dalton 1969 Biochemical studies of isolated Golgi membranes in Subcellular Particles (T. Hayashi, editor). New York, Ronald Press. Page 114.
- Luft, J. H. 1961 Improvements in epoxy resin embedding methods. *J. Biophys. and Biochem. Cytol.*, 9: 406.
- Milomig, G. 1961 A modified procedure for lead staining of thin sections. *J. Biophys. and Biochem. Cytol.*, 11: 736.
- Mollenhauer, H. H., and W. G. Whaley 1963 An observation on the functioning of the Golgi apparatus. *J. Cell Biol.*, 17: 222.
- Novikoff, A. B., E. Essner and M. Quidston 1961 Golgi apparatus and lysosomes. *Federata Proc.*, 23: 1010.
- Novikoff, A. B. and W. Y. Shin 1964 The reticuloplasmic reticulum in the Golgi zone and its relations to microbodies, Golgi apparatus and autophagic vacuoles in rat liver cells. *J. Microscop.*, 3: 187.
- Owens, H. B. and R. B. Bensley 1929 Osmitic acid as microchemical reagent, with special reference to the reticular apparatus of Golgi. *Am. J. Anat.*, 44: 79.
- Peterson, M., and C. P. Leblond 1964 Synthesis of complex carbohydrates in the Golgi region as shown by radiography after injection of labeled glucose. *J. Cell Biol.* 21: 143.
- Pollister, A. W. and P. F. Pollister 1957 The structure of the Golgi apparatus. *Int. Rev. Cytol.*, 6: 85.
- Revel, J. P. and E. D. Hay 1963 An ultrastructural and electron microscopy study of collagen synthesis in differentiating cartilage. *Zeitschrift für Zellforsch.*, 61: 110.
- Sandborn, E., P. F. Koenig, J. D. McNabb, and C. Moore 1964 Cytoplasmic microtubules in mammalian cells. *J. Ultrastructure Res.* 11: 121.
- Schneider, W. C., and E. L. Kuff 1954 On the isolation and some biochemical properties of the Golgi substance. *Am. J. Anat.*, 64: 23.
- Siekevitz, P., and G. E. Palade 1960 A cytochemical study on the pancreas of the guinea pig. V. Incorporation of leucine-¹⁴C.

- into the chymotrypsinogen of various cell fractions. *J. Biophys. and Biochem. Cytol.*, 7, 6.
- Sjostrand, F. S., and U. Hansson 1954 Ultrastructure of the Golgi apparatus of exocrine cells of mouse pancreas. *Exp. Cell Res.*, 7, 415.
- Smith, R. E. 1963 Activity of rat adenohypophysis during secretion. *J. Cell Biol.*, 19, 66A.
- Zaigal, R. F. and A. J. Dalton 1962 Speculations based on the morphology of the Golgi systems in several types of protein-secreting cells. *J. Cell Biol.*, 15, 43.

Abbreviations

C, cisternae	N nucleus
G secretory granules	V vacuole
MVB multivesicular body	ves, vesicles
M, mitochondrion	

PLATE 1

EXPLANATION OF FIGURES

- 1 In the epididymis, the Golgi complex forms an extensive saccular-clear crown composed of cylindrical band of 8 to 10 cisternae, clear vacuoles, and numerous vesicles. A portion of the Golgi apparatus is shown in this electron micrograph. Approx. $\times 18,000$.
- 2 In the cells which compose Brunner's gland, the cisternae number 6 to 11 to packet. Vacuoles with dense contents arise from the innermost cisternae and develop into the mature secretory granules. Approx. $\times 17,000$.
- 3 The cisternae of the plasma cell Golgi apparatus characteristically occur in packets of 4 to 6. The sparse dense granules in the inner region of the Golgi complex may not be related to this cell's main secretory product. Approx. $\times 20,000$.

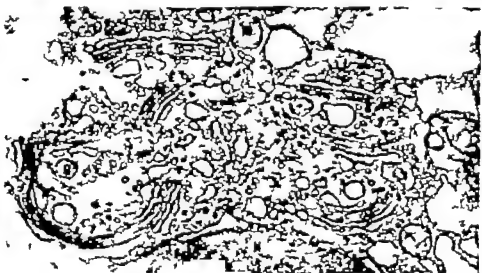
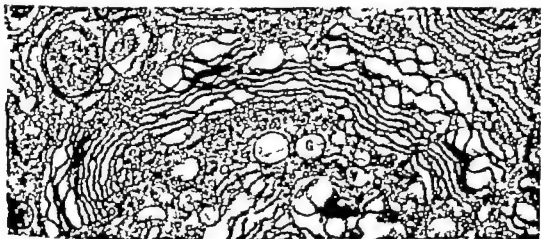
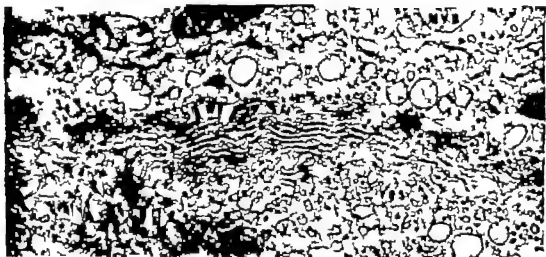


PLATE 2

EXPLANATION OF FIGURE

- 4 After fixation and 40 hours of exposure to aqueous OsO_4 at 40°C , deposits of reduced osmium are localized within the lumens of the outer 1 to 4 cisternae, in many of the vesicles at their ends, and in vesicles aligned along the outer cistern. The plane of section shown in the electron micrograph is perpendicular to the axis of the cells. The epithelial cells of the epididymis seen in the light micrograph insert are sectioned parallel to the cell axis and represent favorable osmium impregnation suitable for both light and electron microscopy. Approx. $\times 12,500$.



PLATE 3

EXPLANATION OF FIGURES

- 5 In the epithelial cells of the epididymis, the vesicles at the ends of the inner cisterna, the vesicles within multivesicular bodies, and the vacuoles associated with the Golgi complex remain free of metallic deposits. Approx. $\times 17,000$.
- 6 In the cells of Brunner's gland the osmium reduction is more consistently found in vesicles along the outermost Golgi cistern and is less uniform in the lumens of the outer cisternae. The osmium impregnation pattern in the plasma cell is similar. Approx. $\times 6,000$.

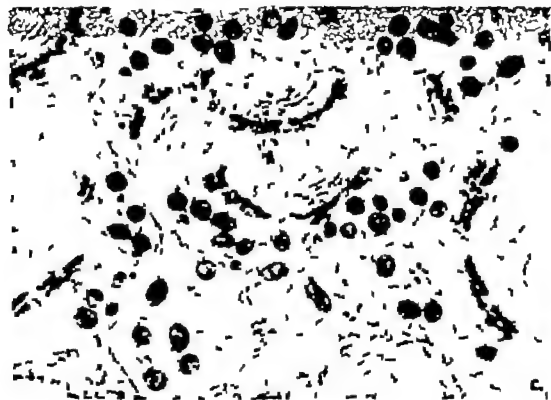
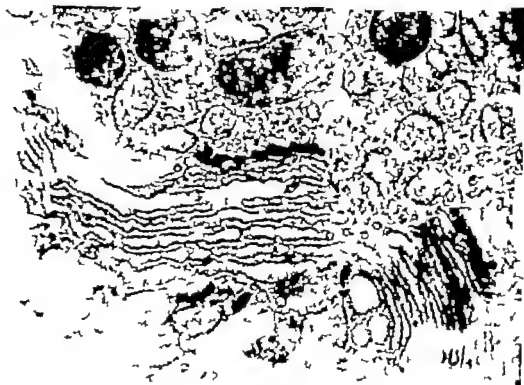
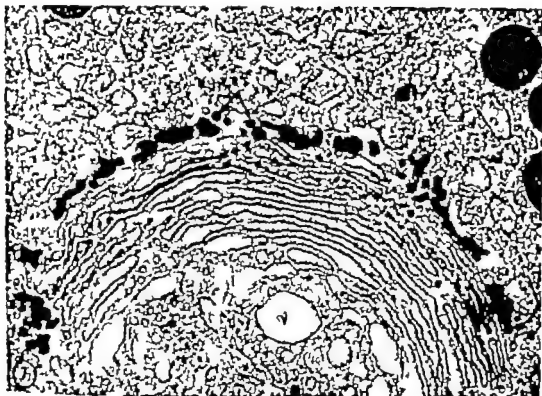


PLATE 4

EXPLANATION OF FIGURES

- 7-8 Portions of the Golgi apparatus from epithelial cells of the epididymis. The dense deposits in the outermost cistern and vesicles extend beyond their membrane limited compartments. Less dense areas in the third and fourth cisternae seem to represent the last and weakest areas of osmium reduction. Figure 7 approx $\times 36,000$
Figure 8 pprox. $\times 46,000$

Daniel S. Friedel and Michael J. Murray



Connective Tissue Responses to Altered Collagen and Bone Implants¹

J. T. IRVING AND S. A. MIGLIORE^{2,3}

*Fourth Dental Center and Harvard School of Dental Medicine
Boston, Massachusetts*

ABSTRACT The ϵ -amino groups of reconstituted collagen were treated in variety of ways and the collagen implanted subcutaneously in rats. After two weeks the implants were removed and examined histologically. A giant cell response was seen around the collagens treated with 1-fluoro-2,4-dinitrobenzene, *p*-nitrobenzoylchloride or carbobenzoxychloride, but not with the other reagents. Parallel experiments with autogenous bone, treated with the same methods, were carried out. A mild giant cell response was found in the untreated bone but was enhanced only in bone treated with the same three reagents. It would appear that the giant cell response was greatly increased when the attached benzene ring had nitro groups in the para position, and also when there was an ester linkage in the attached radicle. It is unlikely that this reaction was immunological in character. The giant cells have many of the properties of osteoclasts. It is suggested that it is the nature of the organic matrix of bone that determines if osteoclasts shall occur.

Irving and Handelman ('63) described a method for studying the resorptive mechanism of bone in which they implanted subcutaneously pieces of bone autogenously derived, and followed the cellular response. Large multinucleated cells appeared around bone whose cells had been killed by repeated freezing and thawing and the same was found if the bone had been previously decalcified rachitic osteoid, on the other hand, did not attract the giant cells till it had become calcified after implantation. The giant cells were frequently seen in Howship's lacunae and had all the enzymes present in osteoclasts. Irving and Handelman ('63) concluded that these giant cells though differing in some ways from osteoclasts were so similar in all material respects that they would serve as a model in a study of the factors governing osteoclasts.

In the present study resorption of implanted collagen, both native and altered chemically was studied. Parallel experiments on implanted bone similarly treated were also carried out. The chemical changes induced involved chiefly the amino groups of lysine and hydroxylysine

ously into rats removed after various intervals and examined histologically. In the second experiment parts of the rats scapula were removed, treated in various chemical ways, implanted subcutaneously into the same animal and examined after 14 days.

Collagen experiments

Preliminary treatment. Two sources of collagen were employed. Collagen was reconstituted at pH 4.5 from the citrate soluble fraction from two-day-old calf skin using the method of Gallop ('55). Collagen was also similarly prepared from the tail tendons of the same rats into which it was finally implanted.

Seven reactions were carried out on collagen before implantation. They are listed below together with the group numbers of the rats into which they were implanted. The reagents used were mild and have been traditionally used in studies on modifications of proteins. The reactions of Groups II-IV were carried out at 0° and those for Groups V-VIII at room temperature (25°). The collagens that were treated

This project was supported by USPHS Research Grant D-13823 from the National Institute of Dental Research.

A post Doctoral Research Fellow supported by the National Institute of Dental Research the time this work was done.

Present address: Department of Orthodontics, School of Dentistry, University of Pittsburgh, Pittsburgh, Pennsylvania.

MATERIALS AND METHODS

Two separate experiments were undertaken. In the first, collagen was treated in various ways implanted subcutane-

with reagents that were not water soluble were repeatedly washed with 50% ethanol and finally with 95% ethanol. Washing was considered complete when the washes contained no visible traces of reagent. In all cases the reaction mixtures were finally dialyzed against frequent changes of distilled water for several days.

Group I Reconstituted collagen with no chemical treatment.

Group II Deamination with nitrous acid (Philpot and Small '38). The collagen was treated in an 0.5 M acetate buffer of pH 4.0 at 0° with 1 M NaNO_2 for 30 minutes. The reaction was stopped by neutralization.

Group III Acetylation with acetic anhydride (Hughes '47). This reaction consisted in slow addition of the anhydride to the collagen suspended in a saturated solution of sodium acetate. The reaction mixture was stirred for a period of 30 minutes.

Group IV Phenylacetylation using the acid chloride. The procedure was similar to that described in Group III.

Group V 3,5-Dinitrobenzoylation using the acid chloride (Mellon '47). A slight excess of the reagent (Schotten-Baumann reaction) was used compared to the calculated -amino groups theoretically available.

(Eastoe '35). The acid chloride was added in anhydrous ether and slowly added while the reaction mixture was subjected to vigorous agitation. 1 N NaOH was added to maintain a pH of 8. The reaction was allowed to proceed for two and one-half hours.

Group VI p-Nitrobenzoylation employing the acid chloride. The procedure was identical to that described in Group V.

Group VII 2,4-Dinitrophenylation using 1-fluoro-2,4-dinitrobenzene (FDNB) (Sanger '45). The reaction was carried out in a medium consisting of an ethanol solution of FDNB and a 2% aqueous sodium bicarbonate solution mixed in a 2:1 ratio. The reaction mixture was constantly agitated for three days at room temperature. The product will be referred to as DNP-collagen.

Group VIII Carboxybenzoylation utilizing the acid chloride (Miller and Stanley '42). The reaction was carried out in a 0.2 M phosphate buffer at pH 8 for two hours. The reagent was slowly added while

the suspension was subjected to vigorous agitation until the concentrate was in slight excess of the calculated amount of -amino groups present in the suspension.

The extent of the reactions of each reagent was determined by a second reaction with FDNB. Each sample was then hydrolyzed and the optical density read at a wave length of 360 m μ . The DNP-collagen reacted with 85% of the estimated -amino groups which agrees closely with the results obtained with dentin collagen by Solomon, Irving and Neuman ('60). Using the DNP-collagen value as an index of 100% the extent of the reactions given by the various reagents used in this study were as follows (in per cent): Dinitrophenylation 100, Deamination, 12, Acetylation, 52, Phenylacetylation, 33, 3,5-dinitrobenzoylation 6, p-nitrobenzoylation 6, carboxybenzoylation 79.

Implantation of collagen

Calf collagen. This was implanted into 108 young adult rats of the Holtzman strain their average weights being 125 g. The implants were placed subcutaneously into the back while the animals were under anesthesia with strict aseptic precautions, and were removed 14 days later. This period was chosen as Irving and Handelman had found this the optimal time for studying the cellular responses. The implant and surrounding tissues were embedded in paraffin and sections stained with hematoxylin and eosin. The distribution of the rats into various groups is shown in table 1.

Autogenous collagen. Six rats had untreated reconstituted collagen implanted, and six were implanted with DNP-collagen. The same time-table as described above was followed.

Early formation of giant cells. Twelve animals were implanted with DNP-calf collagen and the implants were removed daily from two animals on the second to seventh days after implantation.

Implantation of bone

A large part of the scapula was removed from 48 rats and decalcified in 0.5 M sodium ethylenediaminetetraacetate at pH 8.0. The bone was then treated with the same chemical procedures as described

TABLE 1

Number of animals	Type of implant	Group	Chemical treatment	Days in body
18	Collagen (Calf skin citrate soluble fraction)	I	Untreated	14
12	Collagen (Calf skin citrate soluble fraction)	II	Desmination	14
12	Collagen (Calf skin citrate soluble fraction)	III	Acetylation	14
12	Collagen (Calf skin citrate soluble fraction)	IV	Phenylacetylation	14
12	Collagen (Calf skin citrate soluble fraction)	V	3,5-dinitrobenzoylation	14
12	Collagen (Calf skin citrate soluble fraction)	VI	p-nitrobenzoylation	14
18	Collagen (Calf skin citrate soluble fraction)	VII	2,4-dinitrophenylation	14
12	Collagen (Calf skin citrate soluble fraction)	VIII	Carbobenzoylation	14
6	Collagen (Autogenous)	I	Untreated	14
6	Collagen (Autogenous)	VII	Dinitrophenylation	14
12	Collagen (Calf skin)	VII	Dinitrophenylation	2,3,4,5,6,7
6	Scapular bone (Autogenous)	I	Untreated	14
6	Scapular bone (Autogenous)	II	Desmination	14
6	Scapular bone (Autogenous)	III	Acetylation	14
6	Scapular bone (Autogenous)	IV	Phenylacetylation	14
6	Scapular bone (Autogenous)	V	3,5-dinitrobenzoylation	14
6	Scapular bone (Autogenous)	VI	p-nitrobenzoylation	14
6	Scapular bone (Autogenous)	VII	2,4-dinitrophenylation	14
6	Scapular bone (Autogenous)	VIII	Carbobenzoylation	14
8	Collagen (Calf skin)	I	Untreated	28 2 similar implants 14 days each
8	Collagen (Calf skin)	VII	Dinitrophenylation	
8	Scapular bone (Autogenous)	I	Untreated	28 2 similar implants 14 days each
3	Scapular bone (Autogenous)	VII	Dinitrophenylation	
200	Total			

above and 14 days later was implanted into the rat from which it had been taken. After a subsequent 14 days the implant with surrounding tissues was removed, embedded in paraffin and the sections stained with hematoxylin and eosin. The division of the rats into the various groups is shown in table 1.

Tests for immune responses

Landsteiner and Jacobs ('36) Landsteiner and Chase ('37) and Eisen, Orris and Belman ('52) have shown that various chemical changes in collagen can confer immunological properties upon it. To rule out this possibility animals were implanted a second time after removal of the initial implant, and the second implant was allowed to remain a further 14 days. Five animals were treated this way with unaltered collagen, five with DNP-collagen, five with unaltered bone and five with DNP-bone. The reactions in the first and second implants of the respective materials were compared histologically. In addition, a skin test was made with an acetone-ether solution of FDNB according to the procedure of Eisen et al. ('52).

RESULTS

Collagen implants

Group I. The following reaction was noted around reconstituted collagen 14

days after implantation. The reactions around the autogeneously derived collagen and the calf skin collagen were identical. No necrotic or degenerative reaction to the implants was seen in the host tissues and a well-defined fibrous capsule was formed. Fibroblast-like cells infiltrated the entire implant, but no giant cell response was seen in any section (fig. 1). Giant cells were found around hairs that had been accidentally introduced (this was found in all groups) indicating that giant cells could form, given the appropriate stimulus. The implanted collagen stained more strongly with eosin than did that of the host and the collagenous bundles were not arranged in regular fashion.

Groups II to V. The histological appearance of the implants was identical with that of Group I.

Groups VI and VII. In contrast to Groups I to V a very marked giant cell response was found in Groups VI and VII, after 14 days. The background response was similar to that in the previous groups. A fibrous capsule formed and fibroblastic infiltration occurred, but to a lesser extent. The giant cells were similar to those observed by Irving and Handelsman ('63) and were of varying sizes up to 100 μ in diameter and containing as many as 40-50 nuclei (fig. 2). They were found mostly in the fibrous capsule surrounding the im-



Fig. 1. Cellular response around reconstituted calf-skin collagen removed 14 days after implantation. Infiltration by fibroblast-like cells only. Hematoxylin and eosin. 290

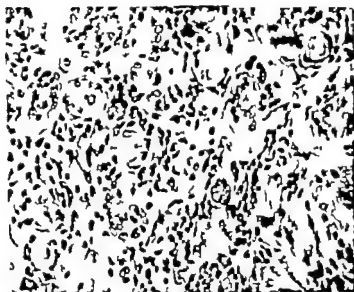


Fig. 2 Cellular response around DNP-collagen (calf-skin) removed 14 days after implantation. Note large number of giant cells. Hematoxylin and eosin. $\times 250$.

plant but many of them had penetrated into the implant and some contained fibrils of altered collagen which could be identified by its characteristic yellow color.

When the reaction was studied daily using implants treated with fluorodinitrobenzene the following was found. The initial reaction was mild inflammation, the predominate cells being polymorphonuclear leucocytes and in addition, young connective tissue cells and capillaries began to proliferate in the area. The young connective tissue cells varied from plump cells with rounded nuclei to spindle cells with small elongated nuclei. By the fourth day the polymorphonuclear leucocytes had disappeared, and what looked like a syncytium of two or more of the young connective tissue cells was seen on the fifth day (fig 3). The next day frank multinucleated cells were visible (fig 4) and they increased in numbers thereafter.

Group VIII. Treatment with carbonylchloride also induced a giant cell reaction, but to a milder degree. The background reaction was the same as in the other groups.

Reactions in implanted bone

Irving and Handelman ('63) had found after 14 days implantation that a number

of giant cells were present around bone either undecalcified with the bone cells killed or decalcified. The same was found in the present results the Group I animals having a moderate number of giant cells (fig 5). Groups II to V showed a response of the same magnitude. Groups VI and VII, however had a very marked giant cell response the cells looking exactly like those in the same groups with implanted collagen (fig 8). The Group VIII rats, implanted with bone had a much more marked response than those of Group I, but not as strong a one as the rats of Groups VI and VII. The results thus ran parallel with those using implanted collagen, except that untreated bone could always attract a few giant cells.

Tests for immune responses

No difference of any kind was seen in the intensity of the response in the first and second implants with collagen or bone and the skin tests gave no reaction to FDNB.

DISCUSSION

These findings show that there is a high degree of specificity of the chemical changes induced in both isolated collagen and bone which govern the appearance of giant cells. They also show that these

above and 14 days later was implanted into the rat from which it had been taken. After a subsequent 14 days the implant with surrounding tissues was removed, embedded in paraffin and the sections stained with hematoxylin and eosin. The division of the rats into the various groups is shown in table 1.

Tests for immune responses

Landsteiner and Jacobs ('36), Landsteiner and Chase ('37) and Eisen, Orris and Belman ('52) have shown that various chemical changes in collagen can confer immunological properties upon it. To rule out this possibility, animals were implanted a second time after removal of the initial implant, and the second implant was allowed to remain a further 14 days. Five animals were treated this way with unaltered collagen, five with DNP-collagen, five with unaltered bone and five with DNP-bone. The reactions in the first and second implants of the respective materials were compared histologically. In addition, a skin test was made with an acetone-ether solution of FDNB according to the procedure of Eisen et al. ('52).

RESULTS

Collagen implants

Group I. The following reaction was seen around reconstituted collagen, 14

days after implantation. The reactions around the autogeneously derived collagen and the calf skin collagen were identical. No necrotic or degenerative reaction to the implants was seen in the host tissues and a well-defined fibrous capsule was formed. Fibroblast-like cells infiltrated the entire implant, but no giant cell response was seen in any section (fig. 1). Giant cells were found around hairs that had been accidentally introduced (this was found in all groups) indicating that giant cells could form, given the appropriate stimulus. The implanted collagen stained more strongly with eosin than did that of the host, and the collagenous bundles were not arranged in regular fashion.

Groups II to V. The histological appearance of the implants was identical with that of Group I.

Groups VI and VII. In contrast to Groups I to V, a very marked giant cell response was found in Groups VI and VII after 14 days. The background response was similar to that in the previous groups. A fibrous capsule formed and fibroblast infiltration occurred, but to a lesser extent. The giant cells were similar to those observed by Irving and Handelman ('63) and were of varying sizes up to 100 μ in diameter and containing as many as 40-50 nuclei (fig. 2). They were found mostly in the fibrous capsule surrounding the im-



Fig. 1. Cellular response around reconstituted calf-skin collagen removed 14 days after implantation. Infiltration by fibroblast-like cells only. Hematoxylin and eosin. 280

A Comparison of the Incisor Teeth of Intact Hypophysectomized and Thyropara-thyroidectomized Rats

J. E. GAVIN

Department of Basic Dental Sciences University of Otago
Dunedin, New Zealand

ABSTRACT Three types of macroscopic incisor abnormality were observed in Wistar rats examined post mortem. Most common was an altered relationship of the incisors to one another due to either fracture, elongation, rotation, malposition, or a combination of these factors affecting one or more incisors. Enamel hypoplasia was evident as opaque whitish blotches, bands or fine transverse striations. Other incisors showed an overall uniform pallor of the enamel. These abnormalities frequently affected the same animal or the same incisor. The associations between them were significant ($P < 0.01$). All the incisors of the intact group were normal and the incidence of abnormalities in hypophysectomized rats was not significantly higher ($P > 0.05$). However of the thyroparathyroidectomized animals 50.8% had an abnormal incisor relationship, 28.4% showed discrete enamel defects and 33% showed enamel pallor. The incidence of all types of abnormality was higher in surgically thyroparathyroidectomized rats ($P < 0.05$) than in other groups. No significant differences were found between completely and incompletely thyroidectomized rats or between subgroups which received different drug treatments. These findings are discussed in relation to similar reports and hypotheses are advanced to explain the abnormalities. Parathyroid deficiency rather than thyroid deficiency appears the most important etiological factor.

Several groups of workers in cancer research have noticed macroscopic and debilitating abnormalities of the incisor teeth of thyroidectomized rats. Bielschowsky and Hall ('53) reported the overgrowth of incisor teeth in surgically thyroidectomized rats. Money and Rawson ('60) observed the fracture of incisors in rats surgically thyroidectomized, and less frequently in those subjected to radiiodine thyroidectomy. Goodall ('63) mentioned over-eruption, fracture rotation and disturbed pigmentation in rats surgically thyroparathyroidectomized. He considered that these changes were accelerated by thyroid replacement therapy. However all these observations were incidental ones and served simply as an explanation for the associated nutritional difficulties and the high mortality in affected groups of animals.

Apart from Jung and Skillen ('29) who described both overgrowth and spontaneous fracture of the incisors of one of two thyroparathyroidectomized rats, detailed descriptions of the incisor changes are not available. Studies primarily con-

cerned with the effects of thyroidectomy and thyroparathyroidectomy on the incisors of the rat (Ziskin, Salmon and Applebaum, '40; Baume and Becks '52; Baume, Becks and Evans '54) describe microscopic changes in the incisors and a reduction in their rate of eruption but do not mention macroscopic abnormalities of the type described above. However opaque spots in the incisor enamel and a tendency for incisors to fracture have been reported associated with parathyroid deficiency by Schour, Chandler and Tweedy ('37). Hammett ('22) appears to have been the only investigator to differentiate between the effects of parathyroid deficiency and a concurrent thyroid and parathyroid deficiency. He concluded that the gross incisor abnormalities were specific effects which followed parathyroidectomy but not thyroparathyroidectomy.

This comparison was undertaken because of this confusion regarding the occurrence and incidence of macroscopic incisor abnormalities in thyroparathyroidectomized rats and the lack of a detailed description of these incisor defects.

MATERIALS AND METHODS

The heads of 138 rats which had been used by Goodall ('63) to study the influence of adrenocortical, thyroid and pituitary hormones on the carcinogenic action of 2 aminofluorene on the liver were examined. All were random bred male Wistar rats from the closed colony of the Otago University Animal Department and were aged between 40 and 70 weeks at necropsy. These animals had been housed in netting fronted metal cages in rooms maintained at $30 \pm 2^\circ \text{C}$. The cage floors were covered with wood shavings which were replaced weekly. Tap water, wheat, and a mash (bran 6 parts, pollard 7 parts, skim milk powder 4 parts, and maize meal 3 parts by weight) to which was added calcium carbonate CaCO_3 1 gm% and calcium phosphate $\text{Ca}_3(\text{PO}_4)_2$ 0.5 gm% were provided ad libitum. In addition, milk (about 10 ml per rat) and a portion of carrot or some other vegetable (about 10 gm per rat) were provided weekly and

cod liver oil (0.5 ml per rat) was given monthly.

Of the heads available 22 were from intact animals, 42 from rats hypophysectomized by the parapharyngeal method at four weeks of age and 74 were from rats surgically thyroparathyroidectomized at the same age. Hypophysectomy was judged complete in all animals examined by the virtually constant post-operative body weight and by the failure of development of the testes as indicated by the complete absence of spermia in sections of the seminiferous tubules. Thyroparathyroidectomized rats were classified as completely or incompletely thyroidectomized using the absence of normal acidophil cells in sections of the adenohypophysis stained with Papanicolaou's stain as modified by Green ('51) as the criterion for completeness. In one subgroup which was given terminal thyroid therapy however a failure to gain more than an average of one gram body weight per week in the first

TABLE 1

Numbers, treatments and distribution of factor abnormalities in the subgroups of rats examined

Surgical	Treatment			Number in subgroup	Malnutritionally	Examined hypopituitary	Examined pairs
	Cortisone	Aminofluorene	Other				
—	—	yes	—	3	—	—	—
—	yes	yes	—	19	—	—	—
			Total	22	—	—	—
Hypophysectomy	yes	yes	—	34	1	—	3
Hypophysectomy	yes	yes	Thyroid supplementation	8	—	—	2
			Total	42	1	—	5
Thyroparathyroidectomy	—	yes	—	8	5	3	—
Thyroparathyroidectomy	yes	—	—	7	3	2	—
Thyroparathyroidectomy	yes	yes	—	32	19	11	9
Thyroparathyroidectomy	—	yes	Terminal thyroid	16	10	4	7
Thyroparathyroidectomy	—	yes	Potassium iodide	11	5	1	1
			Total	74	42	21	1
Proportion of rats with abnormality				Intact	—	—	—
				Hypophysectomized	$2.4 \pm 2.4\%$	—	$11.9 \pm 5.7\%$
				Thyroparathyroidectomized	$56.8 \pm 5.8\%$	$23.4 \pm 5.2\%$	$23.0 \pm 4.9\%$

Numbers underlined indicate standard error

30 postoperative weeks was taken to indicate the absence of thyroid function.

Within each of these three groups subgroups had been treated with topical 2 aminofluorene tri-weekly for 30 weeks (total dose approximately 270 mg) or with 0.5 mg increasing to 2.0 mg of cortisone acetate daily by mouth until death or with both. In addition one subgroup of hypophysectomized rats received a thyroid digest in their drinking water in amounts equivalent to 1.9 mg of L-thyroxine per 100 gm body weight per day and another subgroup received potassium iodide at the rate of 5 mg per 100 gm of body weight daily by the same route. All treatments as far described commenced at eight weeks age. One subgroup of thyroparathyroidectomized rats received a thyroid digest as above commencing at 40 weeks age. The numbers of animals and treatments received by the various subgroups are summarized in table 1.

Heads were selected at random and examined with a 2 X magnifying lens and good lighting. When necessary soft tissue was removed to obtain a full view of the erupted portions of the incisor teeth. If after comparison with several affected rats, doubt still existed as to the structure, color or occlusion of the teeth, the animal was considered normal in that respect.

After classification, the described abnormalities were related to the experimental treatment the animals had received. The significance of differences in the proportion of rats affected by each type of abnormality between subgroups which differed in one type of experimental treatment (tables 3, 4) were determined using the exact probability test of Fisher (30). This test was also used to determine the significance of association between the various types of incisor abnormality.

RESULTS

The incisor abnormalities seen in the examined were of three types. Forty-three rats showed an alteration in relationship of their incisor teeth to the alveolar bone. This was evident from the unusual shape or position of the incisal

edge of the affected teeth. One or more of three factors produced these incisor malrelationships: (i) The fracture of one or more incisors (figs. 1 and 5) in which case the incisal ends of affected teeth were squared or irregular. (ii) The elongation of one or more incisors so that the incisal edges of affected teeth were above or below the normal level (figs. 1-5). In a considerable number of such rats lower incisors were in contact with the palate (figs. 2, 3 and 5) and upper incisors with the cheek pads tongue (fig. 3) or palate. (iii) The malposition of one or more incisors. Some malposed teeth were rotated on their long axes so that the layer of enamel, normally facing directly anteriorly was displaced laterally (fig. 4). In other instances affected incisors emerged from their supporting tissues at an unusual angle (fig. 5) resulting in overlapping or separation of the incisors. In the remaining instances of malposition the affected teeth were displaced bodily a finding which was usually associated with the over-eruption of an opposing tooth. The frequency and combinations of the factors contributing to incisor malrelationships are summarized in table 2.

The next most common type of abnormality noted was a variation in the intensity of enamel pigmentation of one or more incisors. Twenty-one rats showed either white patches (fig. 6) or bands (fig. 1) or a fainter transverse striation (fig. 3) in the orange colored enamel. Such changes

TABLE 2

Analysis of abnormalities of incisor relationship observed in thyroparathyroidectomized rats

Abnormalities observed	Number of animals	Proportion observed (the combination of abnormalities)
Fracture only	2	4.8
Elongation only	2	4.8
Malposition only	3	7.1
Fracture and elongation	5	11.9
Fracture and malposition	3	7.1
Elongation and malposition	15	33.7
Fracture, elongation and malposition	13	28.6
Total	43	100.0

were considered indicative of enamel hypoplasia. A few rats showed a fine transverse grooving of the enamel surface but this was not considered as hypoplasia unless changes in the degree of pigmentation were also present. Seventeen of the rats with enamel hypoplasia also had a malrelationship of their incisors a highly significant association ($P = 0.0013$).

The third type of abnormality noted also concerned the degree of pigmentation of the incisors. In these rats the enamel of affected teeth was noticeably paler in color than that of the corresponding teeth of other rats (fig. 8). Twenty-two rats showed this enamel pallor. Nine of these also had an incisor malrelationship and seven also showed incisor malrelationship and enamel hypoplasia. The association between enamel pallor and incisor malrelationship was highly significant ($P = 0.00061$) as was the association between enamel pallor and enamel hypoplasia ($P = 0.0027$).

None of the 22 intact rats examined showed any abnormality of their incisor teeth.

Of the 42 hypophysectomized rats examined (table 1) only one showed any variation in the relationship of the incisor teeth: the plane of occlusion of the teeth in this enamel was tilted due to the greater length (about 1.5 mm in each case) of the upper right and lower left incisor but all four incisors had a normal incisal bevel. None of the hypophysectomized rats showed any signs of enamel hypoplasia but five had

lower incisors with enamel noticeably paler than normal.

In the group of 74 thyroparathyroidectomized rats (table 1) 42 (56.8%) had some abnormality of incisor relationship. An analysis of these abnormalities is given in table 2. Twenty-one rats (28.4%) in this group had signs of enamel hypoplasia and 17 (23.0%) had two or more teeth with pale enamel.

Probability determinations (table 3) revealed no significant difference between intact and hypophysectomized subgroups or between completely and incompletely thyroidectomized subgroups. The thyroparathyroidectomized subgroup, however, had a significantly higher proportion ($P < 0.01$) of animals with all three types of incisor abnormality than the intact group and a significantly higher proportion with incisor malrelationships and enamel hypoplasia than the hypophysectomized group. The proportion of thyroparathyroidectomized rats with pale enamel is probably significantly higher ($P = 0.049$) than for similarly treated hypophysectomized rats.

Similar probability tests of the significance of the difference in proportion of rats affected by the described types of incisor abnormalities in subgroups which did or did not receive 2-aminofluorene or tizone acetate or potassium iodide therapy did not reveal any significant differences (table 4). Terminal thyroid therapy with having no significant effect on the proportion of rats with incisor malrelationship or

TABLE 3
Comparison of subgroups which were treated with 2-aminofluorene and cortisone but which differed in their surgical treatment

Subgroups compared	Number of rats in subgroups compared	Incisor malrelationship	Enamel hypoplasia	Enamel pallor
Intact	19			
Hypophysectomized	34	$P = 0.64$	—	$P = 0.35$
Intact	19			
Thyroparathyroidectomized	32	$P = 0.00072$	$P = 0.0037$	$P = 0.0082$
Hypophysectomized	34			
Thyroparathyroidectomized	33	$P = 0.0000003$	$P = 0.00012$	$P = 0.049$
Completely thyroidectomized	20			
Incompletely thyroidectomized	12	$P = 0.11$	$P = 0.33$	$P = 0.34$

TABLE 4

Comparison of subgroups of thyroparathyroidectomized rats which were similar except that one group did not receive particular drug treatment

Drug treatment	Numbers in subgroups compared	Significance of the difference between proportions with		
		Incisor malrelationships	Enamel hypoplasia	Enamel pallor
2-Aminofluorene	32 7	$P = 0.35$	$P = 0.62$	$P = 0.13$
Cortisone acetate	32 8	$P = 0.60$	$P = 0.60$	$P = 0.10$
Potassium iodide	11 8	$P = 0.39$	$P = 0.18$	$P = 0.58$
Terminal thyroid	16 8	$P = 0.67$	$P = 0.43$	$P = 0.033$

enamel hypoplasia, did increase the number of rats with pallor of the enamel by an amount which is probably significant ($P = 0.033$). However a comparison of the two subgroups of hypophysectomized rats one of which received thyroid supplementation throughout life, did not show a significant difference ($P = 0.23$) in the proportion with pale enamel.

DISCUSSION

The effects of the various surgical and drug treatments on the incidence of incisor abnormalities was investigated by comparisons between subgroups which differed in regard to one treatment only. However as differences which are not significant when small numbers are compared may prove to be significant when larger numbers are compared only statistically significant differences can profitably be discussed. In this study all significant ($P < 0.01$) and probably significant ($P < 0.05$ but > 0.01) were associated with differences in endocrine balance.

Although incisor abnormalities were not observed in intact animals in this study abnormalities of the relationship of the incisor teeth to one another do occur occasionally in intact rats. Addison and Appleton ('15) in their paper on the growth of the incisors of the albino rat quote Cope who in 1888 stated that nearly all the peculiarities of the rodent dental system and manner of mastication are the mechanical consequence of an elongation of their incisor teeth. These authors also

review the possible causes of incisor overgrowth. In addition to the explanation usually accepted at that time — the accidental breaking off of the opposing tooth — they mention too soft a diet, too rapid formation of tooth tissue a dislocation of one condyle with mandibular deviation and mandibular prognathism. In reviews of experimental studies with the incisor teeth of the rat Schour ('38) and Schour and Massler ('49) state that when an incisor is fractured its opponent continues growing without being worn off at the incisal edge. The eruptive rate of unopposed incisors has been shown to be markedly increased (Schour and Medak, '31; Bryer '37) and this would favor their elongation. Spiral elongation of incisors may also follow a malrelationship of incisal bevels (Schour and Massler '49). However with the exception of the soft diet hypothesis (Addison and Appleton '15) proof that incisor malrelationships can arise in any of these ways appears to be lacking.

The concept of incisor fracture followed in many cases by an elongation of the opposing tooth or teeth and sometimes also by deflection and displacement of unopposed teeth as they erupt towards occlusion, appears the most plausible explanation for the incisor malrelationships observed in this study.

The effects of hypophysectomy on the incisor teeth of the rat have been studied by Schour and Van Dyke ('32) Becka, Collins Simpson and Evans ('46) and

Baume, Becks, Ray and Evans ('54). All agree that there is a marked and progressive reduction in the rate of tooth eruption, an arrest in growth in size of the incisors, a gradual thickening of dentine and cementum and in some cases a severe derangement of the apical tissues of the incisor leading to an almost complete cessation of eruption. From this it seems that incisor fracture is unlikely to be the explanation of the incisor malrelationship seen in one hypophysectomized rat.

With the exception of the difference in proportion of thyroparathyroidectomized and hypophysectomized rats with enamel pallor which was probably significantly higher, thyroparathyroidectomized rats showed a significantly higher proportion of rats with all three types of incisor abnormality than either hypophysectomized or intact rats (table 3). This is consistent with the reports of Jung and Skillen ('29), Bielschowsky and Hall ('53) and Money and Rawson ('60) who observed some of these changes in surgically thyroidectomized rats but contrary to the conclusions of Hammett ('22) who considered that the incisors of thyroparathyroidectomized rats did not differ from those of intact animals.

Only two other attempts appear to have been made to determine the incidence of these abnormalities. Hammett ('22) found one rat out of twenty showing some unspecified dental abnormality 75 days after thyroparathyroidectomy. Money and Rawson ('60) found the proportion of surgically thyroidectomized rats with fractured incisors six months after operation to be 18% and in groups receiving thyroid therapy 35%. These figures agree closely with corresponding proportions with fractured teeth in the somewhat older animals in this study 18.5% and 50% respectively. The proportion of animals showing enamel hypoplasia does not appear to have been previously estimated and enamel pallor in association with thyroparathyroidectomy does not appear to have been previously described. The period of post-operative survival is probably an important factor in the incidence and severity of these abnormalities. Although the various drug treatments did not appear to have any significant effect on the inci-

dence of the abnormalities (table 4) this possibility cannot be excluded.

Because of the intimate anatomical relationship between the thyroid and parathyroid glands in the rat the surgical removal of one tissue must almost invariably affect the other. It follows that the possibility of a concurrent deficiency in both hormones must be considered when such experimental procedures are used. This is rarely done. The most obvious factor which could be involved in the development of the observed incisor changes in surgically thyroparathyroidectomized rats is thyroid deficiency since Money and Rawson ('60) have observed incisor fracture in rats thyroidectomized with radiiodine. Ziskin and Applebaum ('40-'41) and Baume, Becks and Evans ('54) believe that thyroid deficiency can give rise to a hypomineralization of dentin. This could conceivably predispose to incisor fracture and be associated with hypoplasia of enamel. Paradoxically however Money and Rawson ('60) observed a much higher incidence of incisor fracture in surgically thyroidectomized rats which received thyroid replacement therapy and Goodall ('63) considered the development of incisor abnormalities to be accelerated by treatment with thyroid extract or potassium iodide. In the present study thyroid treatment did not prevent incisor abnormalities and the hypophysectomized animals which would be essentially athyroid due to the absence of thyrotrophic hormone did not develop a significantly higher proportion of incisor abnormalities than intact rats. It is probable then that thyroid deficiency is not a major factor in the development of incisor abnormalities described.

The similarity between the observed incisor defects and those described in parathyroidectomized rats by Schour, Chandler and Tweedy ('37) strongly suggests that parathyroid deficiency consequent to surgical thyroidectomy or thyroparathyroidectomy may be an important factor in their causation. But since thyroid levels were not estimated by these authors and parathyroid levels of the animals examined were not known further investigations are needed to confirm the role of parathyroid deficiency in the

development of the incisor changes described.

Enamel hypoplasia, as defined and observed in this study has been reported as a result of a wide variety of experimental treatments. These include hypovitaminosis A and hypovitaminosis D (Schour and Massler 49) fluorosis (McCollum, Simmonds, Becker and Bunting, '25; Hodge, Luce-Clausen and Brown, '39; De Eds 41), treatment with aminocetonitrile and somatotrophic hormone (Selye, '57) surgical thyroidectomy (Baume, Becks and Evans '54) and parathyroidectomy (Schour Chandler and Tweedy '37). In the case of fluorosis and parathyroidectomy incisor fracture and elongation were also described and with the exception of the fluorosis and aminocetonitrile studies where no microscopic examination of the teeth were made, abnormalities of the formation and mineralization of dentine were also present. If we assume from this that enamel hypoplasia is associated with defective dentine structure the significant association found between enamel hypoplasia and incisor malrelationships could be due to a predisposition to incisor fracture.

Schour (34) however described enamel and dentine hypoplasia of uninjured incisors following experimental intra-alveolar fracture or damage to the enamel organ or other incisors. This he has termed an odontocytotoxic reaction a disturbance in the eruption and histological structure of growing teeth caused by an injury to distant teeth and their investing tissues. Until it is known whether or not enamel hypoplasia precedes incisor fracture this mechanism also remains a possible explanation for the association between enamel hypoplasia and incisor malrelationship.

The normal development of the pigmented enamel of the rat incisor has been described by De Eds (41) Pindborg Pindborg and Plum (46) Schour and Massler (49) Butcher (53) and Stein and Boyle (41 '50). A lack of incisor pigmentation sometimes termed depigmentation has been reported following a wide range of experimental treatments the majority of which have been reviewed and classified by Pindborg (53). Many of these treat-

ments are associated with an altered iron metabolism and a reduced iron content of the incisors. However it is unlikely that any dietary deficiency or excess was primarily responsible for the enamel pallor observed as all animals had the same diet.

Unfortunately not all the animals upon which Goodall ('63) based his mean terminal hematocrit determinations were available for examination in this study. However a comparison of the observed proportions of rats showing pale enamel with these mean hematocrit values for comparable subgroups of intact 0% 48.1 ± 1.08 hypophysectomized 8.8% 33.4 ± 1.76 and thyroparathyroidectomized 23.8% 27.8 ± 0.99 rats reveals that the incidence of enamel pallor increases with the degree of anemia. This explanation of the distribution of enamel pallor in this study is in accordance with the reports of Kitchin and McFarland ('33) Ratner ('39) Stein and Boyle (41) and Smith (49) of an association between a lack of enamel pigmentation and anemia.

Alternatively enamel pallor as observed could be explained on the basis of the accelerated rate of incisor eruption which follows both incisor fracture and thyroid treatment. Bryer ('57) and Ulmansky and Shapiro ('63) have observed that incisors regularly trimmed free of contact with opposing teeth and allowed unimpeded eruption show poorly pigmented enamel. Such unimpeded eruption, which is considerably faster than normal incisor eruption in intact rats (Schour 49; Schour and Medak, '51; Bryer '57) would reduce the time available for enamel apposition and pigmentation. A common dependence on incisor fracture may therefore be the explanation for the association found between incisor malrelationship and enamel pallor. This hypothesis is supported by the probably significant increase in the incidence of enamel pallor in the thyroparathyroidectomized animals which received terminal thyroid therapy. Baume Becks and Evans ('54) have shown that thyroid treatment increases the rate of eruption by 27% in thyroidectomized rats. However this hypothesis does not explain the occurrence of enamel pallor in the hypophysectomized rats which did not frac-

ture teeth and in which the eruption rate is up to 76% below that of intact rats (Baume Becks Ray and Evans '54)

ACKNOWLEDGMENTS

The author is indebted to Dr F Bielschowsky and Dr C M Goodall of the Hugh Adam Department of Cancer Research University of Otago Medical School. To the former as Director of the Department for permission to study this material and to the latter for providing the detailed information pertaining to it. And, in addition, to Mr G F S Spears Statistician, University of Otago Medical School, for his advice on statistical methods.

LITERATURE CITED

- Addison, W H F and J L Appleton 1915 The structure and growth of the incisor teeth of the albino rat. *J Morph.*, 26 43-96.
- Baume, L J and H Becks 1952 The effect of thyroid hormone on dental and parodontal structures. *Parodontologie* 6 89-106.
- Baume L J H Becks and H M Evans 1954 Hormonal control of tooth eruption. I. The effect of thyroidectomy on the upper rat incisor and the response to growth hormone thyroxine or the combination of both. *J Dent Res.*, 33 80-90.
- Baume L J H Becks, J C Ray and H M Evans 1954 Hormonal control of tooth eruption. II. The effect of hypophysectomy on the upper rat incisor following progressively longer intervals. *J Dent Res.*, 33 91-103.
- Baume, L J H Becks, M E Simpson and H M Evans 1946 Changes in the central incisors of hypophysectomized female rats after different post-operative periods. *Arch. Path* 41 457-478.
- Bielschowsky F and W H Hall 1953 Carcinogenesis in the thyroidectomized rat. *Brit. J Cancer* 7 355-366.
- Bryer L W 1957 An experimental evaluation of the physiology of tooth eruption. *Int. Dent. J* 7 432-478.
- Butcher E O 1953 Pigment formation in the rat incisor. *J Dent. Res* 32 133-136.
- DeEds F 1941 Factors in the etiology of mottled enamel. *J Amer Dent. Assoc.*, 28 1801-1814.
- Fisher R A 1950 Statistical methods for research workers 11th Ed Oliver and Boyd Edinburgh, p. 97.
- Goodall, C M 1963 The influence of adrenocortical, thyroid and pituitary hormones on the response of the liver to 2 aminoacetic acid. Thesis for M.D. University of Otago Medical School, New Zealand.
- Green, J D 1951 The comparative anatomy of the hypophysis, with special reference to its blood supply and innervation. *Am J Anat* 88 225-311.
- Hammett, F R 1922 Studies on the dental apparatus. VII. A differential effect of thyroparathyroidectomy and parathyroidectomy on the incisor teeth of the albino rat. *Amer J Physiol* 62: 197-201.
- Hodge, H. C., E. M. Loe-Clausen and E J Brown 1939 Fluorosis in rats due to contamination of commercial casein. The effect of darkness and of controlled radiation upon the pathology of the teeth. *J Nutrition*, 17 333-347.
- Jung, F T and W C Skillen 1929 Effects of thyroparathyroidectomy on the teeth of the rat. *Proc. Soc. Exp. Biol. (New York)*, 25 598-600.
- Kitchin, P C., and R D McFarland 1933 Do pasteurized milk cause variation from normal in the crystal structure of enamel formed during the period of use of such milk. *J Dent. Res.*, 13 359-362.
- McCollum, E V N Simmonds, J E Bach and R W Bunting 1925 The effect of additions of fluorine to the diet of the rat on the quality of the teeth. *J Biol. Chem* 63 551-562.
- Money W L, and R W Rawson 1960 The effect of L-thyroxine and 3,5,3',5'-tetraiodo-L-thyronine on the induction of dibenz(a,h)anthracene tumors in the rat. *Advances in thyroid research. Transactions of the 4th International Goitre Conference, London*, p. 383-391.
- Pindborg, J J 1953 The pigmentation of the rat incisor as an index of metabolic disturbance. *Oral Surg.*, 6 780-789.
- Pindborg, E V J J Pindborg and C M Finn 1946 Effect of iron deficiency in rats on incisor pigmentation. *Acta Pharmacol. (Kbh)*, 2: 285-293.
- Ratner S. 1939 The iron content of teeth of normal and anemic rats. *J. Dent. Res* 18 89-92.
- Schour I. 1934 The effect of tooth injury on other teeth. I. The effect of fractures confined to one or two incisors and their keratinized tissues upon the other incisors in the rat. *Physiological Zoology* 7 304-322.
- Schour I. 1938 In: *Dental Science and Art*. 1st ed. Henry Kimpton London, p. 83.
- Schour I, and M Masarik 1949 In: *The Rat in Laboratory Investigation*, 2nd Ed. Haber New York, pp. 104-163.
- Schour I, and N Madlak 1951 Experimental increase in rate of eruption and growth of rat incisor by eliminating nutrition. *J Dent Res* 30 521.
- Schour I, and H B Van Dyk 1932 Changes in the teeth of the white rat following hypophysectomy. *Amer J Anat.*, 50 297-333.
- Schour I, E B Chandler and W R Twiss 1937 Changes in the teeth following parathyroidectomy. I. The effects of different periods of survival, fasting and repeated parathyroidectomies and lactations on the incisor of the rat. *Amer J Physiol.*, 13 945-969.
- Selye H. 1957 Skeletal lesions produced by chronic treatment with somatotrophic hormone and aminoacetonitrile. *J Geront.*, 12 170-174.

- 1 Smith, M. C. 1949 Cited by Schour and Massler, 49, p. 134.
- Sach, G. and P. E. Boyle 1941 Studies on enamel. I. The yellow color of the incisor teeth of the albino rat. *J. Dent. Res.*, 20 301-302.
- Sach, G., and P. E. Boyle 1959 Pigmentation of the enamel of albino rat incisor teeth. *Arch. Oral Biol.* 1 97-105.
- Ulanovsky M. and S. Shapiro 1963 Changes in rat incisors resulting from trauma on the pulp. *J. Dent. Res.*, 42. 1467-1474.
- Ziarkin, D. E., and E. Applebaum 1940 Effect of thyroidectomy upon growing teeth of monkeys. *J. Dent. Res.*, 19 304-308.
- Ziarkin, D. E., and E. Applebaum 1941 Effects of thyroidectomy and thyroid stimulation on the growing permanent dentition of rhesus monkeys. *J. Dent. Res.*, 20 21-27.
- Ziarkin, D. E., T. N. Selmon and E. Applebaum 1940 The effect of thyroparathyroidectomy at birth and at seven days on dental and skeletal development of rat. *J. Dent. Res.*, 19 93-103.

PLATE 1

EXPLANATION OF FIGURES

All incisors shown are those of surgically thyroparathyroidectomized rats

- 1 Showing severe enamel hypoplasia, fracture of both lower incisors and elongation of both upper incisors.
- 2 Showing elongation of the lower left incisor in a rat with uniformly pigmented enamel.
- 3 Showing an elongation of both the animal's left incisors; the lower one has penetrated the palatal mucosa and the upper one passes between lower incisors and is in contact with the tongue. The enamel of the upper incisors shows a fine transverse striation.
- 4 Showing rotation of lower incisors associated with an elongation of the upper incisors.
- 5 Showing an unusual angle of emergence of incisors, fracture of the animal's upper right incisor and an overlapping of the lower incisors. Both lower incisors contact the palatal mucosa.
- 6 The incisors of the half head shown on the right of this illustration are normally pigmented while those on the left show an overall pallor. Those on the left side also show small discrete areas completely devoid of pigment.



The Fine Structure of the Glomerular Nephron of the Toadfish, *Opsanus tau*

RUTH ELLEN BULGER

Department of Anatomy Harvard Medical School, Boston, Massachusetts

ABSTRACT Kidney cell fine structure in the glomerular fish, *Opsanus tau*, varies profoundly with different fixation procedures. An extensive system of cisternae, tubules and irregular-shaped elements of smooth-surfaced membranes are seen in the basal cytoplasm after fixation with 2% OsO₄ buffered with α -collidine. Permanganate fixation demonstrates these membranes as extensions of the basal plasmalemma. Mitochondria and homogeneous bodies surrounded by a single dense membrane lie in close association with the basal membranes. The apical cytoplasm contains an abundance of smooth-surfaced elements whose morphology varies with the fixation procedure used. The fine structure of these cells is discussed with respect to that of other ion transporting tissues and with respect to the concept that basal infoldings are related to "water reabsorption."

Rhodin ('56 '62) examined the fine structure of the kidney tubules of the aglomerular teleost, *Lophius piscatorius*. With the fixation procedures used by him the cells of the aglomerular tubule were found to lack the basal infoldings of the plasma membrane which are present in the cells provided with brush borders in elasmobranch (*Squalus acanthias*) and mammalian kidneys. Due to the absence of glomeruli, urine formed by the aglomerular kidney has been presumed to result entirely from secretion. Inasmuch as basal infoldings were not seen in the aglomerular tubule, Rhodin concluded that basal infoldings of glomerular kidneys are involved in the process of water reabsorption. Because of the far reaching implications of this suggestion, it seemed important to re-examine this question in another aglomerular teleost.

The toadfish, *Opsanus tau*, was selected for this study because of its availability, ease of maintenance, and because it has been studied by light microscopists and physiologists.

MATERIAL AND METHODS

Toadfish *Opsanus tau*, were obtained from the supply department of the Marine Biological Laboratory at Wood's Hole. Some were transported to Harvard Medical School where they were kept in cold oxygenated sea water until used. Others were maintained in tanks of running sea water

at the Wood's Hole Marine Biological Laboratory.

The fish were removed from the sea water and their spinal cords transected. Pieces of kidney tissue were fixed in 1-1/3% osmium tetroxide buffered with α -collidine (Bennett and Luft, '59) in 5% or 8.25% glutaraldehyde with osmium tetroxide post fixation (Sabatini et al. '63) or in 3% unbuffered permanganate. They were dehydrated with cold ethanol and embedded in Epon epoxy resin by the method of Luft ('61). One micron sections stained with toluidine blue were studied with the light microscope. Thin sections were examined on unsupported or supported grids after staining with saturated uranyl acetate and Millonig's ('61) lead tartrate stain. Pictures were taken with RCA-3E or RCA-3G microscopes.

LIGHT MICROSCOPY OBSERVATIONS

The toadfish kidney consists of loosely packed tubules embedded in hemopoietic tissue. The tubules can be divided into two groups on morphological grounds: the kidney tubules proper and the collecting tubules.

The kidney tubules (fig. 1)

The epithelium of the renal tubule consists of a single layer of cells surrounding a lumen which may appear open or closed.

Present address: Department of Pathology University of Washington, Seattle, Washington.

In some regions the epithelial cells are cuboidal and in others they are columnar. The epithelium consists largely of one cell type (the brush border cell) although a second cell type is sometimes found interspersed among these cells.

Microvilli extend from the apical surface of the brush border cell into the lumen. A single cilium is often seen projecting from the cell and parts of several cilia can be resolved in the lumen. Distinct terminal bars are seen at the apical border between cells and a terminal web area traverses the apical cytoplasm between the terminal bars. A pale staining area exists beneath the terminal web and the nucleus lies basal to it. The nuclear position is somewhat apical with respect to the entire cell. The nuclei are sometimes indented and nucleoli are frequently encountered. The cytoplasm immediately surrounding the nucleus and lying basal to it stains intensely due to the concentration of mitochondria and other organelles in this region. A few densely stained bodies lie near the nucleus. In the basal region of certain cells, striations perpendicular to the basement membrane can sometimes be seen.

The kidney tubules are often almost completely surrounded by an endothelium-lined, thin-walled, large caliber vessel.

The collecting ducts (fig. 2)

The kidney tubules connect with collecting ducts. The epithelial cells of the collecting ducts are higher and frequently narrower. Microvilli and an occasional cilium are seen on the apical surface. In contrast to the apical region of the kidney tubular cells the apical region of these cells stains intensely. The nuclei lie in a more basal position and are extremely irregular in shape. Surrounding the collecting ducts are variable amounts of collagen and circumferentially oriented smooth muscle cells.

ELECTRON MICROSCOPY OBSERVATIONS

The kidney tubules

The appearance of the fine structure of kidney tubular cells depends on the fixation procedure used.

A Fixation with 1 1/4% OsO₄, buffered with α -collidine

The majority of the cells making up the wall of the tubule appear to be columnar or pyramidal in shape although some are cuboidal (figs. 4-5). The cell membrane appears to follow a relatively simple course without elaborate interdigitations or infoldings of the basal or lateral surfaces. Microvilli are located on the apical surface (fig. 4). They occasionally appear irregular in shape and contain rows of vesicles. Fine filaments radiate into the lumen from the apical plasma membrane which appear similar to the *stereocilia* or *microvilli* seen on gall bladder epithelium by Yamada ('55). The cells are held together at the apex by a junctional complex (Farquhar and Palade '63) consisting of a tight junction, an intermediate junction, and a desmosome. Additional desmosomes are found along the lateral surface apical to the nucleus (figs. 4-5).

Fine filaments are located in the microvilli and in the cytoplasm immediately beneath the microvilli (fig. 6). The apical cytoplasm is filled with a large variety of smooth-surfaced membranous profiles such as vesicles of varying density, regular or irregular vacuoles, tubules, and vesicles with a double membrane (figs. 4-6). In certain tubules the vesicles predominating near the apical surface tend to be smaller and denser whereas the ones which predominate in the deeper part of the apical cytoplasm are larger, paler and appear less regular in form (figs. 5-6). The apical cytoplasm also contains multivesicular bodies, two types of filaments, a few mitochondria, and a single cilium with its associated centriole. This zone corresponds to the pale staining area seen in 1 μ thick sections described above.

The nucleus lying beneath this apical layer of cytoplasm often has an irregular shape and nucleoli are frequently encountered. Occasional cells are binuclear.

Golgi profiles are located lateral or apico-lateral to the nucleus (figs. 4-6). They consist of membranous cisternae and associated vesicles. The position of the Golgi profiles suggests that the apparatus has the form of a crown on the nucleus.

The mitochondria of the cell are found around the nucleus and in the cytoplasm

lying basal to the nucleus (figs. 4 5 9). They possess relatively few cristae, a moderately dense matrix, and a few small electron dense intramitochondrial granules. The mitochondrial profiles are often elongate.

The most significant feature of the cell is the elaborate system of smooth-surfaced membranes seen in the cytoplasm around and especially beneath the nucleus (figs. 4 5 9). The most frequent appearance assumed by the smooth-surfaced membranes consists of whorls and parallel arrays of cisternae although vacuoles and tubules are also present. The exact configuration and number of these membranes varies from cell to cell. Near the basal region of the cell, the cisternae tend to connect with tubular elements which only rarely can be seen in connection with the basal cell membranes. Mitochondria and homogeneous bodies surrounded by a single dense membrane occupy much of the space between the array of membranes (fig. 9). The homogeneous bodies resemble the microbodies identified in the cytoplasm of mouse proximal convoluted tubular cells by Rhodin ('54). The material in the homogeneous bodies resembles the matrix of the mitochondria.

Some membrane limited non-homogeneous bodies are present which resemble the cytosomes seen in rat proximal convoluted tubular cells (Trump '61) (figs. 4 5).

A few irregularly shaped profiles of rough-surfaced endoplasmic reticulum groups of free ribonucleoprotein particles (RNP) and particles presumed to be glycogen can also be seen in the cytoplasm.

The basal plasma membrane rests on a basal lamina which often consists of two or three interwoven layers. Thin-walled vessels frequently lie close to the basal lamina. The endothelium is of the thin variety with two types of specializations (1) pores bridged by a thin diaphragm and (2) large gaps in the endothelial lining (fig. 4).

A second cell type is found in the wall of the tubule (fig. 5). The nucleus of this cell lies in the basal region of the tubule. The cytoplasm is extremely granular but contains some smooth-surfaced vesicles. The cell often has an irregular shape with cytoplasmic processes extending between

the tubular cells. The usual organelles exist in these cells but in low concentration. Cells with similar morphology have been identified in the proximal tubule of *Fundulus heteroclitus* by Gritzka ('63). He suggested that they are lymphocytes.

Although slight variations in the height of the cells and the amount and appearance of specific organelles were noted from section to section, no attempt was made to correlate these differences with the physiological state of a given tubule or the position along the length of the tubule.

B Fixation with glutaraldehyde buffered with α -collidine post-fixed with OsO₄ buffered with α -collidine

The appearance of the apical region of the kidney cells is markedly changed from that seen after 1½% OsO₄ fixation alone (fig. 7). The cytoplasmic ground substance appears extremely dense and contains a massive network of filaments. The filaments sometimes have a beaded texture and tend to run in bundles. The smooth-surfaced membranes are less conspicuous and of irregular shape. The apical region also contains microtubules, multivesicular bodies, presumptive glycogen granules and an occasional mitochondrion. The three components of the junctional complex can be seen (fig. 7).

The nucleus contains clumps of chromatin especially prominent near the nuclear membrane but also scattered throughout the entire nucleus.

The matrix of the mitochondria, cytosomes, and microbodies appears extremely dense. The distribution, size and shape of these organelles are consistent with that seen after osmium fixation alone.

The extensive system of smooth-surfaced basal membranes is seen as cisternae running perpendicularly to the basal plasmalemma, looping over groups of mitochondria, and returning to the basal region. Communications between the membranes of the cisternae and the plasmalemma appear more frequently with this fixation. Smaller smooth-surfaced elements lie between the mitochondria and may be part of a different system of smooth-surfaced membranes.

Occasional myelin figures are seen in the lateral intercellular spaces.

C Fixation with 3% unbuffered potassium permanganate

Most cellular organelles vary in appearance after permanganate fixation from that seen after OsO_4 fixation procedures. Microvilli are regular unbranched and do not contain vesicles although some areas show bulbous protrusions indicative of swelling (figs. 3-8). The cell membrane of the cilia is still present but the internal tubular structures are not visible. The cytoplasmic ground substance is and just beneath the microvilli and along the lateral border of the cell apical to the nucleus is finely fibrillar and lacks organelles. Although the tight junctions are present, the densities associated with the intermediate junctions and the desmosomes are in general, lacking (fig. 8). The apical cytoplasm is filled with smooth-surfaced membrane profiles predominately in the form of branching cisternae of irregular twisted shapes with narrow lumens. A few vesicular and tubular profiles are also seen (fig. 8). The ends of the cisternae often show bulbous outpocketings. Between the membranous profiles of this region are presumptive glycogen particles and multivesicular bodies of irregular shape.

The nuclear membrane has a wrinkled appearance. The nuclear pores are large and lack a conspicuous diaphragm. Chromatin clumps are seen near the nuclear membrane around the nucleolus, and interspersed in the matrix. The nucleolus appears pale (fig. 3).

Mitochondria lie apical and lateral to the nucleus and fill most of the basal half of the cell (fig. 3). In some regions the mitochondria are elongate and cristae extend across the width as extensions of the inner mitochondrial envelope. In most regions, however the mitochondrial profiles are circular and appear swollen. The cristae in these profiles are crescents, loops, or short plates often seen connecting with the inner envelope. A few mitochondria appear to be hybrids with swollen ends and a narrower mid-piece bridged by cristae. The matrix is pale and contains intramitochondrial granules.

Microbodies are scattered among the mitochondria. They have a single sur-

rounding membrane and a pale matrix. Cytosomes lie near the nucleus. They consist of a variety of components in a dense matrix.

Two types of smooth-surfaced membranes are seen in the basal cytoplasm. The first type resembles those seen in the apical cytoplasm. They show a variety of shapes and are interspersed among mitochondria and other organelles. These membranes appear to be endoplasmic reticulum (fig. 10). The second type of smooth-surfaced membranes seen in the basal cytoplasm with permanganate fixation appear as extensions of the basal plasmalemma. A few of the membranes are true basal infoldings but most seem to surround interdigitating processes. Although most of the processes are completely enclosed by a membrane and therefore cannot be traced to their origin, some adjacent processes can be traced into the same cell. Unless rearrangement occurred during the process of specimen preparation some of the interdigitating processes come from the same cell.

The collecting ducts

A. Fixation with 1% OsO_4 , buffered with α -collidine

High columnar cells line the collecting ducts (fig. 11). The cell membrane follows a relatively simple course but some interdigititation occurs on the lateral surface than is seen in the kidney tubule cells. Long microvilli are present on the apical surface (figs. 11-13). A single cilium and its associated centriole can be seen in the apical region. Since the nucleus lies in a basal position the apical region is large. The apical cytoplasm contains filaments and vesicles as seen in the kidney tubule cells but also contains two additional organelles (fig. 13). The first type consists of electron-dense membrane-bounded granules which often appear round in profile but may exhibit a flattened appearance. The second type consists of stacks of flattened vacuoles similar to those seen in mammalian bladder (Walker '80). Mitochondria, multivesicular bodies, and vacuoles are also found in the apical cytoplasm. The Golgi apparatus is located just beneath this specialized area of cytoplasm.

and apical to the nucleus. It consists of several rows of cisternae which form a cap over the nucleus (fig. 11). Groups of vesicles with intermediate density are generally seen on the nuclear side of the sacs. On the upper side of the cisternae of the Golgi apparatus and adjacent to the Golgi area are several large expanded areas of the Golgi cisternae which appear empty.

The nucleus lies basal to the Golgi apparatus. It is irregular in shape and has deep cytoplasmic indentations. A nucleolus is frequently seen in the nucleus (fig. 11).

The mitochondria are elongate and contain a higher concentration of cristae than those seen in the kidney tubular cell. Their matrix has an intermediate density and contains intramitochondrial granules. The mitochondria are found throughout the entire cytoplasm and not concentrated in the basal region as in the kidney tubular cell.

Although the cytoplasm contains some smooth-surfaced membranes as cisternae, tubules and vacuoles the amount is decidedly less than that seen in the kidney tubular cells. A few profiles of rough-surfaced endoplasmic reticulum and some free RNP particles can be identified.

A thick basal lamina is present and often appears to consist of several interwoven layers. The basal plasma membrane is irregular and the basal lamina follows its contour. The endothelium-lined vessels often lie close to the base of the epithelium. Variable amounts of collagen and smooth muscle cells surround the collecting ducts (fig. 11).

B. Fixation with glutaraldehyde buffered with α -collidine post-fixed with OsO₄ buffered with α -collidine

After glutaraldehyde fixation, some structural variations were noted in the collecting ducts. The apical granules appeared pale and irregular in shape, with a few interruptions in their surrounding membranes (fig. 14). The cytoplasmic matrix was filled with filaments, microtubules, multivesicular bodies, mitochondria, and a few myelin figures. The apical smooth-surfaced membranes were much less conspicuous.

The nuclear chromatin exhibited clumping. Groups of RNP particles and ele-

ments of rough-surfaced endoplasmic reticulum were in abundance and appeared to be well fixed.

C. Fixation with 3% unbuffered potassium permanganate

After permanganate fixation, the apical granules appear pale and are interspersed between vesicular and irregular cisternae of smooth-surfaced membranes (fig. 12). The tight junction is present but the other elements of the junctional complex are not obvious. Cytoplasmic fibrils are not demonstrable with this fixation procedure. The nuclear outline is exceedingly irregular the chromatin is clumped, and the nucleoli are pale. Mitochondria appear somewhat swollen and have a pale matrix. Only a few extensions of the plasmalemma exist in the basal cytoplasm but smooth-surfaced membranes of the endoplasmic reticulum can be seen (fig. 12). RNP particles are not visible with this fixation procedure.

DISCUSSION

Agglomerular marine teleosts have frequently served as valuable experimental animals. Huot ('52) first recognized that certain marine teleost kidneys have no glomeruli. Audigé (10), Marshall and Grafflin ('28) and Grafflin ('29) studied the kidney of the goosefish, *Lophilus piscatorius* and confirmed its agglomerular nature. Many examples of agglomerular species are listed by Edwards ('28). Marshall ('29) was the first to describe the agglomerular kidney of the toadfish. The kidney consists of tubules without glomeruli embedded in what he described as abundant lymphoid tissue. Using Audigé's (10) system for classifying teleost kidneys Marshall concluded that the kidney of the toadfish is mesonephric in type. The greater part of the tubule was described by Marshall ('29) as consisting of high cuboidal, rodlike epithelium which at the end became low cuboidal, more basophilic and lacked striations. The short basophilic segment could be traced into a collecting duct. Grafflin ('31 '37a and b) showed that the entire agglomerular tubule possessed a brush border. Deffrise ('32) noted a long flagellated diplosome, an irregular nucleus a chondriome distributed

throughout the cell, and Golgi varying in number, volume and position.

The composition and flow rate of the urine of the aglomerular teleost approximates that of the glomerular teleost (Edwards and Condorelli, '28 Marshall, '30 '34 Smith, '30 '51 Marshall and Grafflin '32; and Bleter '33a, b). The aglomerular tubules can excrete chloride, creatine, creatinine, magnesium, potassium sulphate, urea, uric acid, and certain foreign substances and dyes. The aglomerular tubules cannot excrete glucose or other sugars, ferrocyanide or albumin which can be excreted by the glomerular tubule under certain conditions.

The secretion pressure measured in the toadfish ureter was shown by Bleter ('31) to be greater than the dorsal aortic blood pressure and probably 4-5 times as high as the blood pressure in the kidney capillaries. The epithelium of the aglomerular tubules can therefore secrete a wide variety of specific substances at a considerable secretion pressure. The elucidation of the fine structure of the aglomerular kidney should provide much information on the machinery used by the cell to carry out these processes. Such a study was originally made by Rhodin ('56) who

ulated that the lack of "basal infoldings" in the aglomerular kidney was related to the specialized function of this kidney and the presence of "basal infoldings" in other tissues was related to the process of water reabsorption. Four lines of evidence suggest that this hypothesis might profitably be re-examined at this time.

1. Morphological variation with multiple fixation procedures

The observed fine structure of toadfish renal tubular cells is to a certain degree dependent on the fixative used. The most striking difference was seen in the morphology of the smooth-surfaced membranes in the basal cytoplasm. After osmium tetroxide fixation they appeared to be intracellular membranes only rarely connecting with the basal surface but after permanganate fixation the membranes appeared as extensions of the basal plasmalemma similar to those seen in

mammalian kidneys. Although it presently is not possible to know the state in the living animal, it seems more likely that fragmentation is occurring at some stage in the osmium and glutaraldehyde fixation procedures than that a fusion of membranes is occurring during the permanganate fixation process. This hypothesis however is highly speculative and needs experimental verification.

Differences in fine structural detail have been demonstrated in a variety of tissues using different fixatives (Ito, '61 Sedo '62 Rosenbluth, '63 Torney '64 Trump and Ericsson, '65 and Bulger and Trump '65b). Such studies indicate the general nature of this problem and emphasize the importance of using multiple fixation procedures in descriptive studies.

2. Morphology of aglomerular and glomerular fish kidneys

A system of basal membranes similar to that found in *Opsanus tau* is seen in extensive regions of the renal tubule of glomerular teleosts such as *Fundulus heteroclitus* (Gritzka, '63) and *Parophrys reticulatus* (Bulger and Trump '65a). The aglomerular fish therefore cannot be separated from the glomerular fish on the basis of the morphology of the basal plasmalemma.

3. Consideration of the function of the aglomerular kidney

Secretion is probably the most important mechanism in the production of urine in the aglomerular kidney. The fact that the urine is hypotonic suggests that reabsorption (as well as secretion) is also occurring. Otherwise one would have to postulate an active water transport mechanism requiring an extremely large energy expenditure to explain the hypotonicity of the resulting urine. The proposed reabsorption might occur through the same cells that are involved in secretion or through a specialized region of the kidney tubule or collecting duct. It is of interest to note that the mitochondria of the kidney tubules are concentrated in the basal region of the cell while the mitochondria of the collecting ducts are concentrated in the apical region.

4 Morphology of related tissues

Although the presence of basal interdigitations and/or infoldings often correlates with the reabsorption of salt, as exemplified by the mammalian proximal convoluted kidney tubule marked reabsorption does occur through cells which lack extensive basal specializations. Examples of transporting cells which lack this marked specialization are the epithelial cells of the gall bladder (Yamada, '65) and the reabsorptive cells lining the intestine (Palay and Karlin '59).

Cells presumably involved in a secretory (not reabsorptive) function which possess basal infoldings or interdigitations include those of the rectal salt-secreting gland of the dogfish (Bulger '63) and the nasal salt gland of marine birds (Doyle '60; Kornick, '63).

Although basal membrane specializations are present in many cell types which are presumably involved in active ion secretion and reabsorption, they are seemingly not a prerequisite. A specialized system of smooth-surfaced intracytoplasmic membranes can be found in actively transporting cells such as the chloride cells of certain fish gills (Kessel and Beans, '62; Philpott, '61 '62; Philpott and Copeland, '63) and the gastric parietal cells (Sedar '61a and b; Ito '61; Ito and Winchester '63). Mitochondria are often found in close association with the basal and the smooth-surfaced membranes in the above cell types.

Extensive membrane specializations are therefore frequently (but not invariably) found in cells involved with the active transport of ions. These specializations, when present, may take the form of infolded or interdigitated basal cell membranes or of intracytoplasmic smooth-surfaced membranes.

ACKNOWLEDGMENTS

This investigation was supported by grants GM 10182 from the USPHS Institute of General Medical Sciences, and G-12916 from the National Science Foundation. The author wishes to express her gratitude to Dr D W Fawcett for his help and encouragement throughout the course

of this study and to Dr B F Trump at the University of Washington where the work was completed.

LITERATURE CITED

- Andigé, J. 1910 Contribution à l'étude des reins des poissons téléostéens. Arch. Zool. exp. et gén., T.4 275-324.
- Bennett, H. B., and J. H. Luft. 1960 a-Cellulose as a basis for buffering fixatives. J. Biophys. Biochem. Cytol., 6 113-114.
- Bleier, R. M. 1931 The secretion pressure of the aglomerular kidney. Am. J. Physiol., 87 66-68.
- . 1933a Excretion of phenol red by the aglomerular kidney. Proc. Soc. Exper. Biol. and Med., 30: 981-984.
- . 1933b Albuminuria in glomerular and aglomerular fish. J. Pharm. and Exper. Therap., 43 407-412.
- Bulger, R. E. 1963 Fine structure of the rectal (salt-secreting) gland of the spiny dogfish, *Squalus acanthias*. Anat. Rec., 147 95-137.
- Bulger, R. E., and B. F. Trump. 1965a A light and electron microscopic study of the mesonephric kidney of the English sole, *Parophrys vetulus*. Anat. Rec., 151 443.
- . 1965b Effects of fixatives on tubular ultrastructure of the aglomerular midshipman, *Porichthys notatus* and the glomerular flounder, *Parophrys vetulus*. J. Histochem. Cytochem., (in press).
- Deftoe, A. 1932 Cytophysiological studies of the nephrocytes of unsegmental aglomerular and glomerular nephrons. Anat. Rec., 54 185-195.
- Doyle, W. L. 1960 The principal cells of the salt-gland of marine birds. Exp. Cell Res., 21 386-393.
- Edwards, J. G. 1928 Studies on aglomerular and glomerular kidneys. I. Anatomical. Am. J. Anat., 42: 78-107.
- Edwards, J. G. and L. Condorelli. 1928 Studies on aglomerular and glomerular kidneys. II. Physiological. Am. J. Physiol., 86 383-396.
- Farquhar, M. G., and G. E. Palade. 1963 Junctional complexes in various epithelia. J. Cell Biol., 17 375-413.
- Grafflin, A. L. 1929 The pseudoglomeruli of the kidney of *Lophtius piscatorius*. Am. J. Anat., 44 441-454.
- . 1931 The structure of the renal tubule of the toadfish. Bull. Johns Hopkins Hosp., 48 260-271.
- . 1937 Observations upon the aglomerular nature of certain teleostean kidneys. J. Morph., 61 155-173.
- . 1937b The structure of the nephron in fishes. Anat. Rec., 68 287-303.
- Gritske, T. L. 1963 The ultrastructure of the proximal convoluted tubule of euryhaline teleost *Fundulus heteroclitus*. Anat. Rec., 145 235-256.
- Huot, A. 1902 Recherches sur les poissons Lophobranchés. Ann. d. Sci. Nat. (Zool. et Paleont.) T.14 197 258.

- Ito S. 1961 The endoplasmic reticulum of gastric parietal cells. *J. Biophys. Biochem. Cytol.*, 11 333-347
- Ito, S. and R. J. Winchester 1963 The fine structure of the gastric mucosa of the bat. *J. Cell Biol.*, 16 541-577
- Kaseel R. G. and H. W. Beams 1962 Electron microscope studies on the gill filaments of *Fundulus heteroclitus* from sea water and fresh water with special reference to the ultrastructural organization of the chloride cell. *J. Ultrastruct. Res.*, 6 77-87
- Komnick, H. 1963 Elektronenmikroskopische Untersuchungen zur funktionellen Morphologie des Ionentransportes in der Salzdrüse von *Larva argenteus*. I. Teil Bau und Feinstruktur der Salzdrüse. *Protoplasma*, 56 274-314
- Luft, J. H. 1961 Improvements in epoxy resin embedding methods. *J. Biophys. Biochem. Cytol.*, 9 409-414
- Marshall, E. K., Jr. 1929 The aglomerular kidney of the toadfish (*Opsanus tau*). *Bull. Johns Hopkins Hosp.*, 43 95-101
- 1930 A comparison of the function of the glomerular and aglomerular kidney in toadfish. *Am. J. Physiol.*, 94 1-10.
- 1934 The comparative physiology of the kidney in relation to theories of renal secretion. *Physiol. Rev.*, 14 133-159
- Marshall, E. K., Jr. and A. L. Grafflin 1928 The structure and function of the kidney of *Lophius piscatorius*. *Bull. Johns Hopkins Hosp.*, 43 825-836
- 1932 The function of the proximal convoluted segment of the renal tubule. *J. Cell and Comp. Physiol.*, 1 161-176
- Millonig, G. 1961 A modified procedure for lead staining of thin sections. *J. Biophys. Biochem. Cytol.*, 11 736-739
- Palay S. L. and L. J. Kardin 1959 An electron microscope study of the intestinal villus. I. The fasting animal. *J. Biophys. Biochem. Cytol.*, 5 363-372
- Philpott, C. W. 1961 The adaptive morphology of the chloride secreting cells of *Fundulus* as revealed by the electron microscope. Abstract, 1st annual meeting of the Am. Soc. Cell Biology Chicago p. 167
- 1962 The comparative morphology of the chloride secreting cells of three species of *Fundulus* as revealed by the electron microscope. *Am. J. Rec.* 142: 267
- Philpott, C. W. and D. E. Copeland 1963 Fine structure of chloride cells from three species of *Fundulus*. *J. Cell Biol.* 18 389-404
- Rhodin, J. 1954 Correlation of ultrastructural organization and function in normal and experimentally changed proximal convoluted tubule cells of the mouse kidney. *Karolinska Institutet, Stockholm, Thesis*
- 1956 Studies on the nephron structure in mouse, goosefish and dogfish. Paper read at the meeting of the Royal Society in October 1956, Ciba Foundation, London.
- 1963 Electron microscopy of the kidney. In *Renal Disease*, Ed. by D. A. K. Kirk. Blackwell Scientific Publications, Oxford
- Rosenbluth J. 1963 Contrast between osmium fixed and permanganate-fixed toad spinal ganglia. *J. Cell Biol.* 16: 143-157
- Sabatini, D. D., K. Benach and R. J. Berez 1963 Cytochemistry and electron microscopy. The preservation of cellular ultrastructure and enzymatic activity by aldehyde fixation. *J. Cell Biol.*, 17 19-58
- Sedar A. W. 1961a Electron microscopy of the excretory cell in the bullfrog (*Rana catesbeiana*). I. The non-acid-secreting gastric mucosa. *J. Biophys. Biochem. Cytol.*, 9 1-12
- 1961b Electron microscopy of the excretory cell in the gastric glands of the bullfrog *Rana catesbeiana*. II. The acid-secreting gastric mucosa. *J. Biophys. Biochem. Cytol.* 9 47-57
- 1962 Electron microscopy of the excretory cell in the gastric glands of the bullfrog *Rana catesbeiana*. III. Permanganate fixation of the endoplasmic reticulum. *J. Cell Biol.* 14 152-156
- Smith, H. W. 1930 The absorption and excretion of water and salts by marine larvae. *Am. J. Physiol.*, 23 480-503
- 1951 *The Kidney: Structure and Function in Health and Disease*, Oxford University Press, New York
- Turney J. M. 1954 Differences in membrane configuration between osmium tetroxide-fixed and glutaraldehyde-fixed ciliary epithelium. *J. Cell Biol.*, 23 656-664
- Trump B. F. 1961 Electron microscopic study of the uptake, transport, and storage of colloidal materials by the cells of the vertebrate nephron. *J. Ultrastruct. Res.*, 5 291-310
- Trump B. F. and J. L. E. Erickson 1965 The effect of the fixative solution on the ultrastructure of cell and tissues. *Symposium on Quantitative Electron Microscopy* Ed. C. J. Bahr and E. Zettler. Lab. Invest. (in press)
- Walker B. E. 1960 Electron microscopic observations on transitional epithelium of the mouse urinary bladder. *J. Ultrastruct. Res.* 3 345-361
- Ymada, E. 1955 The fine structure of the gill bladder epithelium of the mouse. *J. Biophys. Biochem. Cytol.*, 1 445-456

PLATES

PLATE 1

EXPLANATION OF FIGURES

- 1 A light micrograph from a 1μ section of the renal tubules of the toadfish. The epithelium consists of a single layer of cells which demonstrate microvilli projecting into the lumen (1) distinct terminal bars between cells, nuclei (n) lying in a slightly apical position surrounded by densely staining cytoplasm which is the result of a high concentration of mitochondria and other organelles. The tubules are often surrounded by thin-walled vessels () Stained with toluidine blue $\times 700$.
- 2 A light micrograph from a 1μ section of a collecting duct of the toadfish. The epithelial cells lining the collecting duct are higher and narrower than the renal tubular cells. The nuclei (n) are extremely irregular in shape and occupy a basal position in the cell. Variable amounts of collagen and circumferentially oriented smooth muscle cells can be seen surrounding the collecting ducts. Stained with toluidine blue $\times 700$.
- 3 An electron micrograph of the cells lining the renal tubule of the toadfish. Microvilli (mv) extend into the lumen. The apical cytoplasm is filled with smooth-surfaced membrane profiles. Chromatin clumps are seen in the nucleus (n). Mitochondria (m) lie apical, lateral, and basal to the nucleus. Smooth-surfaced membranes are seen in the basal cytoplasm. Fixed in 3% potassium permanganate. Stained with uranyl acetate and Millonig's lead tartrate, $\times 5,900$.

Ruth Ellen Sulzger

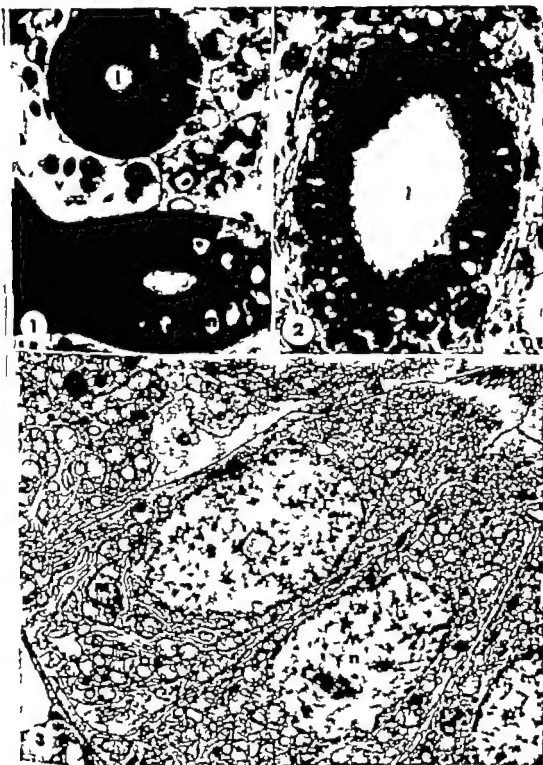


PLATE 2

EXPLANATION OF FIGURES

- 4 An electron micrograph of the cells lining the renal tubule of the toadfish. Microvilli (mv) extend into the lumen. The apical cytoplasm is filled with vesicles (v). With this fixation the cell membrane follows a simple course without elaborate plications. The nucleus (n) has a homogeneous appearance. The mitochondria (m) are elongate with dense matrix material. Golgi apparatus (g) is seen lateral to the nuclei. Smooth-surfaced membranes lie in the basal cytoplasm but connections with the basal plasmalemma are rare. An endothelium-lined vessel is seen at the right. The endothelium demonstrates gaps (double arrow) and pores bridged by thin diaphragm (single arrow). Fixed in 1½% OsO₄ buffered with ε-collidine. Stained with uranyl acetate and Millonig's lead tartrate × 8,100.
- 5 An electron micrograph of the cells lining the renal tubule of the toadfish. Microvilli extend into the lumen (l). The Golgi apparatus (g) lies lateral to the homogeneous nucleus (n). The mitochondria (m) and microbodies (mb) are concentrated in the basal cytoplasm. Cytosomes (c) are seen near the nucleus and an example of the second cell type is evident (II). Fixed in 1½% OsO₄ buffered with ε-collidine. Stained with uranyl acetate and Millonig's lead tartrate × 8,300.



PLATE 3

EXPLANATION OF FIGURES

- 6 An electron micrograph of the pical region of the kidney tubular cells fixed with 1½% OsO₄ buffered with α-collidine. Microvilli (mv) extend into the lumen. With this fixation procedure the apical cytoplasm is filled with vesicles (v) of varying density; those nearer the lumen containing more electron dense substance. The nucleus (n) appears homogeneous. Stained with uranyl acetate and Millonig lead tartrate × 13,700.
- 7 An electron micrograph of the pical region of the kidney tubular cells fixed with glutaraldehyde buffered with α-collidine. The pical cytoplasm is filled with filaments (f) and microtubules (mt). A few smooth-surfaced membranes of irregular shape are seen. Stained with uranyl acetate and Millonig lead tartrate × 17,600.
- 8 An electron micrograph of the pical region of the kidney tubular cells fixed with 3% unbuffered potassium permanganate. Microvilli (mv) extend into the lumen. Except for narrow zones under the microvilli and along the lateral plasmalemma, the pical cytoplasm is filled with irregularly shaped smooth-surfaced elements. Stained with uranyl acetate and Millonig lead tartrate × 15,400.

Each Electron Micrograph



PLATE 4

EXPLANATION OF FIGURES

- 9 An electron micrograph of the basal region of the kidney tubular cells fixed with 1½% OsO₄ buffered with *s*-collidine. An elaborate system of smooth-surfaced membranes is seen consisting of whorls and parallel arrays of cisternae, vacuoles, and tubules. No connections of the smooth-surfaced membranes are seen in this picture. Mitochondria (m) and microbodies (mb) lie between the smooth-surfaced membranes. A lateral cell membrane (lcm) is also evident. Stained with uranyl acetate and Millonig lead tartrate, × 13,400.
- 10 An electron micrograph of the basal region of the kidney tubular cells fixed with 3% potassium permanganate. The majority of the smooth-surfaced membranes in the basal cytoplasm appear to be extensions of the basal plasmalemma. At the arrow second type of smooth-surfaced membrane is seen which is interpreted as endoplasmic reticulum. Stained with uranyl acetate and Millonig lead tartrate, × 24,700.

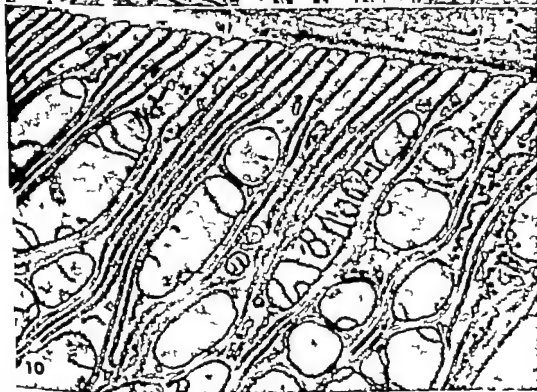
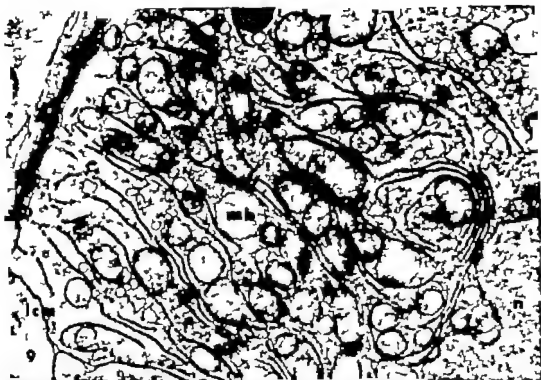


PLATE 5

EXPLANATION OF FIGURE

- 11 An electron micrograph of the cells lining a collecting duct. Microvilli (mv) extend into the lumen. The apical cytoplasm contains mitochondria (m) vesicles () granules (gr) and stacks of flattened vacuoles (va). The Golgi (g) often lies apical to the irregular nuclei (n). Some smooth-surfaced membranes can be seen in the basal cytoplasm. The basal plasmalemma is irregular and the basal lamina (bl) follows its contours. Variable amounts of collagen and smooth muscle cells (sm) surround the collecting ducts. Fixed in 1½% OsO₄ buffered with ε-collidine. Stained with uranyl acetate and Millonig's lead stain. × 6,200.

Ruth Ellen Ridger

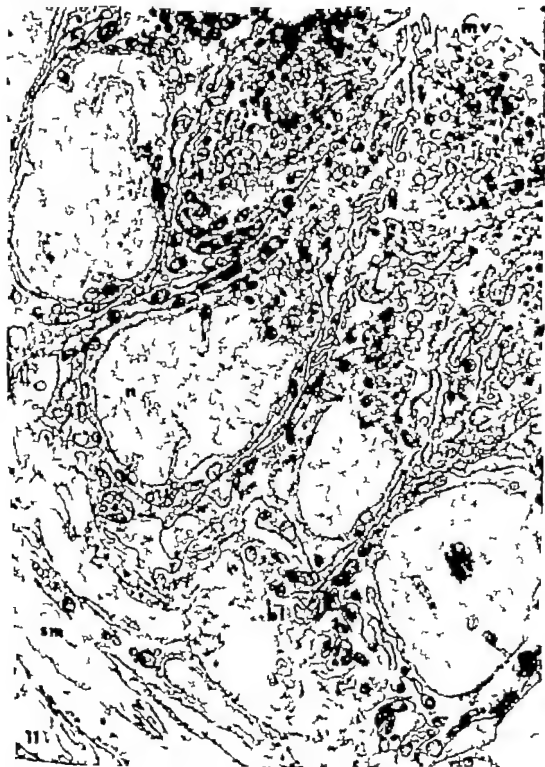


PLATE 8

EXPLANATION OF FIGURES

- 12 An electron micrograph of the cells lining a collecting duct after fixation in 3% potassium permanganate. The apical granules (gr) appear pale with this fixation procedure. The nuclei (n) have irregular outlines and contain clumped chromatin. Stained with uranyl acetate and Millonig's lead tartrate $\times 8,900$
- 13 An electron micrograph of the apical region of collecting duct fixed with 1½% OsO₄ buffered with α -collidine. The cytoplasm in this region contains filaments (f) mitochondria (m) vesicles () multivesicular bodies (mvb) granules (gr) and stack of flattened vacuoles (vs). Stained with uranyl acetate and Millonig's lead tartrate, $\times 14,600$
- 14 An electron micrograph of the apical region of collecting duct after fixation with 5% glutaraldehyde and post-fixation with 1½% OsO₄ buffered with α -collidine. The apical granules (gr) appear irregular in shape and contain pale matrix. The apical cytoplasm contains filaments (f) microtubules (mt) mitochondria (m) free RNP particles, rough-surfaced endoplasmic reticulum (rer) some myelin figures (mf) and Golgi apparatus (g). Stained with uranyl acetate and Millonig's lead tartrate $\times 15,300$



12



13



The Distribution Within the Brain of Ferritin Injected into Cerebrospinal Fluid Compartments

II. PARENCHYMAL DISTRIBUTION¹

MILTON W. BRIGHTMAN

Laboratory of Neuroanatomical Sciences, National Institute of Neurological Diseases and Blindness, National Institutes of Health, Bethesda, Maryland

ABSTRACT The electron lucent channels, about 200 Å-wide, between the plasmalemmas of adjacent cell processes within the brain are true pericellular spaces along which ferritin molecules can move. The micelles, visualized electromicroscopically move through the spaces until they encounter an interglial fusion or its myelin counterpart. The interspace between glial processes is abruptly sealed by these intermembranous fusions or occasionally distended by dense filler capable of trapping ferritin. The cerebral interspace is thus highly variable in width and content.

Molecules initially enter the interspace by passing across the basement membrane of the glial border fronting the subarachnoid space whence they are pinocytosed by the underlying glial processes and, at the subarachnoid border of the anterior medullary velum, by also passing directly between adjacent ependymal extensions. Once having entered the parenchymal interspace, micelles can be pinocytosed by neuronal somata and processes and, to a greater degree, by glial fibers. Pinocytosis by the thicker rather than the attenuated portions of glial fibers suggests that the plasmalemmas on the opposite sides of process must be separated by critical distance before pinocytotic indentations can be formed. The thinner portions thus offer greater barriers to the movement of micelles than do thicker regions.

The early concept of a system of anastomosing extracellular spaces permeating the cerebral parenchyma held that the subarachnoid compartment communicates with perivascular lymph spaces and ultimately with the perineuronal sacs of Obersteiner (1870) and the periglial spaces described by Weed ('23). It was not until 20 years ago that the careful analysis of Patek (44) subsequently confirmed by others (Woodham and Millen, '55) relegated the spaces about capillaries and cell bodies to those of shrinkage artifacts.

The basic method used in such experimental analyses was and remains the intrathecal injection of solutions or particulate suspensions with histological determination of their eventual distribution. Neither colloidal suspensions of mercuric sulfide nor aggregates of carbon particles could be traced beyond the cul-de-sac formed by termination of the true perivascular spaces about the larger parenchymal vessels. Woodham and Millen ('54) have given a comprehensive account of the identity and extent of the true peri-

vascular spaces and associated artifactual spaces.

The advent of electron microscopic studies soon reinforced the conclusion that there were no real spaces around cerebral capillaries, neurons, or glial cells (Dempsey and Wislocki, '55 Wyckoff and Young, '56). The dense packing of interdigitating glial and neuronal processes was inconsistent with the system of spaces discernible at the level of light microscopy. Such spaces were equated rather with the watery cytoplasm of tremendously swollen glial processes fronting the capillary wall (Maynard, Schultz, and Pease '57) and neuronal surface or ascribed to gross shrinkage incidental to preparative techniques. These earlier electron micrographs revealed, however that all cell bodies and their processes were separated by an electron lucent gap too narrow to be resolved with light optics (e.g. figs. 5 and 6). According to some authors, this tiny interval of about 200 Å between adjacent plas-

¹A report (Brightman, '63b) of this work was presented before the American Association of Neuro-pathologists, June 1964.

malemmas does not represent a real extracellular space since it does not enlarge in response to experimental hydration of the brain (Gerschenfeld et al. '59). The relative constancy of the interval in such tissue has been attributed to a displacement of water into cells rather than between them and is in keeping with the hypothesis that the lucent gap is occupied by the hydrophobic lipid leaflets belonging to the unit membrane of adjacent cells (Sjöstrand '58). According to this model of the plasmalemma, there would be no room for an interspace into which water could flow. On the other hand evidence of the entry of substances into neural though extra-cerebral tissue supports the contention that the spaces between adjacent Schwann cell membranes of peripheral nerve represent a real highly hydrated gap along which diffusion can take place (Robertson, '57). Thus the large ferritin molecule can enter Schwann cell channels in the toad spinal ganglion (Rosenbluth and Wissig, '64) and similarly the smaller ferrocyanide molecule can diffuse between neural processes and glial-like processes of Müller cells within the amphibian retina (Lasansky and Wald '63).

The present report extends these last observations to the mammalian brain. The characteristic 200 Å wide interval between adjacent neuronal and glial processes and between the membranes bounding the synaptic cleft are found to be true intercommunicating spaces along which the protein molecule ferritin can move (Brightman '62 '65b).

MATERIALS AND METHODS

Ferritin solutions from which the cadmium had been removed by extensive dialysis were injected into the lateral cerebral ventricles of 12 male rats and into the cisternae magnae of four male rats in amounts ranging from 15 mg to 100 mg of ferritin. After periods of 12 minutes to three and one-half hours the brains of the animals were fixed by perfusion through the cerebral ventricles or the aorta with buffered osmium solutions. Some of the material illustrating the subependymal tissue of brains not injected with ferritin was taken from Syrian ham-

sters. The tissue was prepared by current methods for examination with the electron microscope, details of the experiments being given in a previous account (Brightman '65a).

RESULTS

After intraventricular injection, the larger number of ferritin micelles traversing the ependyma was pinocytosed and stored within cytoplasmic inclusions while a small but appreciable amount moved intercellularly to become trapped within the dense extracellular pools lying between the bases of some ependymal cells (Brightman '65a). Consequently even after three and one-half hours following the intraventricular injection of large amounts (80 mg to 100 mg) of protein very few micelles remained free to enter the interstices throughout the subependymal neuropil. When however large amounts (100 mg) of ferritin were injected into the subarachnoid space of the cisterna magna, micelles entered the 200 Å wide interstices and the cell processes of the neural parenchyma. The following observations are based on the distribution of ferritin within the parenchyma of the anterior medullary velum and adjacent medulla oblongata and cerebellum the comparatively greater concentration of ferritin within the thin velum appeared to be the sum of both inter- and intracellular passage from ventricular and subarachnoid compartments. The structure of the subarachnoid vessels, glial border of the velum and cerebellum, and the underlying neuropil, will be described in relation to the routes of passage taken by ferritin.

A. Glial border of the subarachnoid space

Between the velum and cerebellum lay a subarachnoid space containing large-calibered thin walled vessels, a few arachnoid trabeculae with their mesothelial cells and a poorly developed pia (Fig. 1). Scattered bundles of pial collagen lay next to the velar and cerebellar border (Fig. 2). The free subarachnoid border of the velum consisted of intermingled extensions of both glial and ependymal cells whereas the free cerebellar border was composed of glial processes only. Immediately over-

The concentration of ferritin, site of its injection, the total time permitted for its circulation before the tissue was fixed, the region from which the tissue was taken, and the stain used, are stated. Sections illustrating the distribution of ferritin were taken from three rats; those of the non-injected brains from one rat and two Syrian hamsters.

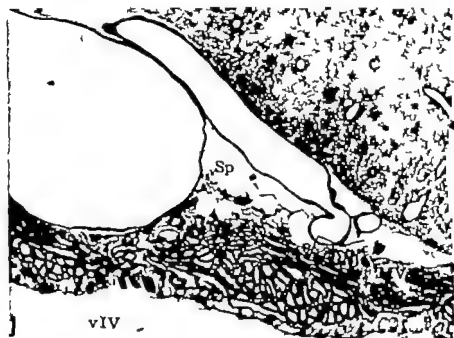


Fig. 1 The parenchyma of the anterior medullary velum (MV) lies close to both ventricular (IV) and subarachnoid (Sp) compartments. The ependyma of the velum lies lowermost, that of the medulla oblongata (not shown) would lie inferiorly. Large thin-walled blood vessels abut against velum and cerebellum (C). The inset corresponds to the region depicted in the next micrograph. Toluidine blue. $\times 500$.

of either border was a bilaminar external coat made up of a lucent lamina applied directly to the plasmalemma and a basement membrane. The free plasmalemma of the cerebellar border was comparatively straight whereas that of the velar border was frequently invaginated. These invaginations, rimmed by the lucent lamina, were filled with basement membrane material (figs. 2 and 3). The free plasmalemmas facing the subarachnoid space and lining the filled invaginations bore dense patches of cytoplasm (figs. 2 and 3) corresponding to the "half-desmosomes" occurring at epithelial-external coat interfaces (Jakus, '61).

The lateral plasmalemmas of adjacent ependymal processes at the subarachnoid border of the velum were usually not fused but merely apposed, so that their interspace opened directly onto the lucent lamina within the subarachnoid space (fig. 4).

However at variable distances from the free surface this 200 Å-wide interspace was occluded by intercellular fusions of undetermined extent. Moreover that portion of the interspace immediately contiguous with the invaginations was sometimes closed by five layered intercellular fusions some of which were zonular in extent (fig. 3). At the cerebellar border the 200 Å wide interspace between contiguous glial processes was always sealed from the subarachnoid space by internembranous fusions. These fusions whether situated at the brain surface or within the parenchyma, occurred between glial, ependymal, or both processes but never involved neuronal processes. The interspace was obliterated throughout the length of these junctions by an apparent fusion of the outer leaflets of adjacent plasmalemmas.

mas (Peters '62) In places the fused leaflets were discernible as a median dense lamina (insets to figs. 17 and 19)

Ferritin injected into the subarachnoid compartment accumulated at the surface of and within the substance of the plicated basement membrane fronting the cerebrospinal fluid (figs. 2, 3 and 4) A few micelles, however, passed through the dense substance of the basement membrane to enter the lucent lamina where they lay randomly scattered, even beneath the half-desmosomes. Particles, together with the substance of the lucent lamina, were incorporated within coated indentations of the plasmalemma (inset, fig. 3) and within pinocytotic vesicles (fig. 4)

B Neuropil

As elsewhere in the brain the subependymal and subpial neuropil was constituted, in part, by fascicles of very small neuronal processes separated usually by 200 Å clefts (fig. 5) or by considerably larger spaces of irregular configuration (inset A of fig. 6) These finest processes about 0.1 μ in diameter were so small that they contained only isolated profiles of smooth endoplasmic reticulum and a few narrower thicker walled neurotubules (fig. 5) The much larger pre-synaptic axonal endings contained a few granular synaptic vesicles in addition to the more numerous agranular vesicles (fig. 5) The agranular vesicles were tightly clustered in crystalline array within a few axonal terminals (fig. 5 inset B) situated randomly throughout the subependymal neuropil (cf Bunge et al. '65) The fascicles synaptic endings (Peters and Palay '65) and neuronal somata were all encapsulated by glial processes. These glial processes contained filaments as did those forming the subarachnoid border and perivascular endfeet. It was, therefore, assumed that all of these fibers belonged to astrocytes. Glycogen granules also occurred within some of the parenchymal glial fibers (fig. 6) Both glial and dendritic processes even when adjacent to well fixed axons were often swollen to varying degrees (fig. 5)

Throughout most of their extent, glial and neuronal processes were separated by 200 Å-wide channels containing a lucent substance. The channels were irregularly

widened into confluences between three or more processes (figs. 6, 7, 8 and 11). At far fewer sites, the space between glial processes, though not between neuronal processes, was also abruptly distended but filled with an amorphous afibrillar dense substance (fig. 6) These dense pools were continuous with the usual 200 Å-wide interspace at one point and occluded by an interglial fusion at another point (fig. 6).

Figures 2 and 3 100 mg ferritin into ventricle IV for two hours. Subarachnoid border of the velum. Uranyl acetate.

Fig. 2 The border of the velum (MV) faces the subarachnoid space (Sp) within which ferritin lies upon and between pial collagen thick micelles lie within vacuoles and freely dispersed in the cytoplasm of an adventitial or pial cell. Particles also lie within the space between the cell and the smooth muscle cell of the vessel (BVL) × 30,000.

Fig. 3 Canalicular invaginations of the pial plasmalemma facing the subarachnoid space are filled with external coat material containing ferritin. The luminal interspace between such contiguous glial processes is closed by laterobranched fusions one of which has been sectioned transversely (lower left corner). Many free micelles lie scattered within the cytoplasm of one of these cells. A fascicle of glial filaments has been cut transversely in the cell at the extreme left (center) × 30,000.

Figure 3 Inset figure 4 and Figure 5 Inset A 100 mg ferritin into lateral ventricle for two hours. Subarachnoid border of chor. Third acetate

Inset The ependymal or glial plasmalemma fronting the subarachnoid compartment faces coated invaginations containing ferritin. Here the micelles within both lumen and basement membrane of the external coat. × 80,000

Fig. 4 Ferritin molecules enter the luminal interspace (arrow) between some glial and ependymal processes in addition to entering the processes pinocytotically. Note the ferritin-laden vesicles. × 70,000.

Figure 5, Figure 6, and Figure 6 Inset A subependymal neuropil from the hemisphere

Fig. 5 The subependymal neuropil consists of bundles of axonal twigs, larger pre-synaptic axons containing a few granular vesicles (a rows) and dendrites (D) all ensheathed with glial processes () All processes are separated by spaces about 200 Å-wide. × 30,000.

Inset A Ferritin occurs within the luminal spaces of a comparable portion of neuropil. All of these processes are probably astrocytes. × 60,000.

Inset B The interstices of the neuropil are irregular in shape and width. Synaptic vesicles are occasionally aligned in crystalline array. Ventricle III subependyma from rat. Third acetate. × 25,000.



Figure 2



Figures 3 and 4

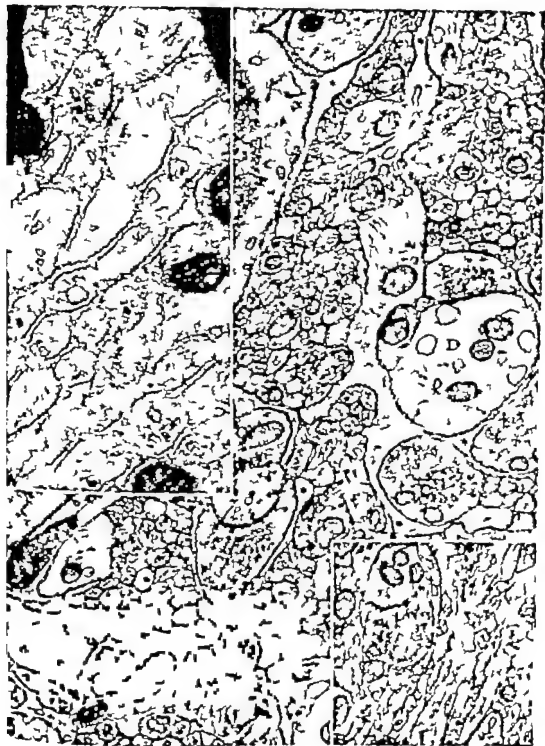


Figure 8

1 Intercellular ferritin

Ferritin entered the interspaces within the medulla oblongata, cerebellum, and velum in large amount about 1 to 3 hours after the injection of 80 to 100 mg of protein. The molecules entered the interspaces by passing across the ependyma of the medulla, the pia-glial border of the cerebellum, and across both such regions of the velum (fig. 1). In the velum ependymal processes extended from ventricular to subarachnoid surface; micelles were thus able to pass between adjacent processes to enter the parenchyma from both compartments. In contrast, particles entered the interspaces in the molecular layer of the cerebellum only after being pinocytosed by the glial processes (and by artifactual diffusion across disrupted cell membranes); there was no passage between glial processes. Nevertheless appreciable numbers of molecules moved into the interspaces situated at least 30 μ from the subarachnoid surface of the cerebellum.

Within the usual 200 \AA wide intercellular channels of these regions micelles occurred immediately adjacent to either plasmalemma, or anywhere across the width of the channels (inset A of fig. 5 fig. 7). Either the entire length of the interspace was completely filled with particles or partly filled by clusters (fig. 7). Within confluences which did not contain filler there were more molecules than in an equivalent length of 200 \AA wide channel (inset B to fig. 6 A of fig. 9 fig. 8 and fig. 19). Although there was a tendency for most of the molecules to aggregate near the plasmalemma, they were also distributed elsewhere within these lucent confluences.

Occasionally a portion of a synaptic cleft contained ferritin which had moved as far as the dense lamina within the cleft (fig. 7 and inset). It would therefore appear that the narrowed interspace at either end of the synaptic cleft (Van Der Loos '63) is patent. Usually however the micelles were restricted to the small peripheral pocket of interspace preceding the narrowed portion (fig. 7). The synapse and the adhering fascia between adjacent ependymal cells are thus structurally similar. In addition to having a dense subjacent cytoplasm (asymmetric at the syn-

apse) the interspace of both junctions is filled with a dense substance. Though this substance may act as a cement, as inferred from the cohesiveness of pre- and post-synaptic terminals of homogenized cerebral tissue (Whittaker and Gray '62), it nevertheless permits the passage of ferritin molecules. The only portions of the intercellular space which never contained ferritin were those occluded by the interplasmal fusions (insets to figs. 6 17 and 19 fig. 21).

2 Intracellular ferritin

Although some vacuoles (figs. 8 and 9) and almost all multivesicular bodies, whether encountered within glial (figs. 8 and 9) or ependymal (figs. 10 and 12) processes, segregated large amounts of ferritin, the chief depot was the dense body (cf. Rosenbluth and Waisig '64). As in ependymal cells both simple and complex dense bodies became filled with micelles about 2 hours following the injection of large amounts of ferritin. In some of the dense bodies (inset to fig. 8) the numerous micelles were packed in crystalline order (Brightman, '65 a). Within small or loose complex dense bodies the dense matrix of the body was obscured by the many parti-

Fig. 6 The glial processes within the subventricular neuropil contain filaments and are separated by a space about 200 \AA wide which at one point, is obliterated by an intermembranous fusion (above arrow) and elsewhere contain dense filler (below arrow). The plasmalemmas of the dense pools bear half-desmosomes. A coated pinocytotic pocket occurs at the upper right and lower center $\times 30,000$.

Inset A The irregularities in shape and breadth of the lucent interspaces are observed. Lead monocold $\times 15,000$.

Inset B Ferritin occurs within the 200 \AA wide spaces and more abundantly within the lucent confluences between neural and glial processes but never within lateral sulci (between arrows). Lead citrate. $\times 100,000$.

Figures 7 & 8, and their insets: 100 mg ferritin into ventricle IV for two hours. Molecular layer of the cerebellum. Uranyl acetate.

Fig. 7 These interspaces also contain vacuoles, two of which lie within the synaptic cleft (right arrow) that narrows, then expands into a pocket containing four micelles. Three particles lie within cytoplasmic vesicle at the left (left arrow) $\times 90,000$.

Inset Seven ferritin molecules have moved into the synaptic cleft as far as the dense intermediate lamina (arrow) $\times 130,000$.



Figure 6



Figure 7

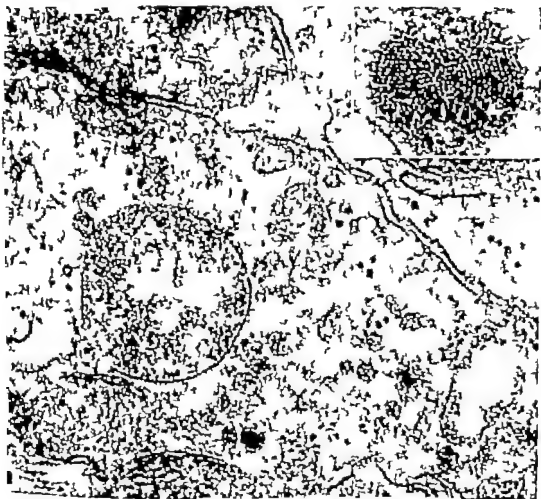


Fig. 8. The thick portion of glial process situated near the border of the parenchyma contains many ferritin-filled pinocytotic vesicles. The contents of one vesicle are continuous with those of large vacuole. Micelles occupy the 200 Å-wide interspace and the wider confluence between the processes situated left of the inset. $\times 100,000$.

Inset. Ferritin molecules are arranged in crystalline fashion within the dense body of another glial process. $\times 130,000$.

cles whereas the large presumably lipid droplets were free of micelles. It is noteworthy that while the plasmalemma of the thicker glial processes was able to form pinocytotic vesicles, the cell membrane of the attenuated sheets, about 200 Å-wide was not (figs. 9, 13, 16, 17, and 21).

The neuronal processes of the neuropil were also capable of pinocytosing ferritin, but to a smaller extent than the glial processes. Within axonal, pre-synaptic endings almost all of the vesicles were of the synaptic type and did not take up ferritin. Occa-

sionally however "coated" vesicles lay among the synaptic vesicles and were observed to arise from either axonal (fig. 11) or dendritic plasmalemmas (Andres, '64). Multivesicular bodies more common in dendrites than in axons, were the primary depot for pinocytosed ferritin within neuronal processes. These large coated indentations in the plasmalemma of both soma and processes of neurons engulfed ferritin molecules and the surrounding medium (figs. 11 and 12). In the perikarya, the micelles were sequestered within multive-

sicular bodies (inset of fig. 12) the participation of dense bodies was undetermined

3 Free ferritin

Some glial and neuronal processes not only contained pinocytosed membrane-enclosed protein, but in addition, micelles which were randomly dispersed throughout the cytoplasm. The intracellular deposition of free molecules not enclosed within a membrane is almost certainly an artifact due to disruption of the plasmalemma (Brightman '65a). At some synapses free ferritin was strikingly confined to the dendritic terminal. However it is significant that few or no particles entered the intervening synaptic cleft (fig. 13). Damage to the dendritic plasmalemma thus probably occurred at some other level, so that any particles which did enter the cleft had moved between the synaptotemnas not across them. Another possibility accounting for the deposition of free ferritin within a section of a cell bounded by an apparently intact plasmalemma, is membrane rupture resulting in the entry of molecules followed by reconstitution of the plasmalemma (Chambers and Chambers '61). The multiple interperiod lamellae of the myelin sheath formed a continuous ve-layered interglial fusion which completely excluded ferritin whether it was artifactually or physiologically distributed. Nevertheless it is stressed that free ferritin was also deposited within some axonal processes presumably by diffusion across a plasmalemma damaged at another level (e.g. at a node the soma or a dendrite).

Within all types of cell processes, the endoplasmic reticulum and most mitochondria did not contain ferritin. In processes filled with free ferritin dense bodies could be devoid of micelles which were distributed indiscriminately upon and between cytoplasmic filaments just as they were within damaged ependymal cells (Brightman '65a). It is important to note that the frequent damage to the glial processes bordering the subarachnoid space could have been responsible for the initial entry of numerous ferritin molecules into the subpial interspaces. The micelles could then have diffused or been carried into the further reaches of these interstices mured by intact plasmalemmas (cf Bondareff '64).

4 Perivascular ferritin

The vessels within the subarachnoid space had a large caliber with a relatively thin wall consisting of endothelium and a single layer each of smooth muscle and adventitial connective tissue cells. A shared, bilaminar external coat lined the endothelial and smooth muscle cells to completely fill the spaces between these cells (figs. 16 to 18). However on the surface facing the adventitia, the smooth muscle cell was covered by a basement membrane applied directly to its plasmalemma (figs. 16 to 18).

Ferritin injected into the subarachnoid compartment came to lie between and upon collagen fibers (fig. 2) and within the pinocytotic vesicles and vacuoles of adventitial cells (fig. 16). Many particles were also freely dispersed within the cytoplasm of some of these cells. The external coat over the smooth muscle surface facing the adventitia was bilaminar. Numerous molecules entered the lucent lamina by diffusing across a disrupted plasmalemma, by circumventing the cells, or by pinocytotic transport (fig. 16). Once inside the

Fig. 9 and Inset A 100 mg ferritin into ventricle IV for two hours. Medulla oblongata. Low citrate.

Fig. 9 The thicker portion of perivascular glial foot contains ferritin-laden vesicles. Micelles lie within the perivascular space, and within the individual and shared basement membranes of the glial cell, pericyte, (the new upper right) and endothelial cell (right, half of space). $\times 80,000$.

Inset A Ferritin-containing vesicles lie within the thicker portion of a glial process near vessel. Particles occupy the lucent laminae of the interspace and the basement membrane shared by glial and endothelial cell. $\times 80,000$.

Inset B A dense body in the pericyte beside a parenchymal capillary is tightly packed with pinocytosed ferritin. The vessel lumen is to the extreme right. A vesicle (arrow) enclosing ferritin lies within the thicker part of glial foot which branches (dashed line) between two sheet processes. $\times 50,000$.

Figs. 10 to 13 100 mg ferritin into lateral ventricle for two hours. Velum. Uranyl acetate.

Fig. 10 Ferritin micelles are contained within the multivesicular body of dendrite. It makes synaptic contact with three axons. $\times 80,000$.

Fig. 11 The plasmalemma of axonal process (probably axonal) forms a deep invagination containing ferritin. $\times 80,000$.



Figure 9



Figures 10 and 11



Fig. 12 Ferritin occupies the coated indentation in the cell membrane of neuronal soma and the cooperatively small vesicles of an adjacent glial process (at the right) $\times 80,000$. Inset: In another neuronal soma, ferritin molecules lie within the matrix of multivesicular body $\times 80,000$.

lamina, the molecules did not pass into the basement membrane (figs. 14 to 18). So effective was this barrier that almost all of the myriad goblets, that are presumed to be pinocytotic and that are formed by the underlying sarcolemma contained only dense basement membrane material and no ferritin molecules whatever (figs. 14 and 18).

Within the parenchyma, half-desmosomes between plasmalemma and external coat were far more prevalent on the perivascular glial feet around large vessels than they were around capillaries (cf. Donahue, '64). Some of the glial processes bordering the subarachnoid space the large vessels within the parenchyma, and some capillaries, typically ended in a T-shaped configuration the cross-bar of

which was formed by a sheet lying parallel to the surface of the endothelium (figs. 9, 18 and 19). These neighboring horizontal glial sheets were very thin, being 200 to 500 Å wide; their plasmalemma was no less undulating than the remainder of the plasmalemma, and they met either as end-to-end or imbricated intercellular fusions. Some ferritin molecules were distributed within the parenchymal interstices on one side of the subendothelial sheets while many more accumulated within the basement membrane on the opposite side (fig. 19). The high frequency of intermembranous fusions between perivascular glial feet and the exclusion of micelles from these junctions suggested that the exchange of ferritin across the wider glial processes occurred mainly by pinocytosis.

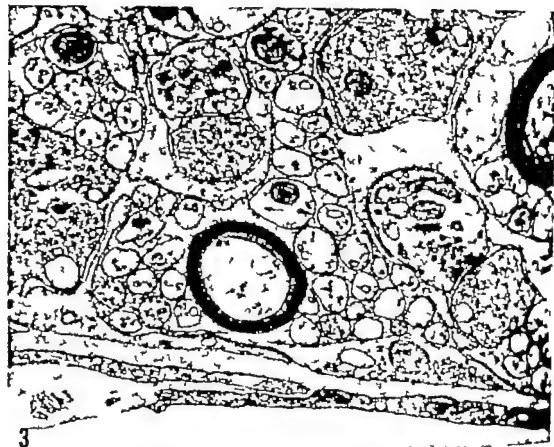


Fig. 13 A common "polarized artifact" consists of freely dispersed ferritin localized to the cytoplasm of dendritic post-synaptic endings. Adjacent perivascular glial feet overlap to form what are probably three intermembranous fusions. Medulla oblongata. 100 mg ferritin into ventricle IV. Lead citrate. $\times 35,000$.

In fact, ferritin-containing pinocytotic vesicles were numerous within the thicker portions of the processes (figs 8 and 9). Significantly though the plasmalemmas of the very thin portions of these processes did not form any pinocytotic indentations. Pericytes (periendothelial cells exclusive of muscle cells) embedded within the basement membrane also pinocytosed ferritin (inset B of fig. 9). A few of the remaining particles which diffused into and through the periendothelial basement membrane were finally pinocytosed by the endothelium.

True perivascular spaces as defined by investigators using light microscopy (Patek, 44 Woollam and Millen '54) communicate with the subarachnoid space and extend only about larger blood vessels as

far as the point where pial and arachnoidal linings unite (Woollam and Millen, '54). Viewed electronmicroscopically these spaces are connective tissue spaces, i.e. those lined by a basement membrane and containing collagen or connective tissue.

Fig. 14 Micelles migrate up as but cannot penetrate the basement membrane covering the smooth muscle cell of this subarachnoid vessel. The many goblets formed by the endothelium consequently contain basement membrane material but no ferritin. The adventitial cell is not shown. Two clumps of ferritin micelles over at the left. Lead citrate. $\times 80,000$.

Fig. 15 A perivascular smooth muscle cell and its basement membrane have been sectioned tangentially. Some ferritin particles appear to lie within but may in fact, rest on top of the membrane. Vesicles and goblets do not contain ferritin. A portion of damaged adventitial cell appears at top and bottom. Lead citrate. $\times 80,000$.



Figures 14 and 15

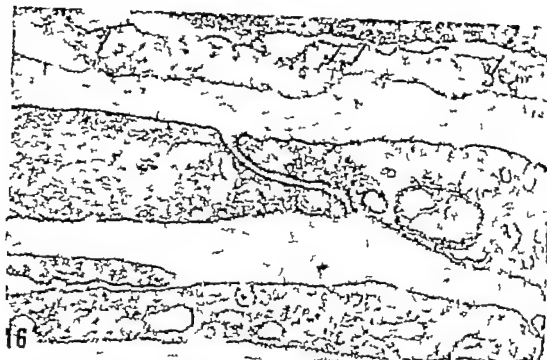


FIG. 16. Ferritin is confined to the lucent lamina and excluded from the basement membrane of the external coat capping the smooth muscle cell (extending across the middle of the figure) of the subarachnoid vessel. Vesicles (arrows) within the adventitial or pia cell (at top) are either pinocytosing molecules from or releasing them into the lucent lamina. $\times 80,000$.

lla. However we have not as yet observed any formation corresponding to a fusion between the lining mesothelial cells. Rather the cul-de-sac is closed by a fusion between the basement membrane lining the glial border of the parenchyma and the blood vessel wall (Nelson Blinzinger and Hager '61). In a few instances, the perivascular space extended as far as the capillaries. Ferritin molecules penetrated the terminal reaches of the spaces up to the point of coalescence between the basement membrane covering the glial border and the pericyte or endothelial cell of the vessel wall (fig. 20). Some ferritin micelles, however, entered the basement membrane beyond its point of fusion. Near this point, the mesothelial lining had disappeared leaving the glial border covered only by basement membrane just as it was in comparable regions of the subarachnoid border. Pinocytotic uptake by glial processes could occur from these perivascular sites though none was observed in the present study.

DISCUSSION

Extracellular space

The electron lucent gap, about 100 \AA wide between the plasmalemmas of adjacent cell processes within the mammalian brain represents a real pericellular space along which ferritin molecules can move. This conclusion has subsequently been confirmed by the finding that thorotrast can also enter these spaces (Lowe '65). The movement of ferritin into the synaptic clefts and dense pools further signifies that these dense portions of the interspace like those of the ependymal fascia adherens (Brightman '65a) are continuous with the rest of the extracellular space. The movement of micelles into these denser reaches of the interspace occurred prior to fixation, allowing sufficient time for still viable cells to pinocytose micelles within these regions. Pinocytosis could not have been performed by fixed cells (Brightman '65b). Nevertheless preliminary observations suggest that "dying" cells might

be capable of actively incorporating particles. Endothelial and glial cells of a rat, killed by exsanguination and thence left for 45 minutes at about 4 C prior to the intracisternal injection of ferritin were still able to pinocytose micelles.

The only portion of the interspace which does not allow the passage of protein is that occluded by the five-layered interglial junctions analyzed in detail by (Peters, '62). In all of the regions so far examined, these intercellular fusions occur only between ependymal, glial, or both cells and not between neuronal processes. The interperiod lamellae of the myelin sheath are the counterparts of such fusions and likewise exclude ferritin.

The occurrence of ferritin within the 200 Å-wide interspace is at variance with the finding that, after aldehyde fixation adjacent plasmalemmas of neuronal and glial cells are often fused by five-layered junctions (Schultz and Karlsson, '65). However these contacts are most prevalent where there is widespread swelling of cell processes. Similarly the pre-fixation swelling that results from asphyxia also leads to an increase in the number of such contacts (Van Harnveld, Crowell and Malhotra, '65). It would, therefore appear certain that the ubiquity of these contacts which are spurious appositions rather than fusions, is the consequence of artifactual swelling either prior to or coincident with fixation. By the same token some of the five-layered junctions in the present material may likewise be artifacts. Moreover if the widespread appositions formed between swollen processes act as fusions, then substances injected after swelling has occurred would be excluded from the obliterated interspaces. The same pictorial evidence could be obtained where ferritin particles could not enter the occluded interspace of a true, pre-existing fusion or where they had been squeezed from the space during artifactual formation of close apposition.

The present experiments demonstrate striking variations in breadth and content of the cerebral interspace. Not only are there regional differences in the width of interspace (Horstmann and Meves '59) within a very short distance the usual 100 Å-wide interglial space is abruptly

obliterated at one point and as abruptly distended with or without dense filler at an adjacent point. Estimates of the size of the cerebral interspace measured by physiological techniques (e.g. Davson and Spaziani '59; Reed and Woodbury '60; Streicher '61) yield average values which cannot take into account these disparities. Conversely the present results cannot provide a measure of the maximal size of the interspace but do set a lower limit of 100 Å, the diameter of the ferritin molecule. This molecule could not only have diffused through the intercellular channels but could also have been carried along by bulk flow of interstitial fluid. Regardless of the mechanisms, the movement would be influenced by the extracellular filler.

This filler is, presumably equivalent to basement membrane material. The space containing the perivascular membrane may likewise be regarded as a dense pool of fairly uniform width though its paren-

Fig. 17 A capillary within the subependymal neuropil is surrounded by layers of glial foot processes united by extensive intermembranous fusions (dashed lines). The glial processes are recognized by their filaments, large mitochondria, and lipid droplets. The cell to the top is probably neuron. Hamster. Region of ventricle III. $\times 20,000$.

This inset, figure 20 and its inset: 100 mg ferritin into ventricle IV for two hours. Medulla oblongata.

Inset: Micelles occupy the lucant confining space on either side of an interglial fusion but never occur within this type of junction. Part of the median dense lamina of the junction is discernible. $\times 100,000$.

Fig. 18 The perivascular glial sheath consists of processes, some of which are shaped as "T" (dashed lines). The cross-bars are finely attenuated sheets intervening between neuronal processes and perivascular basement membrane. These sheets do not form pinocytotic invaginations. The strands of the processes are broader than the sheets. Subependyma of ventricle III. Hamster. $\times 40,000$.

Fig. 19 Ferritin particles occur on either side of the perivascular sheet process (continuous with dashed lines) but are not incorporated within it. Molecules occupy all of the interspaces but are excluded from the interglial fusion (right arrow) and the myelin lamellae (top right) $\times 80,000$.

Inset: Two perivascular sheet processes expand into club-shaped endings which meet as an end-to-end, five-layered fusion. The expansions contain vesicles, the sheet portions do not. Ferritin lies on either side of the sheets. $\times 100,000$.

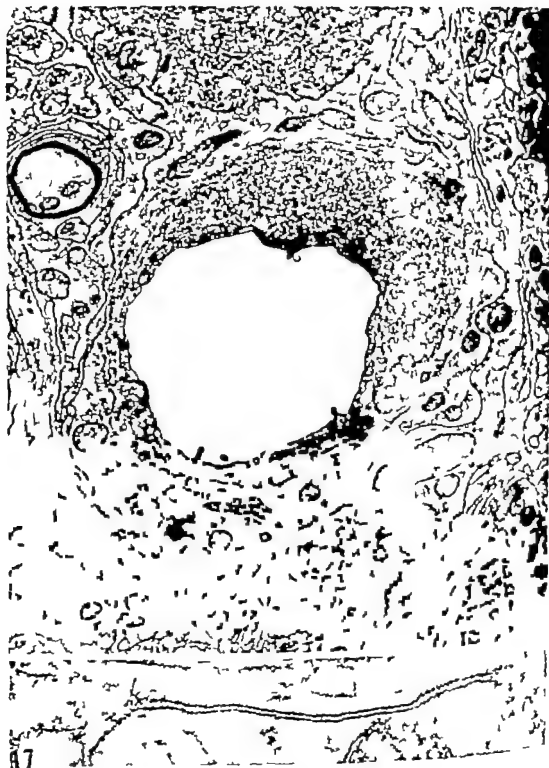
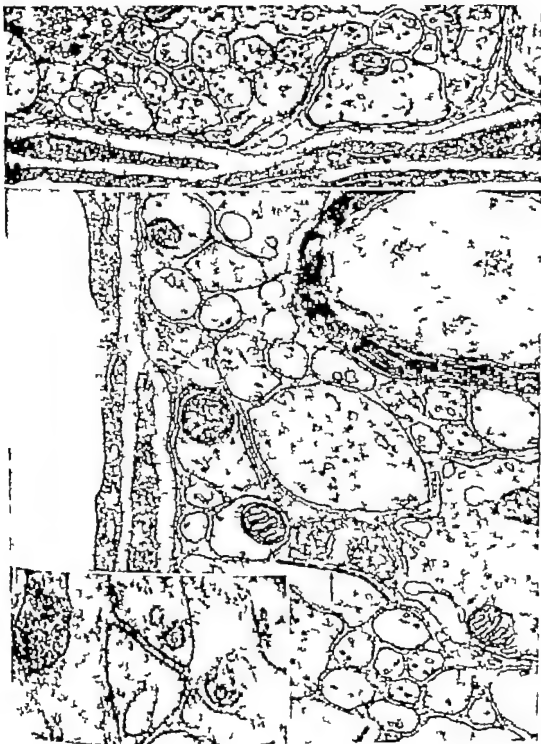


Figure 17



Figures 18 and 19



Fig. 20 The perivascular space, bounded by basement membranes of the glial border (above) and the endothelium (below) contains ferritin. The micelles have moved as far as the terminus formed by coalescence of the basement membranes (arrow). Medulla oblongata, 35 mg ferritin dose, 18 minutes.

chymal extensions apparently do not anastomose with the isolated dense lacunae. At the subarachnoid surface the dense canalicular invaginations of the plasma lemma are comparable to the tubular network of basement membrane in the electric organ of *Torpedo* (Sheridan '65). The parenchymal filler demonstrable with different fixatives appears to be analogous with that occurring in the neurosecretory organ of the insect *Leucophaea maderae* (figs. 2, 13 and 22 of Scharrer '63), the interglial spaces in the ganglia of the leech (Cogeshall and Fawcett '64), and the inter-neuronal spaces about Mauthner's cell in the goldfish (Robertson, Bodenheimer and Stage '63). In the insect organ the dense filler shares a connective tissue space with collagen. In rat brains examined so far the subependymal and cerebellar neuropil and that of the olfactory bulb (Reese and Brightman, '65) contain dense pools too few and circumscribed to account for a periodic acid-Schiff-positive ground substance (Hess '55). Nevertheless these isolated dense pools represent a fundamental variant of the interspace and occur throughout the brain from the ependyma to the glial border of the subarachnoid space (fig. 21).

As in the renal glomerulus (Farquhar, Wilsig and Palade '61) and the area postrema of the brain (Dempsey and Whitely '55) the cerebral basement membrane function as a filter for colloidal particles. The basement membrane covering the glial border of the subarachnoid space accumulates ferritin but permits some to diffuse into the lucent lamina from which the micelles are available for pinocytosis. How-

Fig. 21 This schematic diagram depicts the routes of passage which ferritin takes to move from the ventricle (V) and subarachnoid space (Sp) into the parenchyma. Each dot represents ferritin molecule, the heavy lines represent intercellular fusions, and the filamentous patches on the bottom of the axolemma, half-dimensions. Two clusters of neuronal processes are depicted at the left and right near the bottom.

- A, axon forming synapse with dendrite.
- BM, basement membrane of the glial border; the perivascular basement membrane is not labeled.
- BV, blood vessel containing two red blood cells; the endothelium is vertically hatched.
- E, ependymal cell; the ependymal crurae (E) at the bottom occurs in the ventricle.
- G, glial cell process (horizontally hatched); glial foot process (dashed lines) divide into two sheet processes one of which is encircled.
- P, dense pool; large focal confluences (P) occurs to the left of a pool.

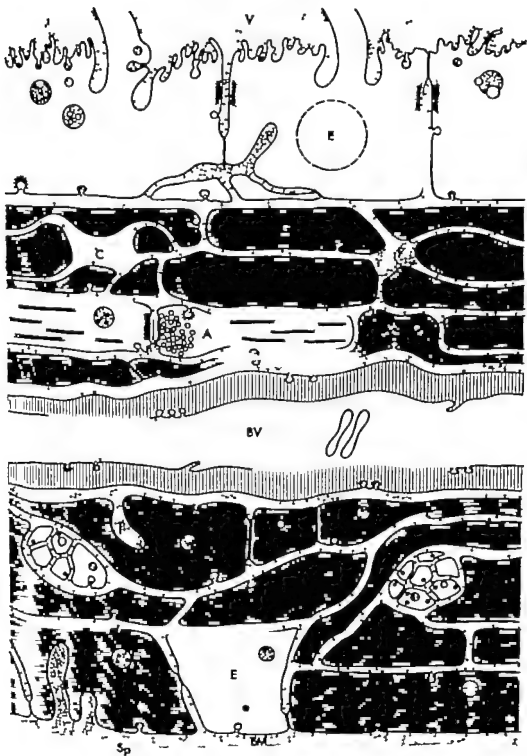


Figure 21

ever ferritin cannot even enter the basement membrane around the smooth muscle cells of subarachnoid arteries. It would therefore appear that the properties of these two basement membranes are different.

It is likely that ferritin is not as free to move within the dense pools of the parenchyma as within the 200 Å wide clefts or the intercellular distensions not containing filler. It is also conceivable that the filler may affect the mobility of much smaller substances as well. If one makes the following assumptions viz. that the basement membrane-like filler is comparable to the proteinpolysaccharide complexes derived from connective tissue then salts or ions may also be "trapped." For example such complexes *in vitro* inhibit "the coming together of microcrystals of calcium phosphate" (Weinstein, Sachs and Schubert, '63). It is suggested, therefore that the lacunae containing dense filler may serve as ionic pools.

Bennett ('63) has postulated that the basement membrane surrounding striated muscle cells acts to keep potassium ions from diffusing away from the immediate vicinity of the sarcolemma. A comparable impediment to ionic diffusion by extracellular filler may occur but only between pericytial or glial processes and not between neurons in the rat brain. Until it is known whether ions are indeed held within the filler and whether electrical activity of neurons is modulated by such interglial sources of ions the supposition of functioning ionic pools can only be conjectural.

Blood-brain barrier

The variations in size and content of the interspace are also pertinent to a consideration of the blood-brain barrier. The variable exclusion from the cerebral parenchyma of many unrelated substances injected intravascularly has recently come to be regarded as a reflection of the absence of an appreciable extracellular space (Edström '58 Dobbing '63). Certain regions lacking this barrier e.g. the area postrema are characterized by large extravascular spaces within which can accumulate particles of colloidal size such as silver salts (Dempsey and Wislocki '55 Van Breeman

and Clemente, '55) and albumin (Brown, '61). It is self-evident that if all the parenchymal interspaces were as wide as the focal confluences considerably more ferritin could be accommodated. However, though most of the interspace is narrow it is patent save where it is actually obliterated by intermembranous fusions.

The barrier to the entrance of silver salts from blood into neural parenchyma has been attributed either to interstitial ground substance or to the glial plasmalemma (Dempsey and Wislocki, '55). The present findings suggest, however that provided there is endothelial transport of substances from the blood stream, the perivascular basement membrane may stand as the primary barrier to movement of colloidal particles from blood to parenchyma just as it does in the opposite direction for intracisternally injected ferritin. The thicker perivascular glial processes do not present a barrier insofar as they are capable of pinocytosing ferritin.

One would expect that the very thin sheet-like extensions of these glial processes would be less of a barrier than the thicker portions. Paradoxically however, ferritin is pinocytosed by the thicker portions only (figs. 8 and 9). The thin glial sheets and their basement membrane may therefore constitute a double barrier over part of a vessel wall. The consistent absence of pinocytotic vesicles within the attenuated sheets suggests further that the plasmalemmas at the two opposite surfaces of a process must be separated by a critical distance (greater than approximately 300 Å) before a pinocytotic indentation of the plasmalemmas can be formed. This hypothesis derives support from the relationship between the degree of separation of two charged parallel plates and the electrostatic repulsive forces acting between them. As Curtis ('62) points out, the mutual repulsion increases markedly as the plates approach one another. A similar relationship may obtain when the two parallel cell membranes (plates) of a single sheet process approach each other where the process thins out. The resulting mutual repulsion may be sufficiently great to prevent further approximation i.e. formation of pinocytotic indentations of either plasmalemma.

The present results are also relevant to the question whether the compositions of the cerebrospinal fluid and extravascular fluid of the cerebral parenchyma are equivalent. The distribution of ferritin indicates that the composition of the interstitial fluid is the sum of both extracellular and intracellular contributions. A small amount of protein is able to pass directly into the interstices of the subependymal parenchyma by moving across and between ependymal cells of the ventricular border. A second surface of entry is the subarachnoid border. Here, in the regions examined, the glial cells do not form a continuous layer of cells connected by fused junctions. Consequently much of the external coat over this glial border is directly exposed to cerebrospinal fluid. At the velar border substances have ready access to the interspace that opens into the external coat. Elsewhere however contiguous glial processes are fused and the contribution from the subarachnoid compartment would have to move across this glial border pinocytotically. As we have seen, these glial cells are indeed capable of pinocytosis. Despite their capability it appears from other studies that ions (Morita, Kobayashi and Ito '64) rather than large particles such as frondexin complexes (Iwanowski and Olaszewski, '60) and albumin (Klatzo et al. '64) readily cross this border.

An additional though limited route is provided by the perivascular spaces. Fluorescein-labeled albumin, though it does travel along the perivascular sheaths of large parenchymal vessels does not cross the subarachnoid border (Klatzo et al. '64). The true perivascular space also serves as a channel for the entrance of ferritin (fig. 20) and of large aggregates of serum albumin within human gliomas (Rabmond, '64). Ferritin diffuses at least as far as the end of the cul-de-sac formed where the lining basement membranes coalesce (fig. 20). The comparatively rare occurrence of micelles within the deeper reaches of the perivascular space would indicate that the passage of ferritin from the subarachnoid space into the neuropil was largely effected directly across the glial border of this compartment.

At sites where the glial plasmalemma and its external coat had been artifactually breached the cytoplasm of glial and neighboring neuronal processes are replete with freely dispersed ferritin. It is emphasized that although a considerable proportion of the ferritin must have initially entered the interspace across disrupted cell membranes, the micelles were able to move for some distance along a patent interspace mured by apparently intact plasmalemmas.

Pinocytosis

In vitro and as viewed with phase optics only glial cells rather than nerve cells, are able to pinocytose protein (Klatzo and Miquel, '60). In situ and at high resolution the micropinocytosis and storage of ferritin can be observed in both glial processes, and to a lesser extent, in neuronal processes. The plasmalemma of ependymal (Brightman '63) and glial cells, those of neurons and satellite cells (Rosenbluth and Wissig, '64) and other cells (Wissig, '62; Roth and Porter '64) can form coated spherules comprising one type of vesicle capable of pinocytosing protein. As both coated and uncoated vesicles laden with ferritin occur in the same section it would appear that in the rat brain the second and more numerous type of vesicle able to pinocytose protein is the uncoated one.

The comparatively brisk glial uptake, manifested by the relatively large number of ferritin-laden vesicles and vacuoles within the thicker glial processes is consistent with the supposed role of glia as nutritional intermediary between endothelium and neuron (Achucarro '18). This inference based literally on the intermediate location of glia between blood and neuron has been coupled with the assumption that as there is no appreciable interspace transport of substances must be entirely transglial (Edstrom, '58). The present experiments tend to support this contention insofar as the interspace immediately surrounding vessels is occluded by fusions between perivascular glial feet (Peters, '62) so that ferritin is first shunted across their cytoplasm. Where the vessel wall is confronted by neuronal processes, however no such occlusions of the interspace would occur to block intercellular movement. Moreover once having crossed

the perivascular glial border even large molecules can reach the plasmalemma of neuronal and glial cells by moving along a patent interspace without necessarily having to pass further through cytoplasm (fig 21)

LITERATURE CITED

- Achucarro N 1918 On the evolution of the neuroglia and specially their relations to the vascular apparatus. *J Nerv Ment Dis.* 48 333-342.
- Anders, K. H. 1964 Mikropinozytosen im Zentralnervensystem. *Zeit. f Zellforsch.*, 64 63-73.
- Bennet, H. S. 1963 Morphological spectra of extracellular polysaccharides. *J Histochem. Cytochem.* 11 14-23.
- Bondareff W 1964 Distribution of ferritin in the cerebral cortex of the mouse revealed by electron microscopy *Exper Neurol.* 10 377-382.
- Brightman, M. W 1962 An electron microscopic study of ferritin uptake from the cerebral extricles of rats. *Anat. Rec.* 142 319 (abstract)
- Brightman, M. W and S. L. Palay 1963 The fine structure of ependyma in the brain of the rat. *J Cell Biol.* 19 415-439
- Brightman, M. W 1963a The distribution within the brain of ferritin injected into cerebrospinal fluid compartments. I. Ependymal distribution. *J Cell Biol.* (In press)
- Brightman, M. W 1963b The distribution within the brain of ferritin injected intraventricularly. *J Neuropathol. and Exper Neurol.* 24 147 (abstract)
- Brown, P 1961 Albumin, connective tissue space and the blood-brain barrier. *Bull. Johns Hopkins Hosp.* 106 200-207
- Bunge P M, Bunge and E. R. Peterson 1965 An electron microscope study of cultured rat spinal cord. *J Cell Biol.* 24 163-191.
- Chambers, R., and E. L. Chambers 1961 Exploration into the nature of the living cell. *Harvard Uni. Press*, p. 100.
- Coggeshall, R. E., and D. W. Fawcett 1964 The fine structure of the central nervous system of the leech, *Hirudo medicinalis*. *J Neurophysiol.* 27 229-239.
- Curtis, A. S. G. 1962 Cell contact and adhesion. *Biol. Rev.* 37 82-129.
- Davson, H., and E. Spariani 1959 The blood-brain barrier and the extracellular space of brain. *J Physiol.* 149 135-143.
- Dempsey E. W and G. B. Wislocki 1955 An electron microscopic study of the blood-brain barrier in the rat, employing silver nitrate as vital stain. *J Biophys. Biochem. Cytol.* 1 243-256
- Dobbing, J 1963 The blood-brain barrier. Some recent developments. *Guy's Hospital Reports* 112 267-268.
- Donahue S. 1964 A relationship between fine structure and function of blood vessels in the central nervous system of rabbit fetuses. *Amer J Anat.* 115 17-28.
- Edström, R. 1958 An explanation of the blood-brain barrier phenomenon. *Acta Physiol. Neurol. Scand.* 33: 403-416.
- Farquhar, M. G., S. L. Weiss and G. E. Palade 1961 Glomerular permeability. I. Ferritin transfer across the normal glomerular capillary wall. *J Expil. Med.* 113: 47-66.
- Gerschenfeld, H. M., F. Wald, J. A. Zacharich and E. D. P. De Robertis 1959 Function of astroglia in the water-ion metabolism of the central nervous system. *Neurology* 9 412-425.
- Hess, A. 1955 Blood-brain barrier and ground substances of central nervous system. *A. M. A. Archiv. Neur. and Psychiat.* 73 380-386.
- Horstmann, E., and H. Meves 1958 Die Feinstruktur des molekulären Rindenstroms und ihre physiologische Bedeutung. *Z. Zellforsch.* 49 509-504
- Iwanowski, L., and J. Olaszewski 1960 The effects of subarachnoid injections of iron-containing substances on the central nervous system. *J Neuropathol. Exper. Neurol.* 19 433-448.
- Jakins, M. A. 1961 The fine structure of the human cornea. In: *The Structure of the Eye*. Smelser, G. K. (ed. Academic Press, New York) p. 343-366.
- Klatzo L., and J. Biquel 1960 Observations on pinocytosis in nervous tissue. *J Neuropath. and Exper. Neurol.* 19: 475-487
- Klatzo, L., J. Biquel, P. J. Ferris, J. D. Fryer and D. E. Smith 1964 Observations on the passage of the fluorescently labeled serum proteins (FLSP) from the cerebrospinal fluid. *J Neuropath. and Exper Neurol.* 23 11-23.
- Lasensky A., and F. J. Wald 1963 The extracellular space in the rod retina as defined by the distribution of ferrocyanide a light and electron microscope study. *J. Cell Biology* 11 463-470.
- Lase, S., J. M. Petty and C. Belter 1963 An electron microscopic study of the fine structure of subarachnoid and intraventricular choroid plexus. *Anat. Rec.* 181 280 (abstract).
- Maynard, E. A., R. L. Schultz, and D. C. Foss 1957 Electron microscopy of the vasculature of rat cerebral cortex. *Am. J. Anat.* 75 408-433.
- Morita, S., Y. Kobayashi, and Y. Ise 1964 A radioautographic study of the synthesis of phosphorus compounds in central nervous tissue of the dog. *J Neurochem.* 11 125-127
- Nelson, E., D. Bluminger and H. H. Fox 1961 Electron microscopic observations on subarachnoid and perivascular spaces of the Syrian hamster brain. *Neurology* 11 225-233.
- Obersteiner H. 1870 Über einige Lymphgefäße im Gehirn. *Sitzungsberichte Akad. Wiss. (Wien)* 61 57-66.
- Palade, P. 1944 The perivascular spaces of the mammalian brain. *Anat. Rec.* 85 1-21
- Peters A. 1962 Plasma membrane contacts in the central nervous system. *J. Anat. Lond.* 96 237-248.
- Peters, A., and S. L. Palay 1965 An electron microscope study of the distribution and per-

- tems of astroglial processes in the central nervous system. *J. Anat.*, 99 419 (abstract).
- Lisacoff, A. J. 1964 Localization of radio-labeled serum albumin in human glioma. *Archiv Neurol.*, 11 173-184.
- Levi, D. J., and D. M. Woodbury 1960 ^{59}Fe distribution in cerebral cortex, cerebrospinal fluid, and plasma of rats. *Pharmacologist*, 2 92 (abstract).
- Levi, T. S. and M. W. Brightman 1965 Unpublished observations.
- Lehmann, J. D. 1957 New observations on the ultrastructure of the membranes of frog peripheral nerve fibers. *J. Biophys. Biochem. Cytol.*, 3 1043-1048.
- Lehmann, J. D., T. S. Bodenheimer and D. E. Stages 1963 The ultrastructure of mauthner cell synapses and nodes in goldfish brains. *J. Cell Biol.*, 19: 179-200.
- Loewenstam, J. and S. L. Wisig 1964 The distribution of exogenous ferritin in toad spinal ganglia and the mechanism of its uptake by neurons. *J. Cell Biol.*, 23: 307-323.
- Lock, T. F. and K. R. Porter 1964 Yolk protein uptake in the oocyte of the mosquito *Anopheles gambiae* L. *J. Cell Biol.*, 20 313-322.
- Scharrer, B. 1963 Neurosecretion XIII. The ultrastructure of the corpus cardiacum of the insect *Leucophaea maderae*. *Z. Zellforsch.*, 60, 781-794.
- Shelden, M. N. 1965 The fine structure of the electric organ of *torpedo marmorata*. *J. Cell Biol.*, 24: (no. 1) 129-141.
- Schultz, R. L. and U. Karlsson 1965 Fixation of the central nervous system for electron microscopy by aldehyde perfusion, II. *J. Ultrastr. Res.* 15: 187-206.
- Sjöstrand, F. S. 1958 Ultrastructure of retinal and synapses of the guinea pig eye as revealed by three-dimensional reconstructions from serial sections. *J. Ultrastr. Res.*, 2, 122-170.
- Stretcher, E. 1961 Thiocyanate space of rat brain. *Am. J. Physiol.*, 201 334-336.
- Van Breeman, V., and C. Clements 1953 Silver deposition in the central nervous system and the hematoencephalic barrier studied with the electron microscope. *J. Biophys. Biochem. Cytol.*, 1 161-165.
- Van Der Loos, H. 1963 Fine structure of synapses in the cerebral cortex. *Zellforsch.*, 60 815-825.
- Van Harnveld, A., J. Crowell and S. K. Malhotra 1965 A study of extracellular space in central nervous tissue by freeze-substitution. *J. Cell Biol.*, 25 117-137.
- Weed, L. H. 1923 The absorption of cerebrospinal fluid into the venous system. *Am. J. Anat.*, 31 191-221.
- Weinstein, H., C. R. Sachs and M. Schubert 1963 Protein polysaccharide in connective tissue: Inhibition of phase separation. *Science*, 141: 1073-1076.
- Whittaker, V. P. and E. C. Gray 1962 The synapse: Biology and Morphology. *Br. Med. Bull.*, 18 323-328.
- Wisig, S. L. 1962 Structural differentiations in the plasmalemma and cytoplasmic vesicles of selected epithelial cells. *Anat. Rec.*, 142 292 (abstract).
- Woodham, D. H. M., and J. W. Millen 1954 Perivascular space of the mammalian central nervous system. *Biol. Rev.* 29 251-281.
- 1958 The perivascular spaces of the mammalian central nervous system and their relation to the perineuronal and subarachnoid spaces. *J. Anat.*, 89 193-200.
- Wyckoff, R. W. G., and J. Z. Young 1936 The motoneuron surface. *Proc. Roy. Soc., B* 144, 440-450.

Growth of the Rat Epiphyseal Cartilage Plate Following Partial Amputation¹

DAVID J. SIMMONS AND RUDOLPH F. NUNNEMACHER
*Radiological Physics Division, Argonne National Laboratory
Argonne, Illinois and Department of Biology, Clark University
Worcester, Massachusetts*

ABSTRACT Following hemi-resection of the rat distal femoral epiphysis with its growing epiphyseal cartilage, the cut surface of the cartilage is sealed-off by trabecular bone and the cells fail to undergo further growth and maturation at that site. However, since the peripheral rows of cartilage cells survive and continue to proliferate, the cellular activity gradient causes the epiphyseal remnant to rotate about the fixed cut surface of the cartilage toward the amputated side. In these experiments, the degree of epiphyseal rotation following partial amputation was compared to the longitudinal growth of the contralateral intact femurs in normal and estrogen-treated rats. While estrogen treatment retarded both the growth of intact femurs and epiphyseal rotation, the ratios of these growth measurements calculated at different time intervals following osteotomy (0-4 4-7 7-9 weeks) were identical to those of the control series. It was concluded that partial amputation per se had no demonstrable effect on the vitality of the surviving chondrocytes of epiphyseal cartilages; moreover these cells were entirely responsive to the growth depressing action of estrogen.

The pioneering experiments of Stephen Hake (1737) established that the bones of the appendicular skeleton grow in length from their ends. The growth centers are known to be the highly specialized epiphyseal cartilage plates and the microscopic anatomy of these cartilages was first described by Muller (1858). Dodds (34) investigated the formation of the epiphyseal disc from the unorganized primitive cartilage of the epiphysis and the pattern of cell division which marshals the cells into more or less regular columns. The cartilage is stratified by a cellular size gradient (4 zones) owing to a gradual but coordinated series of age changes in each column. The epiphyseal cartilage is a cell renewal system, for the maintenance and rate of skeletal growth depends upon the continuing mitotic activity of the cells in the zone of proliferation (Zone 2—Dodds 34). Recent autoradiographic studies of chondrogenesis in the rat after labeling the cartilage cells with tritiated thymidine has furnished additional information about the pattern of cell division (Rigal, '62) and the generation times of the cells (Kember '60).

The proliferative and functional (matrix formation) activities of the cartilage cells are a sensitive measure of the nutritional (Acheson, '59; Bernick et al. '60; Saxton

and Silberberg, '47) and endocrine (Silberberg and Silberberg, '56) status of growing animals.

Arrested or reduced growth has been observed in limbs following experimental compression of epiphyseal cartilages in many species (Arkin and Katz, '58; Duben '58; Rooney '63; Siffert, '56; Sijbani '63; Strohino et al. '56). Small defects produced in growing cartilage plates by surgical incision (Haas '17-'19), needle puncture (Ollier 1867) or by drilling (Ford and Key '58; Imbert, '51) do not generally result in reduced growth. The growth retarding effect of defects produced by trauma or surgical procedure seems to be proportional to the size of the defect, and is caused by the formation of a cancellous bone bridge crossing the defect to fuse the epiphysis to the metaphysis (Campbell et al. '59; Ford and Key '58; Nunnemacher '39; Salter and Harris '63; Siffert, '56). Large defects in intact cartilages may also produce gross epiphyseal deformities (Siffert '56). Partial amputation of the cartilage plates of rat femurs also produced an epiphyseal metaphyseal bridge across the cartilaginous stump, and arrested the growth of the plates at that site (Nunnemacher '39). However because the cells of

¹This work was performed under the auspices of the U. S. Atomic Energy Commission.

the original surviving cartilage continued to grow mature and participate in the process of endochondral ossification the surviving epiphysis rotated about the zone of arrested growth toward the amputated side (figs. 5-7). Similar results were reported in the dog (Campbell et al., '59) and rabbit (Salter and Harris, '63) following an osteotomy of this type.

In these studies partial amputation of the distal epiphyseal cartilages of femurs in young growing rats resulted in the rotation of the surviving hemi-epiphysis. In view of the obviously altered tissue and vascular environment presented to the residual cells after partial amputation, it is of particular interest to determine if the chondrocytes were functioning as normally as those in intact bone. The growth retarding effect of estrogen, which is well characterized in rats is tested in a parallel study. Estrogen treatment results in thinner growth cartilages by repressing chondrocyte proliferation (Silberberg and Silberberg '41) and interferes with metaphyseal bone resorption (Lindquist et al. '60 Silberberg and Silberberg '42 Urist et al. '48). Bone lengthening as a function of the growth of the normal and estrogen-treated rat epiphyseal cartilages is compared with the degree of rotation of a partially amputated cartilages.

METHODS

Thirty male albino rats 31 days of age were housed in cages of ten animals each and fed a diet of Purina Laboratory Rat Chow and water ad libitum. The rats were 29 days old at the time of operation. Under ether anesthesia and aseptic conditions the femoral artery and vein of the left leg was ligated and the tibia was amputated at the knee joint. The condyles of the distal femur with its articular and growth cartilages was removed by making two intersecting cuts at right angles with a jewelers saw (figs 5-6)—the first along the median plane of the bone and the second at right angles to the long axis at the metaphyseal-epiphyseal junction. On the right side the tibia was not amputated and the femur served as the control bone.

A second series of 30 rats subjected to the same operation received daily sub-

cutaneous injections of 0.07 mg. estradiol benzoate in oil (Schering). Hormone treatment was initiated one day postoperatively and was terminated a day prior to sacrifice. Six rats from each series were sacrificed by ether anesthesia at 4, 7, 9, 11 and 13 weeks after the operation. The control and operated femurs from each animal were recovered at autopsy. The length of the control femur was measured. The tissues were subsequently fixed in Hellys fluid, decalcified in 10% nitric acid, and embedded in paraffin. The tissues were sectioned longitudinally on a rotary microtome at 8 μ and every fifth section was mounted serially and stained with Harris hematoxylin and eosin.

The slides of the intact control bone and the slides of the distal hemi-epiphyses from the partially amputated femurs of untreated and estrogen-treated rats which had undergone rotation postoperatively were projected on sheets of paper. The normal angle of the epiphyseal disc (fig. 5, Angle *abc*) was determined by projecting a line (*bc*) perpendicularly from a line (*bd*) drawn normal to the long axis of the bone. Growth of the original cartilage plate following partial amputation was then estimated by measuring the degrees of rotation of the disc from the normal angle about the "fixed" point *b* (fig. 7—Angle *abc'*). Point *b* could be considered as a fixed point because the cartilage plate became quite thin and inactive at that site. The formation of fibrous repair tissue and bone around the cut edge of the cartilage plate during repair resembles the condition described by Dawson ('39) in aged rats as lapsed union in which no further growth of cartilage occurs. In lapsed union, an atrophied epiphyseal disc persists, but it is sealed off by the epiphyseal bone above and by a continuous plate of bone across the metaphysis at the ossification front. This "sealed" appearance characterizes the femoral cartilage of normal senescent rats which grow very little. However after amputation cellular growth continued at the periphery of the surviving cartilage plate and the activity gradient resulted in epiphyseal rotation.

Estradiol benzoate was generously supplied through the courtesy of Dr. R. E. Barlow, Schering Corporation.

RESULTS

Weight gain. Figure 1 indicates that the untreated rats were heavier than the estrogen-treated rats at all experimental intervals. The most rapid weight gain in both series occurred during the first seven weeks. However while the estrogen-treated series failed to increase their weight thereafter the controls continued to gain significantly until 9-11 weeks. At 13 weeks the difference between the groups was nearly two-fold.

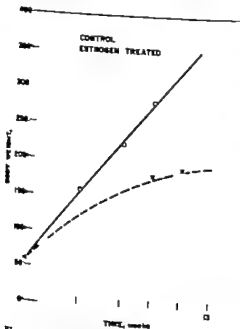


Fig. 1 A plot of body weight vs. time (weeks) indicates that estrogen-treated rats fail to normal weight-gain increments.

Growth of the femur The changes in length have been plotted in figure 2. The pattern of longitudinal growth is very similar to the weight gain data pre- above. Growth increments were greatest during the first seven weeks and the femurs from the untreated rats were slightly longer than those from rats receiving estrogen. While the latter fail to elongate appreciably after seven weeks, the from untreated rats continued to grow from 9-11 weeks. A good correlation for the relationship between body weight and femur length for both series of animals (fig. 3)

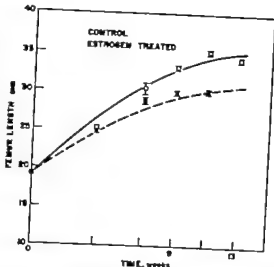


Fig. 2 A plot of femur length vs. time (weeks) which indicates that estrogen treatment inhibits bone growth in rats.

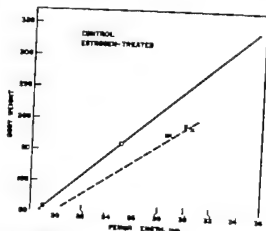


Fig. 3 The relationship between body weight and femur length in normal and estrogen-treated rats. The plot shows that there is a good correlation between these parameters.

The difference in the gross lengths of the bones probably reflects the decreased proliferative activity of the cells in the growth cartilages following estrogen treatment. The epiphyseal discs are always thicker in the femurs of untreated rats (table 1 figs 8,9). The amount of intercellular matrix was also greater in the cartilages from the intact control femurs of untreated rats, indicating further that the cellular synthesis of mucopolysaccharides was impaired by the action of the hormone.

TABLE 1
Epiphyseal plate thickness in normal and estrogen-treated rats

Weeks of treatment	No. of rats/group	Control	Estrogen treated	
		Cartilage thickness	Cartilage thickness	p value
		mm	mm	
0	6	0.401 ± 0.056	—	—
4	6	0.385 ± 0.030	0.248 ± 0.028	> 0.01
7	6	0.195 ± 0.023	0.137 ± 0.005	> 0.03
9	6	0.218 ± 0.005	0.138 ± 0.020	> 0.01
11	6	0.178 ± 0.004	0.154 ± 0.009	> 0.01
13	6	0.171 ± 0.018	0.135 ± 0.004	> 0.01

Larger numbers of irregular bone trabeculae were observed in the metaphyses of estrogen-treated rat femurs than in the controls presumably because of failure of the resorptive mechanism rather than any increased rate of bone formation (Urist et al. 48).

Histology and rotation of partially amputated Cartilages. In the control femurs after partial amputation the appearance of the original surviving cartilage plate at the cut edge was not unlike that of "lapsed union" (Dawson, 29). The cartilages were thinner and the columnar pattern of the surviving cells was disorganized. The metaphyseal trabeculae were short and fused (at 4 weeks) with the cancellous repair bone tissue which sealed off the cut surface of the cartilage. At the cut end then these changes suggest a retardation if not a complete cessation of growth. The rows of cartilage cells and the intercellular matrix were better preserved at the outer edge of the original cartilage plate and the endochondral trabeculae were quite long (fig. 10). It was this cellular activity gradient which was responsible for the rotation of the cartilages toward the amputated side. Effective growth and rotation of the partially amputated control cartilages was rapid throughout the first nine weeks of the experiment and the growth of the remaining hemiepiphysis closely paralleled the growth of the intact cartilage in the unamputated bone (fig. 4).

In the femurs from estrogen-treated rats, the remnant of the original cartilage plate was severely atrophied over a greater distance from the cut end than in the controls (fig. 11). Metaphyseal bone formation had nearly obliterated the marrow elements after seven weeks of hormone treat-

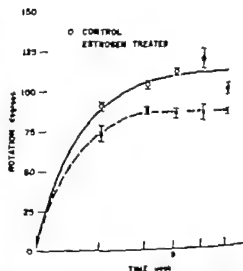


Fig. 4. A plot of the degree of rotation of partially amputated femoral epiphyseal cartilages vs. time which indicates that estrogen treatment inhibits the postoperative growth of the chondrocytes to the remnant of the femoral cartilage plate (compare with fig. 2). Since rotation might be expected to continue until the cut side of the epiphysis abutted the cut side of the shaft (i.e., 110°) the variability in the control data at 11 and 13 weeks suggests failure to remove equal amounts of tissue during amputation. Few degrees of rotation are required for large epiphyseal remnants to achieve epiphyseal metaphyseal contact with the cut surfaces.

ment, and the trabeculae were confluent with the cancellous bone bridging the epiphysis-metaphysis at the cut end of the cartilage plate. The arrangement of the unresorbed metaphyseal trabeculae resembled the "lapsed" appearance of the regions of atrophied cartilage. Effective growth and rotation of the amputated cartilages ceased after seven weeks (fig. 4) compared with nine weeks in the controls. The inability of the viable chondrocytes to

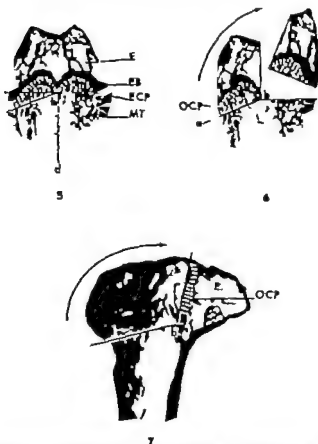


Fig. 5 A drawing of the distal end of rat femur. E, epiphysis; EB epiphyseal bone; ECP epiphyseal cartilage plate; MT metaphyseal trabeculae. Angle abc — normal angle of the epiphyseal cartilage plate.

Fig. 6 A diagram of the distal end of rat femur showing partial amputation of the epiphyseal cartilage plate. OCP original cartilage plate; arrow direction of rotation (ab — refer to Fig. 5)

Fig. 7 A drawing of the distal end of rat femur nine weeks after partial amputation of the epiphyseal cartilage. Note the extreme rotation of the cartilage (OCP) around the fixed point b. Angle abc' is the angle of rotation (compare with Fig. 5) E, epiphysis.

TABLE 2
Ratio of change in rotation to change
in femur length

Experimental period weeks	Control	Estrogen-treated
0-4	15.3	14.8
4-7	2.6	2.8
7-9	1.2	1.0

remain normal growth probably reflected, to large measure a lower cellular activity gradient attributable to the effect of the hormone rather than to the degree of atrophy of the cartilage plate.

The virtual correspondence between ratios of the mean change in angle of rotation to mean change in the length of the intact contralateral femur calculated for the early experimental periods (table 2) in both series suggests that partial amputation per se did not affect the vitality of the surviving peripheral cells and cartilage growth. The change from 0-4 weeks demonstrates particularly well that the smaller rotation of cartilages after estrogen-treatment reflects the differences observed for the intact femurs. The abrupt decrease in the ratios at 4-7 weeks and 7-9 weeks suggests that physiologic growth was

slowed and perhaps that further rotation beyond 75-80° was impeded by the physical resistance of the cut edge of the shaft.

DISCUSSION

Effect of estrogen on bone growth

The present experiment has confirmed previous reports that the administration of estrogen to rats diminishes their body weight (Bernick and Ershoff '63; Bugbee and Simond '26; Clausen and Freudenberg '39; Griffith and Young '42; Mathews et al. '42) owing to decreased consumption and utilization of food (Day and Follis, '41). The growth of bone was also reduced in this study by estrogen which inhibited chondrocyte proliferation in the epiphyseal growth cartilages (Bernick and Ershoff '63; Day and Follis '41; Dziewiatkowski et al. '57; Silberberg and Silberberg '41; Simpson et al. '42). Priest et al. ('60) have also demonstrated that the uptake of radioisotopes in the cartilages of estrogen-treated rats is diminished, indicating that the hormone interferes with mucopolysaccharide synthesis. Histochemical alterations of the ground substance of bone and cartilage tissue in estrogen-treated rats have been found by Bernick and Ershoff ('63). Autoradiographic investigations in mice with labeled estrogenic hormones have shown that bone is a target organ for estrogens (Budy '55; '60; '62; Bengtsson and Ullberg '63) but similar data are not available for the rat. However, while it is recognized that the osseous response to estrogen differs considerably in these species (Urist et al., '48) the effect of the hormone on the growth cartilage is at least qualitatively similar (Simmons '63). The skeletal responses to estrogen in the rat are age dependent. Talbot ('39) and Urist et al. ('48) found that the changes were not manifest in animals younger than a month old and were most pronounced during the period of active growth between one and three months of age.

Effects of partial amputation on epiphyseal cartilage structure These studies have shown that the physiologic aging of a cartilage may be accelerated by partial amputation, leading to early growth arrest at the cut surface. This was accomplished by the formation of bony repair tissue

bridging the cartilaginous stump, and the appearance of the epiphyseal plate at this site was not unlike that of "lapsed" union described first by Dawson ('29). While the amputated cartilages were thinner than those of the unoperated limb in the untreated rats, the amputated cartilages of estrogen-treated rats were atrophied severely for some distance back from the cut surface. However, the peripheral rows of chondrocytes were viable. The structure of the remnant of the original cartilage plate following amputation in the rats not treated with estrogen was quite similar to that observed by Nunnemacher ('39) in rats and by Campbell et al. ('59) in the dog.

Mechanism of epiphyseal cartilage rotation. Postoperative rotation of the partially amputated cartilages in rat femurs was observed in all cases. Because the histologic findings described above indicated (a) that the "lapsed" cut end of the cartilages constituted a fixed non-growing site and (b) that the peripheral rows of chondrocytes were viable, it is certain that the rotation reflected the cellular activity gradient of the residual living cells. Nunnemacher ('39) found that rotational deformities failed to occur if an osteotomy was performed on cartilages after they had closed. The failure of the amputated epiphyses of estrogen-treated rat femurs to rotate as much as the amputated control epiphyses seems to be due largely to the reduced proliferative potential of the viable chondrocytes as a direct consequence of the action of the hormone. However, there are probably also fewer viable cells in the amputated cartilages of estrogen-treated bones relative to the controls owing to the pronounced atrophic changes at the cut end.

It is not known if the actual growth (rotation) of the amputated cartilages was diminished in the present study. It was obviously impossible to measure the longitudinal growth of a bone which was deforming in the manner described. However, when the degrees of epiphyseal rotation were compared to the growth in length of the intact contralateral limb (Table 2), it appeared that the growth potential of the surviving cartilage cells was undisturbed. The abnormal cellular environment pre-

vided by the presence of repair tissue early in the experiment seemed to have little effect on the vitality of the residual cartilage cells. Any damage to the epiphyseal and metaphyseal vascular supply during amputation was in all probability transient. There was no evidence of cell death or abnormal thickening of the cartilage plate stamp which occurs following suppression of blood flow to the epiphyseal and metaphyseal sides of the cartilage respectively (Trueta and Amis, '60). The process of endochondral ossification, which was normal in the control bones, may fall if the metaphyseal circulation is suppressed. Rachtic-like thickening of the growth cartilages of rats (Brashear '59) and man (Hüfner '27) has been observed after experimental epiphyseal fracture owing to failure of the metaphyseal blood supply to reach the hypertrophic cells of the epiphyseal disc. A similar effect on rabbit tibial cartilages was observed by Yabaley and Harris ('85) following periosteal stripping and nutrient-artery destruction. While experimentally compressed epiphyseal discs of rabbits result in shorter limbs (Sjibrant '63) and torsional deformities (Arkin and Katz, '58) the effects of compression on the thickness of the discs is somewhat variable. Although the tibias were removed during amputation in these experiments it was not apparent that cartilage growth was appreciably affected by the failure of the bone to bear weight.

LITERATURE CITED

- Acheson, R. M. 1959 Effects of starvation, epiphyseal, and chronic illness on the growth cartilage plate and metaphyses of the immature rat. *J. Anat.*, 93: 123-130.
- Arkin, A. M., and J. F. Katz 1958 The effects of pressure on epiphyseal growth. The mechanism of plasticity of growing bone. *J. Bone Int. Surg.*, 38-A: 1099-1078.
- Bergman, G., and S. Ullberg 1963 The autoradiographic distribution pattern after administration of diethylstilbestrol compared with that of natural oestrogens. *Acta Endocrinologica*, 43: 561-570.
- Borsick, S., B. Ershoff and L. A. Savetta 1960 Effect of ascorbic acid deficiencies upon the bones and teeth of rats. *Anat. Rec.*, 130: 183-194.
- Borsick, S., and B. H. Ershoff 1963 Histochemical study of bone in estrogen-treated rats. *J. Dent. Res.* 42: 961-968.
- Brashear, H. R., Jr. 1959 Epiphyseal fractures. A microscopic study of the healing process in rats. *J. Bone Int. Surg.* 41-A: 1063-1064.
- Budy, A. M. 1955 Metabolism, excretion and retention of C¹⁴ labeled estrone in immature mice. *Arch. Int. Pharmacodyn.*, 103: 435-452.
- 1960 Skeletal distribution of estrone-16-C¹⁴. *Chin. Orthop.*, 17: 178-183.
- 1962 Radioactive oestrogens and bone. In *Radioscopes and Bone* (ed. P. Lacroix) Blackwell, pp. 327-340.
- Bugbee, E. P. and A. E. Simond 1926 Effects of injection of ovarian follicular hormone on body growth and sexual development of male and female rats. *Endocrinology* 10: 360-369.
- Campbell, C. J. A. Gabsolia and G. Zancoschi 1959 The effects produced in the cartilaginous epiphyseal plate of immature dogs by experimental surgical trauma. *J. Bone Int. Surg.*, 41-A: 1221-1240.
- Claessen, F. W. and C. B. Frandenberger 1939 Comparison of effects of male and female sex hormones on immature female rats. *Endocrinology* 25: 585-592.
- Dawson, A. B. 1929 A histological study of the persisting cartilage plates in retarded or leaped epiphyseal union in the albino rat. *Anat. Rec.*, 43: 109-123.
- Day H. G., and F. H. Polka, Jr. 1941 Skeletal changes in rats receiving estradiol benzoate as indicated by histological studies and determinations of bone ash, serum calcium and phosphatase. *Endocrinology* 26: 83-93.
- Duben, W. 1936 Experimental research into the later behavior of temporarily arrested epiphyseal plates. *Brunn's Beitr. Klin. Chir.*, 193: 201-207.
- Dziwiltkowski, D. D., F. Bronner N. DeFrenante and R. M. Archibald 1957 Some aspects of the metabolism of sulf. 35-S³⁵ and calcium-45 in the metaphyses of immature rats. Influence of β -estradiol benzoate. *J. Morphol. Biochem. Cytol.*, 3: 151-160.
- Enlow, D. H. 1922 A study of the postnatal growth and remodeling of bone. *Am. J. Anat.*, 110: 79-102.
- Feel, L. T. and J. A. Kay 1956 A study of experimental trauma to the distal femoral epiphysis in rabbits. *J. Bone J. t. Surg.*, 38-A: 84-92.
- Haas, R. L. 1917 The relation of the blood supply to the longitudinal growth of bone. *J. Orthop. Surg.*, 18: 157-171, 305-310.
- 1919 The changes produced in the growing bone after injury to the epiphyseal cartilage plate. *J. Orthop. Surg.*, 1: 87-99, 165-173.
- Halse, S. 1937 Vegetable statics (cited by D. H. Enlow 1922; P. Lacroix, 1926 and H. A. Sissons, 1956).
- Hilber, B. 1927 Congenital constriction of limbs. *Med. J. Australia*, 1: 233 (only).
- Imbert, R. 1951 Pathologie expérimentale de l'appareil de Croissance des os Longs. *Marseille Chir.* 3: 561-590.
- Kember, N. F. 1960 Cell division in endochondral ossification. *J. Bone Int. Surg.*, 42-B: 834-839.
- Lacroix, P. 1949 L'Organisation des Os. Editions Desoer Liège.

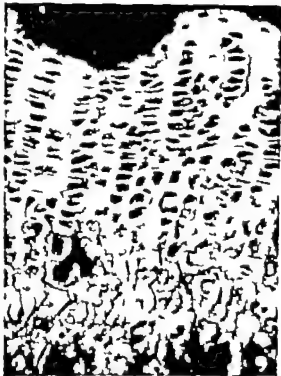
- Lindquist, B. A. M. Budy F. C. McLean and J. L. Howard 1960 Skeletal metabolism in estrogen-treated rats studied by means of Ca^{45} . *Endocrinology* 66: 100-111.
- Mathews C. B., E. L. Schwab and F. E. Emery 1942 The effect of continued oral administration of stilbestrol on body growth and organ weights of adult uncastrated and castrated female rats. *Growth*, 6: 7-22.
- Müller H. 1856 Ueber die entwicklung des knochenstoffs nebst bemerkungen ueber den bau rachitischen knochen. *Zeitschr. f. Wissensch. Zool.*, 9: 147-233.
- Nunnamacher R. F. 1939 Experimental studies on the cartilage plates in the long bones of the rat. *Am. J. Anat.*, 65: 253-269.
- Osler L. 1887 *Traité expérimental et clinique de la régénération des os et de la production artificielle du tissu osseux*. Vol. 1 Paris, Masson et Fils, pp. 336-338, 386-392.
- Priest, R. E., R. M. Koplitz and E. P. Benditt 1960 Estradiol reduced incorporation of radioactive sulfate into cartilage and aortas of rats. *J. Exper. Med.*, 112: 225-236.
- Rigal W. M. 1968 The use of tritiated thymidine in studies of chondrogenesis. In *Radioisotopes and Bone* (eds. P. Lacroix and A. M. Budy) Blackwell, pp. 197-219.
- Rooney J. R. 1963 Epiphyseal compression in young horses. *Cornell Veterinarian*, 53: 567-574.
- Salter R. B. and R. Harris 1963 Injuries involving the epiphyseal plate. *J. Bone J. t. Surg.*, 45-A: 587-622, 1963.
- Saxton, J. A., J. and M. Silberberg 1917 Skeletal growth and aging in rats receiving complete or restricted diets. *Am. J. Anat.*, 81: 445-476.
- Sjstrandlj S. 1963 Inhibition of tibial growth by means of compression of its proximal epiphyseal disc in the rabbit. *Acta Anat.*, 65: 278-283.
- Silberberg, M., and R. Silberberg 1941 Further investigations concerning the influence of oestrogen on skeletal tissue. *Am. J. Anat.*, 69: 295-331.
- 1942 Effects of endocrines on sex changes in the epiphyseal and articular cartilages. *Endocrinology* 31: 410-418.
- 1950 Steroid hormones and bone. In *Biochemistry and Physiology of Bone* (ed. C. H. Bourne) Academic Press, pp. 623-670.
- Simmons, D. J. 1963 Cellular changes in the bones of mice as studied with tritiated thymidine and the effects of estrogen. *Chakral Orthopaedics* no. 86, pp. 176-180.
- Simpson, M. E., E. A. Kibrick, R. Beck and H. M. Evans 1942 Effect of crystalline estrogen implants on the proximal tibia and coxofemoral function of young female rats. *Endocrinology* 30: 286-294.
- Sissons, H. A. 1956 The growth of bone. In *Biochemistry and Physiology of Bone* Academic Press, pp. 443-474.
- Strobino, L. J. P. C. Colonna, R. S. Budy and T. Leinback 1958 The effect of compresses on the growth of the epiphyseal bone. *Sect. Gynec. Obstet.*, 103: 85-93.
- Talbot, N. B. 1939 The effect of estrogen on the skeletal age of immature rats. *Endocrinology* 25: 325-327.
- Trueta, J. and V. P. Amato 1960 The vascular contribution to osteogenesis. III. Changes in the growth cartilage caused by experimentally induced ischaemia. *J. Bone J. t. Surg.* 42B: 571-587.
- Urist, M. R., A. M. Budy and F. C. McLean 1948 Species difference in the reaction of the mammalian skeleton to estrogens. *Proc. Soc. Exper. Biol. Med.*, 66: 334-326.
- Y. Bailey R. H. and W. R. Harris 1963 The effect of shaft fractures and peripheral stripping on the vascular supply to epiphyseal plates. *J. Bone J. t. Surg.*, 47-A: 831-868.

PLATE

PLATE 1

EXPLANATION OF FIGURES

- 8 A photomicrograph of the distal end of normal rat femur at four weeks. The epiphyseal cartilage (Z1-Z4) is thick and there is abundant intercellular matrix. Z1 resting cell zone; Z2, zone of cell proliferation; Z3, zone of individual cell growth; Z4 zone of cell hypertrophy. Hematoxylin and eosin. 370 X
- 9 A photomicrograph of the distal end of femur from a rat treated with estrogen daily for four weeks. The epiphyseal cartilage is thinner than the controls and the amount of intercellular matrix is reduced (compare with fig. 8) Hematoxylin and eosin. 370 X
- 10 A photomicrograph of the distal end of an untreated rat femur four weeks after partial amputation of the epiphyseal cartilage. The rotated original cartilage plate (OCP) is thinner than the unamputated cartilage (compare with fig. 8) but the cut end (CE) is sealed-off by facing of trabecular bone which extends into the metaphysis (MT) E, epiphysis. Hematoxylin and eosin. 80 X
- 11 A photomicrograph of the distal end of the femur from a rat treated with estrogen four weeks after partial amputation of the epiphyseal cartilage. The rotated original cartilage plate (OCP) is thinner than either the unamputated cartilage (compare with fig. 9) or the partially amputated cartilage of the untreated rats (compare with fig. 10). The cartilage appears to have lapsed over large distance from the cut end (CE); the cell columns are very short at this center of rotation which is sealed-off by a facing of irregular trabeculae MT metaphysis; E, epiphysis. Hematoxylin and eosin. 80 X



Phase Microscopic Observations of Rat Incisor Enamel¹

DENNIS WEBER

Marquette University School of Dentistry

ABSTRACT Thin ground sections (4-10 μ) of rat incisor enamel were prepared in appropriate planes using modified hand grinding technique. Phase microscopic observations of these sections confirmed the previously defined rod arrangement in the inner layer of enamel, and also demonstrated high degree of structural orientation in the outer layer of enamel. The initial layer of enamel formed was found to present morphologic picture which has not been previously defined a series of inter connected pillars of enamel on an elevated base which has "fish net" appearance in tangential section.

Tomes (1850) describing the structure of rodent incisor enamel, stated: "The supposed fibres (rods in present terminology) are composed of layers of fibres and each layer of a single series, the fibres of which are parallel to each other and at right angles with those composing the layers immediately above and below. In the outer part of the enamel the fibres of all the layers become parallel, and lamination ceases. Most recent authors (Watson and Avery '54; Butcher '56; Frank and Sognnaes, '60; Helmke and Rau, '62; Bouysse, Guilhem and Vialle '62) agree with Tomes' description of the basic pattern of rod orientation in the inner layer of enamel. Much controversy still exists, however as to the nature of the rod structure in the outer layer of enamel. Frank and Sognnaes ('60) deny the existence of rods in this layer while Watson and Avery ('54) showed considerable reservation when they stated "the rod structure if indeed there is a rod structure is not formed in the outer enamel in the same way as that of the inner enamel."

Although many of the early investigators utilized ground sections for the study of the incisor enamel of rodents none of them used sections which were thin enough to realize the maximum resolution of the light microscope. Recent refinements in technique (Fremlin, Mathleson and Hardwick, '81) permit the preparation of sections of human enamel as thin as 2 μ . Using a modification of this technique thin ground sections of rat incisor enamel were being prepared in this laboratory for a study dealing with the alteration of amelogenesis

after the subcutaneous injection of sodium fluoride. Initial observations of sections taken from the control group of animals indicated that the outer layer of enamel possessed a highly oriented structural pattern. This study was therefore undertaken to define more clearly the outer layer of enamel as well as to re-evaluate the inner layer of enamel.

MATERIALS AND METHODS

Fifty-day-old Sprague-Dawley rats were used as experimental animals. The animals were killed with ether; the incisors with the surrounding soft tissue and alveolar bone intact, were dissected free fixed in absolute ethanol and embedded in methyl methacrylate using the method described by Yaeger ('58). Thin ground sections (4-10 μ) of the incisors were prepared in six different planes:

- a. A tangential section through the inner layer of enamel.
- b. A tangential section several microns above the dentino-enamel junction.
- c. A tangential section several microns below the dentino-enamel junction.
- d. A mid-sagittal section at right angles to the dentino-enamel junction.
- e. A mid-sagittal section at a 45 angle to the dentino-enamel junction.
- f. A transverse section at a 45 angle to the long axis of the tooth.

This investigation was supported by U.S. Public Health Service Support grants 1S01FR-03348-01 and 1S01FR-03348-04 from the Division of Research Facilities and Resources, National Institutes of Health, Bethesda, Maryland.

Sections a, b and c were taken through areas of mature enamel.

Sections d, e and f were taken in areas where the enamel had reached its definitive width but had not fully mineralized. These different planes of section are illustrated in figure 1

Since the section preparation was the most crucial area in this investigation the author will discuss in detail the method that was used. Fremlin, Mathelson and Hardwick ('61) have described an excellent method for the preparation of thin ground sections of human enamel. The present author (Weber '64) recently described a rapid technique for the preparation of sections of human enamel in the 20 to 30 μ range. Neither of these techniques, however, was found to be adequate for this particular investigation. The method reported by the author would not produce sufficiently thin sections and the previously mentioned authors technique would not allow the preparation of the entire width of a tooth as small as the rat incisor. A modification employing aspects of both techniques was devised. The methacrylate-embedded incisor was ground to the desired plane of section using a conventional dental model trimmer. This surface was then finished on a glass plate using no. 4/0 emery paper followed by vitrified alumina on microcloth. The prepared surfaces of two specimen blocks one cut in a transverse plane and the other cut in a longitudinal plane are shown in figure 1. The specimen block was then glued to a standard microscope slide with Eastman 910 adhesive. Initial reduction of the specimen to approximately 70 μ was accomplished by a previously described technique (Weber '64). Reduction of the specimen to approximately 15 μ was accomplished by hand grinding on no. 4/0 emery paper. Final reduction and polishing were done with gold rouge on a silk cloth. It was at the stage of reduction from

70 μ down that this method differed from the method of Fremlin et al. They used abrasives dispersed in a liquid medium. Using that technique it was found that the dispersed abrasive particles removed the methacrylate surrounding the small specimen almost immediately without appreciably reducing the thickness of the specimen. Further grinding reduced the specimen in width as well as in thickness so that when the specimen was sufficiently thin the surface layer of enamel was lost. If however the specimen was reduced to the 15 μ level with no. 4/0 emery paper (here the abrasive particles are fixed to a paper backing) the methacrylate and the tooth were equally reduced. Extreme care was taken during this step. A piece of cloth was placed between the glass plate and the abrasive paper; this acted as a cushion and decreased the possibility of fracturing the specimen. Because of the large size of the abrasive particles on the emery paper (17 μ) one might expect this abrasive to leave deep scratches over the entire surface of the specimen and render it unsuitable for microscopy. Practically however this was not the case. Even specimens viewed before the final reduction and polished with gold rouge were found to be reasonably satisfactory (if mounted in immersion oil) for phase microscopy. The one drawback to this method was that the specimens were not planoparallel. Obviously this is inevitable in any free-hand grinding technique. This is not at all objectionable however when viewing small areas within the section.

A special method of embedding was used for preparing planes a, b and c. The definitive width of rat enamel is approximately 80 to 100 μ . This makes the specimen orientation in the block quite critical if tangential sections are to be prepared to any degree of accuracy and consistency. Only the erupted incisal portion of the tooth was used for the tangential plane.

Abbreviations

D.d, dentin
E.e, enamel
p, pulp
rl, rod, longitudinal section
rc, rod, cross section

il, inner layer of enamel
ep, enamel pillar (vertical projection of enamel)
hl, horizontal layer of enamel
de, dentino-enamel junction

sm, ameloblasts
is, interrod substance
tr, transitional row
I, incisal
B, basal

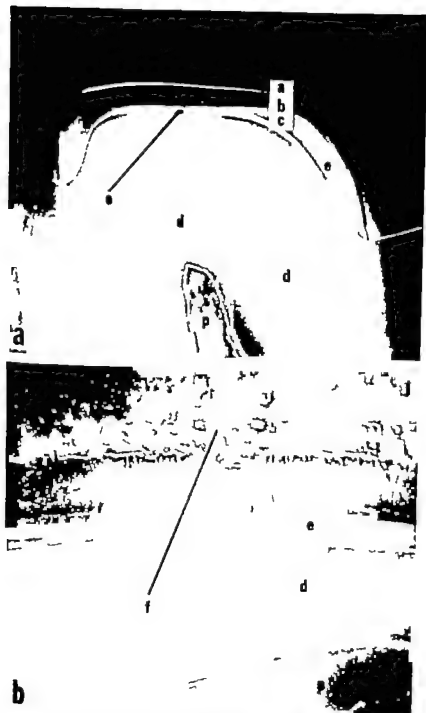


Fig. 1 These two photomicrographs demonstrate the prepared surfaces of the blocks prior to gluing the specimen to the glass slide and also illustrate the planes of section described in the text. (a) transverse section. (b) longitudinal section, ($\times 100$)

of section. The labial surface of the enamel was positioned against the flat surface of a microscope slide and then embedded in methacrylate in this position. As a result of this embedding the labial surface of the enamel was in a point to-point contact with the glass slide and completely surrounded by a surface of methacrylate which was on the same plane as this contact and as flat as the microscope slide. This embedding was accomplished in the following manner:

1. The base of a cylindrical vial was removed and the vial was sealed to the surface of a glass slide with partially polymerized methyl methacrylate.
 2. A section of the incisor approximately 10 mm in length was cut from the appropriate area of the tooth and the lingual surface glued to a cotton swab stick. The opposite end of the stick was inserted into a cork.
 3. The vial was partially filled with methacrylate and the mounted specimen inserted into the vial so that the labial surface of the enamel was in contact with the surface of the glass. The methacrylate was then polymerized using a dry heat oven.
- The steps in this procedure are illustrated in figure 2. With the specimen so oriented in the block it was relatively easy to prepare tangential sections in the previously indicated planes. Several swipes of the specimen across no. 4/0 emery paper exposed the inner layer of enamel (fig. 2c). The other two planes were reached by further grinding with constant pressure on the exposed enamel surface until light microscope with reflected light.
- The photomicrographs were taken with a Leitz Panphot using a dark-field and phase objective. The section was stained with a green fast blue. Specimen was mounted in mounting medium (index of refraction 1.5150) and a radiogram was taken. The Philips contact exposure was 2 MA, 10 min. The emulsion was developed in D19. The film was developed in Kodak X-ray Developer for six minutes at 20 C.

oped in Kodak X-ray Developer for six minutes at 20 C.

The one H&E stained section shown in this paper was taken from a control group of animals used in a previous investigation. It was demineralized in HNO₃. A longitudinal section was cut at 10° and stained and mounted in a routine manner.

OBSERVATIONS

The inner layer of enamel

With the exception of the first layer of enamel laid down by the ameloblasts, the general morphology of the inner layer of enamel corresponded to previous descriptions: an alternating crossing of rods, from layer to layer. This was most obvious in longitudinal sections which were prepared at a 45° angle to the long axis of the tooth (figs. 3, 7 and 8). Theoretically if the present concept of rod orientation is correct, this plane of section should cut alternating layers of rods in cross and longitudinal section. In practice it did. Tangential sections of the inner layer showed the typical herring bone pattern associated with this layer (fig. 4). Though the rod orientation showed a remarkable repeat pattern, many deviations did occur. Branching of rods cut in a longitudinal plane (fig. 8) and adjacent bundles of rods cut in cross section (fig. 3) instead of cross and longitudinal section were seen quite frequently. The layers of rods themselves represented relatively straight lines with a slight bend (fig. 14) or curvature in the outer third of the inner enamel. Layers were inclined at about 30° toward the apical end of the tooth. The rods were roughly rectangular in shape and appeared most distinct in longitudinal section. Interrod spaces were seen in tangential section in either an individual homogeneous layer or in the peripheral enamel. The enamel face structure and composition were a unique feature. There was no evidence of a unique feature. There was no evidence of a unique feature.

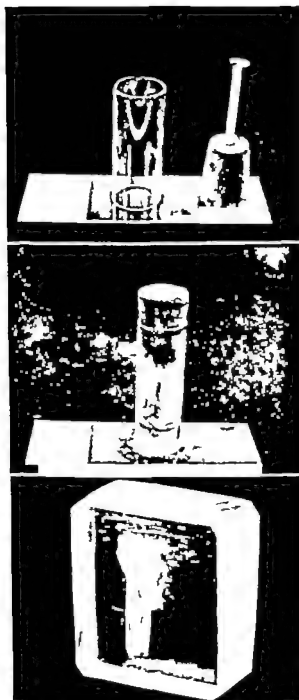


Fig. 2 Photographs illustrating the embedding technique used for the preparation of sequential sections: (a) shows glass vial with base removed and specimen mounted on stick, (b) shows embedded specimen, (c) shows the prepared surface of the specimen.

dentin which was from 1 to 2 μ in thickness. Bars of enamel projected upwards from this initial layer at 4 μ intervals giving this layer an appearance similar to a series of pillars on a slightly elevated base (fig. 9). These pillars or bars of enamel were approximately 4 μ in height thus giving this layer a total width of about 6 μ . Viewed in tangential section (fig. 11 and 12) this layer of pillars had a fish net appearance which indicated that the pillars seen in transverse and longitudinal section were interconnected and formed a continuous network. This zone was present in developing enamel and mature enamel. The microradiogram (fig. 6) indicated that this layer had the same radiodensity as the rest of the inner enamel. Figure 5 is an H&E stained section which also demonstrates this layer. Figure 10 is a diagrammatic three dimensional wax reconstruction of this layer showing the relationships between the component parts.

There was a narrow transitional zone (fig. 13) between the inner and outer layer of enamel. This zone appeared to be very fibrous and lacked any definite structural pattern.

The outer layer of enamel

Viewed in longitudinal section the outer layer of enamel presented a highly fibrous appearance. These fibrous elements were parallel to one another and inclined at about a 45° angle to the dentino-enamel junction. Transverse plane *f* (fig. 1b) cut these elements at approximately 90° thus revealing their cross sectional morphology. This layer presented structures which could be termed rods and interrod substance (fig. 13). The rods in cross section appeared as elongated ovals which were staggered in relation to one another so that the end of one rod was next to the middle of an adjacent rod. The cross sectional area of a rod near the inner layer of enamel was less than the cross sectional area of a rod at or near the surface of the enamel. There appeared to be slightly more interrod substance in the lower levels of the outer layer of enamel than at the surface area. It was interesting to note that even near the surface where the rods have their greatest diameter they were still considerably smaller than the diameter of the

ameloblasts. This rod pattern was very distinct, or invisible when the outer layer was viewed in longitudinal section. Figures 7 and 14 indicate areas which might be the boundaries between individual rods. A series of triangular shaped spaces was seen below the surface layer (fig. 7 and 14). The bases of these areas were directed towards the surface.

DISCUSSION

Section preparation technique

The section preparation technique described in this paper should have many applications. Though this investigation was not concerned with the surrounding soft tissues it is evident in figure 13 that the morphology of the ameloblasts, as well as their spatial relationship to the enamel, is well demonstrated. Sections of alveolar bone with the surrounding fibrous and cellular elements present have been prepared at thicknesses below 3 μ rather routinely. Thus we have a technique for investigating the mineralized tissues together with their formative elements without having to introduce the process of demineralization. These sections can easily be demineralized on the slide by any of the routine methods thereby allowing comparisons between mineralized and demineralized areas in the same section. Using such means studies are presently under way in this laboratory to determine the organic-inorganic relationships in mature rat enamel. Initial results have been informative and will be reported at a later date.

Rat enamel

The present author has probably viewed thousands of sections of rat incisors cut in every conceivable plane yet never noticed the unique structural arrangement presented by the initial layer of enamel. After recognizing it in the thin ground sections used in this investigation he checked other sections (demineralized) available to him and found it to be present in all instances. This layer is demonstrated in many photomicrographs appearing in the literature but has not been remarked upon. Along with the above observations the fact that it is present in all of the ground sec-

zone, no matter what the plane of section, tends to dispel the possibility of this zone being an artifact. That this zone is most obvious in these thin ground sections might be explained by the fact that the pillars of enamel are interconnected and thus would tend to obscure the zone in sections that were greater than 5-10 μ in thickness (fig 10). It is somewhat difficult at present to explain why this zone is not seen in published electron micrographs. Frank and Sogames ('60) describe the formation of a continuous horizontal layer of pre-enamel matrix (0.5 to 2 μ in width) which they refer to as the "inner enamel." This corresponds dimensionally to the initial layer of enamel described in this paper. They further describe a vertical budding continuous with the horizontal layer of enamel. The buds were said to increase in length and width, eventually to form longitudinal rods. These buddings correspond dimensionally to the pillars described in this paper. Nylen and Scott ('60) describe a similar picture except that they term the vertical projections interrod substance. The thin sections utilized for electron microscopy could easily pass through the interconnecting bridges in this zone and thereby obscure the true three dimensional morphology of this layer. Such a plane of section is illustrated in figure 10. It would appear from this investigation that this zone constitutes a distinct structural pattern which is not related to interrod substance or the formation of rods in the remainder of the inner layer of enamel. Of course this layer is continuous with the outer layer but their exact interrelationship could not be determined at this microscopic level.

Watson and Avery ('54) have shown an electron photomicrograph of a replica of the etched surface of a hamster incisor. This photomicrograph demonstrates oval structures similar to the ones shown in this light microscopic study. They however consider this degree of organization compared to the inner layer of enamel. The section of the outer layer of enamel shown in this paper shows a high degree of organization and represents the one area of rat incisor enamel which exhibits rods and interrod substance. The transverse section shown by the present author is taken

through an area of developing enamel. It had not completely mineralized but had reached its definitive width and was acid soluble. Sections of mature enamel of the outer layer were very difficult to prepare. They did, however present the same appearance that is demonstrated in the section of developing enamel. Investigations underway in this laboratory indicate that the interrod area shows a high concentration of organic material. The fact that the rods themselves are smaller in diameter than the ameloblasts makes it highly unlikely that one ameloblast is responsible for the production of one enamel rod. That the rods are not readily visible in longitudinal sections can be explained by their cross-sectional dimensions and their spacial arrangement. Their narrow widths and their staggered positions would tend to present a homogeneous field in sections greater than 5 μ in thickness. Further evaluation of this zone is necessary. Probably low magnification electron microscopy would be very enlightening.

Bouyassou Guilhem and Vialle ('62) indicate that the layers of rods bent in the outer third of the inner layer and became perpendicular to the dentino-enamel junction while the rods in the outer layer became perpendicularly directed as they approached the surface. While a slight curvature of the layers of rods in the outer third of the inner enamel was noted in this investigation the layer direction never approached a 90° angle to the dentino-enamel junction. These authors used demineralized sections from the basal end of the tooth. The slight curvature present could easily be accentuated during sectioning. No change in rod direction was seen in the outer layer in this investigation. The photomicrograph published by the above authors, indicating the change in rod direction in the outer layer of enamel, was not convincing to this author.

Bouyassou Guilhem and Vialle ('62) have pointed out the questionable use of the term rodent enamel because this could refer to structurally different types of enamel. Tomes (1850) pointed out the variations which occur in enamel in the order Rodentia many years ago. The order Rodentia was previously divided into two sub-orders the Simplicidentata (one pair

of incisors) and the *Duplicidentata* (two pairs of incisors). The *Duplicidentata* have been placed in the separate order *Lagomorpha* and the order *Rodentia* is now divided into three sub-orders. Basic differences exist in the enamel structure in members of the suborders. Rat (sub-order *Myomorpha*) enamel is structurally different from guinea pig (sub-order *Hystriocomorpha*) enamel. The present author agrees with Bourysson et al. that the term "rodent enamel" should be eliminated.

ACKNOWLEDGMENT

The author wishes to thank the members of the Dental Materials Department for their technical advice on section grinding and polishing. The photomicrographs were taken by Mr. Anthony Kuzma.

LITERATURE CITED

- Bourysson, M., A. Gullhem and M. P. Viall 1962 Contribution à l'étude optique de la matrice fibrillaire de l'émail dans des dents croissances continue et à croissance limitée. Bull. Group. Int. Rech. Sc. Stom., 5 199-241.
- Butcher E. O. 1956 Enamel rod matrix function in the rat's incisor. J. Am. Dent. Assoc., 53 707-712.
- Frank, R. M., and R. F. Sognnaes 1960 Electron microscopy of matrix formation and calcification in rat enamel. Arch. Oral Biol., 1 339-348.
- Franklin, J. H., J. Mathieson and J. Martell 1961 The preparation of thin sections of dental enamel. Arch. Oral Biol. 8 55-60.
- Helmcke, J. G., and R. Rau 1962 La structure de l'émail des rongeurs (souris et rat). I.D. Group. Int. Rech. Sc. Stom., 5 177-196.
- Nylen, M. U. and D. B. Scott 1960 Electron microscopic studies of odontogenesis. Jour. Int. St. Dent. Assoc., 39 406-421.
- Quigley M. B. 1959 Electron microscopy of developing enamel matrix in the Syrian hamster. J. Dent. Res., 38 180-187.
- Tomes, J. 1850 On the structure of the dental tissues of the order Rodentia. Phil. Trans. 140 529-567.
- Watson M. L., and J. E. Avery 1954 The development of the hamster lower incisor as observed by electron microscopy. Am. J. Anat., 95 109-161.
- Weber D. F. 1964 A simplified technique for the preparation of ground sections. J. Dent. Res., 43 482.
- Yasger J. A. 1958 Methacrylate embedding and sectioning of calcified bone. Stain Tech., 33 229-239.

PLATE I

EXPLANATION OF FIGURES

- 3 A longitudinal section through the inner enamel layer cut at a 45° angle to the long axis of the tooth which demonstrates rods cut in transverse and longitudinal planes. Double arrow indicates deviation from the normal pattern; group of adjacent rods cut in cross section, ($\times 970$)
- 4 A tangential section through the inner layer of enamel which demonstrates the herring bone pattern associated with this layer. Arrow points to an individual rod which has been cut obliquely ($\times 970$).

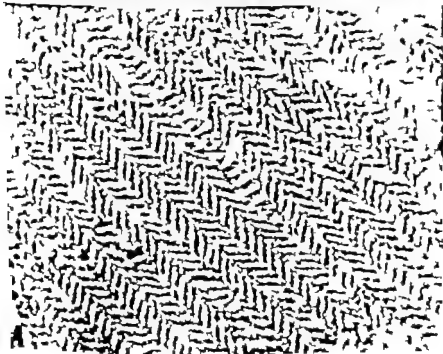
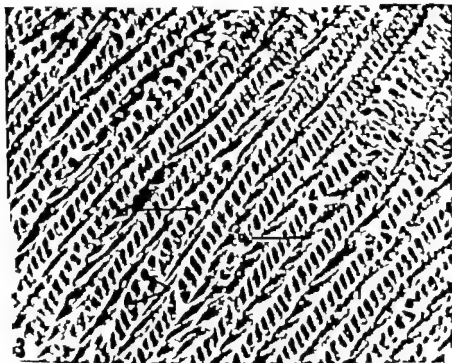


PLATE 2

EXPLANATION OF FIGURES

- 5 A demineralized H&E stained longitudinal section demonstrating the pillars (arrow) of enamel found in the innermost 1 year ($\times 400$).
- 6 A mikroradiogram of longitudinal section demonstrating that the pillars (arrow) of enamel are as radiodense as the rest of the developing enamel, ($\times 250$)
- 7 A longitudinal section cut at a 45° angle to the long axis of the tooth demonstrating the fibrous appearance of the longitudinally cut rods. Arrow (x) in outer layer of enamel indicates possible demarcation between rods. Arrow (y) indicates triangular spaces below the surface layer ($\times 700$)
- 8 A longitudinal section cut at 45° angle to the long axis of the tooth demonstrating the occasional branching (arrow) of rods, ($\times 700$)

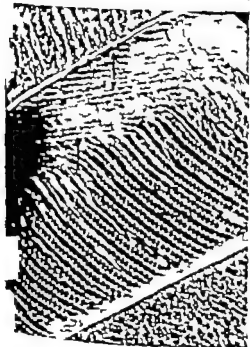
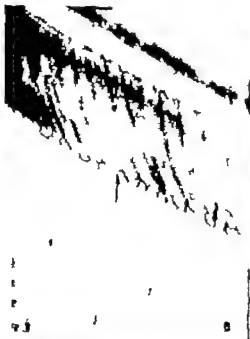


PLATE 3

EXPLANATION OF FIGURES

- 9 A longitudinal section cut at right angle to the long axis of the tooth demonstrating the divisions of the innermost layer of enamel, (X 870).
- 10 A diagrammatic three dimensional wax reconstruction of a rectangular section taken from the innermost layer of enamel. (C) Represents a cross-sectional view (L) represents a longitudinal view and (S) a tangential view. Line (a) indicates that thin section such as those used for electron microscopy could pass through an area in this zone and fail to give true picture of the morphology. The two parallel lines (b and b-) indicate that a thick section through this area could also produce a misleading picture.

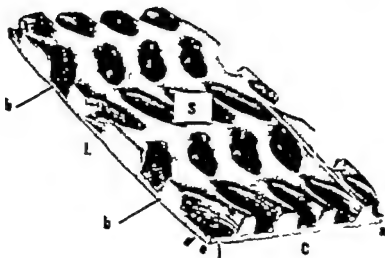


PLATE 4

EXPLANATION OF FIGURES

- 11 A tangential section through the innermost layer of enamel and the dentin showing the fish-net appearance of this layer in tangential section. The arrow points to the vertical projection which would be seen if cross section were prepared along the black line, ($\times 270$)
- 12 A tangential section through the inner layer of enamel. The arrow points to site of junction between vertical projections which are interconnected, ($\times 270$)

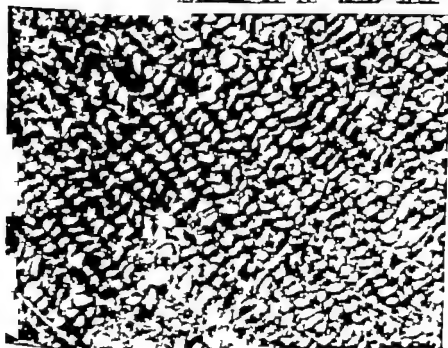
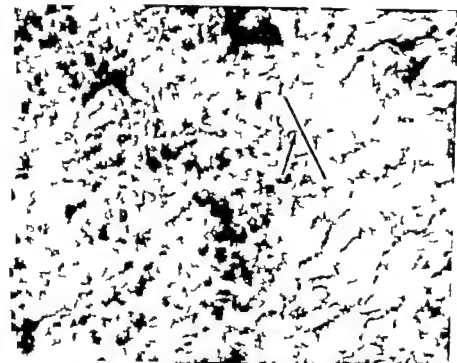
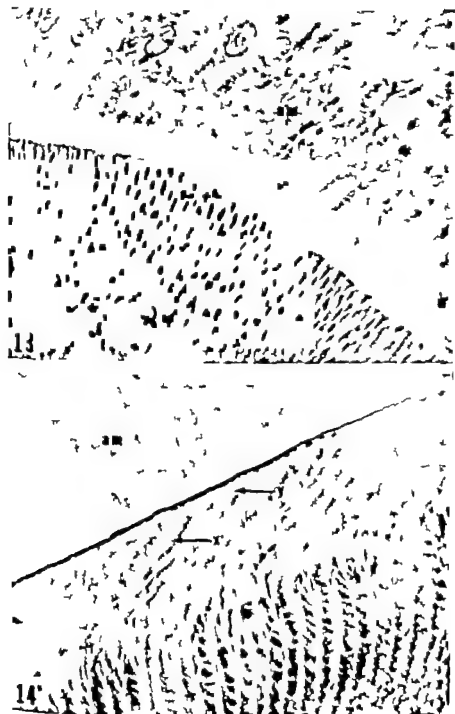


PLATE 5

EXPLANATION OF FIGURES

- 13 A transverse section at a 45° angle to the long axis of the tooth demonstrating rods and interrod substance in the outer layer of enamel. Transitional zone is shown in lower left hand corner ($\times 970$).
- 14 A longitudinal section at right angles to the long axis of the tooth. (x) indicates possible boundary between rods in the outer layer of enamel, arrow (y) points to sub-surface triangular space ($\times 970$)



Electron Microscopic Observations of Neurosecretory Granules Nerve and Glial Fibers and Blood Vessels in the Median Eminence of the Rabbit¹

P. E. DUFFY AND M. MENEFEE

Department of Pathology Division of Neuropathology College of Physicians and Surgeons Columbia University New York and
Department of Anatomy State University of New York Syracuse

ABSTRACT The median eminence of the rabbit has been studied electron microscopically and the neurosecretory granules in the nerve terminals of the external layer were shown to be smaller and have denser central core than the granules composing Herring bodies which are generally larger and have a paler core which is finely granular or vesicular. It was proposed that the small dense granules, which may represent neurosecretory substances destined to reach the pars distalis via portal veins, reach the nerve terminals in the external layer via certain dilated fibers described in this paper which contain identical granules. Some may also arise from the small dense granules occasionally seen in Herring bodies.

The demonstration of neurotubules within Herring bodies and the continuity of nerve fibers into Herring bodies, as well as the demonstration of myelin around some aggregates of large pale granules such as those seen in Herring bodies are further evidence that Herring bodies are dilated axons. Wide perivascular connective tissue spaces and interfilillary spaces were generally seen in the external but not the internal layers. The absence of neurosecretory granules from the perivascular connective tissue spaces suggests that neurosecretory granules go into solution before entering the connective tissue space. Some fibers containing neurosecretory granules, however, penetrated through the basement membrane into the perivascular spaces and certain unidentified electron dense granules were seen beneath the basement membrane of blood vessels.

The importance of neuroendocrine function is well illustrated by the accumulated information on the relationship of the pituitary stalk to the pars distalis of the pituitary gland as well as by the connections of some hypothalamic nuclei to the pars nervosa.

The portal veins of the hypophysis were originally noted by Professor F. L. Ratner of Bucharest (unpublished) and described in detail by Pope and Fielding ('30) and later by Wislocki and King ('36) Wislocki ('37 '38) Green and Harris ('47) Wingstrand ('51) McConnell ('53) and Kureb et al ('54). The significance of the portal system of veins and its role in the regulation of adenohypophyseal functions including the control of ovulation has been reviewed by Harris ('60) and Diepen ('62) and studied by many others (Green and Harris '47 Everett '58 Benoit and Assenmacher '55 '59 Okamoto and Ihara, '60 Vazquez Lopez

49 Ralph, '59 Stutinsky '58; Rinné '60 and Wingstrand '51). Electron microscopic studies with specific emphasis upon the median eminence portion of the neurohypophysis have also been published (Okabe '62 Barry and Cotto '61; Oota and Kobayashi '62 '63 Hirano et al. '62 Green and Van Breeman '55).

Since the early descriptions of neurosecretion (Scharer '33a '33b) and the use of the chrome hematoxylin stain technique of Gomori by Bargmann ('49) the formation of neurosecretory substance in nerve cells of the supraoptic and paraventricular nuclei and its transmission to the posterior pituitary has been recognized and elaborated upon (Bargmann and Scharer '51 Scharer and Scharer '54 Le Gall, '59 Sloper '58 Green and Maxwell, '59 and Green '51). Some aspects of the

¹This work was in part supported by U. S. Public Health Service grants BR01571, GM-1402, 5T1-5065-0 and Health Research Council, City of New York grant U1075.

ultrastructure of this part of the neurohypophysis have also been described (Palay '57; Roth and Luse, '64).

The present work was undertaken to study further the ultrastructure of neurosecretory granules in the infundibulum and to compare the structure of neurosecretory granules in the external layer of the median eminence with those in the tractus hypophyseus. It was also our purpose to examine the fibers in which neurosecretory granules are seen. We have in addition studied the relation of nerve terminals and glial cells to blood vessel walls and any morphological evidence of transport of neurosecretory substances across the vessel walls. Portal veins outside of the median eminence and blood vessels in the external and internal layers of the median eminence were examined. The arrangement of fibers in the external and internal layers of the median eminence were compared in regard to their light and electron microscopic appearances. The nerve and glial cells of the median eminence are the subject of a subsequent communication.

METHODS AND PROCEDURES

Thirty-eight adult female rabbits were caged in separate cages for 4-6 weeks subsequently anesthetized with veterinary nembutal. In three of the rabbits the neurohypophysis was approached by a direct surgical procedure and sections removed for light microscopy and stained with hematoxylin-eosin thionin paraldehyde-fuchsin (Gomori, '50) or chrome-alum-hematoxylin (Gomori 41 Bargmann, 49). In 35 rabbits perfusion was performed according to the method described by Palay et al ('62) using 0.25% glutaraldehyde adjusted to pH 7.4 with phosphate buffer (Sabatini et al. '63). The brain was removed including the separate anterior and posterior pituitary stalks which occur in the rabbit and the pituitary gland. Tissues removed at all levels from the hypothalamic nuclei to the pituitary gland were post fixed in cold 2% osmium tetroxide buffered to pH 7.4 with veronal acetate (Palade '52) which contained 0.04% calcium chloride. The tissues were then dehydrated through graded ethanol solutions and embedded

in Epon-812 (Luft, '61). Thick sections were examined by phase microscopy or stained with toluidine blue for light microscopy. Subsequent thin sections were cut on an LKB-ultramicrotome mounted on grids coated with collodion, and stained with lead or uranyl acetate (Watson, '53). Grids were examined in RCA model EMU-3F or Elmiskop I electron microscopes.

OBSERVATIONS

The median eminence of the infundibulum can be divided into an external (EL) and an internal layer (IL fig. 1) as described earlier by Herring ('08) and Nowakowski ('51).

By light microscopy the external layer (EL figs. 2, 3) appears to be composed of many closely apposed parallel fibers perpendicularly oriented to the surface and relatively few nuclei are present. By contrast the internal layer (IL fig. 2) has many nuclei, an appearance of a looser arrangement of cellular elements, multidirectional glial fibers traversed by the fibers of the tractus hypophyseus (Bargmann, 49) and is lined on its inner surface by the ependymal cells of the infundibular recess (IR fig. 2). The ventral surface of the external layer is surrounded by the pars tuberalis (fig. 1 and T figs. 3) which forms a cuff around it. Between the pars tuberalis (T fig. 4) and the external layer (EL fig. 4) there is often a space which may at times be larger due to artifactual retraction, referred to in this paper as the tuberoventral space. Within this space are some of the arterial branches which supply the median eminence and in thick sections of epon embedded material stained with toluidine blue one can also see portal veins (fig. 4). From here veins extend into the pars tuberalis and along its surface to the pars distalis (fig. 1).

Although by light microscopy the external layer of median eminence appears to be composed of closely packed parallel fibers electron microscopy demonstrates many interfibrillary spaces (5 fig. 5) and a great variety of shapes of fibers (fig. 5 B).

In addition the surface of the external layer which by light microscopy appears only moderately indented, is covered by a

basement membrane which, with the underlying fibers, forms a deeply undulating pattern (fig. 5 arrow). Fibers along the external layer of the median eminence sometimes had a broader zone of electron density along the limiting membrane at the surface adjacent to the basement membrane than along their other membranes. In the internal layer the cytoplasmic membranes were closely apposed to each other as elsewhere in the central nervous system (fig. 7).

Herring bodies identified by Gomori (chrome alum-hematoxylin) stain, were seen with the electron microscope to consist of large masses of neurosecretory granules surrounded by a limiting membrane (H fig. 8). The membrane surrounding the granules sometimes formed oval shapes but in other instances there were irregularly lobulated forms or points of constriction which caused the formation of dumbbell shapes (fig. 9). The granules of Herring bodies were not consistently uniform in size, electron density or morphology. Most of the granules had an average diameter of 200–300 m μ and usually a moderately dense homogeneous finely granular or vesicular content (fig. 10). The differences between these granules and those to be described in nerve terminals can be appreciated in electron micrographs showing granules in nerve terminals (NT fig. 8) adjacent to Herring bodies (H fig. 8). Some variation in the degree of density was observed in granules of Herring bodies but there was little tendency to either extreme electron density or electron density. When the center of a granule was somewhat denser a clear halo often separated it from the surrounding membrane. A different granule form was present infrequently within Herring bodies; these were smaller in size, had a denser central core and a more definite halo surrounding the central core (fig. 8 arrow). Herring bodies were most common in the internal layer and at the junction of the internal and external layers of the median eminence. Usually the aggregates of granules forming Herring bodies were surrounded by a limiting membrane without a myelin sheath but dilated forms with myelin sheaths and an identical granule content were also seen

(fig. 11). Scattered between the granules in Herring bodies there were tubules (fig. 9 arrows and fig. 11) resembling neurotubules.

Different but also large processes not infrequently seen in the external layer formed round, oval, bilobed, or irregular shapes. There was very little background density in these structures but they contained neurosecretory granules having a very dense central core, a clearer wider surrounding halo and an average size similar to granules seen in nerve terminals as described subsequently in this paper (fig. 12). An occasional tubule (fig. 12, arrow) similar to those in nerve fibers was also seen within these structures. Synaptic endings were sometimes present on the surfaces of these membrane bounded structures.

Nerve terminals containing neurosecretory granules were identified in both the internal and external layers but were more numerous in the latter or in the internal layer at the junction with the external layer (figs. 13, 14, 15). The large number of terminals in these sites is indicated by their presence in almost every thin section (fig. 7 arrows). Those in the external layer sometimes extended to the surface where they were apposed to the basement membrane but many terminated deep to the surface layer.

The nerve terminals contained synaptic vesicles (fig. 14 arrow and fig. 15) with an average diameter of 20–40 m μ . Many also contained neurosecretory granules (fig. 14 crossed arrow and figs. 16, 17) having a very dense central core surrounded by a clear zone which in turn was bounded by a membrane. The average diameter of the dense central core was 40–80 m μ while the diameter measured at the external limiting membrane was 70–120 m μ . At times the external membrane was seen without any central density.

The blood vessels of the median eminence were most numerous near the junction of the external and internal layers. Some blood vessels were surrounded by a wide connective tissue space (CT fig. 18) and these were more frequent in the external layer than in the internal layer. Blood vessels without a visible connective

tissue space were sometimes surrounded by glial processes but elsewhere nerve terminals ended directly upon the basement membrane of endothelial cells. End-foot processes lying upon the basement membranes were common (fig. 19). Although most of the deep vessels had walls composed of a single layer of endothelium other vessels had one or two layers of smooth muscle cells.

Endoplasmic invaginations into the lumen of some vessels in the form of villi were not uncommon and varied greatly in shape and size (figs. 20-21). An unevenly distributed electron density was also observed in many of these villi. Pinocytic vesicles were seen along both the external and internal endothelial surfaces of some blood vessels.

Portal vessels between the median eminence and the pars tuberalis (tubero-eminential space) were larger than those in the median eminence. These vessels were usually lined by a thin layer of endothelium (E, fig. 22) and had many fenestrations (fig. 22, arrows) covered by a diaphragm. The vessels were often surrounded by one or two pericytes and were situated within the space lined on one side by the basement membrane of the external layer of median eminence and on the other by the basement membrane of the pars tuberalis. Some of these vessels were deeply embedded and partially surrounded by the basement membrane of the external layer. Nerve terminals sometimes abutted directly upon the basement membrane of the external layer which in turn was apposed to the basement membrane of the portal vessels. The limiting membrane of some nerve fibers and terminals in the external layer showed semi-circular profiles (fig. 22, crossed arrows). The membrane forming these was more electron dense than the limiting membrane of the same fibers elsewhere. Across the base of these protrusions there was sometimes a suggestion of continuity of the limiting membrane of the nerve fiber but this was always less dense than that part of the membrane forming the protrusion.

Neurosecretory granules were often collected at one end of a nerve terminal adjacent to the endothelium of a blood

vessel or were outside of the connective tissue space but generally no secretory granules were present either in the connective tissue space or within the lumen of blood vessels. This was also true of neurosecretory granules in the cells of the pars nervosa of the same animals. Certain unidentified electron dense bodies were seen in two separate animals (fig. 18, arrow and fig. 23). These dense bodies were circular in form with an average diameter of 40 mμ and were present in small clusters beneath the basement membrane or as small "packets" in the endothelial cytoplasm. Nerve terminals abutting upon the basement membrane outside the connective tissue space of the same blood vessels had a marked grouping of synaptic vesicles immediately adjacent to the basement membrane. The limiting membrane of nerve terminals where such groups of synaptic vesicles were present was indistinct but elsewhere the membrane of the same nerve terminals was sharply delineated. Although no neurosecretory granules were seen free within the connective tissue space small groups of granules of similar size and appearance were sometimes seen in the connective tissue space within membrane bounded structures (fig. 24). The appearance suggested cytoplasmic prolongations or fibers which penetrated the basement membrane and were cut in the section either obliquely or in cross-section.

DISCUSSION

The electron microscopic observations of the neurosecretory substances in the median eminence of the rabbit suggest that they occur in at least two separate granular forms. One of these granule forms is smaller and has a very dense central core surrounded by a wide halo. They are located within nerve terminals distributed primarily in the external layer or at the junction of the external and internal layers of the median eminence (figs. 13-17) in areas which do not stain with the Gomori chrome-alum-hematoxylin method. The second kind of granule is larger and has a finely granular or vesicular central core which generally is only faintly electron dense (fig. 10). These are in large masses identified as Herring bodies

(figs. 8, 9) located for the most part in the internal layer where they can be stained with the Gomori chrome-alum-hematoxylin method.

It is of interest to compare these neurosecretory granules with those of the posterior pituitary and with granules of the median eminence and pituitary stalk described in other publications and in different species. Differences in external diameter, structure and staining qualities have been recorded but certain parallelisms also exist.

The size of neurosecretory granules in nerve terminals explicitly in median eminence was recorded by Oota and Kobayashi ('63) in the bullfrog as 55-180 μ . Kobayashi et al. ('61) said they measured 60-100 μ in the parakeet and Oota and Kobayashi ('62) noted corresponding granules in the pigeon median eminence as 55-156 μ . The sizes indicated above are therefore not significantly different from the ones we measured in the rabbit. Monroe ('65) has described the neurosecretory granules in the neurohemal regions of the median eminence and stem of the rat as smaller than those in the neurohypophysis. The smaller granules she describes probably correspond to the small dense granules which we saw in the external layer of median eminence. Neurosecretory granules in the internal layer of median eminence may be as large or even larger than those in the posterior pituitary.

In the posterior pituitary neurosecretory granules were measured in the rat by Palay ('57) 100-150 μ ; Hartmann ('58) 100-180 μ and Bretschneider ('58) 100-200 μ . Granules in this site were also recorded in the dog by Fujita ('57) 100-300 μ and by Bargmann and Knoop ('57) 120-180 μ . Bargmann et al. ('57) found them 150-300 μ in the snake. Fujita and Hartmann ('61) studied the rabbit and reported neurohypophysis granules having an average diameter of 110 μ , a maximum diameter in controls of 200 μ but an increase in size to 300 μ after treatment with adrenaline.

The external diameter of granules in the supraopticohypophyseal tract or infundibular process are generally about the same size, or somewhat larger than those

in the posterior pituitary (Bretschneider '58 Gerschenfeld et al., '60 Palay '57; Fujita, '57 Green and Van Breeman, '55 Barry and Cotte '61). Although neurosecretory granules vary in regard to size in different species there appears to be a similar pattern in relative sizes in the same anatomical locations (Green and Van Breeman, '55).

An exact comparison of sizes of neurosecretory granules in different studies and animals is often difficult because some investigators have not been specifically interested in comparing granules in separate areas of the median eminence and have therefore designated the size of granules in the stalk, neurohypophysis or infundibulum without differentiating external or internal layers. Differences incurred by the state of the animal, the effects of fixation sampling and other variables may also be misleading. Nonetheless our results indicate that neurosecretory granules in nerve terminals of the external layer of median eminence of the rabbit are smaller (70-120 μ) than those in Herring bodies (200-300 μ). A comparison with the results in other studies demonstrates that although there appear to be species differences and variations in altered physiological states the intraterminal granules of the median eminence are generally smaller than the majority of large pale granules forming Herring bodies or those in the posterior lobe.

Another characteristic which distinguishes neurosecretory granules from each other is the density and structure of the central core and the corresponding clarity of the surrounding halo. The small granules in nerve terminals in the external layer (figs. 13-17) have a much denser more homogeneous central core than the large pale granules in Herring bodies (figs. 8-10) which have a finely granular or vesicular central core. The granules in nerve terminals in the posterior pituitary are often slightly denser than those in Herring bodies. Any of these may have a lucent phase at which time they differ only in respect to size. Granules having a central density equal to the small granules in nerve terminals of the external layer were seen within

dilated fibers described in this paper (fig 12) but similar ones in small numbers are also seen between the larger granules of Herring bodies. Although small dense granules are sometimes present in Herring bodies and large pale granules may occur in nerve terminals in the posterior pituitary it is significant in our opinion that the large pale granules with finely granular or vesicular cores seen in Herring bodies are never seen in nerve terminals of the external layer.

Our observations on size and morphology of the small dense granules in nerve terminals in the external layer of the median eminence suggest that they are not derived from the large pale granules in Herring bodies of the supraopticohypophyseal tract. The possibility that the large pale granules in Herring bodies might decrease in size and increase in density and approach the external layer must be considered since in the neurohypophysis of the toad Gerschenfeld, Trautman, and DeRobertis ('60) reported that granules increase in size from 62 μ in the hypothalamus to 135–150 μ in the hilar region but are reduced to 115 μ in the terminal fibers of the neurohypophysis. We believe that a similar transformation in the external layer is unlikely because the differences in the granule sizes, and in the density and structure of their central cores is greater and because no transition forms from the large pale granules are seen in the nerve terminals of the external layer whereas they are not rare in the terminal fibers of the posterior pituitary.

The size and appearance of the small granules in the nerve terminals of the external layer suggests that they may come from the dilated fibers described in this paper (fig 12) which contain only small dense granules. The general configuration of these processes and the presence of a small number of neurotubules usually widely separated from one another suggests that these are dilated neural processes. Some of the small dense granules of the external layer may also arise from the small dense granules sometimes seen in Herring bodies.

The substance in Herring bodies which it is generally accepted is destined for the

posterior pituitary may well be incorporated only in the large pale granules with finely granular or vesicular cores.

Support for the proposal that the small granules of the external layer may represent a different substance from the majority of granules in Herring bodies is also gained from special stains and is important because of the role of median eminence in control of the pars distalis (Harris '35 '80). The Gomori chrome-alum-hematoxylin reaction obtained in the tractus hypophyseus is not present in the external layer. Wingstrand ('51) had commented upon material which stained with aldehyde-fuchsin in the median eminence but only part of this was stained with chrome-alum-hematoxylin. A number of workers have shown that fibers from infundibular nuclei ending in the posterior median eminence are aldehyde negative (Okabe '62, Christ '51) while Nowakowski ('51) also said that nerve fibers from the infundibular nucleus are finer than tract fibers and are Gomori negative. Hirano, Ishii, and Kobayashi ('62) studied the effects of prolonged dark photoperiods upon the median eminence of the Passerine Bird *Zosterops Palpebros Japonica* and concluded that the activity of the median eminence and pars nervosa are separately controlled. These studies are consistent with the proposal that the small dense granules in nerve terminals in the external layer of the median eminence are different in morphology and function from the larger granules in Herring bodies. It seems probable that the small dense granules are the substances which enter the portal veins to reach the pars distalis and exert control on pituitary secretion but confirmation of this by other techniques is necessary.

A consideration of the structure of Herring bodies other than neurosecretory granules contained within them is of some consequence. As pointed out by Gross and Maxwell ('59) the electron microscope reveals many confusing details about Herring bodies. They showed that the material in Herring bodies is composed of (1) structures easily identified as mitochondria (2) material resembling to plasma (3) fragments like neurosecretory (4) rarely small dark granules (5) and

momentously pale and dark granules with folds resembling the cristae of mitochondria. Green and Maxwell also said that the granules which they described in Herring bodies are also found in structures resembling nerve fibers and containing neurofibrils. They felt that the large pale granules could not clearly be distinguished from mitochondria but they were not convinced that these paler granules were related to mitochondria. We believe that the large pale granules in Herring bodies in our preparations can be distinguished from mitochondria by the absence of a double limiting membrane the lack of cristae, and the presence of a finely granular or vesicular content not seen in mitochondria. It was suggested that Herring bodies are dilated axons containing neurosecretory granules (Bargmann, '49). This concept is further supported in our study by the identification of neurotubules traversing between granules (figs. 9-11) and by demonstration in longitudinal section that nerve fibers become abruptly widened where masses of neurosecretory granules are present. Also some dilated axons containing large pale granules were seen surrounded by myelin sheaths. It is our impression that the slightly dilated fibers containing small numbers of granules are stages in the formation or dissolution of the more complete Herring body. Many of the nerve fibers which we saw in the external layer were smaller in diameter than those in the internal layer and they rarely had a myelin sheath. These smaller fibers may correspond to the smaller shorter Gomori negative fibers which Clark ('51) believes arise in the nucleus infundibularis and which were discussed by Diepen ('62) and were shown in light microscopy by Spatz et al. ('48) and Nowakowski ('51). Though some fibers in the external layer of median eminence are probably branches from the supraoptico-hypophyseal tract (Oota and Kobayashi, '63) the concept that many come from other sources such as the nucleus infundibularis is supported by many investigators. In birds such fibers are directed especially to the posterior median eminence (Okabe, '62; Kobayashi et al., '61). These proposals for the origin of fibers to the external layer of median eminence perhaps

coincide with our proposal of the origin of the small dense granules seen in nerve terminals in the external layer from the dilated fibers described in this paper which contain only small dense granules. Perhaps some also come from the small dense granules occasionally seen in Herring bodies. Other methods for specific identification must be employed.

The nerve terminals in which the small dense neurosecretory granules are contained in the rabbit are similar to those described by Palay ('57) in the rat neurohypophysis. Upon cursory examination of the external layer and junction of external and internal layers the number of small granules in nerve terminals appear deceptively few because large congregations of such terminals are rare. In almost every thin section of external layer however some of the nerve terminals are seen (fig. 7 arrows) so that the total representation of these terminals and granules is quite large.

The anatomical relationship between nerve terminals, blood vessels, and inter-fibrillary spaces presents a number of possible mechanisms for transfer of neurosecretory substances to the portal veins. Blood vessels within the median eminence in some instances have a connective tissue space (usually in the external layer) and elsewhere lack a connective tissue space (usually in the internal layer). Also the nerve terminals may be separated from the blood vessels by glial processes or end directly upon the basement membrane. The failure to identify neurosecretory granules within the connective space or in the endothelium or lumina of blood vessels suggests that granules go into solution before traversing the external basement membrane of the connective tissue space which is in keeping with the observations of others (Green and Maxwell, '59; Palay '57). At some sites however the transfer may take place from the fibers which appear to extend directly through the basement membrane into the connective tissue space (fig. 24). These are similar to the nerve terminals observed by Oota and Kobayashi ('62) and may correspond to the terminals described by Fujita and Hartmann ('61) as lying free in the connective tissue space.

Villous projections into the lumen of blood vessels were described by Fawcett ('59) but he felt that they were too few to be a significant feature of capillary structure. Kisch ('57a, '57b) spoke of such villi as tentacles. Villi having variable density were shown in some blood vessels of the median eminence (figs. 20-21) but it is not known whether they take part in transfer of neurosecretory substances.

Since on two occasions we saw small electron dense spherical bodies beneath the endothelial basement membrane and within the endothelium (fig. 23) the possibility that under some circumstances the dense core of neurosecretory granules may be transferred in this form must still be entertained. It was, however, seen only rarely in a large sampling and could represent many other substances. Glycogen, for example, which has been described in axons and nerve terminals of the neurohypophysis (Roth and Luse '64) bears some resemblance to these dense bodies though they do not appear identical in morphology.

The presence of a connective tissue space around many blood vessels of the external layer but not the internal layer is of interest. Oota and Kobayashi ('62) commented upon the wide connective tissue

between the parenchymal tissue of eminence and the capillaries of the portal vessels but their tissue sampling for electron microscopy was at two depths within the external layer. The connective tissue space around blood vessels of the external layer is like that seen around blood vessels in many parts of the body and the absence of such a space in the internal layer is like the arrangement in the other sites of the central nervous system. It is of interest to recall in connection with the presence of a connective tissue space around most blood vessels of the external layer that dyes which do not pass the blood brain barrier do readily traverse in the median eminence.

The presence of spaces between fibers in the external layer of the median eminence (figs. 5-6) may be of significance and one must consider that the terminals which lie immediately adjacent to these spaces may discharge neurosecretory material directly into these spaces from whence the

material could reach the surface basement membrane and portal veins of the tubero-eminent space. It seems unlikely that the spaces described are due to artifactual retraction because of their shape and since they were present to about the same degree in all preparations in which the internal layer showed no significant spaces between limiting membranes. The scattered distribution of nerve terminals in the external layer with or without relation to blood vessels would be consistent with this. Also the large portal veins in the space between the median eminence and pars tuberalis have a large surface exposure to the surface basement membrane (fig. 22) by the manner in which they are often ensconced into the surface layer. Evidence to demonstrate or disprove transfer of neurosecretory material at this site is needed and perhaps could be done by the use of dyes or radioactively labeled substances.

ACKNOWLEDGMENT

Schematic diagram, modified from Handbook of Physiology Section 1: Neurophysiology Volume II, page 1041 is reproduced with permission of Prof. Dr. Engelhardt, Bargmann and Diaper.

The authors gratefully acknowledge the technical assistance of Mrs. Ursula Feller and Mr. Gamil Debbas.

LITERATURE CITED

- Bargmann, W. 1949 Über die neuroendokrine Verknüpfung von Hypothalamus und Neurohypophyse. *Z. Zellforsch.* 34: 410-433.
Bargmann, W. and A. Knoop 1957 Elektronenmikroskopische Beobachtungen an der Neurohypophyse. *Zell. f. Zell- und Mirk-anat.* 46: 242-251.
Bargmann, W. and E. Scharrer 1951 The site of origin of the hormones of the posterior pituitary. *Ann. Scientist.* 39: 233.
Bargmann, W., A. Knoop and A. Thiel 1957 Elektronenmikroskopische Studie an der Neurohypophyse von *Tritidonoros natrix* (180). *Beiträge zur Kenntnis der Pars Innervata*. *Zell. f. Zell- und Mirk-anat.* 47: 114-125.
Barry, J. and G. Cottis 1961 Étude préliminaire au microscope électronique de l'axe hypothalamo-médian. *De Ciba*. *Zell. f. Zell- und Mirk-anat.* 47: 714-724.
Benoit, J. and L. Assenmacher 1953 La neurole hypothalamique de L'Arrière Pituitaire. *Conadrotrope*. *J. Physiologie* 6: 527-567.

- 1959 The control by visible radiations of the gonadotropic activity of the duck hypophysis. Recent Progress in Hormone Research, 14: 143-164.
- Reichsneider H. 1938 Die Feinstruktur des serösen Paranechyma von Infundibulum und Neurohypophyse. II. Die Neurosekretion. Z. Mikr-anat. Forsch., 64: 575-590.
- Choi, J. 1951 Über den Nucleus infundibularis beim erwachsenen Menschen. Acta Neurolog., 3: 287-335.
- Dejcs, R. 1952 Der Hypothalamus. In: Handbuch der mikroskopischen Anatomie des Menschen. W. Arnold, J. J. Springer, Berlin, Bd. IV/7.
- Ernst, J. W. 1958 Neuroendocrine mechanism in control of the mammalian ovary. In: Columbia University Symposium on Comparative Endocrinology. Ed., A. Gorbman, John Wiley and Sons, Inc., New York, pp. 174-1866.
- Fewell, D. W. 1959 The Fine Structure of Capillaries, Arterioles and Small Arteries. In: The Microcirculation Symposium on Factors Influencing Exchange of Substance Across Capillary Wall. Eds., S. B. M. Reynolds and E. W. Zweifach, U. of Ill. Press, Urbana.
- Fujita, H. 1957 Electron microscopic observations on the neurosecretory granules in pituitary posterior lobe of dog. Arch. histol. jap., 13: 163-172.
- Fujita, H., and J. F. Hartmann 1961 Electron microscopy of neurohypophysis in normal, adrenaline-treated and pilocarpine treated rabbits. Zeit. f. Zellf. u. Mikr-anat. 54: 734-743.
- Gordonfield, H. M., J. H. Tramezzani and E. DeRobertis 1960 Ultrastructure and function in neurohypophysis of the toad. Endocrin., 66: 741-762.
- Good, G. 1941 Observations with differential stains on known islets of Langerhans. Am. J. Path., 17: 305-400.
- 1950 Aldehyde-fuchsin: new stain for elastic tissue. Am. J. Clin. Path., 20: 665-668.
- Greer, J. D. 1951 The comparative anatomy of the hypophysis, with special reference to its blood supply and innervation. Am. J. Anat., 66: 213-312.
- Greer, J. D. and G. W. Harris 1947 Neurovascular link between the neurohypophysis and adenohypophysis. J. Endocrinol., 5: 136-146.
- Greer, J. D., and D. S. Maxwell 1959 Comparative Anatomy of the Hypophysis and Observations on the Mechanism of Neurosecretion. In: Columbia University Symposium on Comparative Endocrinology. Ed., A. Gorbman, John Wiley and Sons, Inc., New York, pp. 268-372.
- Greer, J. D. and V. L. van Breemen 1955 Electron microscopy of the pituitary and observations on neurosecretion. Am. J. Anat., 67: 177-203.
- Kern, G. W. 1953 Neural Control of the Pituitary Gland. Edward Arnold, Ltd., London.
- 1960 Neuroendocrine relations. Res. Fed. Assoc. Nerv. Ment. Dis., 40: 380-403.
- Hartmann, J. F. 1958 Electron microscopy of the neurohypophysis in normal and histamine-treated rats. Zeit. f. Zellf. Bd. 49: 291-308.
- Herring, P. T. 1908 The histological appearance of the mammalian pituitary body. Quart. J. Exper. Physiol., 1: 121-159.
- Hirano, T. S. Ishii and H. Kobayashi 1953 Effects of prolongation of daily photoperiod on gonadal development and neurohypophyseal hormone activity in the median eminence and the pars nervosa of the passerine bird, Zosterops palpestris japonica. Annotationes Zoologicae Japonenses, 23: 64-71.
- Klach, B. 1957 Elektronenmikroskopische Untersuchung des Hormons und der Kapillaren. Dtsch. Med. Wochr. 82: 605-606.
- 1957b Der Ultramikroskopische Bau der Capillarwand. Acta Physiol. Pharm. Neerlandica, 6: 334-338.
- Kobayashi, H., H. A. Barn, B. S. Makioka and Y. Hyodo 1961 The hypothalamo-hypophyseal neurosecretory system of the parakeet, melospittacus undulatus. Gen. and Comp. Endo., vol. 5 and 6, 1: 545-584.
- Legatt, H. 1959 Contribution à l'étude morphologique et expérimentale du système hypothalamo-neurohypophysaire de la Poule Rhode Island. Thèse d'agrégation, Univ. Catholique de Louvain, Nancy.
- Luft, J. H. 1961 Improvements in epoxy resin embedding methods. J. Biophys. Biochem. Cytol., 9: 409-414.
- McConnell, E. M. 1953 The arterial blood supply of the human hypophysis cerebri. Anat. Rec., 115: 178-203.
- Monroe, B. G. 1963 Comparison of the fine structures of median eminence and neural stem with that of the neural lobe of the hypophysis of the rat. Abn. Amer. Assoc. of Anat. confs., 78th Annual Session (April) Miami Beach Fla.
- Nowakowski, H. 1951 Infundibulum und Tuberkelstratum der Katze. Deutsche Zeit. f. Nervenk., Bd. 165: 261-339.
- Okamoto, S., and Y. Ihara 1960 Neural and neurovascular connections between the hypothalamic neurosecretory center and the adenohypophysis. Anat. Rec., 137: 455-499.
- Okabe, A. 1953 The fine nervous, neurosecretory and glial structure of the median eminence in the white-crowned sparrow. Neurosecretion, Eds., H. Heller and R. B. Clark, Academic Press, London and New York, pp. 199-206.
- Oota, Y. and H. Kobayashi 1962 Fine structure of the median eminence and pars nervosa of the pigeon. Annotationes Zoologicae Japonenses, 23: 123-134.
- 1963 Fine structure of the median eminence and the pars nervosa of the bullfrog. Zeit. f. Zellf. u. Mikr-anat., 60: 667-687.
- Palade, G. E. 1952 A study of fixation for electron microscopy. J. Exp. Med. 95: 235-298.
- Paley, S. L. 1957 The fine structure of the neurohypophysis. In: Progress in Neurobiology II. Ultrastructure and Cellular Chemistry of Neural Tissue. Ed., H. Waelch F. B. Hoeber-Harper New York, 249 pp.

- Palay S. L., S. M. McGee-Russell, S. Gordon and M. A. Grillo 1962 Fixation of neural tissues for electron microscopy by perfusion with solutions of osmium tetroxide. *J. Cell Biol.*, 12: 383-410.
- Papa, G. T. and U. Falding 1930 A portal circulation from the pituitary to the hypothalamic region. *J. Anat. Lond.*, 65: 88-91.
- Ralph, C. L. 1959 Some effects of hypothalamic lesions on gonadotrophin release in the hen. *Anat. Rec.*, 134: 411-423.
- Rinné, U. K. 1960 Neurosecretory material around the hypophyseal portal vessels in the median eminence of the rat. *Acta Endocrinol.*, 35 Suppl. 57.
- Roth, L. A., and S. A. Lane 1964 Fine structure of the neurohypophysis of the opossum. *J. of Cell Biol.*, 20: 459-472.
- Sabatini, D. D., K. Bensch and R. J. Barnett 1963 Cytochemistry and electron microscopy. The preservation of cellular ultrastructure and enzymatic activity by aldehyde fixation. *J. Cell Biol.*, 17: 19-33.
- Scharrer, E. 1933a Über neurokline organe der wirbeltiere. *Verhandl. Deutsche zool. Ges.*, 35: 217-220.
- 1933b Über die Zwischenhirndrüse der Säugetiere. *Sitzber. Ges. Morphol. u. Physiol. München*, 42: 36-41.
- Scharrer, E., and B. Scharrer 1954 Hormones produced by neurosecretory cells. Recent Progress in Hormone Research, 10: 183-240.
- Sloper J. D. 1958 Hypothalamo-neurohypophyseal neurosecretion. International Review of Cytology Academic Press Inc., New York. Vol. II, pp. 337-369.
- Spatz, H., R. Diepen and V. Gump 1943 *Die Anatomie des Infundibulum und des Tuberculum beim Kaninchen*. *Dtsch. Zts. f. Nervenhilfunde*, 159: 229-268.
- Stutinsky F. 1958 Rapports du neurosecretor hypothalamique avec l'adenohypophyse dans des conditions normales et experimentales. In: "Pathophysiologie Diencéphalica. Ed. S. B. Curri, L. Martini and W. Leric. J. Springer Vienna, pp. 79-103.
- Vazquez-Lopez, E. 1949 Innervation of the rabbit adenohypophysis. *J. of Endocrinol.*, 6: 159-168.
- Watson, M. L. 1958 Staining of tissue sections for electron microscopy with heavy metals. *J. Biophys. Biochem. Cytol.*, 4: 473-478.
- Wingstrand, K. G. 1951 The Structure and Development of the Avian Pituitary. C. W. K. Gleerup, Lund.
- Whitlock, G. B. 1937 The vascular supply of the hypophysis cerebri of the cat. *Ann. Rec.*, 69: 361-387.
- 1938 The vascular supply of the hypophysis cerebri of the Abroton monax and its Assoc. for Res. in Nerv. and Ment. Dis. Proc. 17: 48-68.
- Whitlock, G. B., and L. S. Klag 1938 The permeability of the hypophysis and hypothalamus to vital dyes, with a study of the hypophyseal vascular supply. *Am. J. Anat.*, 44: 421-472.
- Xeroub, G. P., M. M. L. Pykard and P. M. Daniel 1934 The hypophyseal portal system of vessels in man. *Quarterly J. Exp. Physiol.* 39: 219-229.

Abbreviations

CT connective tissue space	IR, infundibular recess
E, endothelium	S spaces between fibers of
EL, external layer	external layer
II, Herring bodies	SO supraoptic nucleus
IL, internal layer	SOT supraopticohypophyseal
L, lumen	tract
NT nerve terminal	T pars tuberalis
PV paraventricular nucleus	TE, tuberoinfundibular space

PLATE 1

EXPLANATION OF FIGURE

- 1 Schematic diagram of the infundibulum and pituitary gland of the rabbit. The external and internal layers, the portal veins, and supraopticohypophyseal tract are shown. Dotted areas surrounding the infundibulum indicate the pars tuberalis. (Modified from Handbook of Physiology Section 1 Neurophysiology volume II)

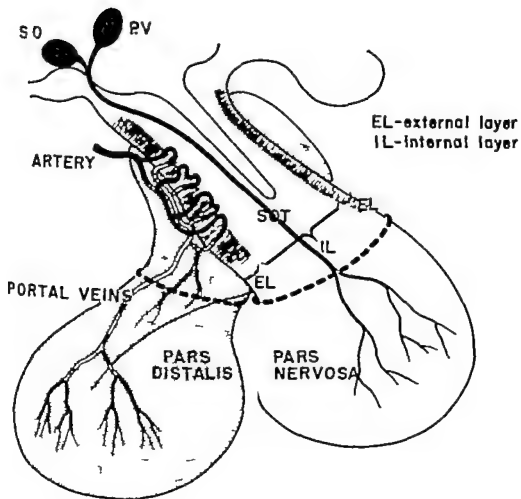


PLATE 2

EXPLANATION OF FIGURES

- 2 Cross section of median eminence showing the pars tuberalis, the external and internal layers of median eminence and portion of the infundibular recess. H & E. $\times 130$.
- 3 Cross section of median eminence shows the arrangement of cells in pars tuberalis, the relatively small number of nuclei in the external layer and a part of the more cellular internal layer H & E. $\times 120$.

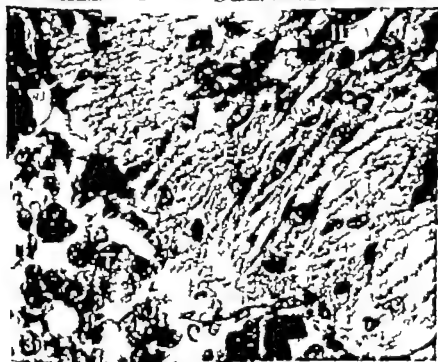


PLATE 3

EXPLANATION OF FIGURE

- 4 Cross section median eminence; epon embedded thick section. Note vessels in tuberoeminential space as well as some in pars tuberalis and one large vein lined by a single layer of endothelial cells in median eminence Toluidine blue stain. $\times 750$.



PLATE 4

EXPLANATION OF FIGURE

- 3 External layer of median eminence to show interfibrillary spaces and deep indentations of basement membrane (arrow) which separates the external layer from the tuberoemboental space. $\times 30,800$.

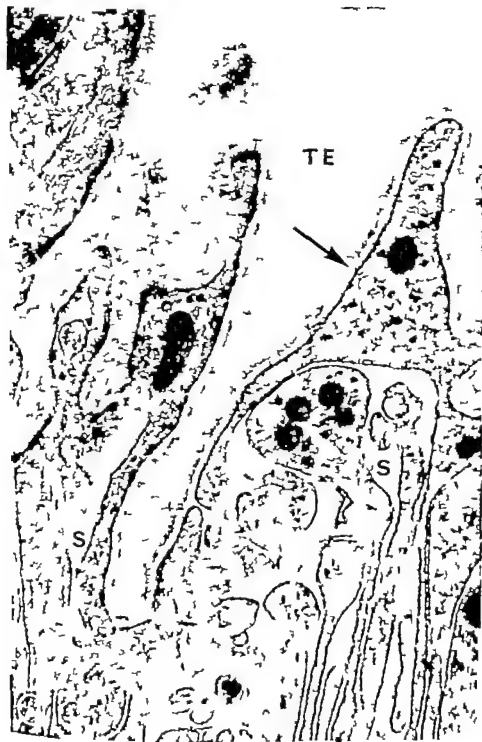


PLATE 5

EXPLANATION OF FIGURES

- 6 External layer of median eminence. Great variety of shapes and sizes of fibers and many interfibrillary spaces are shown. $\times 25,400$.
- 7 Internal layer of median eminence at junction with external layer. Neurosecretory granules seen as small dots in many portions of the section within nerve terminals (arrows) and elsewhere in the section. Cytoplasmic membranes are closely apposed in contrast to those of external layer. $\times 8,000$.



PLATE 6

EXPLANATION OF FIGURE

- 8 Internal layer demonstrating portion of large Herring body below and smaller part of one bova. Granules within Herring body differ from those in neurosecretory nerve terminal shown. One of the smaller granules rarely seen in Herring bodies is shown at arrow
X 16,400



PLATE 7

EXPLANATION OF FIGURES

- 9 Herring body with central constriction. Tubules seen at arrows. $\times 21,740$
- 10 Neurosecretory granule of Herring body. Fine vesicular structures within granule. $\times 45,000$.
- 11 Portion of Herring body extending vertically across the field. Tubules are present in the center surrounded by large granules and a myelin sheath. A node of Ranvier is seen at lower portion of the dilated fiber. $\times 30,000$.



PLATE 8

EXPLANATION OF FIGURE

- 12 Membrane bound structure containing tubules (arrow) and small granules with dense cores. $\times 27,500$.



PLATE 9

EXPLANATION OF FIGURES

- 13 Nerve terminal containing neurosecretory granules (arrow) $\times 18,000$
- 14 Nerve terminal containing synaptic vesicles (arrow) and neurosecretory granules with dense cores (crossed arrow) $\times 33,000$.
- 15 Nerve terminal; showing neurosecretory granules with various sizes and densities of central cores and synaptic vesicles. Note small nerve fiber at left containing one neurosecretory granule. $\times 27,500$.
- 16 Neurosecretory granules and synaptic vesicles in nerve terminal. Note differences in size and density of central core $\times 56,000$.
- 17 Neurosecretory granules. $\times 88,000$.

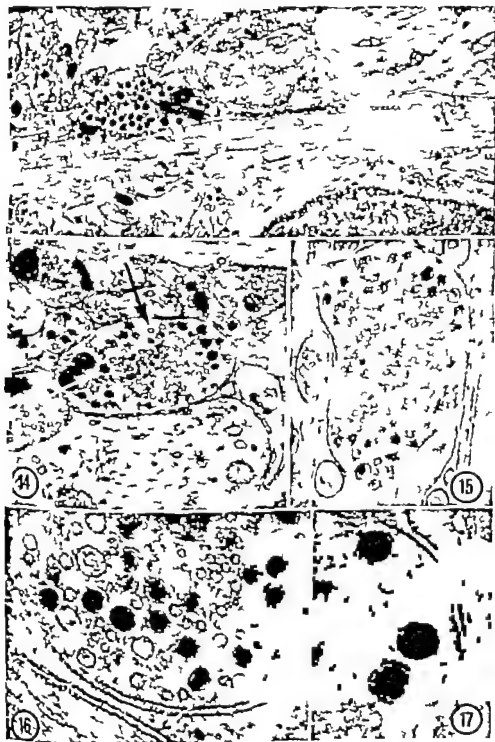


PLATE 9

EXPLANATION OF FIGURES

- 13 Nerve terminal containing neurosecretory granules at arrow $\times 16,000$
- 14 Nerve terminal containing synaptic vesicles (arrow) and neurosecretory granules with dense cores (crossed arrow) $\times 33,000$.
- 15 Nerve terminal; showing neurosecretory granules with various sizes and densities of central cores and synaptic vesicles. Note small nerve fiber to left containing one neurosecretory granule. $\times 37,500$.
- 16 Neurosecretory granules and synaptic vesicles in nerve terminal. Note differences in size and density of central core $\times 36,000$.
- 17 Neurosecretory granules. $\times 38,000$.



PLATE 11

EXPLANATION OF FIGURES

- 19 Blood vessel; foot processes ending upon basement membrane. No connective tissue space is visible. See arrow pointing to basement membrane. $\times 30,000$.
- 20 Endoplasmic villus. $\times 30,800$.
- 21 Endoplasmic villus. $\times 52,800$.



PLATE 11

EXPLANATION OF FIGURES

- 19 Blood vessel; foot processes ending upon basement membrane. No connective tissue space is visible. See arrow pointing to basement membrane $\times 30,000$.
- 20 Endoplasmic villus. $\times 30,800$.
- 21 Endoplasmic villus. $\times 82,800$.

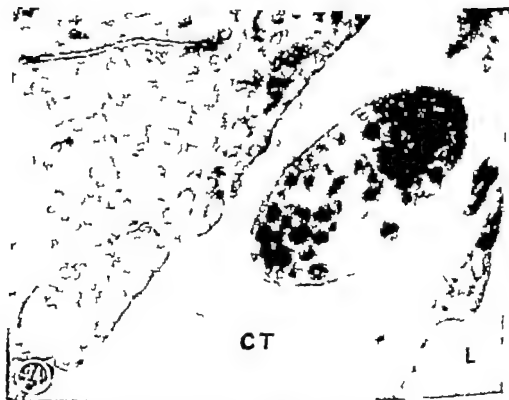


PLATE 13

EXPLANATION OF FIGURE

- 23 Blood vessel wall with connective tissue space. Arrow indicates basement membrane. Note small dense granules beneath basement membrane and in small pocket in endothelium. $\times 40,700$





34. Process containing neurosecretory granules in connective tissue space $\times 38,500$

The Study of Calcification of Mammalian Cartilage in Norm and Pathology by Stain Historadiography¹

F. BOHATIRCHUK

Department of Anatomy Faculty of Medicine University of Ottawa,
Ottawa 2, Canada

ABSTRACT The combined technique of histology and radiography — stain historadiography (Bohatirchuk, '57) — was used for studies of cartilage calcification. The main advantages of the technique are a. X-ray specificity in the detection of calcium; b. the possibility of morphological visualization of calcium in biological tissues at microlevel. Three patterns of cartilage calcification were observed: 1. columnar; 2. expansive; 3. ubiquitous. Stain historadiographs suggest that the cartilage cell rather actively participates in the calcification: a. calcium deposits are often found within the cytoplasm and cell membrane; b. some cartilage cells are frequently entrapped in intracellular lacunae. The latter phenomenon is especially often observed in the ubiquitous type of calcification.

The micromorphology appears to be a neglected field in studies of calcium-containing tissues in general, and of the calcifying and calcified cartilage in particular. The majority of authors are occupied with problems of biochemistry and physiology of calcification especially with those of bone growth. Consequently the knowledge of the above problems has been enriched immensely during the last 50 years while the comprehension of the calcification morphology continues to be based mainly on findings of former authors.

According to the views accepted now in the literature crystals of calcium salts (hydroxyapatite) are deposited during the calcification of growing cartilage into the intercellular (ground) substance. Due to this calcium impregnation the cartilage becomes opaque, hard and brittle (Eger '60). It is believed that mature cartilage cells mostly degenerate and die during this process. A few authors (among them Enlow '62, Fawcett and Bloom, '62) admit that some cartilage cells survive the calcification and are converted into osteocytes.

Almost all the authors (to mention only a few of them: Weidenreich '30, McLean and Bloom, '40, Maximow and Bloom '44, Ham, '52, Pritchard, '56, Ham '57, Fawcett and Bloom, '62) consider that the calcium impregnation does not involve the cartilage cell. Follis ('60) is quite categorical in this respect. He says (p. 245, no. 3) "The deposition of hydroxyapatite

takes place in a certain area of the matrix and only in the matrix, never in the cells at least as far as present techniques allow us to judge. The latest works of electron microscopists confirm in general the above views (Cameron '63). There are only a few dissenters. Shin-Izi Ziba ('10) has seen calcium in cytoplasm of calcifying cartilage cells in some growing bones of the human ear. The possibility of calcification of cartilage cells is admitted also by Todd ('13), Retterer ('17), Fell ('25) and Suzuki ('63).

Oddly enough to the best knowledge of this writer such a specific and reliable detector of calcium as X-rays were used only in four works on the problems of calcification in biological tissues. Owen et al. ('55) and Wallgren ('57) were dealing with problems of bone growth and mineralization, but did not discuss the cartilage calcification; Lagergren et al. ('62) studied the calcification and bone formation in chondrosarcoma. By making use of microradiography these investigators found that cartilage cells of the above tumors became partially or completely calcified. Suzuki ('63) in his recent work mentioned above also used X-rays among other methods. He found intracellular mineralization in chondrocytes of the epiphyseal plate of the slider turtle. Bohatirchuk ('57) in his first publication on stain historadiography

¹The work on stain historadiography of calcified tissues is supported by research grants from the Medical Research Council of Canada.

lography pointed out that this new technique permitted him to see calcium within the cartilage cell. However at that time this finding was not elaborated.

Since 1957 this new technique (called stain historadiography) has been used in studies of several bone problems (Bohatirchuk, '59 '60 '63a,b). It is thought to be of interest to inform about the latest results obtained with this technique in the Department of Anatomy of the University of Ottawa on the calcification of cartilage.

MATERIAL AND METHOD

Stain historadiography (Bohatirchuk, '57 '61 '63a,b) was used exclusively in this work. The routine details of the method are described in these publications and therefore will not be discussed here. However it is necessary to point out the latest improvements of the technique.

1 The new model of "K" microtome (Jung, Heidelberg, Germany) used by us at the present time has an electric motor which moves the block across a blade of extra hard steel. This device permits us to obtain serial sections of natural (undecalcified) calcium-containing tissue 5 microns and thinner with a smooth surface and of a uniform thickness.

2 The staining by thionin and picric acid (Schmødl) and the counterstaining by acid fuchsin were found to be the most suitable for growing and calcifying cartilage in bioplastic sections.

3 All historadiographs of this work were made with x-rays obtained at tensions between 8 and 12 kv. These rays have a wave-length sufficient for the visualization of calcium but they are too hard for the differentiation of soft tissue.

Material for this work comprised bones and cartilage of:

(1) three human fetuses of ages from about two and one-half to three and one-half months;

(2) one guinea pig, two cats, six rats and 12 rabbits (from new-born to about 8 weeks);

(3) two calcified intervertebral discs and one calcified cartilage of the tenth rib from aged persons (this material was obtained from the morgue of the Department of Anatomy).

(4) two rabbits with calcifying callus cartilage which developed after an autologous bone transplant. In this experiment pieces of rabbit tibia were transplanted into the muscular bed of the shoulder of the same animal. Both rabbits reported on here were sacrificed one month after the transplantation. The complete results of these experiments will be published elsewhere.

(5) three rabbits with the calcifying callus cartilage which developed consecutively on the fourth, tenth and twelfth day after the experimental fractures of tibia and fibula.

About 1,000 historadiographs and stained sections of the material mentioned above were studied for this work.

SOME COMMENTS ON THE READING OF STAIN HISTORADIOGRAPHS OF CALCIUM-CONTAINING TISSUES

The whitest color in an original historadiograph corresponds to the maximum amount of calcium, the blackest — to its absence. If the historadiograph is made under the technical conditions mentioned above, all transitions between these two extremes are seen in different shades of a grey color.

However, not every white or greyish spot in a historadiograph represents calcium of tissue section. Similar images may be caused by particles of dust or by some foreign inclusions, e.g. by those in the photoemulsion or in the bioplastic. All these pseudo-images can be differentiated from images of the tissue calcium by the following signs:

(1) they are present not only within the radiographed field of the specimen, but are seen outside of it;

(2) they usually have outlines much sharper than those of tissue calcium;

(3) they disappear or are displaced in serial historadiographs.

After it has been established that a white or greyish spot in the historadiograph represents the tissue calcium, it is necessary to determine the level of the section from which this calcium is projected. For instance, in case of a cartilage cell, it must be determined whether the calcium belongs to the cell or is projected into the cell area from levels either in

front or behind the cell. The most reliable conclusion can be made from a historadiograph of a section no thicker than the average thickness of a tissue element which was the subject of study e.g. that of a cartilage cell. Accordingly if the thickness of the section is no greater than 10 or 15 μ , one can be sure that calcium is conspicuous within the area of the cartilage cell belongs to that cell. In the determination of the level the following two geometrical properties of x-rays have also to be considered

(1) Images of structures lying at the same level should have a similar degree of marginal sharpness

(2) the closer the structure is to the photoemulsion the sharper should be its image.

The alternate study of historadiograph and stained specimen can be of help if calcium is seen not only in the historadiograph but appears also red or reddish in the corresponding stained section. Then its level can be determined in microscopical studies of stained sections by making use of the micrometer even if the sections are thicker than 10 or 15 μ .

The symmetry of images in both the historadiograph and the stained section allows also to localize calcium. For instance if an image of calcium as seen in the historadiograph has symmetrical outlines with a cartilage cell as seen in a corresponding place of the stained section one can assume that calcium belongs to the cell.

Any undecalcified hard tissue especially bone and sometimes calcified cartilage may be split during cutting. The resulting calcium artifacts can be differentiated from tissue calcium by comparing historadiographs of several subsequent sections. Images of the tissue calcium are seen in the same place and they have more or less symmetrical outlines while calcium artifacts are spread over the entire historadiograph and their outlines have many asymmetrical dentations, sharp protuberances and fissures (Bobatirehuk, '63)

At the comparison of a stained specimen and the corresponding historadiograph it is necessary to take into consideration that the minimal asymmetry in the picture of some detail is possible even in authentic

images due to a slight displacement of tissues during staining, mounting, etc.

RESULTS

Calcifications of hyaline and fibrocartilage were the subject of this study. The morphological peculiarities of calcification of these two types are to the best knowledge of this author not discussed in the literature. Therefore a scheme of different patterns of this calcification is proposed which was found to be the most appropriate in the reported studies. According to this, three main patterns have to be distinguished (1) columnar (2) expansive and (3) ubiquitous. All three were observed in the calcifying hyaline cartilage and only the latter — ubiquitous — in fibrocartilage.

1 Columnar pattern

The columnar pattern was seen exclusively in the calcifying hyaline cartilage during bone growth. It was seen in longitudinal bone sections along and within columns of cartilage cells. Two modifications of the pattern were observed (a) primary or prenatal, and (b) postnatal.

(a) *Prenatal calcification.* Calcification of this modification was observed in diaphyses of tubular bones. In the human embryo (approximately 10 cm long) the middle part of the cartilaginous diaphyses of metacarpal and metatarsal bones was seen already impregnated with calcium (figs 1 2). A net of tiny primary trabeculae was observed here surrounded by a case of compact bone. Zones of cartilage growth and the subsequent calcification were conspicuous at both the proximal and the distal ends of the calcified anlage. In each of these zones the subzones of the proliferating and the mature cartilage cells were distinguished. Although traces of calcium were seen in historadiographs of some specimens within the subzone of proliferating cells neither the distribution nor the localization of this calcium were sufficiently clear to draw any conclusion. A definite image of calcium within cytoplasm cell membrane and nucleus of many cells was observed in the subzone of mature cartilage (figs 3 4 4bis). Calcium here was seen in the ground substance also i.e. between cells (calcified

or not calcified) Some of these deposits were quite large like those in the middle part of the diaphysis. In this case they were seen in historadiographs of several subsequent serial sections.

(b) *Postnatal calcification* Stain historadiographs showed the much more pronounced columnar arrangement of cartilage cells during the postnatal (endochondral) bone growth than was seen before birth. As in the prenatal calcification, calcium deposits in the subzone of proliferating cartilage did not bear features definite enough for a conclusion either on their exact localization or on any other morphological details. However this writer believes that further development of the historadiographic technique will permit the higher magnification of historadiographs at which even the traces of calcium should be identified with morphological structures.

The densest calcium deposits were conspicuous in historadiographs within the subzone of mature cartilage as longitudinal (sagittal) strips of a white color. They were on the average a few millimeters long and from several to 100 μ wide, but were subject to large variations even within the length of one strip. Between these dense calcium deposits one could see either black or greyish-white spaces. Stained specimens showed that mature cartilage cells were present in both spaces. In other words some cells were partially or completely calcified others calcium-free (figs. 5 6 7). The comparative study of identical places of historadiograph and stained specimen revealed that calcium was present not only in cytoplasm and nucleus of numerous cells but also in their membranes (figs. 6 7). The density and distribution of calcium in the above cell elements varied. The calcified membranes were frequently seen in cells lying outside of the calcified strips (fig. 8).

2 Expansive pattern

The expansive pattern was characterized by the centrifugal spreading of the calcifying area from a primary anlage or a center of ossification localized approximately in the middle of the cartilaginous model. The mature cartilage cells were seen within the area of this anlage sur-

rounded by proliferating cells. In bigger center subzones of mature and proliferating cartilage were seen at periphery of the expanding calcified cartilage. No definite arrangement in columns was observed in this pattern. Both subzones of this proliferating and mature cartilage were much narrower in the expansive pattern than those in the columnar one.

The centers of ossification were distinguished in historadiographs by their size and structure. The primary anlage was seen as a group of tiny white tortuous lines. Stained specimens showed that these lines were x-ray images of the calcified intercellular (ground) substance located between mature cells. At this stage of the centers development no calcium was seen within the cells, probably because the concentration of calcium was too weak to be visualized by x-rays. Even the softest historadiographs of such small centers did not reveal any change of x-ray absorption coefficient within the cells area.

Within bigger centers calcified strips appeared thicker continuing one into another and forming a net (fig. 10).

In centers several millimeters large the intracellular calcification was frequently conspicuous in historadiographs (fig. 11).

The expansive pattern was observed in calcifying flat bones and in epiphyses of long tubular bones.

The entombment of cartilage cells into intraosseous lacunae was rarely observed in this pattern.

3 Ubiquitous pattern

In the ubiquitous pattern deposits of calcium were seen within large areas of cartilage. The irregular morphological features of these deposits the absence of any definite starting point of the calcification and the fact that they were always conspicuous in large numbers even at the beginning of calcification (e.g. in newborn animals) suggested the idea that they all appeared probably at the same time. This pattern justified the hypothesis of many authors that some biochemical changes within the entire calcifying area have to precede the calcification. The ubiquitous pattern was observed in b-

types of cartilage: in hyaline as well as in fibrocartilage.

A. Ubiquitous pattern in the calcifying hyaline cartilage

(a) *Ubiquitous pattern during bone growth.* Malleola and condyl of tubular bones were observed calcifying after the ubiquitous pattern. The calcification of one intrajoint sesamoid bone in a rat proceeded probably after the mixed pattern; it started possibly with the ubiquitous and continued with the expansive spreading of calcium (fig. 15).

Histoadiographs revealed that calcium within small areas was present among cells like in the other patterns. Nevertheless, no division was seen on subzones of proliferation and maturation as in other patterns and the columnar arrangement was observed only rarely. Cells were seen everywhere in calcified as well as in non-calcified cartilage (fig. 14).

The histoadiographs revealed within the entire calcified area black holes of different sizes. The smallest holes were larger than the usual intraosseous lacunae and had a somewhat round shape. Stained specimens showed that either single or groups of cells were present within these holes (fig. 16).

(b) *Ubiquitous pattern in the healing experimental fracture.* The development of a cartilaginous callus prior to the osseous one was observed in three cases of experimental fractures (the complete report on the results of this experiment will be published elsewhere). Figures 17 and 18 present stain histoadiographs of the rabbit which was sacrificed on the tenth day after the experimental fracture. All the stages of the new bone organization can be seen here. In the central parts of both figures several small calcium deposits are conspicuous distributed among cartilage cells. These minute deposits evidently represent the initial stage of calcification in this area. In other parts of the larger deposits are seen which surround cartilage cells and occasionally fuse. This stage was considered to be the more advanced one representing probably the beginning of a trabecular organization of new bone (fig. 18 at arrows and fig. 19).

The latter observation contradicts the generalization of Weidenreich ('30) that trabecula can originate only from trabecula. In the right upper corner of figure 17 and in the left upper of 18 another type of the trabecular organization is seen which is more in agreement with the statement of Weidenreich cited above. Here a stage of a cartilaginous trabeculae precedes its calcification. Within these trabeculae numerous flattened cartilage cells are seen of which the distribution and outlines suggest the possibility that they will be the future osteocytes. The entombment of cartilage cells into intraosseous lacunae was observed also in another type of the trabecular organization described above but it was not so typical as in the latter.

(c) *Ubiquitous pattern in the calcifying cartilage developed in the autologous bone transplant.* In both cases of autologous bone transplants discussed in this article numerous structures similar to cartilaginous exostoses developed on the surface of the transplanted bone. The ubiquitous pattern of calcification of these structures was obvious even in the smallest exostoses. In one case a thick layer of organized bone was seen at the periphery of exostosis (fig. 20). The partially or completely calcified cartilage cells were frequently seen within the entire area of calcification (fig. 21).

(d) *Ubiquitous pattern in the calcifying rib cartilage of an aged person.* Calcium deposits were seen in the middle of cartilage close to the bony part of the rib. They were very dense and solid. Evidently both cartilage cells and ground substance were involved in the calcification.

B. Ubiquitous pattern in the calcifying fibrocartilage

The irregular morphological features of the ubiquitous pattern were especially pronounced in the calcifying intervertebral discs. One could observe calcium deposits distributed in the examined area here and there on a considerable distance one from another (fig. 22). Outlines of these deposits were very irregular and they were conspicuous in cells as well as in the ground substance. Some calcifications as seen in a histoadiograph of one section were as large as 1 mm and one could

follow them on the depth of several consecutive sections. The osseous structure was rarely observed even within large calcium deposits. One must not confuse these mostly structureless deposits with lippings which have the osseous structure and another origin (Bohatirchuk, '57b)

LITERATURE CITED

- Bohatirchuk, F. 1957 Stain historadiography. *Stain Techn.*, 32: 67-74.
- 1957b Aging and osteoarthritis. *Canad. Med. Assoc. J.* 76: 106-114.
- 1959 Microradiographical data on fibered bone. *Anat. Rec.*, 133: 203-218.
- 1960 Micromorphological data on aging bone atrophy as seen in microradiographs and colored specimens. *Amer. J. of Gerontology* 15: 143-148.
- 1961 Medico-biologic research by microradiography. *Encyclopedia of Microscopy* pp. 591-629 ed. by G. Clark, Reinhold Publ., New York.
- 1963a A study of bone resorption and osteoclast* problem by stain historadiography. *Am. J. Anat.*, 119: 117-138.
- 1963b Use of x-rays in the detection of calcium in biological tissues: a microlevel. *Canad. Med. Assoc. J.* 89: 1171-1177.
- Cameron D. A. 1963 The fine structure of bone and calcified cartilage. *Clin. Orthopaedics*, 26: 199-228.
- Eger W. 1960 Mineralstoffwechsel des Knochens unter Ausschluss der Altersvorgänge. *Verhandlungen Dtsch. Orthop. 48 Kongress Vorträge*.
- Enlow D. H. 1963 A study of post-natal growth and remodelling of bone. *Am. J. Anat.*, 110: 78-102.
- Fawcett, D. W. and W. Bloom 1962 A text book of histology. W. B. Saunders, Philadelphia.
- Fellis, R. A. 1960 Calcification of cartilage. *Calcification in biological systems*, pp. 245-259 edit. by R. Sognnaes. *Amer. Assoc. Adv. Sc. Publ.*, Washington.
- Fell, H. B. 1923 The histogenesis of cartilage and bones in the long bones of embryo fowl. *J. Morph.*, 40: 417-459.
- Hans, A. W. 1933 Some histophysiological problems peculiar to calcified tissues. *J. Bone Joint Surg.*, 34A: 701-728.
- 1957 Histology 3rd Edition. J. Lippincott Company Montreal, Canada.
- McLean, F. C., and W. Bloom 1940 Calcification and ossification. Calcification in growing bone. *Anat. Rec.*, 78: 333-361.
- Maximow A. A., and W. Bloom 1944 A text book of histology. W. B. Saunders, Philadelphia.
- Owen, M., J. Jowett and J. Vargha 1953 Investigations of the growth and structure of the tibia of the rabbit by microradiography and autoradiographic techniques. *J. Bone Joint Surg.*, 37B: 324-342.
- Pritchard, J. J. 1956 General anatomy and histology of bone. *The Biochemistry and Physiology of Bone* pp. 1-23, edit. by G. H. Brown. *Acad. Press Publ.*, New York.
- Retterer E. 1917 De l'origine et de la structure du système médullaire du cartilage et de l'os. *Compt. Rend. Soc. Biol.*, 80: 86-90.
- Suzuki, H. K. 1963 Studies on the osseous system of the slider turtle. *Ann. of the New York Academy of Sciences*, 109: 351-410.
- Todd, T. W. 1913 Preliminary communication on the development and growth of bone and relation thereto of several histological elements concerned. *J. Anat. Physiol.* 47: 177-183.
- Wallgren, G. 1937 Microradiographical studies of developing bone in embryos. *X-ray Microscopy and Microradiography* pp. 441-463 ed. by V. E. Coslett, A. Engstrom and H. R. P. ity. *Acad. Press*, New York.
- Weidenreich, F. 1930 Das Knochengewebe. *Handbuch der mikroskopischen Anatomie des Menschen*, Vol. 2, by Mikendorf. J. Springer Berlin.
- Zilbs SShtn-Ird 1910 Ueber die chondroplastische Ontogenese bei endochondraler Ossifikation des menschlichen Fibrachien. *Zschr. Morph. Anthr.* 13: 137-174.

PLATES

PLATE 1

EXPLANATION OF FIGURES

Figures of this work are mostly given at magnifications smaller than those used at the study. This is done in order to make it easier for the reader to compare the identical places of the stained specimen and its historadiograph.

All the reproductions of the historadiographs are in their natural color (see text).

Calcium-containing tissues (e.g. bone) as seen in stained specimens are reproduced either grey or white depending upon their color in originals.

- 1 Macroradiographs of the right foot, human embryo 10 cm long; left — natural size right — photographically enlarged to approximately $\times 5$. Calcified diaphyses of metatarsal bones; advanced calcification of end phalanges.
- 2 Macroradiographs of the left hand of the embryo of figure 1 made with the same technique. The more advanced stage of calcification of the end phalanges.
- 3 A — Stained specimen, B — Historadiograph. An oblique section to the frontal plane proximal end of diaphysis of metacarpal 4, embryo of figure 2, 5a section, approx. $\times 180$. Although dots and lines of a slightly white color are seen here in the substance of proliferating cartilage they cannot definitely be identified with any crystal elements. In the substance of mature cartilage calcium deposits are seen within few cells (note the matching areas of cells and their x-ray images at the corresponding arrows).
- 4 A — Stained specimen, B — Historadiograph. Longitudinal section, proximal end of diaphysis of metatarsal 4 embryo of figure 1 8 μ , approximately $\times 180$. At middle arrows the initial stage of the organization of a trabecula. Two cells beside of it are partly calcified. At other arrows cartilage cells are seen with the different calcium content in their cytoplasm or membrane.

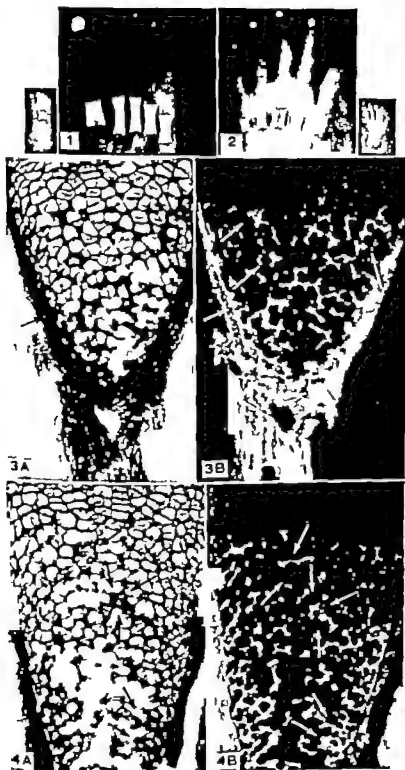


PLATE 2

EXPLANATION OF FIGURE

- 4 bis A, A — stained specimens; B, B — historadiograph new-born rabbit, metatarsal, oblique cut 5μ . Identical places are designated by X. A, B — $\times 120$ A, B — $\times 250$. Although the rabbit is newborn the cartilage is calcified after the prenatal pattern as yet. Cartilage cells are encircled in all figures which are undergoing complete or partial calcification. Note the calcification of membranes in several of these cells. Similar groups of cells are seen also in other places of figures.



PLATE 3

EXPLANATION OF FIGURES

- 5 A — Stained specimen, B — Historadiograph. Rat, two weeks old, proximal tibia epiphysis, 10 μ , approximately $\times 140$. Columnar pattern. Subzone of mature cartilage. Historadiograph shows longitudinal white stripes and between them two kinds of spaces of black color — image of calcium-free cartilage (both the mature cells and the ground substance) and \dagger white or grey color — the image of the same elements as above but containing calcium. The configuration and localization of many calcium-containing elements lead no doubt that they are images of partly or completely calcified cartilage cells. Transverse white lines between several vertical stripes are probably images of calcified cell membranes. Note that some of these lines are seen within the calcified ground substance. If they would belong to the latter then they should not be seen so clearly.
- 6 A — Stained specimen, B — Historadiograph. Rabbit, 10 days, proximal tibia epiphysis, 10 μ , approximately $\times 250$. Columnar pattern, subzone of mature cartilage. Arrows point to identical places where three partly or completely calcified mature cells are conspicuous on each side. Note the lower cell on the right. Its calcified membrane is seen on the background of calcified ground substance.
- 7 A — Stained specimen, B — Historadiograph. Rat, two weeks, proximal tibia epiphysis, 10 μ , approximately $\times 250$. Columnar pattern, subzone of mature cartilage. Calcification is not so regular as in figures 5 and 6. Vertical stripes are more tortuous and they frequently cross one another. However several partly or completely calcified cells are seen (at arrows and in other places).
- 8 A — Stained specimen, B — Historadiograph. Rabbit, three weeks, proximal femur epiphysis, 10 μ , approximately $\times 400$. Columnar pattern, subzone of mature cartilage. A group of three cartilage cells with the calcium present in their cytoplasm and membranes (at arrows).

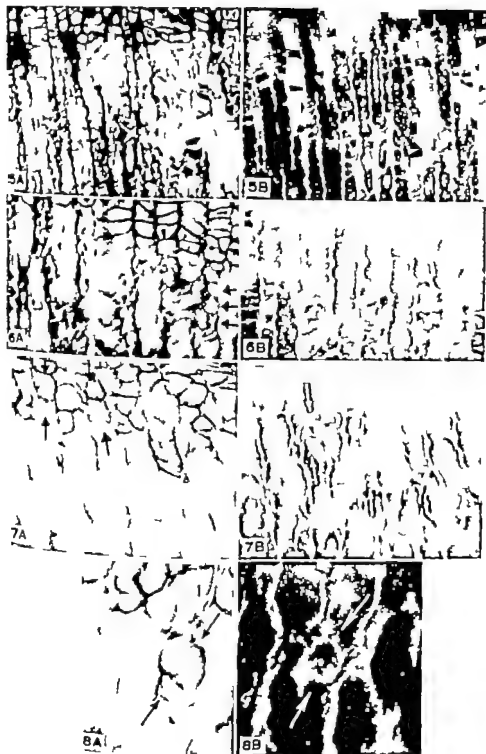


PLATE 3

EXPLANATION OF FIGURES

- 5 A — Stained specimen, B — Historadiograph. Rat, two weeks old, proximal tibia epiphysis, 10 μ , approximately $\times 180$. Columnar pattern. Subzone of mature cartilage. Historadiograph shows longitudinal white strips and between them two kinds of spaces of black color — image of calcium-free cartilage (both the mature cells and the ground substance) and of white or grey color — the image of the same elements as above but containing calcium. The configuration and localization of many calcium-containing elements leave no doubt that they are images of partly or completely calcified cartilage cells. Transverse white lines between several vertical strips are probably leaders of calcified cell membrane. Note that some of these lines are seen within the calcified ground substance. If they would belong to the latter then they should not be seen so clearly.
- 6 A — Stained specimen B — Historadiograph. Rabbit, 10 days proximal tibia epiphysis, 10 μ , approximately $\times 250$. Columnar pattern, subzone of mature cartilage. Arrow point to identical places where three partly or completely calcified mature cells are conspicuous on each side. Note the lower cell on the right. It calcified membrane is seen on the background of calcified ground substance.
- 7 A — Stained specimen B — Historadiograph. Rat two weeks, proximal tibia epiphysis, 10 μ , approximately $\times 250$. Columnar pattern, subzone of a mature cartilage. Calcification is not so regular as in figures 5 and 6. Vertical strips are more tortuous and they frequently cross one another. However several partly or completely calcified cells are seen (at arrows and in other places).
- 8 A — Stained specimen B — Historadiograph. Rabbit, three weeks, proximal tibia epiphysis, 10 μ , approximately $\times 400$. Columnar pattern subzone of mature cartilage. A group of three cartilage cells with the calcium present in their cytoplasm and membrane (at arrows).

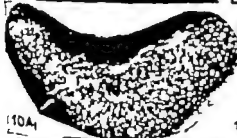


PLATE 4

EXPLANATION OF FIGURES

- 9 A — Stained specimen, B — Historadiograph. Rat, one week, 10 μ , both at low magnification. At arrows talus and navicular are seen calcifying after the expansive pattern. The almost uniform structure of calcium distribution in the central and peripheral parts of calcifying bones.
- 10 A and A' — Stained specimens, B and B' — Historadiographs. Rat, two weeks, talus (A,B) and navicular (A' B') 10 μ , approximately $\times 80$. Expansive pattern. The beginning trabecular organization in central parts of both bones. Note that the net of trabeculae is denser at periphery than in center although the central trabeculae are thicker.
- 11 A — Stained specimen, B — Historadiograph. Rat, two weeks, proximal tibia epiphysis, 10 μ , approximately $\times 180$. Expansive pattern. Stars indicate the identical parts of both figures. 1 side of oval several cartilage cells are seen with partly or completely calcified protoplasm. At upper right of oval in B one cell is conspicuous with traces of calcium in its cytoplasm and membrane (thin white line in B crossing the black background).



PLATE 8

EXPLANATION OF FIGURES

- 14 A — Stained specimen, B — Historadiograph. Rat, two weeks, femur area of distal condylus, 10 μ , approximately $\times 80$. Ubiquitous pattern. Calcium deposits are seen within large area of the calcifying cartilage. Several cells are seen entombed within cavities of an organizing bone. Some of these cavities are quite large with two or more cartilage cells inside some are of the size of intraseous lacunae with only one flattened cell.
- 15 A — Stained specimen, B — Historadiograph. Rat, four weeks, 10 μ , approximately $\times 180$. Ubiquitous pattern. Sesamoid bone within knee joint (fabella?). The thick layer of the compact bone at the periphery. Note that although the border line between calcium-containing and calcium-free tissue is clearly seen in B (upper part of figure) the same line is not definite in A.
- 16 High power view of an area of bone of 15A (approximately $\times 600$). Different cartilage cells are conspicuous entombed within cavities of the compact bone.



PLATE 7

EXPLANATION OF FIGURES

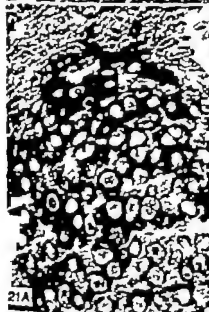
- 17 A — Stained specimen, B — historadiograph. Rabbit, experimental fracture 12th day 5 μ , approximately $\times 120$. (Stars are placed within the images of identical bone fragments.) Ubiquitous pattern. One can see in central part of the figures the initial stage of calcium deposition. The starting trabecular organization is seen at the periphery of the bone area. In the right upper corner of the figure one can see many cartilage cells entombed into lacunae of newly organized bone.
- 18 A — Stained specimen, B — Historadiograph. Rabbit the same as in previous figure another area of callus, 5 μ , approximately $\times 120$. Ubiquitous pattern. In central parts the separate calcium deposits start to confluence together. At arrows in the lower part of the figure one can see the starting organization of a trabecula. At left of the figure cartilaginous trabeculae are seen with many flattened cartilage cells within. Historadiograph shows that these cells are already entombed into cavities of the organizing bone.
- 19 Historadiograph of another area of the specimen of figure 17. Approximately $\times 120$. Different stages of trabecular organization of partly calcified cartilaginous callus.



PLATE 8

EXPLANATION OF FIGURES

- 20 A — Stained specimen, B — Historadiograph. Rabbit, autologous bone transplant, one month after the graft, 5 μ , approximately $\times 120$. Ubiquitous pattern. Several cartilaginous exostoses on the surface of transplanted bone showing different stages of a new bone development. The thick layer of the compact bone at the periphery of the big exostosis.
- 21 A — Stained specimen B — Historadiograph. Rabbit, autologous bone transplant, one month after transplantation, 5 μ , stained specimen : approximately $\times 100$, historadiograph at approximately $\times 250$. Ubiquitous pattern. At arrows and in other parts several partially or completely calcified cells are present. In the upper part of the figure a few cartilage cell are entombed in large cavities.
- 22 A — Stained specimen B — Historadiograph. Man, approximately T9 intervertebral disc 10 μ , approximately $\times 180$. A somewhat chaotic character of the ubiquitous pattern is particularly well conspicuous in this calcification. Calcium deposits of different size, shape and localization are seen everywhere within the area of calcification. None of these deposit has definite bone structure.



On the Cytology and Cytochemistry of the Opossum's Bronchial Glands¹

SERGEI PITRIMOVITCH SOROKIN

Department of Anatomy Harvard Medical School, Boston, Massachusetts

ABSTRACT The numerous compound acinar, mixed, bronchial glands of the opossum¹ lungs collectively provide a large surface for secretion. The secretory material is made by two types of cells located in the acini and smaller ducts. Mucus is produced by mucous cells that are similar to those found elsewhere. A fluid of unknown composition appears to be secreted by hydrotic cells. The acini are encircled by myoepithelial cells and the larger ducts are lined by morphologically unspecialized cells. The hydrotic cell, type of "special serous cell," is cytologically the most interesting of the elements present. It is not appreciably basophilic and lacks secretion granules, but it is rich in glycogen and contains many mitochondria with high succinate dehydrogenase activity. The basal surface is divided into irregular compartments by grooves, some of which are occupied by processes from stellate myoepithelial cells. The apical surface is villous and extends far down the sides of the cell as intercellular canaliculi. This surface has adenosine triphosphatase activity and is contacted by the agranular nucleus and numerous small vesicles in the subjacent cytoplasm. The bronchial glands are classified in the discussion, and special features of the hydrotic cells are compared with those possessed by other types of cells that engage in ion-segregation or ion-secretion. The glands are thought to assist in temperature regulation.

During a histochemical survey of lungs from the Virginia opossum (*Didelphys virginiana* Kerr) the mixed bronchial glands attracted attention because of a metabolic capacity greater than is typically present in bronchial glands of other animals (Sorokin, '62); secretory acini were strongly reactive for succinic dehydrogenase. Closer study has revealed that these bronchial glands bear a general resemblance to salivary and sweat glands, but the ducts are less well developed. Secretion is produced by two types of acinar cells. One is a typical mucous cell. The other shares some characteristics with serous cells from certain salivary glands and clear cells from eccrine sweat glands, but it is more appropriately placed in the broader category of cells specialized for the reparation of ions. This category includes cells from the kidney tubules, the stomach, the salt glands of marine birds and reptiles, and the rectal gland of sharks, in addition to those from the salivary and sweat glands. The cells in the bronchial glands, nevertheless, present their own variations on the cytological plan common to ion-segregators, and for this reason a detailed light and electron microscopic study of these glands is given here.

Why the opossum possesses such highly developed bronchial glands is uncertain. It may be that they function primarily in heat exchange, for the animal relies heavily on salivation and respiratory water loss for evaporative cooling (Higgenbotham and Koon, '55). The secretory proficiency of this slaving marsupial has not escaped notice in folklore (Hartman '52).

MATERIALS AND METHODS

Six adult opossums, five female and one male furnished lungs for the light microscopy and cytochemistry reported; of these three provided the specimens for electron microscopy. Prior to death by ether anesthesia, one animal was given an intraperitoneal injection of 10 mg pilocarpine nitrate in 2.5 ml saline. Within ten minutes 30 ml of saliva was collected as it dripped from the mouth, a 20- to 30-fold increase over normal. The sodium and potassium levels of this saliva were measured by flame photometry.

Light microscopy was carried out on sections of Bouin-fixed paraffin-embedded tissue stained by various procedures. Tis-

¹Supported by Research Career Development Award and Research Grant GM-10948-03 to the author from the United States Public Health Service.

sue fixed in Rossman's fluid was stained by the periodic acid-Schiff (PAS) method. Additional slides were prepared from epoxy-embedded material that had been intended primarily for electron microscopy. Others were made from gelatin-embedded frozen sections that had been fixed in 10% buffered formalin and stained with Sudan black B from thick (40 μ) slices impregnated with silver (Richardson, '60) and from fresh-frozen sections that had been cut on a cryostat and reacted for various enzymes. Succinic dehydrogenase was demonstrated using Nitroblue tetrazolium as hydrogen acceptor (Nachlas et al. '57). Adenosine triphosphatase (ATP) activity at pH 7.2 and 9.4 was revealed by a modification of the Gomori metal-salt procedure (Padykula and Gauthier '63; Padykula and Herman '55). Alkaline and acid phosphatases (Barka and Anderson, '63) were also studied by the Gomori method. Non-specific esterase activity was revealed using α -naphthyl acetate and fast blue RR (Pearse '60). Parotid glands of the pilocarpine-stimulated opossum were also studied for succinic dehydrogenase and esterase in order to compare their enzymic activities with those of the bronchial glands. Control reactions were performed for the cytochemical determinations. In the PAS reaction a control lacking periodic acid was carried out on material embedded in plastic in addition to a diastase control on paraffin sections.

Electron microscopy was pursued on material fixed in cold 1% osmium tetroxide and variously buffered at pH 7.2-7.4 by barbiturate phosphate or α -collidine. Additionally some specimens were immersed in 2% glutaraldehyde buffered in cacodylate and postfixed in osmium (Gordon et al. '63). All specimens were embedded in epon thin-sectioned, stained with Karnovsky's lead plumbite method A (Karnovsky '61), coated with carbon and examined in electron microscopes RCA models EMU 3E, 3F or 3G. In general the phosphate-buffered preparations (Millonig '61) were most satisfactory. There is some evidence however that proteins in such material are slightly more extracted than from tissues fixed in the presence of some other buffers (Luft and Wood '65) but

less extracted than from tissues buffered in α -collidine. Additional details of procedures followed may be found in the legends to the figures.

RESULTS

General description of the glands

The bronchial glands are abundantly distributed throughout the tracheal and bronchial passages of the opossum (fig. 4). Although individually small, the glands in the aggregate present a large surface to the bronchial lumen. According to histological convention (Bloom and Fawcett, '62) the glands are compound acinar structures. They usually have one or two and sometimes three orders of branching from a main duct (figs. 3, 7) which varies in length. Most of the secretory portions lie deep to the muscularis. Superficial acini nevertheless may open directly into a bronchial crypt. Terminal ramifications of the glands frequently are bound by connective tissue into lobules that include fat cells and comparatively large nerves. These regions are well vascularized. The glands extend down the bronchial tree until the adventitia becomes thin. They are reduced in number around bronchioles that have an inside diameter of ca 400 μ and disappear along the course of the next branching.

Secretory cells occupy the acini and much of the length of the ducts. Non-secretory cuboidal cells line little more than the main duct that leads to the surface epithelium. Mucous cells line the openings of the glands (figs. 8, 10). They line the ducts and form acini. Mucous secretory cells are found peripheral to the mucous cells. The non-mucous cells may be classified in the heterogeneous group of apical serous cells that differ in important details from the usual serous or serotympanic or (Stormont '32) in this paper they will be called hydrotic cells because they are called water-shedding cells of sweat glands and certain salivary glands. In the bronchial glands such cells usually form their own acini (figs. 5, 7) but they may occur among mucous cells or be grouped in crescents (fig. 10). All cells of both acini and crescents are drained by

capillaries that open into the lumen of the duct. The secretory capillaries extend along the lateral walls of hydrotic cells as lengthy intercellular canaliculi (fig. 11). Myoepithelial cells envelop the acini in arachnean processes. The myoepithelial investment extends along that part of the ducts lined by mucous cells (fig. 28) and terminates where these cells are replaced by non-secretory epithelium. The conformation of acinus and mucous duct is represented by a drawing (fig. 1) based on tracings made by camera lucida.

From the comparatively large nerves that come near the bronchial glands numerous small bundles of a few unmyelinated axons diverge toward the acinar clusters and ramify among the individual acini. Some nerves run along the periphery of the acini in the connective tissue that separates acini from the capillaries. Before turning inward they separate into three or more individual axons. Other nerves end near small ganglion cells that lie outside the acini. From these ganglion cells fine processes are directed toward the acini and extend part way along the ducts.

Cytochemistry

Structural materials and cell products. Mucus-secreting cells of the bronchial glands give a positive PAS reaction attributable to mucoproteins and mucopolysaccharides. In epon-embedded tissue the deposits of mucus occupy most of the cytoplasm (fig. 6) they are uneven in staining and coarse in granularity. Due to its basophilia the mucus both inside the cell and the lumen is readily identified in routine acid (1%) sections stained with toluidine blue (fig. 7). In frozen sections its metachromasia is pronounced. Hydrotic cells are not basophilic. They contain abundant glycogen (fig. 8). In electron micrographs glycogen occurs in loose aggregates as it is in dispersed form (figs. 15, 17, 19). Epithelial cells contain little or no glycogen (figs. 6, 25).

Cells of the bronchial glands are stained lightly with Sudan black (fig. 10) owing to their content of phospholipid but little glycide is evident. Intercellular digitations and canaliculi make the boundaries

of the cells stand out clearly after staining with the lipid dye.

Enzymic activity. The bronchial glands are the most reactive structures for succinic dehydrogenase in the opossum's lungs and in that respect easily surpass the bronchial epithelium (fig. 4). In contrast, bronchial glands and epithelium of man are almost equally reactive (Sorokin, '60). Within the opossum's glands this enzymic reaction of mitochondria is most intense in peripheral acini (fig. 9) where it is largely localized within the hydrotic cells. There the activity is nearly at the level present in parietal cells of the stomach (Padykula, '52) in cells of cardiac muscle, proximal and distal tubules of mammalian kidneys (Stenberg et al. '56) and other organs having intense oxidative metabolism. Succinic dehydrogenase is only moderately active in the ducts (fig. 9). In the opossum's parotid glands however the ducts are more reactive than the acini.

The bronchial and parotid glands exhibit the same distribution of activity for non-specific esterase as described for succinic dehydrogenase. In bronchial glands the enzyme is active in the acini (fig. 13) whereas in parotid glands it is mainly in the striated ducts (fig. 14).

After reaction for adenosine triphosphatase the acinar cells of the opossum's bronchial glands attract notice primarily for the darkening of their surface membranes. Fresh-frozen sections fixed in formal-calcium and subsequently incubated with ATP and dinitrophenol at pH 7.2 reveal the branching system of secretory capillaries and intercellular canaliculi (fig. 11). A fainter reaction within the cells may be attributed to mitochondria. Because the canaliculi are formed principally between hydrotic cells (*vide infra*) the chief locus of the enzyme is on the luminal surface of these cells. The basal surface is less active. Unfixed frozen sections incubated in ATP at pH 9.4 also reveal the canaliculi. At that pH however additional cytoplasmic activity within myoepithelial and hydrotic cells obscures the clarity of the surface-membrane localization (fig. 12). Alkaline phosphatase at pH 9.4 is confined to capillaries that encircle the acini. Acid phosphatase at pH 5 is visible in the glands as a cytoplasmic

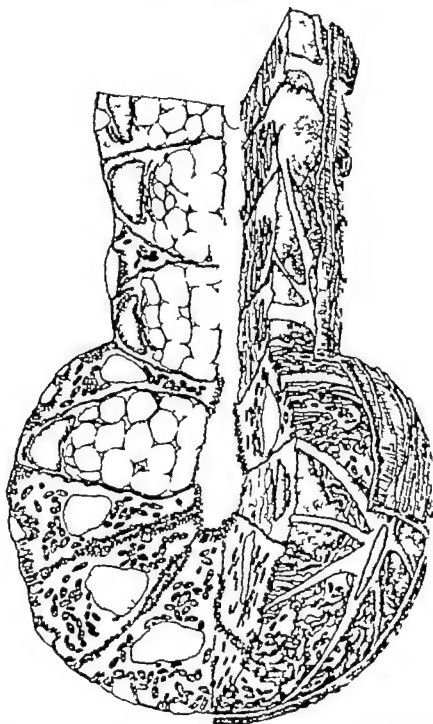


Fig. 1 A representation of an acinus and mucous duct in the bronchial gland of the opossum. On the left quadrant has been cut way to show section through the cells. Hydroptic cells have pical analiculi, basal grooves, and a cytoplasm rich in mitochondria. Mucous cells have apical secretory droplets. On the right, part of the basement membrane has been removed to expose the rugose basal surfaces of hydroptic cells and the microvilli.

section equal in intensity to that seen in the bronchial epithelium. A few granules per cell contain heavy lead deposits; they range in size from less than 1μ in diameter to somewhat more (fig. 8). Fainter cytoplasmic staining exhibits a reticular pattern and may be localized on intracytoplasmic membranes.

Electron microscopy

Within the acini all secretory cells are irregular in shape; such irregularity is more pronounced among hydrotic than mucous cells. For this reason it is difficult for one to obtain vertical sections that extend from free surface to base. Where both mucous and hydrotic cells are present in the same acinus the mucous cells appear to occupy the center and the non-mucous

the periphery. The latter rest on a wide base and taper toward the apex (figs. 6, 16) while the former are wide on top and narrow at the bottom (fig. 6). In the comparatively rare pure mucous acini the cells have wider bases. Along the ducts, mucous cells are more regularly prismatic (figs. 10, 28).

Hydrotic cell

1 *Topography* Surface features of the hydrotic cell are represented in a drawing based on electron micrographs (fig. 2). At the base, the cell is divided into a number of irregular compartments by criss-crossing grooves. Between them the compartments reach the basement lamina (fig. 15). Most of the grooves are filled with narrow (ca. 800 \AA) cytoplasmic leaflets that ex-

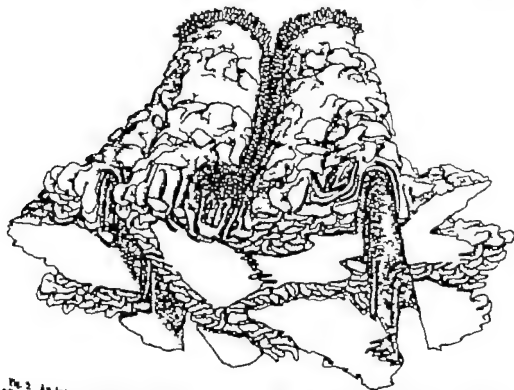


Fig. 2. An interpretation of the shape of hydrotic cells. The bottom and sides of two hydrotic cells are shown, as viewed from below. An overlying third cell has been removed. The basement lamina has been stripped off revealing the basal compartments. The two prominent grooves develop into processes from myoepithelial cell. Other grooves are less straight and are filled with thin cytoplasmic leaflets. Where the two cells meet some of these leaflets interdigitate. On the basal surface cytoplasmic flaps occur irregularly and from the apex an intercellular canaliculus extends down the interface between the cells and ends near the basal grooves. Microvilli occur along apical and canalicular surfaces. Beneath the microvilli, the canaliculus is isolated by continuous terminal bar and by desmosomes.

tend from the overlying cell (figs. 15 17 18). Others are occupied by tapering processes of myoepithelial cells (figs. 15 23). Larger processes extending from the base of one hydrotic cell may undermine a neighboring cell. At such points the cytoplasmic leaflets from the two cells interdigitate (fig. 17).

Vertical ridges of cytoplasm, areas with and without intercellular digitation and intercellular canaliculi are found at the sides of the hydrotic cell. The ridges give the cell a stellate shape when viewed from above. They are largest toward the base, where they are elongated to form the processes that extend under neighboring cells. At areas of interdigitation the adjacent cells are provided with cytoplasmic leaflets like those at the base. Some of these areas are continuous with the basal grooves. Desmosomes occur sporadically along the interfaces. Four or more canaliculi contact each cell. These canaliculi (figs. 15 18 19 21 22) range from 0.5 to 1.5 μ in diameter. They originate as intercellular channels near the basement membrane where they are in close relation to the grooves beneath the cells (fig. 18). They may also continue from short intracellular canaliculi. Each intercellular canaliculus drains two or three adjacent cells. Several of these channels come together to form a larger channel which leads to the lumen of the acinus (fig. 22). Microvilli extend into the canaliculi from the cells that form their walls (figs. 15 22). Terminal bar complexes (Palade and Farquhar '63) close off the potential space between cells (figs. 15 22) and isolate the canaliculi from the basal grooves.

The apex of the hydrotic cell is covered with short microvilli similar to those that line the canaliculi. The microvilli are though for the most part straight and simple, sometimes are clubbed and more rarely branched. They have a sparse coating of filaments, the *antennulae microvillares* (Yamada '35; Ito '65).

2. Internal organization. Within the hydrotic cell the central nucleus contains dispersed chromatin (figs. 8 15 16) and the cytoplasm is replete with mitochondria and glycogen. The mitochondria are short rods with considerably developed internal structure. The cristae are abundant angu-

lar and often branched (figs. 17 19, '66); the matrix contains granules. By far the greater part of the granular matter in the cytoplasm is glycogen (figs. 17 19 21). Such granules are larger than ribosomes and stain more heavily with lead (Revel '64). The ribosomes are not sufficiently numerous to provide appreciable cytoplasmic basophilia. A minority of them is attached to membranes of the endoplasmic reticulum which in this cell is only modestly developed (figs. 15 17). The apical surfaces. Multivesicular bodies are occurs as tubules and vesicles in the cytoplasm beneath the apical and canaliculi surfaces (figs. 15 20 21). The Golgi apparatus exists as several aggregations of lamellae and vesicles that measure about 1 μ across. Most frequently it is situated near the intercellular canaliculi (figs. 15, 20) or near the nucleus. Centrioles usually lie just deep to the apical or canaliculi surfaces. Multivesicular bodies are fairly numerous and have no preferred location. Such bodies are known to be reactive for acid phosphatase (Robbins et al. '64) and perhaps are related to the large eosinophilic residual bodies that abound in this cell and are its most reactive site for that enzyme (figs. 15 '60; cf. fig. 8).

3. Secretion. The microscopic appearance of the hydrotic cell supports the concept that it produces a watery secretion. The following observations from electron microscopy bear on the process of secretion. (1) The canaliculi surface frequently is marked by cavitations from the canaliculi lumen (fig. 19). Some of these appear to be continuous with the apical surface of the subjacent cytoplasm (fig. 21). (2) Numerous discrete small vesicles about 400-500 \AA in diameter are found in the lumens of the intercellular canaliculi (fig. 22). These vesicles exhibit a range of sizes similar to those in multivesicular bodies (fig. 20 inset) and neuronal synapses. The intracanaliculi vesicles increase in number toward the apical surface (cf. figs. 18 '60 21 22) as if they were being secreted or extruded progressively from base to apex. In the acinar lumen they become mixed with the electron-opaque mucus. (3) Within the hydrotic cells similar vesicles are seen near the Golgi apparatus in the cy-

plasm beneath the free surface and in the microvilli (figs. 20-22). They are not found near the cell base. (4) A flocculent material, more dispersed than in blood vessels (fig. 27) is present in the lumens of the canaliculi (figs. 19-21) and in the granular reticulum beneath the free surface (fig. 20). (5) Neither flocculent material nor the small 400-500 Å vesicles are present in the grooves beneath the cell (fig. 18). Micropinocytotic vesicles (diameter 600-800 Å) are infrequently seen at the base and are absent from apical and subcellular surfaces.

Following administration of *pilocarpine* glycogen disappears from hydrotic cells, but mucous cells retain much of their secretion (fig. 5). In electron micrographs the fine structure of the cells is so distorted as to resemble poor fixation. The mitochondria and endoplasmic reticulum are greatly swollen, and the microvilli fill the canaliculi. In some specimens from untreated animals, hydrotic cells present a less extremely swollen appearance (fig. 16) possibly having been fixed while actively secreting (Lehninger '84; Sedar and Friedman, '81). The saliva collected from the treated opossum comes from various sources: the major and minor salivary glands and the bronchial glands. It is isotonic with respect to serum and contains $\text{Na} = 73 \text{ mEq/l}$; $\text{K} = 9.3 \text{ mEq/l}$, $\text{Na/K ratio} = 7.8$.

Mucous cell

1. *Topography* In comparison with the hydrotic cell, the mucous cell has a less ridgy topography. Its base is fairly smooth and its lateral walls trace a gently undulating contour as they flanch to meet the upper surface. The apex is broad and domed. Its microvilli are short and thick set. Interdigitations of adjacent mucous cells, or of mucous and hydrotic cells, are simpler than those of adjacent hydrotic cells (fig. 1). Desmosomes are abundant along the sides. At the apex both like and unlike cells are joined by terminal overlap but extensions from one cell may intercellular canaliculi are not found between mucous cells. They may occur however between mucous and hydrotic cells.

2. *Internal organization* The mucous cell of the bronchial gland resembles other mucous cells of mammals. Nuclear chromatin is more condensed than in the hydrotic cell (figs. 23-28). The basal cytoplasm contains most of the granular endoplasmic reticulum free ribosomes and mitochondria. The supranuclear region is occupied principally by the Golgi apparatus. Its lamellae surround individual mucous droplets (figs. 23-28). Larger droplets in the apex are separated by strands of cytoplasm in which the paired centrioles may be found. Multivesicular and residual bodies are distributed throughout the cytoplasm but are less abundant than in the hydrotic cell. In sum, the mucous cells of acini and ducts are richer than hydrotic cells in granular endoplasmic reticulum and secretory matter but poorer in mitochondria and glycogen.

Myoepithelial cell

1. *Topography* The stellate myoepithelial cell encircles the other acinar cells. It lies just inside the basement lamina. There it is related principally to the hydrotic cells, as the latter occupy more of the acinar base than mucous cells. From the myoepithelial cell body numerous slender cytoplasmic processes fan out upon the basement lamina (figs. 1-12) and may branch near their termination. Cross sections of these ovoid processes can be seen every few microns along the perimeter of an acinus (fig. 15). They may be less than 0.5μ in diameter and are finer than the myoepithelial processes in sweat glands of the monkey (Terzakis, '84). The myoepithelial cell interlocks with adjacent cells by means of a few small cytoplasmic projections. These are most numerous around the cell body (fig. 16) and at the ends of the processes. Desmosomes occur at various points (fig. 23 inset, fig. 23) and condensations of electron-opaque material lie adjacent to large areas of the basal plasma membrane.

2. *Internal organization* The myoepithelial cell resembles smooth muscle in the appearance of the myofilaments, the presence of electron-opaque areas in the cytoplasm (fig. 25) and in the disposition of the organelles. In electron micrographs the chromatin in its sausage-shaped nu-

cleus is nearly as condensed as in the mucous cell (figs. 16, 23). The myofibrils run in the long axis of the cell. Along the processes they again run lengthwise and at the angles of junction between process and cell body the filaments change direction abruptly (fig. 25). The organelles include multivesicular bodies in their number and are stowed in what space remains beside the nucleus and along the processes. Micropinocytotic vesicles and a few alveolate vesicles containing a fuzzy lining occur at cell surfaces.

Non secretory cell of the duct

In the larger ducts of the bronchial glands the epithelial layer is one or two cells thick. The surface cell is roughly cuboidal; the lower cell is elongated. The nucleus occupies much of the cell. In the cytoplasm few organelles are present to obscure the filamentous cytoskeleton (fig. 29). The apical surface is smooth except for very few microvilli. Notably absent is any evidence of basal compartmentation and mitochondrial stratification as is seen in the epithelium of the striated ducts of salivary glands (Scott and Pease '59, Parks '61) whose cells are considered to take part in the secretory process (Parks, '62).

Connective tissue capillaries and nerves

Near the acini of the bronchial glands the collagenous connective tissue contains few large bundles. The acini are held in a matrix of tiny fibrils permeated by fine reticular fibers recognizable by their cross-banding, and equally fine elastic fibers, recognizable by their electron-permeability (figs. 16-27). Against the acini the matrix material appears condensed into a basement lamina some 300 Å in thickness and a similar condensation of material occurs around capillaries (fig. 27).

The capillaries closest to the acini belong to the fenestrated type that is characteristic of many viscera (Fawcett '63). In the endothelial cell illustrated (fig. 27) the Golgi apparatus is conspicuously developed. More generally these cells are noteworthy for the demarcation of the cytoplasm into thick and thin areas. The thicker areas contain organelles and serve

as points for junction of adjacent cells. Many micropinocytotic vesicles are present, on upper and lower surfaces. The thin areas are about 300 Å thick and are laterally fenestrated as in renal glomeruli and peritubular capillaries (Pease '53). The pores have only a thin membrane across them. From the pores the minimum distance to the base of the gland is less than 1 μ. Like pial cells in the choroid plexus (Maxwell and Pease '56) pericytes interpose cytoplasmic extensions between capillaries and the base of the gland. The extensions frequently remain clear of the fenestrated areas (fig. 27). In sections where no capillaries are encountered, the acini appear encapsulated by a single layer formed by thin processes from connective tissue cells.

Between capillaries and acini unmyelinated nerves penetrate the delicate connective tissue sheath and course through the periacinar matrix. The neuronal processes contain mitochondria and vesicles measuring 300-500 Å and near the glandular base lose their Schwann cell envelope (fig. 24). The intraneuronal vesicles have electron permeable centers; according to Richardson ('64) they may be considered the linergic. No process bearing mitochondria and synaptic vesicles has been seen on the epithelial side of the basement lamina, although processes with similar diameters have been found in grooves between acinar cells.

DISCUSSION

Functional organization of the bronchial glands. By morphological criteria, the acini and smaller ducts of the opossum bronchial glands comprise its secretory region. In this region the hydrotic cells for the most part lie peripheral to the mucous cells. Such an arrangement is also found in glands of the eustachian tube in mice (Ludman and Mitchell, '55) and portions of the sublingual glands of cats and dogs (Shackelford and Klapper '62) but is not typical of the major salivary glands. In the bronchial glands the secretory acini and not the ducts are the sites most reactive for succinic dehydrogenase and nonspecific esterase. This is also true of the avian salt glands (Elli et al '63) and human eccrine sweat glands (Montagna and Far

mann, '55; Montagna, '55) despite notable activity for succinic dehydrogenase present in the excretory ducts of the sweat glands. Such a histochemical pattern contrasts with that typical of salivary glands where succinic dehydrogenase is more active in the ducts than in the acini. firmly established for salivary glands of rodents (Padykula, '52; Nachlas et al. '57; Dewey '58) the histochemical localization of succinoxidase activity is similar in the parotid gland of the opossum and the salivary glands of other animals, even if secretory acini differ in reactivity among the different glands and species (Arvy '61). In the opossum a parotid gland and in the principal submaxillary glands of the vampire bat (DiSanto '60) non-specific esterase, like succinic dehydrogenase is active principally in the ducts. Where the ducts of exocrine glands exhibit greater enzymic activity they appear to be more involved in the secretory process as in the salivary ducts (Parks, '62) and possibly in the sweat ducts (Lloyd, '57). Judged by their variable length, their histochemical behavior and the unspecialized appearance of their lining, the larger ducts of the bronchial glands appear to function chiefly as conduits.

Classification of the secretory cells Of the numerous small exocrine glands found along the internal passages of mammals, few receive more than passing attention. Like the cells of the more prominent salivary glands (Bensley '08; Stormont, '32; Bence, '47; Leblond, '50; Junqueira et al. '51; Wimsatt, '56; DiSanto '60; Shackelford and Klapper '62; Quintarelli, '63; Shackelford, '63; Munger '64) secretory cells in the acini of these little glands exhibit considerable variation within and among species (cf. Goco et al., '63); but the modifiers used to describe them rarely exceed serous and mucous. In the literature on salivary glands the inadequacy of this terminology has been pointed out repeatedly and terms like "apocrine", "sero-mucoid", "pseudo-serous", and "pseudomucous" have been coined to characterize the salivary cells more accurately. The same terminological deficiency arises in describing the small exocrine glands. Much of the trouble stems from the association of specific cytological

properties with the terms serous and mucous. A pure serous cell (Leblond, '50) or a serozytogenic cell (Stormont, '32) is typified by a pancreatic zymogen cell or a gastric chief cell. A mucous cell is typified by an intestinal goblet. In practice the term serous has been applied widely and uncritically to any non mucous secretory cell in such a gland. Some of these scarcely resemble pancreatic zymogen cells. The hydrotic cells of the bronchial glands, for example, lack the cytoplasmic basophilia and secretory granules that they would possess if they were pure serous cells. Hydrotic cells, moreover do not contain extensive ordered, lamellae of granular endoplasmic reticulum as do zymogen cells (Palade et al., '61). The sparsity of ergastoplasm indicates that the product of these cells is not predominantly proteinaceous. The shape of the hydrotic cell is complex to provide extensive absorptive and secretory surfaces within a compact form, and to permit close contact with the contained organelles. Mitochondria with high succinoxidase activity and agranular membranes of the cytoplasm are the most prominent of these organelles. Glycogen is abundant in the matrix. Such features are characteristic of cells that work against elevated concentration gradients and appear in both water-secreting and ion-secreting elements. Familiar examples of such modified mammalian cells are found in the salivary glands (Scott and Pease '59; Parks, '61; Tandler '62; Kurtz '64; Shackelford and Schneyer '64) the sweat glands (Hibbs, '58; Munger '61; Munger and Brustlow '61; Ellis, '62; Terzakis '64) the renal tubules (Pease '55b; Clark, '57; Rhodin, '58) the choroid plexus (Maxwell and Pease '58) the ciliary body (Pease '58; Torrey '63; '64) and the stomach (Sedar and Friedman, '61; Sedar '64; Ito '61; Ito and Winchester '63). Examples from other classes are found in the salt-secreting glands of birds (Schmidt Nielsen '60; Doyle '60; Fawcett, '62; Kornick, '63) and marine turtles (Ellis and Abel, '64) the inner ear of lizards (Hamilton '65) the tubules of reptilian (Anderson, '60) and amphibian kidneys (Christensen, '64) the stomach of amphibians (Sedar '61) gills of teleosts (Copeland and Dalton, '59; Kessel and Brame, '60).

- Sorokin, S. P. 1960 Histochemical events in developing human lung. *Acta Anat.*, 40 105-119.
- 1962 A note on the histochemistry of the opossum's lung. *Acta Anat.*, 50 13-21.
- Sternberg, W. H., E. Farber and C. E. Dunlap 1956 Histochemical localization of specific oxidative enzymes II. Localization of diphosphopyridine nucleotide and triphosphopyridine nucleotide diaphorases and the succinate dehydrogenase system in the kidney. *J. Histochem. Cytochem.*, 4 266-283.
- Stormont, D. L. 1933 The salivary glands. In: *Special Cytology* Ed. E. V. Cowdry Paul B. Hoeber New York, 1 153-194.
- Tandler B. 1962 Ultrastructure of the human submaxillary gland. I. Architecture and histological relationships of the secretory cells. *Am. J. Anat.*, 111 237-307.
- Ternakis J. A. 1964 The ultrastructure of monkey eccrine sweat glands. *Z. Zellforsch. mikroskop. Anat.*, 64 493-509.
- Turney J. M. D. 1963 Fine structure of the ciliary epithelium of the rabbit with particular reference to "infolded membranes," "vesicles," and the effects of Dexam. *J. Cell Biol.*, 17 641-659.
- 1964 Differences in membrane organization between osmium tetroxide-fixed and glutaraldehyde-fixed ciliary epithelium. *J. Cell Biol.*, 23 655-664.
- Tsabo, L., and F. W. Brandt 1962 An electron microscopic study of the Malpighian tubules of the grasshopper *Dissosteira carolina*. *J. Construct. Res.*, 6 28-33.
- Van Breemen, V. L., and C. D. Clemente 1951 Silver deposition in the central nervous system and the hematoencephalic barrier studied with the electron microscope. *J. Biophys. Biochem. Cytol.*, 1 181-186.
- Wetzel J. S. and Hellmann, K. 1960 The sweat glands. *Biol. Revs.*, 35 141-186.
- Whimsatt, W. A. 1956 Histological and histochemical observations on the parotid, sublingual and sublingual glands of the tropical American fruit bat, *Artibeus fuscus* Leach. *J. Morph.*, 99 189-210.
- Yamada, E. 1953 The fine structure of the pil bladder of the mouse. *J. Biophys. Biochem. Cytol.*, 1 445-458.
- Yamamoto, T. 1965 Some observations on the fine structure of the intrapapillary duct passages in goldfish (*Carassius auratus*). *Z. Zellforsch. mikroskop. Anat.*, 63 219-230.

PLATE I

EXPLANATION OF FIGURES

- 1 A thick section (40 μ) indicating the general topography of bronchial gland. The bronchial lumen is above the adventitia below Richardson's silver method. 180 \times
- 2 A low-power view of bronchiole with surrounding bronchial glands. The acini are shown in black. Succinic dehydrogenase, Nitro-blue tetrazolium, pH 7.6 20 min. at 37°C. 25 \times
- 3 A cluster of acini and mucous ducts 20 minutes after administration of pilocarpine. Glycogen is absent from the acini. The dark staining is due to mucus in acinar and duct cells. PAS on frozen section, one hour. 250 \times
- 4 An acinus of the bronchial gland, stained by the PAS method. Mucous droplets in the mucous cell are brilliantly stained (black and gray) is glycogen in the ductal cells. The myoepithelial cell does not stain. PAS on frozen section, lightly counterstained with toluidine blue. 1,900 \times

An frozen section showing acini clustering about the mucous ducts (da k). From the periphery of the duct three orders of branching be deduced. Toluidine blue. 300 \times

OWEN'S BRONCHIAL GLANDS

Lesl. Parnassus, Secotia

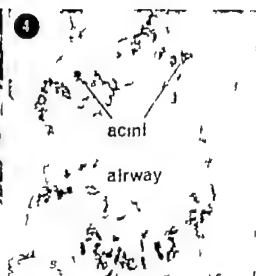
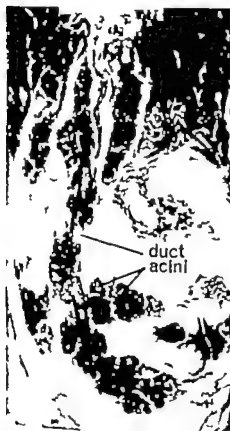
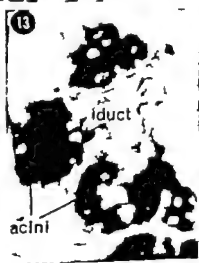


PLATE 2

EXPLANATION OF FIGURES

- 8 Acid phosphatase in glandular cells. The main reaction occurs in large cytoplasmic granules (dark) identified as residual bodies. Fainter staining has a reticular pattern in the cytoplasm. Gomori method. Glycerophosphate, pH 5, one hour at 37°C. 1100 X
- 9 Succinic dehydrogenase in the bronchial gland. The acini are more reactive than the ducts. Nitro-blue tetrazolium pH 7.8, 20 minutes at 37°C. 120 X
- 10 Staining with Sudan black reveals the boundaries of the mucous cells. Staining is similar in acetone-extracted controls. 250 X
- 11 Adenosine triphosphatase at pH 7.2 is especially active at the luminal surfaces of acinar cells. The reaction demonstrates the branching system of secretory capillaries and intercellular canaliculi. Adenosine triphosphate, one hour at 37°C. 800 X
- 12 Adenosine triphosphatase at pH 9.4 is more diffusely reactive in the cytoplasm of acinar cells than at pH 7.2. The processes from myo-epithelial cells are shown. Adenosine triphosphate 30 minutes at 37°C. 520 X
- 13 Non-specific esterase in bronchial glands is more reactive in acini than in ducts. *p*-naphthyl acetate, six minutes at 20°C. 400 X
- 14 In the parotid gland, esterase is more reactive in striated ducts than in acini. *p*-naphthyl acetate six minutes at 20°C. 400 X



myoep

acini

duct

duct

acinus

PLATE 3

EXPLANATION OF FIGURE

- 15 A section through part of an acinus. Portion of several hydrotic cell and two myoepithelial cell processes are shown. A basement lamina courses up the right side of the figure. In the hydrotic cells basal cytoplasmic leaflets, lateral interdigitations and intercellular canaliculi and internal organelles are shown. Mitochondria and glycogen are widely scattered throughout the cytoplasm, as are multivesicular and residual (black) bodies. The granular endoplasmic reticulum is not well developed. The agranular reticulum and Golgi apparatus tend to occur near the luminal surface (top of figure). The myoepithelial cell processes are obliquely sectioned. They rest on the basement lamina. In them, organelles myofilaments and, basally some pinocytotic vesicles can be seen. 17,000 \times

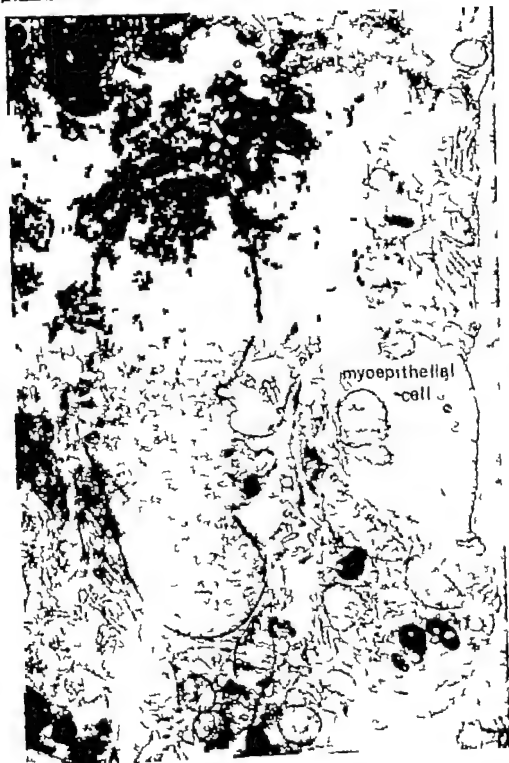


PLATE 4

EXPLANATION OF FIGURES

- 16 Parts of several hydrotic cells and the body of a myoepithelial cell are included in this section of an acinus. It permits an extended view of the alveolus, which is filled with microvilli. One of the hydrotic cells has swollen mitochondria and endoplasmic reticulum. Near its base it interdigitates with the myoepithelial cell (arrows). 8700 \times
- 17 A detailed view of digitations between two hydrotic cells, one dark and the other light. In the cytoplasm the coarser granulation is due to glycogen; the finer to ribosomes. 23400 \times
- 18 A detail from the base of a hydrotic cell. A ductule comes into close apposition with the basal groove. The cytoplasmic leaflets that occupy the groove are less than 0.1 μ wide and may branch. Beneath them lies the basement lamina. 23400 \times

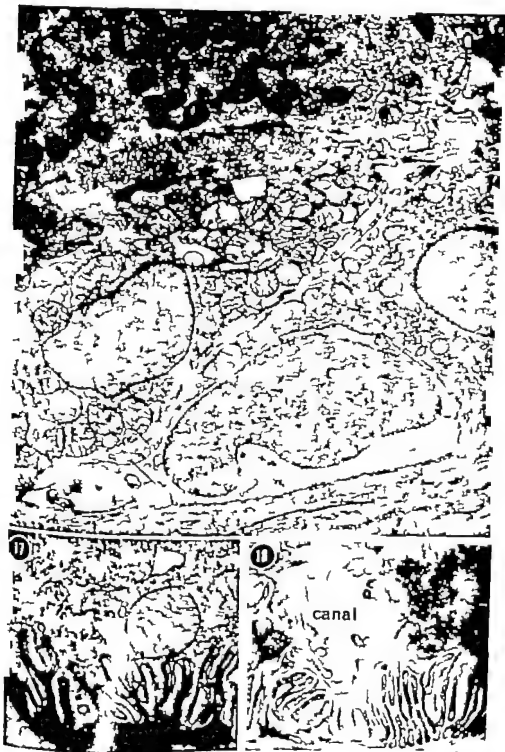


PLATE 5

EXPLANATION OF FIGURES

These figures present morphological evidence of secretion by hydrotic cells. They illustrate intercellular canaliculi and subjacent cytoplasm.

- 19 From this hydrotic cell a cavitation of the surface membrane opens into an intercellular canaliculus. The lumen contains thinly dispersed flocculent material. 27,600 X
- 20 Detail of a cell illustrated in figure 15 showing the subcanalicular cytoplasm. It contains many tubules and vesicles of granular endoplasmic reticulum, among other organelles. Smaller vesicles (400-500 Å) are also present near the Golgi apparatus (1) and in the cytoplasm immediately beneath the canaliculus (2). A few of such vesicles are found between microvilli in the lumen. The large black bodies are lysosomal residual bodies. *Inset* Small vesicles like those above (1, 2) surround multivesicular body which borders another canaliculus. 29,000 X
- 21 An extension from the canalicular lumen into a hydrotic cell. It is interpreted as point of junction between the canaliculus and the cell granular reticulum. 30,000 X
- 22 A grazing section of a canaliculus near its junction with the acinar lumen (right). Some of the microvilli that border the canaliculus are blebbed. The small (400-500 Å) vesicles (cf fig 20) are present in the subjacent cytoplasm in the microvilli (3) and in the lumen (4). The tight junctions and an underlying desmosome (lower left) are prominent. 23,600 X

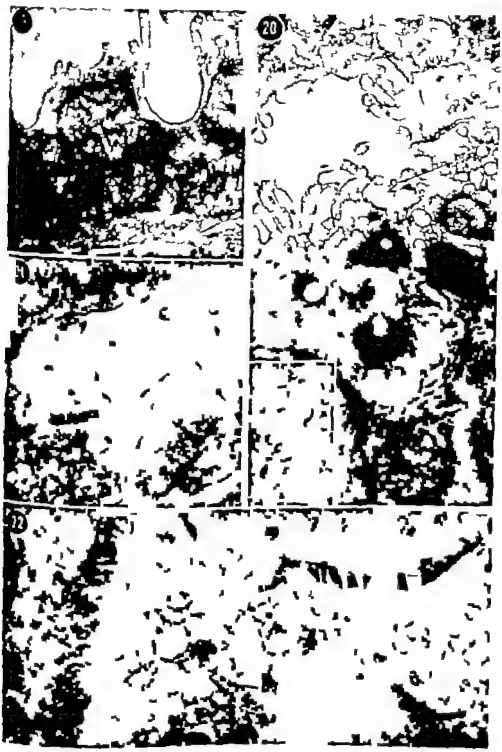


PLATE 6

EXPLANATION OF FIGURES

- 23 A section through an acinus showing some features of the basal surface. A basal groove of hydrotic cell 1 filled with cytoplasmic projection and follows a wavy course (dotted line). A myoepithelial cell process crosses the basal groove and terminates at the base of the figure. Desmosome (arrow); mucous cell (upper right) 11,000 X
1 A desmosome between myoepithelium (above) and hydrotic cell (below) 40,000 X
- 24 Beneath the body of a myoepithelial cell (upper right) neuronal processes are incompletely enveloped by Schwann cell. Intranuclear vesicles are electron-permeable 21,000 X
- 25 Detail of a myoepithelial cell at the junction of several stellate processes. The myofibrils run in several directions. Patches of electron-opaque material occur in the cytoplasm (top center) 17,000 X
- 26 Two swollen mitochondria from figure 10 exhibit branched and angled cristae. The matrix contains small granules. 70,000 X.

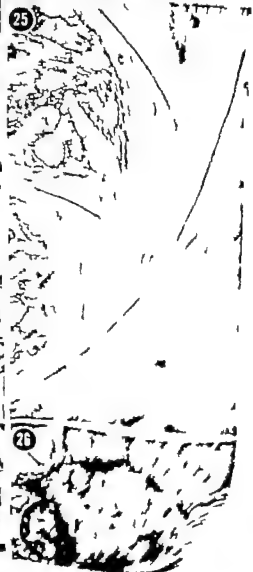
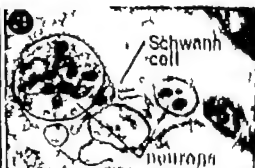


PLATE 7

EXPLANATION OF FIGURES

- 27 A capillary between two acini of the bronchial glands. Fenestrations of the endothelial wall are indicated in part (arrows). The basement lamina of the endothelial cell splits to invest the pericyte. Small nerve processes (lower right) occur in the connective tissue. 13,500 X
- 28 A mucous cell from a small duct of the bronchial gland. Toward the base it touches myoepithelial cell body. Mucus appears as gray material in the lumen of the duct. 8,860 X
- 29 An epithelial cell from a non-secretory duct. Its cytoplasm contains few organelles. 10,100 X



PLATE 7

EXPLANATION OF FIGURES

- 27 A capillary between two acini of the bronchial glands. Fenestrations of the endothelial wall are indicated in part (arrows). The basement lamina of the endothelial cell splits to invest the pericyte. Small nerve processes (lower right) occur in the connective tissue. 13,500 X.
- 28 A mucous cell from a small duct of the bronchial gland. Toward the base it touches a myoepithelial cell body. Mucus appears as a gray material in the lumen of the duct. 6,860 X.
- 29 An epithelial cell from non-secretory duct. Its cytoplasm contains few organelles. 10,100 X.

TABLE 1

Biochemistry of the chromophilic cell types of the anterior pituitary gland of the pine squirrel

Biochemical test	Basophils		Acidophils	Remarks
	Gonadotrophs	Thyrotrophs		
Pink acid-Schiff reaction (PAS)	+++	+	—	Glycogen absent
Dastex (PAS)	+++	+	—	
Acetylation PAS	—	—	—	Reaction due to 1,2-glycol groups
Deacetylation PAS	+++	+	—	
745 without acidification in periodic acid	—	—	—	Free aldehyde groups absent
Re-sulfonated-chloroform PAS	+++	+	—	PAS reaction not due to lipids
McKenzie blue extraction (pH 2.65-7.65)	pH 5-6	pH 5-6	pH 5-6	Mucoproteins, glycoproteins or simple basic proteins present
1% Aqueous toluidine blue for metachromasy	—	—	—	Acid mucopolysaccharides absent
Delayed iron	—	—	—	
Stain blue	—	—	—	
Ironless orange UV	—	—	—	
Barney-hampered blue	—	—	+++	Proteins present
Fast green (pH 1.3)	±	±	++	
Kline reaction	—	—	+	Tyrosine present
Acid ferricyanide method	—	—	—	SH groups absent
Iohaloe acid — Alcian blue	++	—	—	SS groups present
Alcian fast green (pH 8.1)	+	+	+	Only the nuclei are stained demonstrating proteins with basic amino acids
Acid anilindine fast green	+	+	+	Lysine absent
Acidyl green — pyronin G staining	pink	pink	pink	Small amounts of RNA present
Elison acidyl green — pyronin G staining	—	—	—	
Acid B	purple	purple	purple	
Elison extra B	—	—	—	
Sudan black B (room temperature)	+	+	+	Lipids present in the form of lipoprotein complexes
Sudan black B (60°C)	+	+	+	
Oil treatment Sudan black B	+++	+++	+++	
Acid haematein	±	±	+++	Phospholipids present
Pyridine extraction acid haematein	—	—	—	
Carbazole chromation Sudan black B	++	++	++	Coloration mainly in the Golgi apparatus
Forster's "Mordant-staining" method	—	—	—	Acidic lipids absent
Kle blue	—	—	—	Neutral lipids absent
Sudan III and IV	—	—	—	
Forster's test	—	—	—	Fatty acids absent
Periodic acid — Schiff reaction	—	—	—	Lipids containing unsaturated bonds absent
Conant's calcium-cobalt method for alkaline phosphatase	+	+	+	Alkaline phosphatase present primarily in nuclei with traces in the cytoplasm

Biochemical tests performed here are according to PERCIVAL, '80, except the ones marked 2, 3, and 4.
 1. Barney and Lachmanberger, '80. — No reaction
 2. For and Elison, '80. + Weak reaction.
 3. For, '80. ++ Strong reaction.
 4. For, '80. ++ Medium reaction.

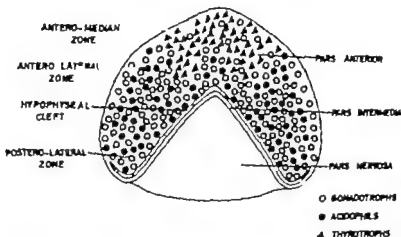


Fig. 1 Semidiagrammatic sketch of section of the pituitary gland showing the regional distribution of gonadotrophs thyrotrophs and acidophils.

the two sexes they do not show any change either during different stages of the reproductive cycle or after gonadectomy. However granulation and staining intensity of these cells is markedly altered by thyroidectomy. On the basis of these criteria it is inferred that these large lightly stained basophils secrete thyrotrophin and they will be referred to as thyrotrophs. They correspond to the thyrotrophs of Purves and Griebach (51a,b). Changes in the basophils following gonadectomy and thyroidectomy will be described in another paper.

The thyrotrophs are usually stained dark purple by AF but not consistently. These cells can be distinguished from gonadotrophs by the use of PFAAB/PAS/OG following which the gonadotrophs are stained purple and thyrotrophs pink. PAS-positive material of the gonadotrophs is resistant to performic acid as by the omission of alcian blue alone from PFAAB/PAS procedure gonadotrophs are stained magenta.

Fluorimetric differentiation between FSH and LH secreting gonadotrophs in the squirrel pituitary is not possible by PAS/methyl blue staining. Methyl blue stains all PAS-positive cells purple but after differentiation and dehydration, the original magenta or pink color is restored. However the two gonadotroph types are distinguished by the differential protein solubility procedures. Immersion of the pituitary gland in 2.5% TCA for 24 hours prior to fixation precipitates only a part of

the PAS-positive material. In PAS/OG stained sections there is a decrease in the number of PAS-positive cells. The dark basophils of the unextracted pituitary are represented by large hollow spheres in the extracted gland. The cells retaining PAS stain are round, feebly stained and are more numerous towards the posterior region of the pars anterior. In shape and distribution they resemble the gonadotrophs of the unextracted pituitary. PAS-positive material is completely extracted from all basophils of the pituitary glands immersed in 0.5% TCA and aqueous phosphate buffer at pH 7.8.

The acidophils occur in clusters of 3-8 or more cells (figs. 7 and 8) and are mainly aggregated in the medullary part of the lateral halves of pars anterior and toward the border facing the pars intermedia (fig. 1). Their nuclei are small, rounded and centrally placed. A small Golgi zone is present in the vicinity of the nucleus. No distinction could be made between the acidophil and basophil cells on the basis of localization of the Golgi zone, as in both types it is mostly juxta-nuclear (fig. 9). The amount of cytoplasm in the acidophils is less than that in the basophils. In sexually mature males and non-pregnant, non-lactating females, only one type of acidophil cell is prominent. The dense and coarsely granulated cytoplasm of these cells is stained red after MTS and orange after Crossman's stain and PAS/OG. These cells which are also present in the pituitary

of juvenile animals, do not fluctuate either in number or in amount of granulation in mature animals and in females during pregnancy and lactation. On the basis of these observations it is inferred that they are somatotrophin (STH) secreting cells and they are referred to as orangeophils.

The cells of the second acidophil type are seen primarily in pregnant and lactating female squirrels. They are present in small numbers in sexually mature females and are poorly represented in the male pituitary gland. These cells are interspersed with orangeophils but outnumber the latter in the peripheral and anterior regions of the acidophil zone. They appear dark brown or dull orange after MTS and are purple after Crossmon's triple stain. In PAS/OG preparations they are indistinguishable from orangeophils as both are stained orange. These purple cells are larger than the orangeophils and contain coarse granulation and hypertrophied Golgi zone. As they are poorly represented in males, in perous non-pregnant and non-lactating females, and are prominent during pregnancy and lactation, they are possibly concerned with the elaboration of prolactin or luteotrophic hormone (LTH). In the present study they are termed carminophils as suggested by Dawson and Friedgood ('38).

The acidophil cell granules are not extracted by 2.5% TCA or by phosphate buffer at pH 7.5. Protein precipitation is observed only in the carminophils, after treatment with 0.5% TCA.

In some sections, basophil cells are seen completely enclosing the acidophils or vice versa (figs. 10 and 11) a phenomenon described as cupping by Purves and Griesbach ('37).

The chromophobes possess a small, round nucleus and are conspicuous by the absence of cytoplasmic granulation. They occupy the interior of the interstitial spaces and are dispersed among the chromophil cell types.

Changes in pituitary cytology during pregnancy and lactation

The gonadotrophs which increase in size and number during early pregnancy remain relatively unchanged in the later stages of pregnancy. These are stained in-

tensely with PAS and show hypertrophied Golgi zones (fig. 13). The cytoplasmic granulation is coarse. During lactation there is a marked decrease in the number of gonadotrophs and they are small with conspicuous Golgi apparatus and coarse and sparsely granulated cytoplasm (fig. 12).

The acidophils increase in number during pregnancy primarily due to the increase in number of carminophil cells. These cells are predominant in the pituitary glands of females in late pregnancy and continue to increase in number during lactation. They are coarsely granulated and possess hypertrophied Golgi apparatuses. Partially degranulated cells are also frequently seen. As no mitoses were observed in the pars anterior the increase in carminophil cell number appears to be due to the granulation of chromophobes and degranulated acidophils.

HISTOCHEMICAL OBSERVATIONS

The various histochemical reactions listed in table 1 show the presence of mucopolysaccharides in the basophil cells. The gonadotrophs in addition possess moderate amounts of cystine groups. A weak RNAase labile basophilia is observed in the cytoplasm. Lipids are present in the form of lipoprotein complexes, as they are detected only after the use of unmasking reagents. Phospholipids are absent, and the few small granules scattered in the cytoplasm may represent mitochondria (fig. 8). Alkaline phosphatase is present primarily in the nuclei.

The acidophil cells lack carbohydrate material. These cells are selectively stained bright blue by the mercury-bromophenol blue reaction (fig. 7). Though the specificity of this method as a histochemical test for proteins has been questioned by Baker ('58) its selective staining of the acidophils in the pituitary gland of the squirrel is very clear. In addition to proteins, traces of tyrosine are also present. These cells are rich in phospholipids (fig. 8) which are removed by pyridine extraction. Traces of RNAase labile basophilia are also present.

Pars intermedia

The cells of the pars intermedia arranged in 3 to 4 layers are uniformly oval

TABLE 3
Comparison of leucocyte cell types in the pituitary glands of squirrel, rat and hamster

Cell type and characteristics	Female (<i>Peromyscus maniculatus</i>)	White rat	Golden hamster (<i>Mesocricetus auratus</i>)
Gonadotrophs			
Shape	Round to oval with eccentrically placed nucleus	Round to oval	Round to oval
Granulation	Coarse	Coarse	
Location and orientation	Randomly distributed in the postero-medial and lateral halves of the pars anterior and occupy the sinusoidal borders	Occupy the lateral halves surrounding large portal vessels	Peripheral
Number in the two sexes	More in male than in female	More in male than in female	Main type in both sexes; fewer in females
Staining reaction			
PAS	Positive (light to intense reaction)	Positive (dark staining)	Positive (intense reaction)
AF	Negative	Neg. tve	Positive
PAS/MS	No distinction between FSH and LH gonadotrophs	Theoretical differentiation into Red and Purple gonadotrophs (Remmel, '67) FSH gonadotrophs stain purple and LH gonadotrophs stain red (Hildebrand et al., '67 and Hildebrand et al., '61)	—
PFAAB/PAS	Purple	Light blue	Light blue
Antihue blue (MTS)	Dark blue	—	—
Gonadotrophs			
Early	Increase in size, number and granulation	Increase in number size, and glycoprotein content	Increase in size and number
Late	Degranulated cells with hyper-trophied Golgi apparatus. Typical "maturation" of secretory cells seen (Hildebrand)	—	—

and are oriented with their long axes perpendicular to the basement membrane. With MTS and PAS/OG only a part of the cell population is stained with aniline blue and PAS respectively while the rest of the cells are unstained. Possibly these represent two different phases in the secretory activity of the same cell type. Sudanophilic material is seen in the cell cytoplasm. Phospholipids are absent. A weak basophilia is noted after methyl green-pyrimin staining. The Golgi apparatus is small and consists of argentophilic rods and granules. It is seen in the vicinity of the nucleus placed generally towards its anterior pole.

DISCUSSION

In the anterior pituitary gland of the palm squirrel as in the rat (Halmi, '50 and '51 and Purves and Griesbach '51a) golden hamster (Serber '58) non-parous female rabbit (Allanson Foster and Menzies, '59) and mouse (Ortman '56 Barnes '62) two types of basophils are recognized following MTS PAS AF and PFAAB/PAS/OG techniques. In the squirrel round or ovoid coarsely granulated and darkly stained cells the gonadotrophs occupy the lateral and postero-medial regions of the pars anterior. These are PAS-positive and AF-negative. The thyrotrophs which are localized in the anteromedian zone of the pars anterior are large rounded or polyhedral and finely granulated. They are AF positive and resemble the condition in the rat (Halmi, '50) which is the reverse of that seen in the golden hamster (Serber '58) where the gonadotrophs are AF-positive and thyrotrophs are AF-negative (table 2).

PFAAB/PAS/OG staining has been used to distinguish between the different basophilic cell types (Pearse, '60). In the pituitary gland of the squirrel the gonadotrophs are stained purple and the thyrotrophs pink by this technique. In contrast to the observations of Adams ('57) and Adams and Pearse ('59) the glyco or mucoproteins of gonadotrophs of the pituitary gland of the squirrel are resistant to performic acid.

Rennels ('57) differentiated tinctorially the red and purple gonadotrophs in the anterior pituitary of the rat by the use of PAS/methyl blue. Hildebrand Rennels and Finerty ('67) and Hellbaum, McArthur

Campbell and Finerty ('61) using PAS/methyl blue described FSH cells as purple staining and LH gonadotrophs as red staining cells. Rennels ('63) in disagreeing with the observations of Purves and Giesbach ('51a) suggested that the PAS-purple, centrally located gonadotrophs are FSH secreting cells and that the PAS-red, peripherally located gonadotrophs are the LH cells. Such tinctorial differentiation of the gonadotrophs was not obtained in the pituitary gland of the squirrel.

Orangeophils in the pituitary gland of the squirrel are presumed to be responsible for the elaboration of STH and the carminophils are considered to be prolactin or lactotrophic or LTH cells. This resembles the condition in the cat and rabbit (Dawson and Friedgood, '38) dog (Hartmann, Fain and Wolfe, '46 and Purves and Griesbach '57) monkey (Dawson, '48) bat (Herliant '58) and wallaby (Ortman and Griesbach, '58). However in man (Folander '49) and the rat (Sanders and Rennels '59) prolactin secretion is assigned to the orangeophils and somatotrophs secretion to the carminophils. Electron microscopic studies of Farquhar and Rinehart ('54) on the rat and those of Barnes ('62) on the mouse also point to a similar distinction between the two acidophilic cell types.

In the pituitary gland of the squirrel the orangeophils and carminophils are also distinguishable on the basis of differential protein solubility properties. Proteins of only the carminophils are precipitated by 0.5% TCA. Our results, based only on histochemical observations, are in agreement with those of Barnett, Roth and Salzer ('61) who by histochemical observations and bioassay procedures confirmed the luteotrophic potency of the cells precipitable by 0.5% TCA treatment, and considered them to be the LTH producing cells. The acidophils in the squirrel hypophysis are rich in phospholipids and proteins and contain traces of RNA.

Elftman ('55 '56 '57 and '58) studied the pituitary gland of the rat and described the localization of phospholipids in the mitochondria and the Golgi apparatus by dichromate sublimate fixation and controlled chromatation technique. In the squirrel pituitary gland processed in a similar

summer the Golgi apparatus and the mitochondria are the only sudanophilic structures, and the cytoplasm of both the acidophils and basophils is colorless. But the amount of the lipid material exposed after controlled chromation is much less than that seen in Sudan black B preparations of the tissue treated by lipoprotein dissolving agents or after staining with acid hematein.

ACKNOWLEDGMENT

Thanks are due to Dr B. R. Seshachar, Professor of Zoology, University of Delhi and Dr H. W. Mosman, University of Wisconsin, for helpful suggestions. One of us (G.K.D.) is grateful to the Council of Scientific and Industrial Research, India for the award of a Research Fellowship. This investigation was supported, in part, by a grant from the Ford Foundation.

LITERATURE CITED

- Adams, C. W. H. 1937 *J. Clin. Pathol.*, 10: 56.
Quoted by Pearse, A. G. E. 1960
- Adams, C. W. H., and J. C. Sloper 1955 Techniques for demonstrating neurosecretory material in the human hypothalamus. *Lancet*, 1: 851-852.
- Adams, C. W. H., and A. G. E. Pearse 1950 Classification of mucoid (basophil) cells in normal and pathological human adenohypophysis. *J. Endocrinol.*, 18: 147-153.
- Altmann, M., C. L. Foster and G. Mendel 1950 Some observations on the cytology of the adenohypophysis of the non-pregnant female rabbit. *Quart. J. micr. Sci.*, 100: 463-482.
- Baker, J. R. 1958 Cytological Techniques. The principles and practice of methods used to determine the structure of the metazoan cell. 2nd edition (1958) Reprinted. Methuen and Co., London.
- Barnes, R. G. 1962 Electron microscope studies on the secretory cytology of the mouse anterior pituitary. *Endocrinology* 71: 618-628.
- Barnett, R. J., A. J. Ladman, M. J. McAllister and E. R. Sperrheim 1958 The localization of glycoprotein hormones in the anterior pituitary glands of rats investigated by differential protein solubilities, histological stains and histochemistry. *Endocrinology* 59: 393-418.
- Barnett, R. J., W. D. Roth and J. Sahner 1961 The histochemical demonstration of the sites of heterotropic hormone in the rat pituitary gland. *Endocrinology* 69: 1047-1059.
- Cleveland, R., and J. M. Wolf 1952 A differential stain for the anterior lobe of the hypophysis. *Anat. Rec.*, 51: 406-418.
- Cosmides, G. C. 1937 A modification of Mallory's connective tissue stain with discussion of the principles involved. *Anat. Rec.*, 69: 23-34.
- Dawson, A. B. 1948 The relationship of pars tuberalis to pars distalis in the hypophysis of the rhesus monkey. *Anat. Rec.*, 102: 103-122.
- 1953 The occurrence of two tinctorial types of acidophils (carminophiles and orangeophils) in the pars distalis of mammalian pituitary gland. *Anat. Rec.*, 145: 315 (abstract).
- Dawson, A. B. and H. B. Friedgood 1958 The occurrence of a second type of acidophile cell in the anterior pituitary of the female cat and its relation to sexual activity. *Anat. Rec. Suppl.*, 70: 21.
- Eftman, H. 1932 A direct silver method for the Golgi Apparatus. *Stain Technol.*, 27: 47-52.
- 1955 Phospholipids of the anterior pituitary. *Anat. Rec.*, 121: 288.
- 1956 Response of the anterior pituitary to dichromate oxidation. *J. Histochem. Cytochem.* 4: 410-411.
- 1957 Phospholipid fixation by dichromate sublimation. *Stain Technol.*, 32: 29-31.
- 1958 Phospholipids of the anterior pituitary. *Anat. Rec.*, 130: 567-580.
- Farquhar, M. G., and J. F. Rhinehart 1954 Cytologic alterations in the anterior pituitary gland following thyroidectomy. An electron microscope study. *Endocrinology* 55: 857-878.
- Flax, M. H., and M. H. Himes 1952 Microspectrophotometric analysis of metachromatic staining of nucleic acids. *Physiol. Zool.*, 25: 297-311.
- Floeder, S. 1949 Changes in the human hypophysis in connection with pregnancy. *Acta Anat.*, 8: 329-346.
- Gomori, G. 1950 Aldehyde-fuchsin: a new stain for elastic tissue. *Am. J. Clin. Path.*, 20: 663-666.
- Halmi, N. S. 1950 Two types of basophils in the anterior pituitary of the rat and their respective cytopathological significance. *Endocrinology* 47: 259-269.
- 1951 Further observations on two types of basophil cells in the anterior pituitary. *Anat. Rec.*, 109: 300.
- Hartmann, J. F. W. R. Fain and J. M. Wolfe 1946 A cytological study of the anterior hypophysis of the dog with particular reference to the presence of fourth cell type. *Anat. Rec.*, 95: 11-27.
- Hellbaum, A. A., L. G. McArthur, F. J. Campbell and J. C. Finerty 1961 The physiological fractionation of pituitary gonadotropic factors correlated with cytological changes. *Endocrinology* 63: 144-153.
- Herlant, M. 1958 Correlations hypophysogonitales chez la femelle de la Chèvre-Souris, *Algeria agoutis* (Borkhausen). *Arch. Biol.*, 67: 89-180.
- Hildebrand, J. E., E. G. Hannels and J. C. Finerty 1957 Gonadotropic cells of the rat hypophysis and their relation to hormone production. *Zucker. Zelforsch.*, 48: 400-411.
- Hoffman, R. A., and M. X. Zarrow 1953 Changes in the cytology of the pituitary gland of *Citellus* as demonstrated by the periodic acid-Schiff reaction. *Anat. Rec.*, 122: 466-487.
- Lillie, R. D. 1951 The alcohols procedure. A differential method segregating the connective

- tive tissue, collagen, reticulum and basement membranes into two groups. *Am. J. Clin. Path.*, 21: 484-485.
- McKeever S. 1963 Seasonal changes in body weight, reproductive organs, pituitary adrenal glands, thyroid gland and spleen of the belding ground squirrels (*Citellus beidleri*) *Am. J. Anat.*, 113: 153-167.
- Ortman, R. 1956 A study of some cytochemical reactions and of the hormone content of the adenohypophysis in normal and in genetic dwarf mice. *J. Morph.*, 99: 417-431.
- Ortman, R., and W. E. Gelesbach 1958 The cytology of the pars distalis of the wallaby pituitary. *Australian J. Exp. Biol.*, 36: 609-618.
- Pearse, A. G. E. 1960 *Histochemistry Theoretical and Applied*. Churchill, London.
- Purves, H. D. 1961 Morphology of the hypophysis related to its function. In *Sex and Internal Secretions*. Young, W. C., ed. Williams & Wilkins, Baltimore, Vol. I, pp. 161-232.
- Purves, H. D., and W. E. Gelesbach 1951a The site of thyrotrophin and gonadotrophin production in the rat pituitary studied by McManus-Hotchkiss staining for glycoprotein. *Endocrinology* 49: 244-264.
- 1951b Specific staining of the thyrotrophic cells of the rat pituitary by the Gomori stain. *Endocrinology* 49: 427-432.
- 1957 A study on the cytology of the adenohypophysis of the dog. *J. Endocrin.*, 14: 361-370.
- Kennels E. G. 1953 Localization of phospholipids in the rat hypophysis. *Anst. Rec.*, 115: 659-671.
- 1957 Two tinctorial types of gonadotrophic cells in the rat hypophysis. *Dtsch. Zellforsch.*, 45: 494-471.
- 1963 Gonadotrophic cells of rat hypophysis. In *Cytologie de l'Adenohypophyse*. Editions du CNRS, Paris. pp.201-214.
- Kanders, A. E., and E. G. Kennels 1959 Evidence on the cellular source of luteotrophin derived from a study of rat pituitary autografts. *Ztschr. Zellforsch.*, 49: 283-274.
- Schrader F and C. Leuchtenberger 1950 A cytochemical analysis of the functional interrelations of various structures in *Arachis hypogaeata* (de Geer). *Exp. Cell Res.*, 1: 431-453.
- Serber B. J. 1958 A cytological study of the anterior pituitary gland of the normal, gonadectomized and thyroid deficient hamster (*Mesocricetus auratus*). *Anst. Rec.*, 131: 173-185.
- Serra, J. A. 1958 A method for the detection of masked lipids. *Revista Portuguesa de Zoologia e Biologia Geral*, 1: 109-120.
- Smith, P. E., and I. F. Smith 1972 The function of the lobes of the hypophysis as indicated by replacement therapy with different portions of the ox gland. *Endocrinology* 7: 578-581.
- Wilson, W. D. and C. E. Erin 1954 Three types of chromophil cells of the adenohypophysis. *Am. J. Path.*, 50: 891-896.

PLATE 1

EXPLANATION OF FIGURES

- 2 Lateral half of the pars anterior of the mature male palm squirrel showing the general distribution and location of the PAS-positive cells. PAS/OG $\times 600$.
- 3 Higher magnification of a portion of figure 2 clearly showing the oval shape of the gonadotrophs. The unstained gray cells represent the acidophils. PAS/OG $\times 1,520$.
- 4 Lateral half of the pars anterior of nonlactating, nonpregnant female palm squirrel. Note the small number of gonadotrophs compared to that of the male (fig. 2). PAS/OG $\times 600$.
- 5 Higher magnification of portion of figure 4 showing the gonadotrophs $\times 1,520$.
- 6 Anteromedian zone of the pars anterior of male palm squirrel showing the large, round thyrotrophs. PAS/OG $\times 1,520$.
- 7 Lateral half of the pars anterior of male palm squirrel showing the distribution of acidophils. (The cells are arranged in clusters in the intranuclear spaces.) Mercury-bromophenol blue $\times 600$.

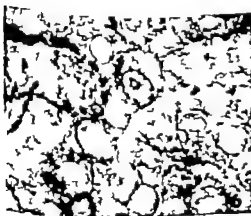
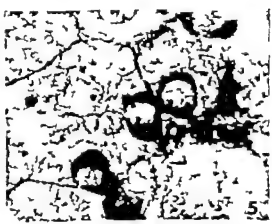
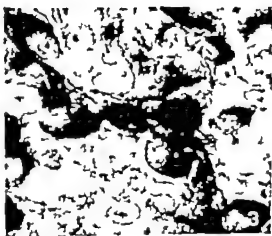
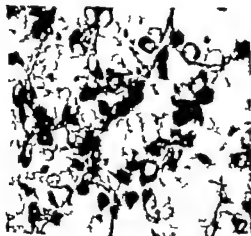


PLATE 2

EXPLANATION OF FIGURES

- 8 Higher magnification of a portion of figure 7 showing the acidophils $\times 1,520$.
- 9 Lateral half of the pars anterior of the pituitary of a male palm squirrel showing the silver impregnated Golgi zones. $\times 800$.
- 10-11 The "cupping" of acidophils by the basophils in the pars anterior. The outer dark zone represents the PAS-positive material of the gonadotroph and the inner gray zone represents the acidophilic area of the cell. PAS/OG $\times 1,520$.
- 12 Lateral half of the pars anterior of a female palm squirrel in late pregnancy. The gonadotrophs show increase in number and granulation. PAS/OG $\times 1,520$.
- 13 Lateral half of the pars anterior of a lactating female palm squirrel showing the degranulating gonadotrophs. The gray cells in the interalveolar spaces represent the acidophils. PAS/OG $\times 1,520$.



PLATE 2

EXPLANATION OF FIGURES

- 8 Higher magnification of portion of figure 7 showing the acidophils $\times 1,520$.
- 9 Lateral half of the pars anterior of the pituitary of a male palm squirrel showing the silver impregnated Golgi zones. $\times 600$
- 10-11 The "cupping" of acidophil by the basophils in the pars anterior. The outer dark zone represents the PAS-positive material of the gonadotroph and the inner gray zone represents the acidophilic area of the cell. PAS/OG $\times 1,680$
- 12 Lateral half of the pars anterior of a female palm squirrel in late pregnancy. The gonadotrophs show increase in number and granulation. PAS/OG $\times 1,520$
- 13 Lateral half of the pars anterior of lactating female palm squirrel showing the degranulating gonadotrophs. The gray cells in the intersinusoidal spaces represent the acidophils. PAS/OG $\times 1,520$.

Effects of Gonadectomy Androgen Administration and Thyroidectomy on the Cytology of the Pituitary Gland of the Five-striped Palm Squirrel *Funambulus pennanti* (Wroughton)

GURMEET K. DHALIWAL AND M. R. N. PRASAD

Physiology of Reproduction Wing, Department of Zoology
University of Delhi, Delhi-7 India

ABSTRACT Changes in the cytology of the pituitary gland of the palm squirrel, *Funambulus pennanti* (Wroughton) following gonadectomy androgen administration and propylthiouracil treatment are described.

Increase in gonadotroph cell number and granulation reaches its maximum by one week after gonadectomy and is maintained at this level during the next three weeks, following which there is gradual decline. Female squirrels show hyper trophic cells with prominent Golgi apparatus at 16 weeks after gonadectomy whereas males show similar changes four weeks after castration, changes which are still clearly noticeable at the end of 48 weeks. Castration cells or silver-ring cells, so characteristically seen in rats, do not occur in gonadectomized squirrels. Thyrotrophs are not affected by gonadectomy. Acidophils quickly decrease in number following gonadectomy and are maintained at this level throughout the post-castration period.

Administration of testosterone propionate to one week castrates causes degeneration in some gonadotrophs while others are coarsely granulated and deeply stained. The degenerated cells are interspersed with the other deeply stained gonadotrophs in the lateral halves of the pars anterior. Testosterone propionate administration to 12-week castrates produces no marked changes in the granule content of the gonadotrophs.

Propylthiouracil treatment causes degeneration of cells located in the antero-medial zone of the pars anterior. Degeneration is partial in animals treated for 18 days but is complete after 30 days of treatment. Acidophils are partially degenerated after 30 days of propylthiouracil treatment.

Cytological study of the pituitary gland of the squirrel, *Funambulus pennanti* (Prasad and Dhaliwal '63; Dhaliwal and Prasad, '65) has shown that the gonadotrophs are located in the postero-medial and lateral halves of the pars anterior; the thyrotrophs occupy the antero-medial zone, and the acidophils occur mainly in the medullary zones of the lateral halves. The present paper deals with changes in these cell types following gonadectomy and administration of androgens and gonotrophic compounds.

MATERIAL AND METHODS

Eighty-four sexually mature palm squirrels, trapped in the vicinity of the Delhi University Campus, were gonadectomized under ether anaesthesia using the sterile technique. Castration was performed through an incision in the scrotum, since the testes in palm squirrels remain scrotal throughout life. Ovariectomy was per-

formed through a mid-ventral incision. Experimental animals and the controls were maintained in the laboratory on a standard diet.

Three milligrams of testosterone propionate (Perandren — CIBA) was administered subcutaneously to a group of six squirrels on alternate days for a period of 21 days, beginning one week after gonadectomy. Another set of six animals was injected with the same dose of testosterone propionate for 45 days beginning 12 weeks after gonadectomy.

For chemical thyroidectomy the animals were fed an aqueous suspension of 5% 6-n-propyl-2-thiouracil 2 cm/day for 2-4 weeks.

Body weights were noted in the beginning and at the end of each experiment. The animals were sacrificed under ether anaesthesia. The pituitary glands were removed and fixed in Dawson's fixative for six hours. Horizontal sections of the pitui-

tary glands were cut at 6 μ and stained in periodic acid-Schiff/orange G (PAS/OG) stain.

Differential counts of basophils, acidophils and chromophobes were made in every tenth section of the pituitary gland with the aid of an eye piece micrometer from ten fields representing approximately all the different areas of the section. The number and size of fields chosen for counts were comparable for all the pituitary glands. About 5 000 cells were counted from each gland. Basophil counts included both gonadotrophs and thyrotrophs and the acidophil counts included both the orangeophils and carminophils.

OBSERVATIONS

1 Changes in the gonadotrophs following gonadectomy

The gonadotrophs show increase in number as well as granulation as early as

two days following gonadectomy (tables 1 and 2). The increase is more apparent in females than in males since the number of gonadotrophs in intact females is less than in males. The cells are coarsely granulated and deeply stained with PAS (figs. 1 and 5). Some cells show accumulation of granules, mainly towards the periphery. The Golgi zone, visible in some cells, presents no striking change. By one week after gonadectomy the number of gonadotrophs reaches the maximum and is maintained at this level up to four weeks post-operatively. Subsequently the general staining intensity and the amount of granulation decreases (fig. 2). A few small, irregular and intensely PAS positive masses are also observed in the middle of the interinsular spaces. The basophil count begins to decline after four weeks of gonadectomy and continues until the termination of the experiment at the end of 48 weeks. Degranulation of gonadotrophs is more in

TABLE 1

Cell counts from the anterior pituitary gland of intact and gonadectomized male palm squirrels

Period after gonadectomy	Basophils	Acidophils	Chromophobes
Intact control (3)	1190 \pm 99	1321 \pm 71	2482 \pm 118
2 days (2)	1294 \pm 94	1324 \pm 49	2396 \pm 35
4 days (3)	1571 \pm 46	1182 \pm 74	2359 \pm 47
1 week (3)	1603 \pm 34	1176 \pm 76	2435 \pm 101
4 weeks (2)	1518 \pm 45	1284 \pm 30	2517 \pm 23
12 weeks (2)	1223 \pm 44	1206 \pm 20	2745 \pm 144
18 weeks (2)	1166 \pm 20	1106 \pm 111	2768 \pm 63
22 weeks (3)	1008 \pm 74	1121 \pm 68	2811 \pm 43
40 weeks (1)	868	1378	3068

Figures in parentheses represent the number of animals in each group.
Mean.

Standard error of the mean.

TABLE 2

Cell counts from the anterior pituitary glands of intact and gonadectomized female palm squirrels

Period after gonadectomy	Basophils	Acidophils	Chromophobes
Intact control (3)	848 \pm 42	1342 \pm 61	2577 \pm 40
2 days (2)	1257 \pm 104	1296 \pm 4	2392 \pm 43
4 days (2)	1287 \pm 51	1187 \pm 121	2336 \pm 53
1 week (4)	1190 \pm 73	1231 \pm 110	2577 \pm 66
4 weeks (3)	1296 \pm 101	1032 \pm 65	2662 \pm 66
12 weeks (2)	1013 \pm 40	1070 \pm 61	2451 \pm 143
18 weeks (2)	956 \pm 16	1039 \pm 31	2606 \pm 95
22 weeks (3)	947 \pm 97	1047 \pm 8	2337 \pm 103
48 weeks (1)	703	1192	3168

Figures in parentheses represent the number of animals in each group.
Mean.

Standard error of the mean.

evidence in the postero-lateral halves of the pars anterior than in the other regions (figs 3 and 4). The Golgi apparatus hypertrophies and in some cells it represents the only PAS-positive structure in the cytoplasm.

Typical castration cells as observed in dems are not seen in the squirrel pituitary gland. Cells with coarse granules and hypertrophied Golgi apparatus are common in females 16 weeks after gonadectomy but in the males they occur four weeks after castration, and some are retained up to 40-48 weeks postoperatively (fig. 8). In these long-term castrates, the number of gonadotrophs is low and the basophil cell counts (tables 1 and 2) probably record primarily the thyrotrophs which do not show any apparent differences in number or disposition except for minor variations in staining intensity. Masses of PAS-positive substances of varying sizes are present in the inter-sinusoidal spaces.

2. Changes in acidophil cells after gonadectomy

The acidophils show an initial decrease in number (tables 1 and 2) in the early castrates and are maintained at this level throughout the experimental period. Except for slight variation in number the acidophils show no change in granulation, shape or staining intensity following gonadectomy.

3. Effect of testosterone propionate treatment on the pituitary cytology of gonadectomized squirrels

Administration of 3 mg of testosterone propionate on alternate days for 21 days to squirrels, beginning one week after gonadectomy results in the reduction of basophil cell number by 32% in males and by 46% in females compared to the castrate controls (table 3 groups II and III). Some of the gonadotrophs are heavily granulated and stained with PAS while others are completely degranulated (fig. 7).

Testosterone treatment, begun 12 weeks after castration and continued for 45 days caused no appreciable change in the number of gonadotrophs (table 3 groups V and VI) but dark staining, coarsely granulated cells predominate. These cells prob-

ably represent the lightly stained basophils of the castrate control group (table 3 group VI). Lightly PAS-positive basophils are absent. Increase in the intensity of staining may possibly be due either to an increase in the rate of hormone synthesis and/or to the storage of the hormone. The gonadotrophs which cannot be differentiated tinctorially into FSH and LH secretory cells represent a mixed population of cells scattered in the lateral halves of the pars anterior with greater concentration posteriorly.

4. Effect of propylthiouracil administration on the cytology of the pituitary gland

Thyroid glands of squirrels treated with propylthiouracil (PTU) up to 30 days showed two- to five-fold increase in weight as compared to those of the untreated normal controls. The cytology of the pituitary glands of animals treated for two days with PTU is normal. After administration of PTU for 15 days marked degranulation is observed in TSH secreting cells. Some cells show partial degranulation while others are completely depleted of PAS-positive granules. A few intensely stained thyrotrophs are also present. In some cases small colloidal masses are evident in the antero-medial zone of the pars anterior. These changes are enhanced in animals which were administered PTU for 30 days. In some pituitary glands of such squirrels the Golgi apparatus is the only structure stainable with PAS (fig. 8). Darkly stained thyrotrophs, seen in squirrels treated with PTU for 15 days are absent. The gonadotrophs appear slightly shrunken with the granules clumped together. Acidophils also show partial degranulation and an apparent decrease in number. These changes follow a similar pattern in males and females.

DISCUSSION

Increase in number and granulation of gonadotrophs following gonadectomy as observed in the present study substantiates the findings of Wolfe and Brown (42) Purves and Griesbach (55) and Farquhar and Rinehart (54) in the rat, and Serber (58) in the golden hamster. In the palm squirrel the basophils attained the maxi-

TABLE 3
Effect of testosterone propionate administration on the anterior pituitary glands of gonadectomized palm squirrels

Experimental groups	Males			Females		
	Basophils	Acidophils	Chromophobes	Basophils	Acidophils	Chromophobes
Group I (One week after gonadectomy)	1605 \pm 34 (3)	1178 \pm 76	2435 \pm 101	1100 \pm 73 (4)	1231 \pm 110	3577 \pm 69
Group II (T.P. treatment beginning one week after gonadectomy for 21 days)	1083 \pm 35 (3)	1298 \pm 33	2724 \pm 42	701 \pm 9 (3)	1281 \pm 47	2786 \pm 54
Group III (4 weeks after gonadectomy)	1516 \pm 45 (3)	1284 \pm 30	2517 \pm 23	1226 \pm 101 (3)	1032 \pm 85	2682 \pm 80
Group IV (12 weeks after gonadectomy)	1323 \pm 44 (2)	1100 \pm 20	2746 \pm 144	1015 \pm 40 (2)	1070 \pm 61	2851 \pm 146
Group V (T.P. treatment beginning 12 weeks after gonadectomy for 45 days)	1123 \pm 28 (3)	1002 \pm 46	2782 \pm 27	1017 \pm 10 (3)	1089 \pm 62	2819 \pm 16
Group VI (16 weeks after gonadectomy)	1185 \pm 20 (2)	1168 \pm 111	2709 \pm 92	966 \pm 16 (2)	1029 \pm 31	2906 \pm 92

Testosterone propionate (Ponasteron - CIBA) - 3 m administered subcutaneously on alternate days.

Mean.

Standard error of the mean.

Figures in parentheses refer to the number of animals in each group.

number by one week after gonadectomy and were maintained at this level for four weeks, after which they declined gradually. As a tinctorial or cytological differentiation between FSH and LH secreting gonadotrophs was not possible, comments on the increase and/or decrease of FSH and LH activities of the gland following gonadectomy cannot be considered until history of the pituitaries is completed. Paesl, de Jongh, Hoogstra and Engelbrecht (35) reported a five-fold increase in FSH content after gonadectomy in female rats while there was no appreciable change in the male LH content increased in both the sexes. Similarly Hellbaum and Greep (40) Purves and Griesbach (55) Wooten, Simpson and Evans (55) and Cozens and Nelson (61) observed that early changes after gonadectomy involved increase in the FSH content, whereas in the late castrates LH activity predominated.

A progressive vacuolation of gonadotrophs resulting in typical castration or "apopting" cells is seen in the rat (Purves and Griesbach, 55) Serber (58) observed the vacuolated gonadotrophs in the male golden hamsters only. Severinghaus (37) castrated guinea pigs for a maximum period of 175 days but did not observe the vacuolation leading to the formation of castration cells as in the rat. Burrows (49) interpreted the difference in vacuole formation in gonadotrophs on the assumption that a lapse of longer post-castration interval was necessary for these changes to take place in guinea pigs. In the present study gonadectomized squirrels were maintained for a maximum period of 48 weeks but no vacuolation, as reported in the rat, was observed in the gonadotrophs. However, the female squirrels exhibited a higher percentage of gonadotrophs with hypertrophied Golgi zones and coarse dark staining granules 16 weeks after ovariectomy while males exhibited such changes four weeks after castration and retained them until the end of 48 weeks.

Reports concerning the effect of gonadectomy on the acidophil cells and the growth hormone content of the pituitary glands are conflicting. Scheldt (74) Severinghaus (33) and Serber (58) reported a progressive decrease in the acidophil number and staining intensity while

Descelin (33) noticed increase in the number of acidophils after gonadectomy. Farquhar and Rinehart (54) observed that degranulation in the acidophil cells up to 35 days after castration, was followed by an increase thereafter. Paesl, de Jongh, Hoogstra and Engelbrecht (35) Contopoulos-Simpson and Koneff (58) and Cozens and Nelson (61) assayed the growth hormone potency of the pituitary glands of ovariectomized rats and found that there was no change in the growth hormone content up to 2 months following ovariectomy. Cozens and Nelson (61) recorded a slight decrease in the growth hormone content in 4-9 months castrate rats. In the palm squirrel the acidophil number decreases in the early castration period and is maintained at this level in long-term castrates. Whether this is indicative of a decrease in growth hormone content cannot be definitely stated until further work on bioassay is completed.

Nelson and Gallagher (35) Wolfe and Hamilton (37) Cutly and Cutly (38) Laqueur and Fluhman (42) Heller Segaloff and Nelson (43) Hellbaum and Greep (43) Paesl, de Jongh and Willemse (58) and Hellbaum, McArthur Campbell and Finerty (61) reported a partial reduction in the gonadotrophic potency of the pituitary glands after androgen administration. Greep and Chester Jones (50) Hoogstra and Paesl (57) and Paesl, de Jongh and Willemse (58) observed that a smaller dose (0.1 to 0.5 mg/day) of testosterone propionate increased the FSH potency of intact females whereas a higher dose (2 mg/day) was required to produce a similar effect in intact as well as in gonadectomized rats (Hoogstra and Paesl, 57). Burrows (49) concluded that the androgens administered in small doses for short periods enhanced the production of FSH while continuation of treatment for long periods resulted in a decrease of FSH accompanied by a complete suppression of LH. Similar decrease in the gonadotrophin content as indicated by the degranulation of the gonadotrophs of the squirrel pituitary gland was observed in the present study. Testosterone propionate was administered to two groups of squirrels — one group gonadectomized for one week and the other for 12 weeks. Changes in the

first group were very striking as shown by a decrease in the basophil number. Moreover many cells which in the castrate control animals were recognized as basophils were represented in testosterone propionate treated animals by degranulated cells thus demonstrating the liberation of the stainable material, probably from the LH secreting cells. In long-term castrates such changes were not seen except for an increase in the staining intensity in some cells. Similar observations were made by Heller Segaloff and Nelson (43) in rats.

In the squirrel pituitary gland the degranulated basophils are distributed in the lateral halves of the pars anterior and are not segregated in separate zones as in the rat (Hellbaum, McArthur Campbell and Finerty '61). These authors recognized the degranulated cells following testosterone propionate injections to castrates, as LH producing basophils by PAS/methyl blue stain and confirmed their findings by bioassay. PAS/methyl blue did not distinguish tinctorially the two types of basophils in squirrel pituitary (Dhaliwal and Prasad '65). The conclusion that the degranulated cells represent LH secreting gonadotrophs and that the heavily granulated cells are the FSH gonadotrophs is based on extrapolation of the observations of Hellbaum, McArthur Campbell and Finerty ('61) to the squirrel. It is hoped that further bioassay experiments may reveal the functional identity if any of the two types of gonadotrophs.

Extensive degranulation of the thyrotrophs was evident in squirrels treated with PTU for 15 days. A pink staining Golgi apparatus was present in some of the degranulating cells. A few PAS-positive thyrotrophs containing coarse granulation were also seen. After 30 days of treatment degranulation was complete and the only PAS-positive cells discernible were a few which showed coarse bright PAS-positive granules. These granules were comparable to "T" granules of Purves and Griesbach ('56). Similar degranulation and decrease in stainability of thyrotrophs following propylthiouracil or iodothiouracil administration was reported by Purves and Griesbach ('56) Serber ('58) and Peters and Halmi ('61). Lightly stained AF positive Golgi apparatus was also reported in the

degranulating thyrotrophs of the rat pituitary (Peters and Halmi, '61). Male and female squirrels were similar in their response to PTU administration in contrast to the findings of Serber ('58) in the golden hamster. She observed that in the female hamster increase in weight of the thyroid gland was greater and the number of hypertrophied basophils was higher than that in the male hamster. Vacuolation of basophil cells observed in the male hamster was not seen in the female.

Acidophils were normal in squirrels which received PTU for 15 days, whereas partial degranulation and an apparent decrease in the cell number occurred in those which received PTU for 30 days. These results are in accord with those of Purves and Griesbach (46) who showed that a slight depression in thyroxin level caused marked changes in thyrotrophs. Acidophils were only partially affected under similar conditions. Peters and Halmi ('61) also reported incomplete degranulation of acidophil cells in rats administered 20 mg of propylthiouracil daily for 28 days.

ACKNOWLEDGMENT

Thanks are due to Dr. B. R. Saxhachar, Professor of Zoology, University of Delhi and Dr. H. W. Mossman, University of Wisconsin, for helpful suggestions. One of us (G. K. D.) is grateful to the Council of Scientific and Industrial Research, India for the award of a Research Fellowship. This investigation was supported in part, by a grant from the Ford Foundation.

LITERATURE CITED

- Burrows, H. 1949. *Biological Actions of Sex Hormones*, 2nd ed., University Press, Cambridge.
- Contopoulos, A. N. M. E. Simpson and A. A. Koneff. 1956. Pituitary function in the thyroidectomized rat. *Endocrinology* 60: 643-651.
- Cooper, D. A., and M. M. Nelson. 1961. Effects of ovariectomy on the follicle-stimulating and interstitial cell-stimulating content of the anterior pituitary of the rat. *Endocrinology* 61: 767-772.
- Cutuly, E., and E. C. Cutuly. 1958. Inhibition of gonadotropic activity by sex hormones in parabiotic rats. *Endocrinology* 53: 568-572.
- Desclis, L. 1933. *Aspects des déterminations des modifications structurales de l'hypophyse résultant de la castration chez le rat mâle*. *Compend. Soc. Biol.*, 114: 533.
- Dhaliwal, G. K., and M. R. N. Prasad. 1965. Cytology and histochemistry of the pituitary

- gland of the five striped palm squirrel, *Flemingia leucophaea* (Wroughton) *Am. J. Anat.*, 117 128-132.
- Jayakar, M. G., and J. F. Ripehart 1954. Electron microscopic studies of the anterior pituitary gland of castrate rats. *Endocrinology* 54 436-441.
- Geop, R. O., and I. Chester Jones 1950. Steroid control of pituitary function. Recent prog. *Endocrine Res.*, 5 197-251.
- McEwen, A. A., and R. O. Geop 1940. Qualitative changes in the gonadotropic complex of the rat pituitary following removal of the testes. *Am. J. Anat.*, 67 287-304.
- 1943. Qualitative changes induced in gonadotropic complex of pituitary by testosterone propionate. *Endocrinology* 32: 33-40.
- McEwen, A. A., L. G. McArthur, P. J. Campbell and J. C. Flarity 1961. The physiological action of pituitary gonadotropic factors correlated with cytological changes. *Endocrinology* 68 144-153.
- Nale, C. C., A. Segaloff and W. O. Nelson 1943. Effect of testosterone propionate on pituitary gonadotropic potency of castrated male rat. *Endocrinology* 33 186-189.
- Nagata, M., J. F. J. A. Paed 1957. The FSH content of the hypophysis of the rat as influenced by androgen. *Acta endocr(Kbh)* 24 230-240.
- Lawson, O. L., and C. F. Fishman 1942. Action of testosterone on the female rat hypophysis. *Endocrinology* 31 300-302.
- Lawson, W. C., and T. F. Gallagher 1933. Studies on the anterior hypophysis. IV. The effect of male hormone preparations upon the anterior hypophyses of gonadectomized male and female rats. *Anat. Rec.*, 64 129.
- Lecl, F. J. A., R. E. de Jongh, M. J. Hoogstra and A. Zeyher 1955. The follicle-stimulating hormone content of the hypophysis of the rat as influenced by gonadectomy and estrogen treatment. *Acta endocr(Kbh)*, 10: 49-60.
- Lecl, F. J. A., R. E. de Jongh and C. H. Willems 1954. Testosterone and the pituitary ICSH content of male and female rats (with additional remarks on body growth). *Arch. Internat. Pharmacodyn.*, 118 317-327.
- Peters, B. H., and N. S. Halmi 1961. Changes in the thyroidectomy cells of the rat pituitary under the influence of large doses of triiodothyronine. *Endocrinology* 68 844.
- Prasad, M. B. N. and G. K. Dhaliwal 1963. Studies on the pituitary gland of the Indian Palm squirrel, *Flemingia leucophaea* (Wroughton). *Curr. Sci.*, 32: 317-318.
- Purves H. D. and W. E. Goeschel 1948. Observations on the acidophil cell changes in the pituitary in thyroxine deficiency states. I. Acidophil degranulation in relation to gonitogenic agents and extrathyroidal-thyroxine synthesis. *Brit. J. Exper. Path.*, 37 170-179.
- 1955. Changes in the gonadotrophs of the rat pituitary after gonadectomy. *Endocrinology* 56 374-386.
- 1958. Changes in the basophil cells of the rat pituitary after thyroidectomy. *J. Endocrin.*, 13: 365-373.
- Schleddt, J. 1914. Ueber die hypophysen bei feminierten Männchen und maskulierten Weibchen. *Zentr. f. Physiol.*, 27 1170.
- Serber B. J. 1958. A cytological study of the anterior pituitary gland of the normal, gonadectomized and thyroid deficient hamster (*Mesocricetus auratus*). *Anat. Rec.*, 131 173-192.
- Servingshaus, A. E. 1933. A cytological study of the anterior pituitary of rat with special reference to the Golgi apparatus and to cell relationship. *Anat. Rec.*, 87 142.
- 1937. Cellular changes in the anterior hypophysis with special reference to its secretory activities. *Physiol. Rev.* 17 558-583.
- Wolfe J. M., and A. D. Brown 1942. Action of diethylstilbestrol on cytological characteristics of anterior pituitaries of female rats, together with certain observations on the effect of castration. *Endocrinology* 31 467-478.
- Wolfe J. M., and J. B. Hamilton 1937. Comparative action of testosterone compounds and estrogens on anterior hypophysis. *Endocrinology* 21 603-610.
- Wooten, E., M. M. Nelson, M. E. Simpson and H. M. Evans 1955. Effect of pyridoxine deficiency on the gonadotrophic content of the anterior pituitary in the rat. *Endocrinology* 56: 50-66.

PLATE 1

EXPLANATION OF FIGURES

- 1 Parous female squirrel, one week after gonadectomy. Coarse and darkly stained granules are seen in the gonadotrophs. PAS/OG $\times 1,520$.
- 2 Parous female squirrel, four months after gonadectomy. Golgi zone is hypertrophied and in some degenerated cells, like the one in the middle of the field, it is the only PAS-positive structure. PAS/OG $\times 1,520$.
- 3 Parous female squirrel, eight months after gonadectomy. Antero-lateral zone of the pars anterior showing occasional gonadotrophs with darkly stained, coarse granulation. PAS/OG $\times 1,520$.
- 4 Same as above. Postero-lateral zone of the pars anterior showing the absence of PAS-positive material in the gonadotrophs. PAS/OG $\times 1,520$.

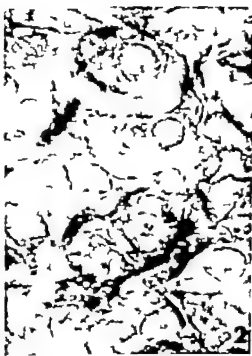
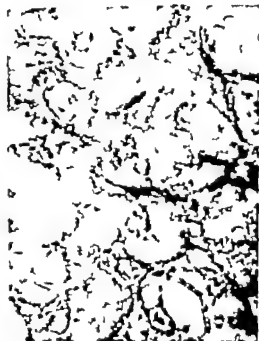


PLATE 2

EXPLANATION OF FIGURES

- 5 Mature male squirrel one week after gonadectomy. Gonadotrophs show coarse darkly stained granules and prominent Golgi zones. PAS/OG $\times 1,320$.
- 6 Mature male squirrel, ten months after gonadectomy. Gonadotrophs with hypertrophied Golgi zone and coarse granulation, resembling the castration cells in the rat, are seen. PAS/OG $\times 1,320$.
- 7 Male squirrel gonadectomized for one week and administered testosterone propionate for 21 days. FSH-secreting gonadotrophs are granulated and stained with PAS (white arrows). LH-secreting gonadotrophs are represented by the degranulated cells (black arrows). PAS/OG $\times 1,320$.
- 8 Female squirrel, administered propylthiouracil for one month. Thyrotrophs are degranulated. PAS-positive Golgi zone is seen in few cells. PAS/OG $\times 1,320$.



Morphologic Heterogeneity of Mouse Paneth Cell Granules before and after Secretory Stimulation¹

MARY W. STALEY AND JERRY S. TRIER

Gastroenterology Research Laboratory Veterans Administration Hospital
and Department of Medicine University of Wisconsin Medical School,
Madison, Wisconsin

ABSTRACT Paneth cells from fasted, fed and pilocarpine stimulated mice were studied with the light and electron microscopes. While human and rat Paneth cells contain structurally homogeneous granules, most mouse Paneth cell granules were found to be structurally heterogeneous both by light and electron microscopy. These structurally heterogeneous granules consisted of an outer rim or halo which surrounded the central core of the granule. These halos varied strikingly in electron density ranging from much paler to much darker than the granule core. Electron density of the halos correlated well with their affinity for toluidine blue in light microscopic preparations. The granule halo could be stained with both alcian blue and with PAS indicating that it contained acid mucopolysaccharide while the central core of the granule could be stained only with PAS and not with alcian blue.

While actively secreting Paneth cells were seen in preparations from fasting mice, the secretory activity was increased after feeding and after stimulation with pilocarpine. The actively secreting mouse Paneth cells discharged their granules into the crypt lumen by merocrine secretion. The fine structure of mouse Paneth cell granules was the same in resting and in actively secreting cells.

Although Paneth cells have been the subject of considerable discussions since their discovery in small intestinal crypts late in the nineteenth century (Schwalbe 1872, Paneth 1888) little is known of their contribution to the function of the small intestine. The morphology of the Paneth cells leaves little doubt that they are zymogenic secretory cells (Patzelt, '38 Hally '58 Trier '63 Behnke and Moe '64) yet the nature and role of their secretory product is not known.

Mouse Paneth cells have been of particular interest to some investigators because of the peculiar morphology of their secretory granules. Leblond ('50) noted that these granules were surrounded by achromatic vacuoles after staining by the periodic acid Schiff (PAS) technique. Utilizing histochemical techniques, Selzman and Liebelt ('61 '62a, b) have presented evidence that the mouse Paneth cell granules are characterized by a central core which is a neutral polysaccharide-protein complex surrounded by an outer rim or halo of acid mucopolysaccharide. This rim if not appropriately stained, appears as an empty vacuole. Hally ('58)

using the electron microscope, also noted vacuoles or halos surrounding mouse Paneth cell granules but interpreted these as probable artifacts of fixation.

It is the purpose of this paper to present further evidence of the morphologic heterogeneity of mouse Paneth cell granules and in addition, to present some observations on the fine structure of actively secreting mouse Paneth cells.

MATERIALS AND METHODS

Random breed adult white mice were used in this study. Animals were studied under the following conditions: six fasted for 24 hours, three fasted for 48 hours, six fasted for 72 hours, nine fed a standard Purina rodent chow pellet diet ad lib, four injected intraperitoneally with 0.3 cm³ of a 0.1% solution of pilocarpine nitrate in isotonic saline (0.3 mg of pilocarpine nitrate) and 15 injected intraperitoneally with 0.75 cm³ of the same pilo-

¹This investigation was supported in part by grant A51-05379 from the National Institutes of Arthritis and Metabolic Disorders, Bethesda, Maryland, and by General Research Support Grant to the University of Wisconsin Medical School from the National Institutes of Health, Division of Research Facilities and Resources, Bethesda, Maryland.

carpine solution (0.75 mg of pilocarpine nitrate). Animals receiving pilocarpine had been fasted for 24 hours and were sacrificed five minutes to three hours after pilocarpine injection. Four rats were also studied: two had been fasted for 24 hours and two were fed. All animals were allowed water *ad lib*.

Animals were sacrificed by cervical dislocation and approximately 0.5 cm of chilled chrome-osmium fixative (Dalton '35) or glutaraldehyde fixative (Sabatini *et al.* '63) was instilled with minimal pressure into the lumen of the third portion of the duodenum. A portion of the proximal jejunum approximately 8 by 8 mm was immediately removed and placed into chilled fixative for four minutes. The tissue was then cut into slices approximately 1 mm wide and 3 to 4 mm in length on dental wax under a drop of fixative and returned to the fixative bottle. After fixation for 1 to 2 hours the osmium fixed tissue was placed in 10% neutral buffered formol for one-half to one hour rapidly dehydrated in increasing concentrations of ethyl alcohol and embedded in epoxy resin (Luft, '61). Tissue was left in glutaraldehyde for two hours, washed in buffered 0.2 molar sucrose solution for four hours (Sabatini *et al.* '63) and then dehydrated and embedded as above. The embedded tissue slices were cut out of the epoxy block, carefully oriented and mounted with epoxy cement on a short aluminum rod machined to fit the microtome chuck. Sections of the whole specimen were then cut approximately 1 μ thick parallel to the plane of the villi with glass knives. These were mounted on glass slides and stained with toluidine blue (Trump *et al.* '61) or by the periodic acid Schiff technique (PAS).

In addition tissue from mice from each group was fixed in Zenker's and neutral buffered formol for paraffin embedment. Serial sections 4 μ thick were cut and stained with hematoxylin and eosin, alcian blue (McManus and Mowry '60), PAS (Pearse '60) and alcian blue-PAS (McManus and Mowry '60).

Chrome-osmium fixed tissue from twelve mice from representative groups was selected for electron microscopic studies.

Two animals had been fasted for 24 hours, one fasted for 48 hours, two fasted for 72 hours, four had been fed and three had been treated with 0.75 mg pilocarpine nitrate and sacrificed at 10, 20 and 30 minutes respectively. In addition, tissue from three rats was examined with the electron microscope. Human material had been studied previously (Trier '63). Suitable crypts with well oriented Paneth cells were selected for electron microscopic study utilizing the toluidine blue stained epoxy sections. The desired area was readily identified on the surface of the tissue block and trimmed for thin sectioning. Correlative observations of the same Paneth cell could thus be carried out with both light and electron microscopes by studying adjacent thick and thin sections. Thin sections were cut with diamond knives on an LKB microtome mounted on carbon coated copper mesh grids and stained with lead solution (Millonig, '61) before examination with an RCA EMU 3G electron microscope.

RESULTS

Light microscopy

In mice Paneth cells form, in part, the base of the crypts and are readily identified by their large secretory granules. In toluidine blue stained epoxy sections of mouse intestine the Paneth cell cytoplasm is more deeply stained than that of the neighboring undifferentiated cells. The supranuclear area is often more lightly stained than the remaining cytoplasm (fig. 1a and 1c) and may contain several secretory granules. The apical half of most Paneth cells is filled with secretory granules which stain in various intensities with toluidine blue.

Four types of mouse Paneth cell granules could be identified after toluidine blue staining (fig. 1). The first were those granules whose entire matrix stained homogeneously with toluidine blue and thus were not enclosed by a halo with staining characteristics different from those of the central portion of the granules (fig. 1a and 1c). The remaining three types of Paneth cell granules were characterized by their halos which surrounded the central portion of the granules. These included granules with a

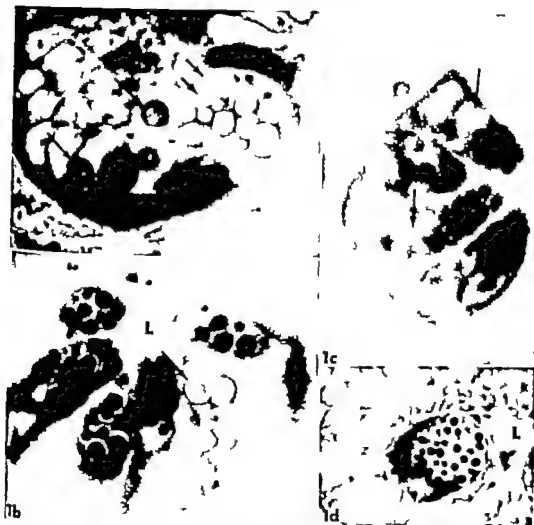


Fig 1 Various Paneth cells in 1 μ thick epoxy sections of osmium fixed mouse jejunum stained with toluidine blue. Paneth cell granules with halo which appears darker than the central core after toluidine blue (long arrows) are seen in figure 1. In the Paneth cell to the right, some granules have pale, thin halo while others show no halo (short arrows). In figure 1b are seen five Paneth cells with halos with intermediate affinity for toluidine blue. Note in addition, the one cell with granules with very pale halos and relatively pale central cores (arrow). In figure 1 four Paneth cells containing granules with no halos or thin halos with stain affinity almost comparable to that of the central cores are seen. Not the pale, soprannuclear cytoplasm (arrow). Figure 1d shows a Paneth cell with granules with relatively large pale halos. L, lumen. All micrographs $\times 2,000$.

halo of variable size which stained very faintly with toluidine blue (fig 1d) granules with a narrow halo with a moderate affinity for toluidine blue stain (fig 1b) and granules with a halo which stained intensely following exposure to toluidine blue and which was darker in appearance than the central core of the granule (fig

1a). Sections of many Paneth cells revealed granules of only one type but occasionally two different types of granules could be identified within one cell (fig. 1a and 1b). Similarly in some crypt sections all the Paneth cells seen contained the same type of granule. In other crypt sections the individual Paneth cells con-

tained morphologically different types of granules. The morphology of the granules was not particularly related to their location in cell cytoplasm and all four types of granules were seen in the supranuclear as well as in the apical regions of the cells. Granules which were morphologically heterogeneous were not always completely enclosed by a halo. Instead, paler or darker staining material was occasionally eccentrically disposed towards one side of the granule (fig 1c). All granules observed could not be readily classified into our arbitrary four groups. Instead granules intermediate in structure between groups were also seen.

When adjacent 1 μ epoxy embedded sections were stained one with toluidine blue the other with PAS. It was found that all halos present in the toluidine blue stained preparations stained more intensely with PAS than did the central core of the granules. Thus even those granules which had very pale halos after toluidine blue staining were characterized by an intensely PAS positive halo. This PAS positive halo was resistant to diastase digestion. Unfortunately we were consistently unable to stain epoxy embedded tissue with alcian blue. Glutaraldehyde-fixed tissue embedded in epoxy resin showed the same staining reactions as did the epoxy embedded osmium fixed tissue. Paraffin sections stained with alcian blue consistently showed staining of the halos with little or no staining of the central core of the granules. Paraffin sections stained with both alcian blue and PAS consistently revealed a magenta central core surrounded by a dark purple halo suggesting affinity of the central core for only PAS and of the halo for both staining reactions.

Although there was much variation from animal to animal, we found that granules characterized by a narrow halo with moderate affinity for toluidine blue were most abundant in the Paneth cells of fasting animals. The granules with a very pale halo of variable size were also commonly encountered while the granules with no halo and with dark halos occurred infrequently. Quantitation of the frequency of occurrence of the four types of Paneth cell granules after feeding and 30 minutes and three hours after pilocarpine stimula-

tion revealed no change in their frequency and their distribution compared to the fasting samples but again, considerable variation was encountered from animal to animal.

Evidence of Paneth cell secretory activity was seen in some crypts of tissue obtained from fasting animals and animals receiving 0.3 mg pilocarpine. In these crypts, material was seen in the crypt lumina with staining characteristics similar to those of the central core of the Paneth cell granules and occasionally a granule could be seen at the apical border of the cell as it appeared to enter the crypt lumen.

In tissues obtained from fed mice and mice sacrificed 30 minutes to two hours after 0.75 mg of pilocarpine, morphologic evidence of secretory activity of the Paneth cells was apparent in many of the crypts. These crypt lumina again contained material with staining characteristics resembling those of the Paneth cell granules and many of the Paneth cells lining these crypts contained few granules while some were virtually depleted of granules. Paneth cells with abundant numbers of granules could at times be found in the same crypt in which cells with only few granules were seen. Evidence of secretory activity was not present in all crypts after feeding and pilocarpine stimulation. Instead, some crypts had no stainable material in the crypt lumen and contained only well granulated Paneth cells.

Toluidine blue and PAS stained sections of osmium fixed upon embedded rat jejunum revealed homogeneous Paneth cell granules without halos both in fasting and fed animals. Similarly human biopsies from fasting subjects (Trier '63) and after pilocarpine stimulation failed to show any evidence of halos surrounding Paneth cell granules both after toluidine blue and PAS staining.

Electron microscopy

Our observations on the structural organization of the Paneth cell agree in general with those previously described in the mouse (Hally '58) in the rat (Behnke and Moe '64) and in the human (Trier '63). The cells are columnar in shape and the nucleus is situated in the basal portion of the cell which is considerably wider

than its apex. The large secretory granules are found between the irregularly shaped nucleus and the luminal surface of the cells. The lateral cell membranes show attachment areas typical for intestinal epithelial (Farquhar and Palade '63) and occasionally interdigitate with lateral membranes of adjacent cells. Short microvilli, irregular in height and distribution are present on the apical cell surface (figs. 2, 4, 8 and 9). An extensive Golgi complex containing many small round vesicles and closely apposed, flattened cisternae bounded by agranular membranes is located above the nucleus and often extends laterally (figs. 2 and 8).

The small Golgi vesicles often contain material of density similar to that of granules in the immediate vicinity of the Golgi material. The relatively dense cytoplasm contains mitochondria, unattached ribosomes, centrioles and many lysosome-like bodies (fig. 2). A well developed granular endoplasmic reticulum composed primarily of closely apposed, flattened cisternae virtually fills the portion of the cell below and lateral to the nucleus and is found between the other organelles in the remaining cytoplasm of the cell. The cisternae of the granular endoplasmic reticulum are filled with moderately dense, finely granular material of electron density similar to that seen in the central core of the granules of most Paneth cells (figs. 2, 4 and 9). However in those cells in which the central core of the granules is pale and the halo dense the contents of the cisternae of the endoplasmic reticulum is frequently of greater density than the central core of the granules (fig. 2 and 8).

The large secretory granules of the Paneth cells consist of a closely packed, relatively dense finely granular material which, when no halo is present, is surrounded by a loosely applied fine membrane (figs. 2 and 8). This membranous envelope often appears incomplete suggesting structural continuity between the granules and adjacent cytoplasm but these breaks more likely represent artifacts occurred during processing due to friability of the membrane. When the outer portion of the granule is composed of a halo this membranous envelope is ap-

plied to the outer limits of the halo thus the halo is truly part of the granule. When a halo is present, a distinct interface but no apparent membrane separates the inner surface of the halo from the central core of the granule (figs. 3, 5, 6, 7 and 8). Material of electron density similar to that of the halos of nearby Paneth cell granules may occasionally be disposed in an eccentric fashion in a Paneth cell granule and thus may not completely encircle the material of density similar to that of the central core of nearby granules. This is particularly apparent in cells which are actively secreting (fig. 4). Similarly less dense material is occasionally seen eccentrically disposed in small granules located within the Golgi region (fig. 8). However in other areas of the cell and in cells not actively secreting well formed halos are the rule in those Paneth cell granules which are heterogeneous in their structure.

Comparison of light microscopic slides of epoxy embedded osmium fixed tissue and electron micrographs of adjacent thin sections of the same Paneth cells indicate that the types of granules noted by light microscopy can readily be identified with the electron microscope. The granules which appear morphologically homogeneous by light microscopy also have no halo on electron microscopic examination. The granules with pale halos following toluidine blue staining are characterized by a relatively electron lucent halo of varying width (figs. 3, 5 and 6). These probably correspond to what Hally ('58) described as granules within empty vacuoles but our micrographs indicate that they contain sparse amounts of finely granular material throughout the substance of the halo (figs. 3, 5 and 8). The narrower halos of intermediate density following the toluidine blue staining are characterized electron microscopically by narrow halos of intermediate densities (figs. 4 and 7) and probably represent Hally's ('58) moderately osmophilic halos. These halos are composed of very small electron dense particles which are more closely packed than in the paler halos. The dark halos are composed of similar material which is even more closely packed but in addition the central core of these granules ap-

appears less electron dense hence the halo appears even darker in relation to the central core (fig. 7 and 8).

During secretion of the Paneth cell granules the fine membrane enclosing the granule appears to fuse with and become incorporated into the apical portion of the cell membrane thus allowing extrusion of the contents of the granule without loss of other cytoplasmic materials from the cell (figs. 3, 4 and 9). This apparent fusion of the membrane surrounding the secretory granule with the plasma membrane results in finger-like extensions of crypt lumina indenting the apical cytoplasm of actively secreting Paneth cells (fig. 3, 4 and 9). Microvilli are less abundant on the apical surface of these actively secreting cells. Material of electron density similar to that of the central core of the Paneth cell granules was regularly seen in the crypt lumina where cells were actively secreting (figs. 3, 4 and 9).

Occasionally membranous elements were apparent in the central dense core of Paneth cell granules (figs. 9 and 10). Although the general organization of these membranes bore some resemblance to the membranes of Golgi cisternae and vesicles granules containing these membranes were not confined to the Golgi region but were occasionally seen near the apical surface of the cell.

The density of the homogeneously granular material forming the Paneth cell granules in the rat jejunum showed some variation from granule to granule (fig. 11) but none of the granules contained a halo. Similarly Paneth cell granules from human biopsies from normal volunteers contained no halo (fig. 12).

DISCUSSION

The light and electron microscopic observations and the histochemical results of this study support previous reports (Leblond, '50; Hally '58; Selzman and Liebelt, '61; '62a, b) that most mouse Paneth cell granules are structurally heterogeneous. The regular observation of halos and their similar staining reactions after both osmium and aldehyde fixation clearly indicates that the halo is not an artifact of fixation but is an integral part of many mouse Paneth cell granules. It

has been histochemically demonstrated that the central portion of these secretory granules contains neutral polysaccharide-protein complex while the halo shows the presence of acid mucopolysaccharide (Selzman and Liebelt, '62b). Our results also indicate the presence of a non-acid mucopolysaccharide in the core of the granule. However the halos in our material stained regularly with both PAS and alcian blue, suggesting they contain both acid and neutral polysaccharide protein complexes (Pearse, '60).

The significance of the different morphologic types of halos observed in mouse Paneth cells with the light and electron microscopes is not clear. If we assume that new Paneth cell granules first appear in the Golgi region, there is no good correlation between the structure and the age of the individual granules. Granules with specific types of halos did not appear with regularity in any particular location within the cell cytoplasm; instead, single Paneth cells most frequently contained granules of a single morphologic type. The similarity of granule structure in non-secreting and actively secreting Paneth cells is further evidence that the age of the granules does not seem to be a major factor in determining their morphology.

The appearance of halos in mouse Paneth cell granules is of particular interest since these were not encountered in Paneth cell granules of the human or rat. If the granules contain digestive enzymes, it would seem possible that dietary factors might play a role in governing the nature of the enzymes present and on this basis the appearance of the granules might differ. Since the human diet is markedly different from that of laboratory mice, this might explain the differences in Paneth granule structure observed in mice and humans. However Paneth cells of the laboratory rat maintained on the same diet as the laboratory mouse have granules with structural features similar to the human (figs. 11 and 12) not the mouse suggesting that Paneth cell structure and diet do not correlate.

Our observations of mouse Paneth cells during active secretion suggest that the fine membrane surrounding the granule fuses with and becomes a part of the

apical cell membrane thus releasing the granule contents into the crypt lumen. This mechanism of secretion in which only the contents of the granule and no other cytoplasmic substances are lost from the cells is characteristic of merocrine secretory cells. It has been described in other cells of similar structure including pancreatic acinar cells (Palade et al. '61) and gastric chief cells (Ito and Winchester '63), as well as in the goblet and undifferentiated cells of the small intestinal crypts (Trier '63 '64). It is of interest that fasting mice showed morphologic evidence of secretion suggesting that a low level of secretory activity exists in Paneth cells even when food is withheld. It should be emphasized, however, that a true fast ing state in the intestine was never really attained in our study. Salivary secretion, gastric secretion and exfoliated cells from the oral cavity, esophagus, stomach and small bowel containing protein, carbohydrate and fat are present in the mouse intestinal lumen even during fasting and may provide sufficient stimulus for a low level of Paneth cell secretion even in the "fasting" animal.

Palade and coworkers ('61) and Caro ('61) have shown that the secretory product in pancreatic exocrine cells is synthesized within the granular endoplasmic reticulum and then transported to the Golgi region where granule formation takes place prior to granule migration into the apical cytoplasm and subsequent secretion at the apical surface. The similarities in structural organization and secretory mechanism among Paneth cells and pancreatic acinar cells suggest that synthesis and secretion of the granules may occur in a similar manner in both cells. Behnke and Moe's observation of material of ordered structure with a 100 Å periodicity which appeared in the ergastoplasmic and Golgi cisterns as well as in the secretory granules of differentiating rat Paneth cells (Behnke and Moe '64) provides some evidence for this sequence of granule synthesis. The membranous elements which we observed in the central portion of some mouse Paneth cell granules (figs. 9 and 10) may be incorporated into the granule during its formation in the Golgi region. However, radioauto-

graphic studies of Paneth cells utilizing radioactive precursors of the granules are needed before the pathway of granule synthesis can be ascertained.

It seems unlikely that the role of the Paneth cell granules in the functions of the small intestine will be clarified until cell fractionation techniques permit isolation of a relatively pure granule fraction for careful biochemical analysis. Similarly, correlative biochemical and morphologic studies will probably be needed to explain the reasons for the striking structural variation of Paneth cells in different mammalian species.

LITERATURE CITED

- Behnke O., and H. Moe 1964 An electron microscope study of mature and differentiating Paneth cells in the rat, especially of their endoplasmic reticulum and lysosomes. *J. Cell Biol.* 22: 633-653.
- Caro, L. G. 1961 Electron microscopic radioautography of thin sections: The Golgi zone as a site of protein concentration in pancreatic acinar cells. *J. Biophysic. and Biochem. Cytol.* 10: 37-45.
- Dalton, A. J. 1955 A chrome-osmium fixative for electron microscopy. *Anat. Rec.* 121: 281.
- Farquhar M. G., and G. E. Palade 1963 Junctional complexes in various epithelia. *J. Cell Biol.* 17: 375-412.
- Hally A. D. 1958 The fine structure of the Paneth cell. *J. Anat.* 92: 208-277.
- Ito, S. and R. J. Winchester 1963 The fine structure of the gastric mucosa in the rat. *J. Cell Biol.* 18: 541-577.
- Leblond, C. P. 1960 Distribution of periodic acid reactive carbohydrates in the adult rat. *Am. J. Anat.* 66: 1-49.
- Luft, J. H. 1961 Improvements in epoxy resin embedding methods. *J. Biophysic. and Biochem. Cytol.* 9: 409-414.
- McLames, J. F. A., and R. R. Mowry 1960 Staining methods — histologic and histochemical. New York, Hoeber Inc., p. 64.
- Milions G. A. 1961 A modified procedure for lead staining of thin sections. *J. Biophysic. and Biochem. Cytol.* 11: 736-739.
- Palade G. P., Bickavita and L. Caro 1961 Structure, chemistry and function of the pancreatic exocrine cell. In: *The Exocrine Pancreas. Normal and abnormal function* Boston, Little Brown and Company p. 23-49.
- Paneth, J. 1918 Ueber die secretirenden Zellen des Dünndarm-Epithels. *Arch. mikr. Anat.* 31: 113-191.
- Patzelt, V. 1936 Der Darm. In: *Handbuch der mikroskopischen Anatomie des Menschen*, edited by W. Heidenreich Vol. 1-2. Berlin, Julius Springer p. 170-137.
- Farmer A. G. E. 1960 Histochemistry theoretical and applied London J. & A. Churchill, Ltd. p. 235.

- Sabatini D. D., K. Benesche and R. J. Barnett 1963. Cytochemistry and electron microscopy: Preservation of cellular ultrastructure and enzymatic activity by aldehyde fixation. *J. Cell Biol.*, 17: 19-53.
- Schwalbe G. 1872. Beiträge zur Kenntniss der Drüsen in den Darmwandungen, ins Besondere der Brünnerischen Drüsen. *Arch. mikr. Anat.*, 8: 92-139.
- Selzman, H. M. and R. A. Ljebelt 1961. A cytochemical analysis of Paneth cell secretion in the mouse. *Anat. Rec.*, 140: 17-22.
- 1962a. Localization of sulfhydryl and disulfide groups of protein in Paneth cell granules of mouse intestine. *J. Histochem. and Cytochem.*, 10: 106.

- 1962b. Paneth cell granule of mouse intestine. *J. Cell Biol.*, 15: 136-139.
- Trier J. S. 1963. Studies on small intestinal crypt epithelium. I. The fine structure of the crypt epithelium of the proximal small intestine of fasting humans. *J. Cell Biol.*, 18: 899-920.
- 1964. Studies on small intestinal crypt epithelium. II. Evidence for and mechanisms of secretory activity by undifferentiated crypt cells of the human small intestine. *Gastroenterology* 47: 480-495.
- Trump, B. F., E. A. Smockler and E. F. Becht 1961. A method for staining epoxy sections for light microscopy. *J. Ultrastruct. Res.* 5: 343-348.

PLATE 1

EXPLANATION OF FIGURES

- 2a. A Paneth cell from mouse 30 minutes after pilocarpine administration located in the base of a crypt between undifferentiated cells (U). The secretory granules (G) are morphologically homogeneous with no surrounding halo and appear enclosed by a loosely applied fine membrane. Several lysosome-like structures (arrows) are seen in the cytoplasm between the nucleus (N) and the secretory granules. The crypt lumen (L) is at the far right of the micrograph. $\times 16,000$.
- 2b. Similar homogeneous appearing Paneth cell granules from a mouse, fasted for three days. The cisternae of the endoplasmic reticulum are filled with finely granular materials similar in density to that of the secretory granules. $\times 13,000$.
3. Apical portion of an actively secreting Paneth cell from mouse 10 minutes after pilocarpine injection. The granules (G) are surrounded by halos of very low electron density secreted material (S) is seen in the crypt lumen proper (L) and in the invagination of the lumen indenting the apical cytoplasm. $\times 17,500$.

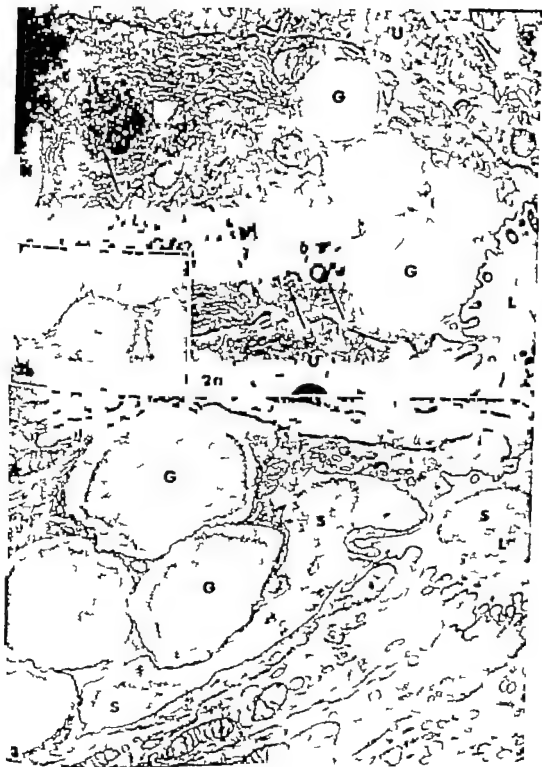


PLATE 2

EXPLANATION OF FIGURES

- 4 Portions of three Paneth cells (P) from a mouse 20 minutes after pilocarpine injection each containing secretory granules with more or less irregularly shaped halos of intermediate electron density. Again, secreted material (S) is seen in the crypt lumen and at the apical surface of the Paneth cell in the lower right of the micrograph. Note the eccentrically disposed halo material (H) in several of the granules of this cell. $\times 15,500$.
- 5 Morphologically heterogeneous Paneth cell granules from fasting mouse. A fine membrane (arrows) surrounds the relatively electron transparent halo while a distinct interface with no discernible membrane separates the halo from the central portion of the granule. $\times 16,500$.
- 6 Paneth cell granules with halos of low density seen in mouse which was fed. The halos are wider and the core of the granules smaller than those in figure 5 demonstrating the structural variation encountered with this type of granule. $\times 21,500$.



PLATE 3

EXPLANATION OF FIGURE

- 7 Portions of four Paneth cells (P) from one crypt from fasting mouse illustrating the variation in granule fine structure encountered in neighboring cells of the same crypt. The two cells in the lower half of the micrograph contain secretory granules surrounded by narrow halos which are less dense than the core of the granules (G_1) while the cells in the upper portion of the micrograph, contain granules with paler central cores surrounded by relatively dense halos (G) $\times 20,500$.

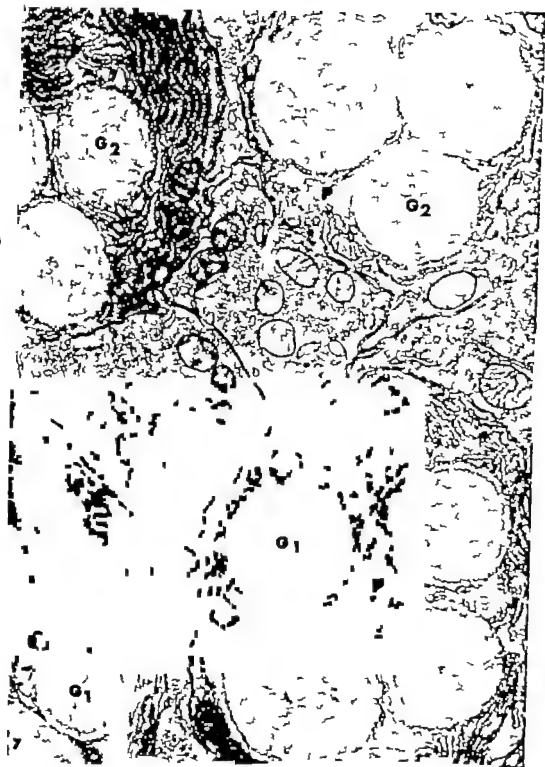


PLATE 4

EXPLANATION OF FIGURES

- 8a A portion of Paneth cell from a fasting mouse. Relatively dark halos surround pale secretory granules (G). In addition, two homogeneous appearing granules (X) and one granule with an eccentric "halo" (E) are seen near Golgi material (arrows). L, crypt lumen. $\times 18,800$.
- 8b Higher magnification of a portion of one of the granules with a dark halo. A distinct membrane (arrows) encloses the granule but no membrane is present at the interface of halo (H) and central core (C) of granule. $\times 48,500$

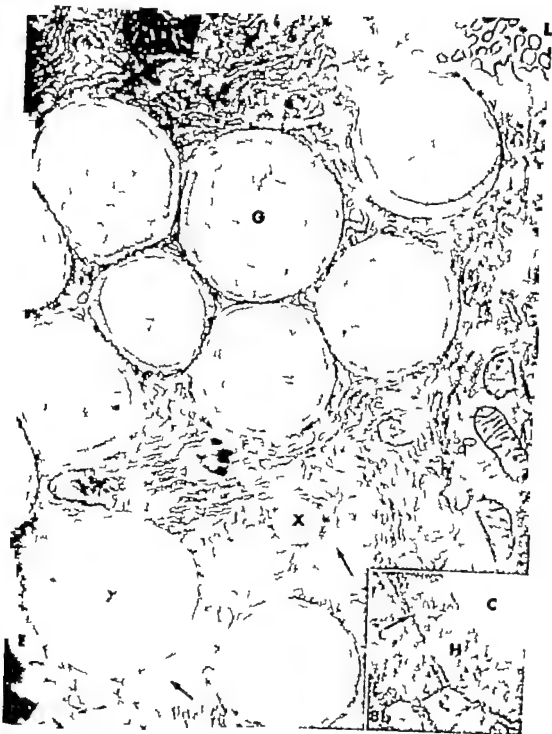


PLATE 8

EXPLANATION OF FIGURES

- 9 Apical half of Paneth cell which is probably actively secreting from fasting mouse. Extruded secretory material (\$) is seen in the crypt lumen. Two irregularly shaped granules contain membranous elements resembling Golgi material (arrows) $\times 22,000$.
- 10 Higher magnification of membranous structures (arrows) within the central core of Paneth cell granule from the same mouse $\times 37,000$.



PLATE 6

EXPLANATION OF FIGURES

- 11 Apical half of Paneth cell from a fasting rat. Note that the granules (G) are structurally homogeneous and smaller than those of mouse and human Paneth cells. L, crypt lumen. $\times 22,000$.
- 12 Apical portion of Paneth cell from fasting normal human. Note that all granules (G) while larger than those of rat Paneth cells, are structurally homogeneous. L, crypt lumen. $\times 22,000$.



Antigen (Ferritin) and Antibody Distribution in the Rat Lymph Node after Primary and Secondary Responses and after Prolonged Stimulation¹

ILHAN BUYUKOZER, KAMILE SEVKE MUTLU AND FRANK A. PEPE
Department of Anatomy School of Medicine University of Pennsylvania
Philadelphia Pennsylvania

ABSTRACT With electron microscopy it was observed that ferritin antigen was taken up in pinocytotic vesicles by the reticular cells. No antigen was observed in lymphocytes, in immature or mature plasma cells after primary and secondary stimulation, or after hyperstimulation. In hyperstimulated tissue larger number of more complex vesicles containing ferritin were visible, more ferritin was found free in the cytoplasm and larger number of multiple-membraned figures were present.

Hyperstimulation led to the appearance of activated fixed reticular cells which were characterized by cytoplasm containing rich endoplasmic reticulum with dilated cisternae and ferritin both free and in vesicles. The activated fixed reticular cells therefore contain antigenic ferritin and have the characteristics of cells engaged in protein synthesis.

Using fluorescent antibody staining no antigenic material was detectable in the antibody producing plasma cells; therefore if antigen fragments not identifiable in electron microscopy are present they are in form not available for antibody staining. Gamma-globulin was not detectable in the activated reticular cell. It may be necessary for the intact antigen to be completely modified and for the cell to lose its fixed position before γ -globulin synthesis can begin.

The response of lymphoreticular tissue to single and multiple injections of various foreign substances has been studied in detail and has been reviewed extensively (Harris and Harris, '60 McMaster '61). Reports on the ultrastructure of lymphoreticular tissue have generally been limited to normal animals to those with latent infection or to animals injected with protein material not identifiable in electron microscopy (Ilhan '61, Thilery '60 Bernhard and Gomboulan '60 Bevilacqua '61). Injection of antigenically inert inorganic substances visible in electron microscopy has been made in some cases (White Coons and Connolly '55 Sorenson '61).

A fundamental question concerning the immune response is: What is the relationship among cells and within a single cell between the localization of the stimulating antigen and the antibody produced? To attempt to answer this, one must at least be able to trace the distribution of the antigen in the cells involved in the immune response and, hopefully be able to detect the subsequent appearance of antibody. Horse spleen ferritin has been used successfully as an antigen in the

rabbit (Granick, 43 Easty and Mercer '58; Serre and Magnan de Bornier '58 Wallensiek and Coons '64). It also is antigenic in the rat as reported in this study. Since ferritin is visible in electron microscopy (Granick, '51; Easty and Mercer '58) we can hope to follow its distribution at least up to the point where it may be broken down into unrecognizable subunits. In the work presented here a systematic investigation has been made of the distribution of antigenic ferritin among the cells of the rat lymph node. The primary and secondary response to ferritin as well as hyperstimulation was studied. Ferritin was found exclusively in the reticular cells. In addition to electron microscopy the antigen distribution as well as the appearance of antibody to horse spleen ferritin in the rat was studied with the fluorescent antibody staining method (Nairn '62).

This investigation was supported by USPHS grant A-4406 and in part by the American Chemical Society Inorganic Grant.

¹Present address: Ilhan Buyukozur University of Ege School of Medicine, Department of Anatomy Bornova, Izmir, Turkey.

²Present address: Kamile Sevk Mutlu, Department of Histology and Embryology of the Medical Faculty of Ankara University Cebeci, Ankara Turkey.

Considerable evidence exists for the transition from a fixed reticular cell to a free reticular cell to an immature and then to a mature plasma cell (Fagraeus '48 McMaster '61). Evidence will be presented for the differentiation of fixed reticular cells into activated fixed reticular cells as a result of hyperstimulation with antigen. Partially activated fixed reticular cells have been described briefly (Bernhard and Granboulan, '60 Wellensiek and Coons '64). It will be shown that under hyperstimulation, the fixed reticular cell can acquire cytoplasmic characteristics of the plasma cell while still retaining recognizable antigen. The hyperstimulated tissue was also compared to tissue from animals injected with ferric hydroxide as a non antigenic particulate substance.

It is presently accepted that the plasma cell is the source of antibody (McMaster '61) yet the presence of the horse spleen ferritin used as an antigen could not be detected in the plasma cell by electron microscopy. The visualization of ferritin in the electron microscope depends on maintenance of the integrity of the ferritin molecule. If the molecule is fragmented the structure of the iron micelle which is the part of the ferritin molecule visible in electron microscopy is disrupted and no longer detectable. In considering theories of antibody formation it therefore becomes important to examine two possibilities: (a) that the plasma cell produces specific antibody in the absence of antigen and (b) that it produces antibody in the absence of whole antigen but in the presence of antigenic fragments. To this end, we have investigated the possibility that antigenic fragments of the ferritin not identifiable in electron microscopy may be present in the plasma cell. This was done using fluorescent antibody staining techniques (Nairn, '62). It will be shown that no detectable antigenic fragments are present in the plasma cell. The antigenic fragments may still be present in some modified form incapable of reacting with antibody in which case they would not be detectable with the fluorescent antibody staining technique. In addition, since the activated fixed reticular cells contain both the injected antigen and cytoplasmic characteristics of protein synthesizing cells it

is possible that they may eventually become mature plasma cells. Fluorescent antibody staining techniques were used to determine if the activated fixed reticular cells contain detectable γ -globulin.

Since the protein ferritin has a high iron content (Granick, '42, '51) we were able to follow its distribution by staining for iron in addition to using fluorescent antibody. Using both methods the distribution of ferritin in the lymph node after successive injections of ferritin could be followed.

MATERIALS AND METHODS

White female rats weighing 150-200 g were used. Horse spleen ferritin (2 X crystalline) in solution was obtained from Nutritional Biochemicals Corporation. This was dialyzed against M/60 PO₄ buffer pH 7.3 for three days with several changes and diluted to approximately 50 mg/ml with saline. The foot pads of rats were injected with 0.02-0.05 ml of the ferritin solution. Injections were made carefully into the corium to avoid hemorrhage. At daily intervals up to seven days after a single injection of ferritin, the animals were injected intraperitoneally with nembutal (0.075 ml per 100 g body weight) and the inguinal lymph nodes removed, cut into small pieces and immediately placed in fixative. Another group of animals received a second injection of ferritin one week after the first. The lymph nodes of this group were removed at daily intervals after the second injection and treated by the same procedure as those of the first group. For hyperstimulation, injections were given on the third, fourth, seventh, tenth, twentieth and twenty-third days following the first injection. If animals were injected further they received two injections per week. Each animal was sacrificed one day after its last injection. All animals received at least six injections of ferritin.

A ferric hydroxide suspension was prepared by adding sodium hydroxide to a 10% solution of ferric chloride until the pH was approximately 11. The final volume of suspension contained approximately 15 gm of $\text{FeCl}_3 \cdot 6\text{H}_2\text{O}$ in 200 ml. The suspension was dialyzed against saline made up in M/60 PO₄ buffer pH 7.4.

and was injected as described for the fer-
ritin.

Electron microscopy

A portion of each lymph node was fixed in 1% buffered osmium tetroxide pH 7.4 according to Palade ('52) for one hour and dehydrated by passing through a graded series of ethanol concentrations into 100% ethanol. The tissue was then brought into embite (Finck, '60) for embedding. Another portion of each lymph node was fixed in formalin and embedded in paraffin for histological examination in light microscopy.

Sections were obtained on a Porter Blum microtome using a diamond knife and were placed on grids coated with a uranyl film stabilized with a film of carbon. The sections were observed without further staining in order to make the ferritin more easily detectable.

Both a Hitachi HS-6 and a Siemens Elmiskop I were used for electron microscopy. Figures 1-3 and 5-7 were taken with the Hitachi, all other electron micrographs were taken with the Siemens.

Hemagglutination

Hemagglutination titration (Kabat and Mayer '51) was used to follow the appearance of antibody in the serum. The hemagglutination reactions were read according to Stavitsky ('54). Blood for this purpose was obtained from the experimental animals after removal of the lymph nodes.

Histochemistry and fluorescent staining

Inguinal lymph nodes were removed after intraperitoneal injection of the animal with nembutal (0.075 ml per 100 gm body weight). For iron determination the nodes were fixed in 95% ethanol, embedded in paraffin, sectioned (6-8 μ thick) and stained for organic iron as well as inorganic iron (Glick, 49). The Prussian blue reaction for ferric iron and the Turnbull blue reaction for ferrous iron were both used.

For fluorescent staining the procedure described by Sainte-Marie ('62) for paraffin embedded tissue gave the best results. In addition to this technique, frozen sec-

tions (25 μ thick) were stained after treatment with desoxycholate to improve permeability to the stain. The sections thus treated were very fragile and difficult to handle. The procedure was as follows: (1) fresh tissue was fixed in 3% formaldehyde in 0.05 M PO₄ buffer pH 7-7.2 at 4 C for one and one-half hours (2) fixed tissue was washed in buffer above at 4 C for one-half hour (3) washed tissue was frozen and sectioned, (4) the sections were placed in cold buffer then transferred to 0.5% desoxycholate in buffer for 5-8 minutes at room temperature (5) sections were washed with cold buffer for one-half hour with three changes (6) sections were transferred to the staining solutions for one-half hour at room temperature, then washed for one-half hour at room temperature. If the sandwich staining technique (Nairn, '62a) was used, restaining and washing was done at this point. The stained sections were brought into 95% ethanol for 15 minutes to fix the stain (Sainte-Marie '62) then washed with buffer and mounted on slides in glycerol (9 parts glycerol plus 1 part buffer).

Impression films were also made by pressing the cut surface of a lymph node against a glass slide. The slide was allowed to dry 5-10 minutes at room temperature and fixed in absolute methanol for five minutes. The slide was transferred to a solution of 0.5% sodium desoxycholate in saline made up in M/60 PO₄ buffer pH 7.3 for 3-5 minutes and washed with the buffered saline with several changes for one-half hour. The slide was stained for one and one-half hours at 37 C in a humid atmosphere to prevent drying. It was washed 24 hours with several changes of the buffered saline and was finally mounted in buffered glycerol (9 parts glycerol plus 1 part buffered saline).

Preparation of normal rat γ -globulin

The blood from 17 normal female rats (200 gm) was obtained by cardiac puncture. Purified normal γ -globulin was isolated from the serum by the ethanol fractionation procedure (Deutsch, '52) as described for rat serum.

Preparation of antisera

For preparation of anti-rat γ -globulin antibody six normal rabbits (8-10 lbs.) were injected with rat γ -globulin. On the first day they received one injection intraperitoneally and one intravenously. Each injection consisted of 0.5 ml of normal rat γ -globulin (10 mg protein/ml) in physiological saline made up in M/60 PO buffer pH 7.4. Two weeks later they received 0.5 ml of the antigen intraperitoneally and these injections were continued once or twice a week for three months. During the injection period as soon as the antibody titer reached a maximum the animals were bled once a week from the lateral ear vein. In this manner 50-60 ml of blood could be obtained from each animal at one bleeding. The final bleeding was by heart puncture. After collecting the blood, it was allowed to clot at room temperature for approximately two hours. The clot was freed from the walls of the beaker and it was allowed to stand overnight in the refrigerator. The serum was removed and centrifuged then frozen until further use.

For preparation of anti ferritin antibody six normal rabbits were injected with ferritin as described above. The solution of ferritin used contained approximately 10 mg of protein per milliliter. Serum was obtained as already described and frozen until further use. In addition normal rabbits were bled to obtain normal serum.

Fractionation of the γ -globulin from immune and normal sera

The antisera and the normal serum were fractionated by the ethanol fractionation procedure (Deutsch '52) as described for rabbit serum. The purified antibody γ -globulins were kept frozen until used. The yields of antibody γ -globulin were as follows: 1400 ml normal serum gave 11 gms normal γ -globulin; 900 ml anti ferritin antiserum gave 5 gms of antibody to ferritin; 900 ml anti rat γ -globulin antiserum gave 6 gms of antibody to rat γ -globulin.

Fluorescent labeling and purification of labeled conjugates

Ferritin as well as antibody and normal γ -globulins were conjugated with fluo-

rescein isothiocyanate (Naim, '62). The conjugates were then dialyzed overnight against saline made up in M/60 PO buffer pH 7.4. All conjugates were then passed through Sephadex (G-25 medium). The purified conjugates were stored frozen. Just before use the conjugates were absorbed with calf liver powder by mixing 1.5 ml of the conjugate plus 100 mg of the calf liver powder. This mixture was stirred at room temperature for one and one-half hours and then centrifuged.

RESULTS

The appearance of circulating antibody was followed in the serum of the hyperstimulated group of animals by hemagglutination titration (Kabat and Mayer '61) and was found to increase during the period over which injections were made. The interval between the first and second injections was three days. Before the third injection there was a rest period of 11 days. A large increase in circulating antibody characteristic of a secondary response occurred after the third injection.

As a result of injection of the horse spleen ferritin into the hind-foot pad, there was an increase in the size of the individual nodes. The wet weight of individual nodes was at least twice that of a normal node. Sometimes a fusion of two or more nodes seemed to occur. In one animal, after 12 injections, a mass of lymphoid tissue with a weight four and one-half times that of a normal node was found. Injection of the $\text{Fe}(\text{OH})_3$ suspension had no effect on the size of the lymph nodes.

Ferritin could easily be identified in electron microscopy by the characteristic tetrad structure of the iron micelles (Fig. 4) or by its high density at lower magnifications (Figs. 1-3). The solution used for injection was also examined by spreading it on a carbon film and the same tetrad structure was observed.

In this study we have paid particular attention to the free and fixed reticular cells, to lymphocytes and to plasma cells. Since the ultrastructural characteristics of these cells have been described extensively (Bernhard and Granboulan, '60; Bessis, '61) only a brief description of pertinent characteristics will be given here. The

cytoplasm of the reticular cells has very little, if any endoplasmic reticulum or processes, but does have many vesicles of widely varying sizes, containing injected material (fig. 1). The cell generally has abundant cytoplasm with long processes. The mature lymphocyte is characterized by a small rim of cytoplasm surrounding a centrally located nucleus (fig. 2) with the cytoplasm practically devoid of organelles. The mature plasma cell is a rounded cell with an eccentrically placed nucleus. It has an abundant rough endoplasmic reticulum with greatly dilated cisternae and a well developed Golgi zone (fig. 5). In addition to the mature form of the plasma cell, immature stages may be observed especially after secondary stimulation of the tissue (fig. 6).

In both those animals given one injection and those given two injections ferritin was taken up exclusively by the reticular cells. It was present both diffusely dispersed throughout the cytoplasm and in vesicles (figs. 1-3). With increasing time after the first injection, vesicles with many layers of membrane became common (fig. 7). The occurrence of these increased somewhat after the second injection. Although ferritin free in the cytoplasm was distributed uniformly throughout the cytoplasm of reticular cells it was rarely found in nuclei or mitochondria. When it was, its presence was associated with areas of poor fixation or when high concentrations were present, abnormal displacement of ferritin in the direction of sectioning (J. M. Marshall personal communication). Pinocytotic vesicles were not seen in mature plasma cells (fig. 5). Ferritin was not observed in the lymphocytes or in mature or immature plasma cells.

In animals which received a second injection of antigen there was a more vigorous uptake of the antigen. This was reflected in more numerous vesicles of larger size. In addition more vesicles were observed of the type shown in figure 3 which probably represents a fusion of several small vesicles with a larger vesicle. Although a small increase in the number of mature plasma cells was observed after the first injection, this in-

crease was greater after the second injection. In addition immature plasma cells (fig. 6) became abundant.

The manner of uptake and cellular distribution of ferritin observed in hyperstimulated animals was no different from that after primary and secondary stimulation. In both instances: (1) uptake was limited to reticular cells and (2) ferritin was found in pinocytotic vesicles as well as free in the cytoplasm. Single vesicles containing uniformly dispersed ferritin were seen as well as complex vesicles containing more densely packed ferritin. However in the hyperimmunized animals these highly complex vesicles (fig. 8) occurred in greater number and were larger. The amount of ferritin free in the cytoplasm was likewise increased. An increase in the number of multiplo-membraned figures was also observed in the reticular cells. Ferritin was not found in the mitochondria or in nuclei even when the concentration of ferritin free in the cytoplasm became very high. The high concentration of ferritin in the reticular cell seen in figure 9 is in striking contrast to the absence of ferritin in the intimately related plasma cell. No evidence was found that would indicate the crossing over of ferritin either endogenous or exogenous, from the reticular cell to the immature plasma cell, the mature plasma cell, or the lymphocyte.

The major difference occurring in the tissue as a result of hyperstimulation with antigen was found in the fine structure of the fixed reticular cells. The primary characteristics of the normal fixed reticular cell (Moo '63 '64; Clark, '62; Han '61; Sorenson '60) are (1) cytoplasm containing many vesicles few ribonucleoprotein particles and little if any endoplasmic reticulum; and (2) long processes the ends of which meet processes of other fixed reticular cells forming the reticulum network of cells in the lymph node. In addition to taking up large amounts of the injected antigen the fixed reticular cell showed changes in its cytoplasm as a result of hyperstimulation. An abundant rough endoplasmic reticulum with dilated cisternae developed until the cytoplasm of the activated reticular cell resembled that of the mature plasma cell in all respects.

except that (1) it contained ferritin both in vesicles and free in the cytoplasm (fig 12); and (2) it maintained the shape and fixed position of the normal fixed reticular cell. This latter characteristic was used for distinguishing between activated fixed reticular cells and plasma cells. Transitional stages from the normal fixed reticular cell to the fully activated fixed reticular cell were observed in some cases, depending on the plane of section it was difficult to determine if the cytoplasm of a plasma cell or that of an activated fixed reticular cell was being observed. However in cases where the cells were clearly identifiable as mature or immature plasma cell ferritin was never observed whereas in cases where the cells were clearly identifiable as fully or partially activated fixed reticular cells ferritin was always observed both free in the cytoplasm and in vesicles. The amount of ferritin in the cytoplasm of the fully activated fixed reticular cell was less than that found in the transitional stages. In figure 10 is an example of the cytoplasm of a normal fixed reticular cell. This particular cell is from hyperstimulated tissue but has not become activated. In figure 11 can be seen the beginnings of the formation of the endoplasmic reticulum in a fixed reticular cell. Some ribonucleoprotein particles can be seen on the membranes of the endoplasmic reticulum as well as free in the cytoplasm. The fully activated fixed reticular cell with dilated rough endoplasmic reticulum can be seen in figure 12. Ferritin is visible in membrane lined vesicles as well as free in the cytoplasm.

Occasionally the activated reticular cells were seen in normal tissue, but this was rare. In order to check the possibility that non-antigenic stimulation of the lymph node might account for their increase in number a suspension of ferric hydroxide was injected into control animals using the same injection schedule as that for ferritin. No difference between this and the normal tissue could be found with respect to the occurrence of activated fixed reticular cells. An example of uptake of the ferric hydroxide suspension by a fixed reticular cell can be seen in figure 13. Dense accumulations

of ingested material are present in vesicles. Uptake was limited to the reticular cells as was the case after injection of ferritin. The amorphous ferric hydroxide was never found free in the cytoplasm. The ferritin formed as a result of uptake of the ferric hydroxide was distributed within the cell in the same manner as that observed after injection of ferritin.

The distribution of the antigen, horse spleen ferritin, could also be followed by staining for iron (Glick, 49). Staining reactions were obtained for organic iron and for inorganic ferric iron (Prussian blue). Staining for ferrous iron was always negative. All tissue from injected animals contained large accumulations of iron containing material. The normal lymph nodes had little iron positive material.

After the first injection the iron was generally found just under the capsule in the subcapsular sinus and in the peripheral parts of the cortex. A few cells containing iron could be found in the medullary sinuses. After the second injection the iron distribution in these areas increased and iron positive material was seen in the deeper parts of the cortex and the medulla (figs. 14 and 15). With increasing number of injections the amount of iron positive material increased in all parts of the lymph node. In figure 16 some of the iron positive material can be seen at higher magnification. Note the appearance of many positively stained granules of widely varying sizes.

In the ferric hydroxide injected animals Prussian blue staining of the nodes for ferric iron showed a larger amount of iron positive material than in the normal nodes. However organic iron staining was practically the same as that in the normal nodes. The Prussian blue positive material was not present in the large quantities observed with ferritin injected material. This may be because the ferric hydroxide suspension showed a tendency to accumulate at the injection site. The iron positive material was distributed throughout the lymph node.

In addition to iron staining fluorescently labeled anti-ferritin antibody was used to determine the distribution of the horse spleen ferritin antigen. Normal tissue

showed no non-specific staining with fluorescein labeled γ -globulin or fluorescein labeled anti-ferritin antibody. In all tissue even completely unstained, autofluorescence of the connective tissue eosinophils was observed. In figure 16 is an example of a section from an injected animal stained with fluorescein labeled normal γ -globulin. No non-specific staining was observed but the autofluorescent eosinophils are visible. These could easily be distinguished from specifically stained cells. The distribution of staining with fluorescent anti-ferritin antibody corresponded exactly to that already described for iron staining in the injected tissue. In figure 17 an example of fluorescent anti-ferritin antibody staining of tissue which received five injections of ferritin is seen. In figure 18 at higher magnification the characteristic pattern of staining observed with the anti-ferritin antibody is visible. This corresponds to the iron positive staining previously described (Fig. 10) and represents staining of ferritin taken up in pinocytotic vesicles by the reticular cells.

In order to detect the presence of γ -globulin containing cells, the tissue was stained with fluorescent anti-rat γ -globulin. This stained both the cells containing normal rat γ -globulin and those containing antibody rat γ -globulin. Since the fluorescent anti-rat γ -globulin gave the least staining reaction of the fluorescent stains used, it was particularly suitable to our search for γ -globulin in activated reticular cells. We looked for a staining pattern consisting of fluorescent foci similar to that obtained with fluorescent anti-ferritin antibody or for fluorescent cells with long processes. Although many stained cells were observed which suggested these characteristics, none were convincing enough for identification as stained activated reticular cells. Rounded cells with an eccentric unstained nucleus characteristic of plasma cells were readily observed both in normal tissue and in injected tissue. They were much more abundant in the injected tissue. An example of a smear preparation stained with fluorescent anti-rat γ -globulin is shown in figure 20. The animal used received one injection of

ferritin. In figure 21 these cells are stained in a section of tissue from an animal injected five times with ferritin.

Staining of only the cells containing specific rat antibody to ferritin was accomplished by two methods. The sandwich technique (Nairn, '62a) involved first staining the tissue with ferritin and then with fluorescent anti-ferritin antibody. In this case cells containing anti-ferritin antibody picked up the ferritin which was subsequently stained by the fluorescent anti-ferritin antibody. In addition, ferritin was labeled directly with fluorescein and used as a direct stain for the antibody containing cells. The intensity of fluorescence obtained with this latter method was much less than with the other methods used. Examples of the staining obtained by both of these methods can be seen in figures 22 and 23. Plasma cells were stained in both cases. In the case of the sandwich staining technique since fluorescent anti-ferritin antibody was used, the reticular cells which picked up the injected ferritin were stained in addition to the antibody containing plasma cells.

DISCUSSION

As seen in the electron microscope the ferritin molecule has a diameter of approximately 100 Å and contains four ferrioxenous micelles each 12.7 Å in diameter located in the center of the molecule (Farrant '34). This structure permits identification of ferritin in tissues. Ferritin is occasionally observed in normal lymph nodes, probably as a result of uptake and digestion of erythrocytes (Beaumont '61a). There is no detectable difference in the electron microscope image of injected horse ferritin and normally occurring rat ferritin. However because of the rarity with which ferritin was seen in normal animals and its great abundance in the experimental animals, it was a simple matter to follow the uptake of the injected material.

Ferritin was taken up exclusively by the reticular cells and was detectable in the cytoplasm in membrane lined vesicles and also freely dispersed. No differences were observed in the manner of uptake after the first and second injections and

after hyperstimulation. However the avidity of uptake was substantially greater after the second injection and after hyperstimulation as evidenced by a greater concentration of ferritin distributed in the cytoplasm and a greater number of vesicles filled with ferritin in the cytoplasm. Since ferritin was found both in vesicles and free in the cytoplasm it is possible that after uptake by pinocytosis it may be released into the cytoplasm by rupture of vesicles. Another possibility is that the ferritin diffused through the membranes of the vesicles. We have never seen evidence of the rupture of vesicles which could not be attributed to poor fixation. Diffusion of ferritin through the membranes would be difficult to observe unequivocally. It has been shown that injected iron compounds when taken up by reticular cells can be utilized in the formation of ferritin (Muir and Goldberg, '61; Richter '59). Therefore another possible explanation for the appearance of ferritin both in vesicles and free in the cytoplasm is that the exogenous (antigenic) ferritin is digested in the vesicles releasing iron compounds which are then utilized in the production of endogenous ferritin (Farquhar and Palade '61). We have seen evidence of digestion of ferritin in vesicles. This is shown in figure 4 where some of the ferritin has become amorphous, indicative of disruption of structure and digestion. Partially digested ferritin, which is seen only in vesicles is the best identification we have for the exogenous ferritin. The ferritin free in the cytoplasm is probably endogenous. Ferritin was not observed in nuclei or in the mitochondria of any of the cells.

After the first injection vesicles containing ferritin were generally characterized by a uniform distribution of ferritin molecules more or less densely packed within the vesicle. With increasing time the more densely packed vesicles were more prevalent. After the second injection and hyperstimulation many examples of more complicated vesicles such as that in figures 3 and 8 were observed. Note the more densely packed ferritin in some areas of the large vesicle in figure 3. This probably represents fusion of several small vesicles with a larger one. If so

the smaller vesicles on fusion seem to have lost their membranes but their contents are still held together in some manner. In addition to vesicles with single membranes, at later times after the first injection vesicles with multiple membranes were observed (fig. 7). These were even more abundant after the second injection and after hyperstimulation. The formation of multiple membranes around the ferritin masses is consistent with similar observations by Sorenson ('61) with colloidal gold.

The major difference between hyperstimulated tissue and that receiving a primary or secondary stimulation was the presence of activated reticular cells at different stages of activation. The fully activated reticular cell is characterized by (1) being part of the reticulum network of reticular cells in the tissue; (2) having cytoplasm with a highly developed endoplasmic reticulum similar to that of the plasma cells; (3) the presence of ferritin in the cytoplasm both free and in vesicles. Occasionally activated reticular cells have been observed in normal and immature tissue (Moe '64; Bernhard and Graboulian, '60; Wellenstiek and Coons, '64) using electron microscopy. These observations were of the first stages in the normal differentiation from the fixed reticular cell as a stem cell to the plasma cell (Fagreaus, '48; McMaster '61). In this process, before the cytoplasm becomes recognizable as that of an immature plasma cell, the reticular cell is freed of its fixed position and becomes rounded. The cell seen in figure 12 is not rounded. It is still fixed in the reticulum but has cytoplasm which is similar morphologically to that of the plasma cell, except that it contains ingested antigen. Therefore under hyperstimulation with antigen differentiation of the cytoplasm of the fixed reticular cell may take place before the cell is able to lose its fixed position in the reticulum. Observation of these fully activated reticular cells gives additional support to evidence pointing to the fixed reticular cell as a stem cell in normal differentiation to the plasma cell. Also the activated reticular cell is the only cell in which clearly identifiable antigen and an elaborate endoplasmic reticulum

characteristic of protein secreting cells was observed together.

During the preparation of this manuscript, Wellenick and Coons ('64) published electron microscopic observations on the distribution of injected horse spleen ferritin in rabbit popliteal lymph nodes. They found ferritin free in the cytoplasm and nuclei of reticular cells both after the first injection and a second injection five weeks later. Some reticular cells contained ferritin only in the cytoplasm. After the second injection ferritin was also found in the cytoplasm and nuclei of many immature and some mature plasma cells. In our observations the appearance of ferritin in nuclei was always associated with areas of poor fixation. In addition depending on the plane of section, we found that activated reticular cells could be mistaken for plasma cells. Whenever we were certain of the identification of a plasma cell we could not observe ferritin in it and likewise when we were certain of the identification of an activated reticular cell we always observed ferritin in it. No detectable intact antigen could be found in mature or immature plasma cells even when these cells were found in contact with reticular cells which contained extremely large amounts of ferritin (figs. 8 and 9).

It is possible to distinguish between destructive and elective theories of antibody formation (Flacher '64) by determining if any part of the antigenic molecule is present in the antibody producing plasma cell. With electron microscopy we have shown that the intact antigen ferritin, is not present in the plasma cell. The possibility that the plasma cell may contain antigenic fragments of the original antigen was investigated by staining with fluorescein labeled anti-ferritin antibody. No staining was observable. Therefore if antigenic fragments are present in the plasma cell they must be present either in concentrations below the limit of detectability with the fluorescent antibody stain or in a form such that they cannot be stained with fluorescent antibody. Considerable evidence is available for the retention of antigen fragments by tissues in a form which is not available for precipitation with antibody (Haurowitz et al.

'55 Hawkins and Haurowitz, '59 Campbell and Garvey '61). These antigen fragments may have only one antigenic determinant per fragment in which case reaction with bivalent rabbit antibody would not produce a precipitate (Pepe and Singer '59). In this case staining of the tissue would only be observed if the antigen fragment was fixed to insoluble material in the cell. Alternatively the antigen fragment may be combined with other cell constituents such that its antigenicity as reflected in its reactivity with formed antibody would be absent but it would still be able to direct the synthesis of specific antibody. Such a situation has the advantage that the synthesis of specific antibody could be directed without the possibility of the antibody blocking the effectiveness of the antigen fragment in the further synthesis of antibody.

An important consideration of this work was to determine if the activated reticular cells produce γ -globulin. No clear-cut evidence of staining of the activated reticular cells was observed. It may be that the large number of brightly staining plasma cells present in the tissue obscured the identification of the less numerous activated reticular cells. However it seems more likely that the ergastoplasm of the activated reticular cell may be for elaboration of enzymes needed to process the antigen still present in the cytoplasm of these cells, and that antibody production by the ergastoplasm is only initiated when all the intact antigen is modified and the cell loses its fixed position to become a plasma cell.

Since the protein ferritin has a high iron content (Granick, '42, '51) its distribution in the lymph node was followed by histochemical methods for iron in addition to fluorescent antibody staining methods. In both cases the presence of ferritin was limited exclusively to reticular cells. After successive injections of ferritin into the foot pad, ferritin was progressively distributed through the subcutaneous sinuses, cortex and medulla, thus following the pathway of lymph from afferent to efferent vessels.

Injection of ferritin into the foot pad resulted in enlargement of the inguinal lymph nodes draining the injected foot.

This is a general result of antigenic stimulation (Ringertz and Adamson, '50)

ACKNOWLEDGMENT

The authors gratefully acknowledge the assistance of Mr Joseph Martin in parts of this work.

LITERATURE CITED

- Bernhard, W. and N. Granboulan 1960 Ultrastructure of immunologically competent cells in Ciba Foundation Symposium on Cellular Aspects of Immunity J. and A. Churchill Ltd. London, p. 92.
- Bessis, M. C. 1961 Ultrastructure of lymphoid and plasma cells in relation to globulin and antibody formation. *Lab. Invest.*, 10: 1040.
- Bessis Marcel 1961a The Blood Cells and Their Formation. In *The Cell* Vol. 5 Ed. by Jean Brachet and Alfred E. Mirsky Acad. Press, New York and London.
- Campbell, Dan H., and J. stine S Garvey 1961 The Fate of Foreign Antigen and Speculations as to its Role in Immune Mechanisms. *Lab. Investigations*, 10: 1126-1150.
- Clarke Sam L., J. 1962 The reticulum of lymph nodes in mice studied with the electron microscope. *Am. J. Anat.*, 110: 217-257.
- Deutsch H. F. 1952 Separation of antibody active proteins from various animal sera by ethanol fractionation techniques. *Meth. in Med. Research*, 5: 284-300.
- East G. C. and E. H. Mercer 1958 Electron microscopic studies of the antigen-antibody complex. *Immunology* 1: 353-364.
- Fagraeus A. 1948 Antibody production in relation to the development of plasma cells. *Acta Med. Scand.*, 130 Suppl., 204: 7-122.
- Farquhar Marilyn G. and George E. Palade 1961 Glomerular permeability II. Ferritin transport across the glomerular capillary wall in nephrotic rats. *J. Exper. Med.*, 114: 669.
- Farrant, J. L. 1954 An electron microscopic study of ferritin. *Biochem. et Biophys. Acta*, 13: 569-576.
- Fueck, H. 1960 Epoxy resins in electron microscopy. *J. Biophysic. Biochem. Cytol.*, 7: 27-30.
- Flacher David S. 1964 Theories of antibody formation A review *Yale J. Biol. and Med.*, 37: 1-30.
- Glick, David 1949 Techniques of Histo and Cytochemistry p. 19-20 Interscience Publishers Inc., New York.
- Granick, S. 1943 Ferritin. I. Physical and chemical properties of horse spleen ferritin. *J. Biol. Chem.*, 146: 451-461.
- 1943 Ferritin IV occurrence and immunological properties of ferritin. *J. Biol. Chem.*, 146: 157.
- 1951 Structure and physiological functions of ferritin. *Physiol. Rev.* 31: 489-511.
- Han, Seong Soo 1961 The ultrastructure of the mesenteric lymph node of the rat. *Am. J. Anat.*, 109: 183-225.
- Harris, T. N. and S. Harris 1960 Cellular sources of antibody: a review of current literature. *Ann. N. Y. Acad. Sci.*, 90: 948.
- Haurowitz, F. W. Friedberg, H. Walker and M. Jensen 1955 The metabolic fate of "internally" and "externally" labeled protein antigens. *Proc. Internat. Conf. on Peaceful Uses of Atomic Energy Geneva*, 13: 545-547.
- Hawkins J. C., and F. Haurowitz 1959 Recovery of intravenously injected protein antigens from rat spleen. *Biochem. J.* 77: 80.
- Kabat, E. A., and M. M. Mayer 1961 Experimental Immunochimistry Second Ed. Charles C. Thomas, pp. 120-122.
- McMaster P. D. 1961 Antibody formation. In *The Cell*, vol. 5, ed. by Jean Brachet and Alfred E. Mirsky Academic Press, p. 233-244.
- Moe R. E. 1963 Fine structure of the interluminal and sinuses of lymph nodes. *Am. J. Anat.*, 112: 311-335.
- 1964 Electron microscopic appearance of the parenchyma of lymph nodes. *Am. J. Anat.*, 114: 341-369.
- Moore B. D., V. R. Minshaw and M. D. Schenberger 1961 The transport and distribution of colloidal iron and its relation to the ultrastructure of the cell. *J. Ultrastruct. Research* 5: 244-255.
- Muhr A. R., and L. Goldberg 1961 Observations on subcutaneous macrophage phagocytosis of iron-dextran and ferritin synthesis. *Quart. J. Exp. Phys.* 46: 289.
- Nairn, R. C. (Editor) 1963 *Fluorescent Protein Tracing*, E. and S. Livingstone Ltd. Edinburgh and London, p. 19-22.
- 1963a *Fluorescent Protein Tracing*, E. and S. Livingstone Ltd., Edinburgh and London, p. 122-126.
- Palade, G. 1962 A study of granules for electron microscopy. *J. Exp. Med.* 65: 235-294.
- Pepe Frank A., and S. J. Singer 1960 Physical-chemical studies of soluble antigen-antibody complexes. X. The reaction of univalent protein antigen with antibody. *J. Amer. Chem. Soc.*, 81: 3576-3587.
- Richter Goetz, W. 1950 The cellular transformation of injected colloidal iron complex into ferritin and hemosiderin in experimental animals. *J. Exp. Med.*, 109: 197.
- Ringertz, N., and C. A. Adamson 1950 The lymph-node response to various antigens. *Acta Path. Microbiol. Scand. Suppl.* 80: 1-49.
- Saint-Marie, G. 1962 A paraffin embedding technique for studies employing immunofluorescence. *J. Histochem. Cytochem.* 10: 250-258.
- Serre, A., and M. B. Magnan de Brozier 1958 La methode de diffusion d'osmium oxyde. I. etude immunologique de la ferritine. *Montpellier Medical*, 53: 119-124.
- Sorenson, George D. 1960 An electron microscopic study of popliteal lymph nodes from rabbits. *Am. J. Anat.*, 107: 73-96.
- Sorenson, G. 1961 Electron microscopic observation on the fate of colloidal gold in popliteal lymph nodes of rabbits. *Anat. Rec.*, 159: 579 (abstract).

- Swetsky A. B. 1964 Micromethods for the study of proteins and antibodies. *J Immun.*, 71 360-367
- Thery J. P. 1960 Microcinematographic contributions to the study of plasma cells in Ciba Foundation Symposium on Cellular Aspects of Immunity J and A. Churchill Ltd., London, p. 59
- Wellsiek, Hans-Jobst, and Albert H. Coons 1964 Studies on antibody production IX. The cellular localization of antigen molecules (ferritin) in the secondary response. *J Exper. Med.*, 119 685-696.
- White R. G., A. H. Coons and J. M. Connolly 1953 Studies on antibody production. III. The alumi granuloma. *J Exper Med.*, 102: 73.

PLATE I

EXPLANATION OF FIGURES

- 1 Portion of reticular cell from a rat lymph node two days after the second injection of ferritin. Many ferritin containing vesicles (f-s) are present in the cell process. One of these can be seen at higher magnification in figure 3. Mag. 18,000 X
- 2 From a rat lymph node one day after the first injection of ferritin. Ly lymphocyte. Mag. 20,000 X



PLATE 2

EXPLANATION OF FIGURES

- 3 From a rat lymph node two days after the second injection of ferritin. In this higher magnification of the largest vesicle in figure 1, individual ferritin molecules are resolved. Ferritin molecules are also present in the cytoplasm. M g. 100,000 X
- 4 High magnification of the contents of vesicle one day after the first injection of ferritin. The tetrad characteristic of ferritin can be seen (f) A mass of partially digested ferritin is also visible (fe-d) Mag. 480,000 X



PLATE 3

EXPLANATION OF FIGURE

- 5 A mature plasma cell with highly developed ergastoplasm, two days after the first injection of ferritin. N nucleus, G, golgi. Mag. 20,000 X



PLATE 4

EXPLANATION OF FIGURES

- 6 A mature plasma cell (PI) surrounded by immature plasma cells (IP) two days after the second injection of ferritin. Mag. 10,000 x
- 7 A reticular cell containing multiple membraned vesicles (m) and ferritin free in the cytoplasm, six days after the first injection of ferritin. Mag 100,000 x

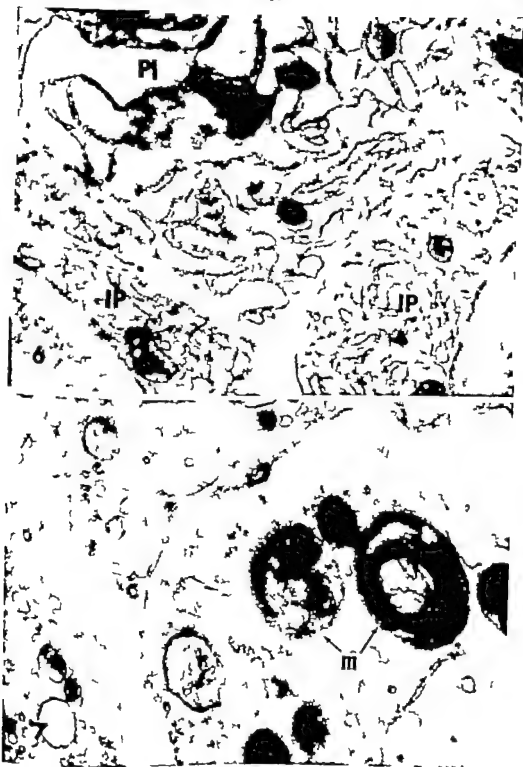


PLATE 5

EXPLANATION OF FIGURES

- 8 Lymph node from rat injected six times with ferritin. Many large complex vesicles containing ferritin are present in reticular cell (R) which is closely associated with plasma cell (Pl) Mag. 50,000 \times
- 9 From lymph node of rat injected 15 times with ferritin. Note heavy concentration of ferritin in the reticular cell (R) in contrast to absence of ferritin in the intimately related plasma cell (Pl) Mag. 50,000 \times

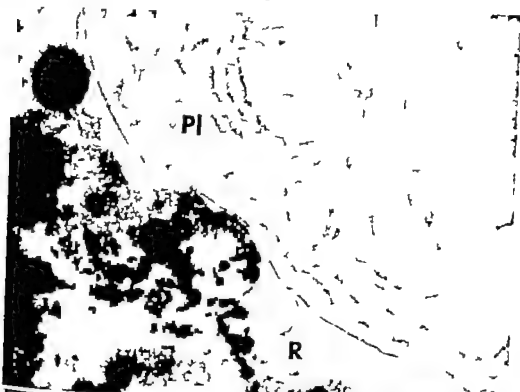


PLATE 6

EXPLANATION OF FIGURES

- 10 Portion of normal fixed reticular cell containing ingested ferritin, from a rat lymph node injected six times with ferritin. fe-v ferritin containing vesicles. Mag. 40,000 X
- 11 Portion of a partially activated fixed reticular cell from a rat lymph node injected six times with ferritin. Some rough endoplasmic reticulum (e.r.) and free ribosomes () can be seen in addition to ingested ferritin (fe-v) Mag. 35,000 X

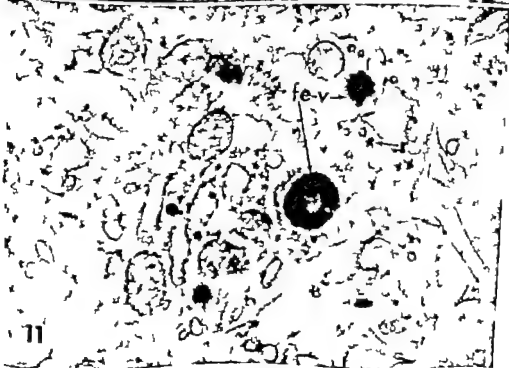
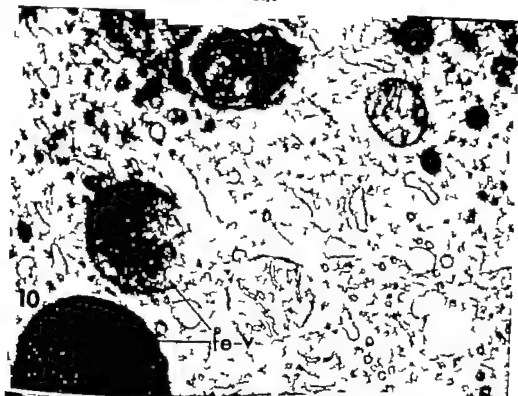


PLATE 7

EXPLANATION OF FIGURE

- 12 Portion of fully activated reticular cell from a rat lymph node injected six times with ferritin. Cytoplasm has an abundant rough endoplasmic reticulum (er) as well as complex vesicles containing ferritin (fe.) Mag. 20,000X In the inserts ferritin can be seen both in the vesicles and free in the cytoplasm. Mag. 100,000X

Sam Serebreny, Kamille Sevkil Muffin and Frank A. Pope

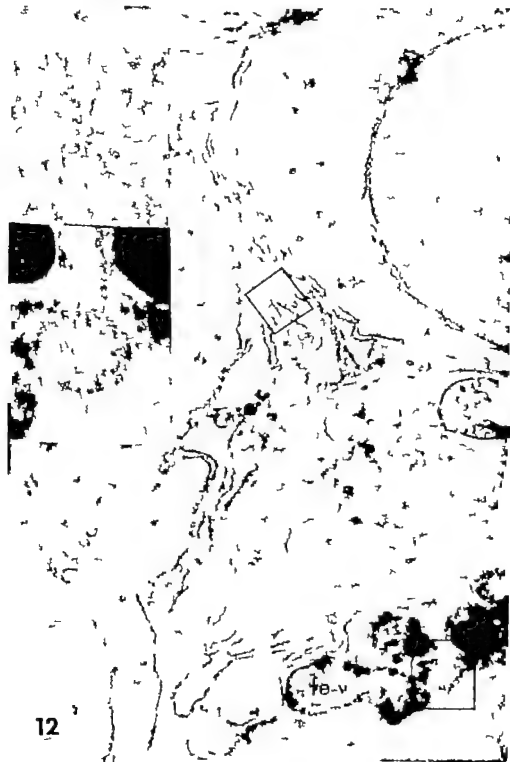


PLATE 8

EXPLANATION OF FIGURES

- 13 From lymph node of a rat injected six times with ferric hydroxide. The fixed reticular cell (R) contains ingested ferric hydroxide (FH). Also, some ferritin can be seen free in the cytoplasm. Mag. 35,000 \times .
- 14 From lymph node of rat given two injections of ferritin. Paraffin section stained for organic iron. Iron positive material is present deep in the cortex. Mag. 450 \times .
- 15 From lymph node of rat given two injections of ferritin. Paraffin section stained for organic iron. Iron positive material is also present in the medullary cord. Mag. 450 \times .

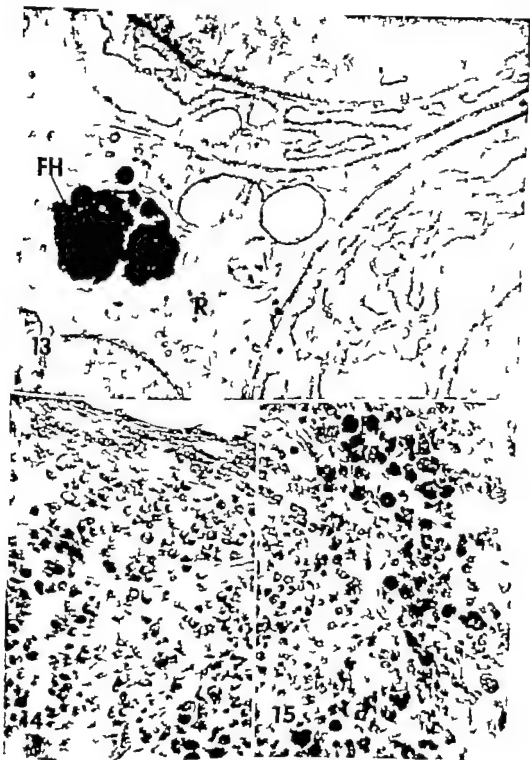


PLATE 9

EXPLANATION OF FIGURES

- 16 From lymph node of rat given five injections of ferritin. Paraffin section stained with fluorescein labeled normal γ -globulin. Auto-fluorescent eosinophils are visible. Mag. 500 \times
- 17 From lymph node of a rat given five injections of ferritin. Paraffin section stained with fluorescein labeled anti-ferritin antibody. Mag. 500 \times
- 18 From lymph node of a rat given five injections of ferritin. Paraffin section stained with fluorescein labeled anti-ferritin antibody. Granular structure of the specific staining is seen at this magnification. Mag. 2,400 \times (enlarged from 1,000 \times)
- 19 From lymph node of rat given five injections of ferritin. Paraffin section stained for organic iron. Granular structure of the staining can be compared with that of figure 18. Mag. 2,400 \times (enlarged from 1,000 \times)

Don Reynolds, Kazuo Seki, Mutsa and Frank A. Pope

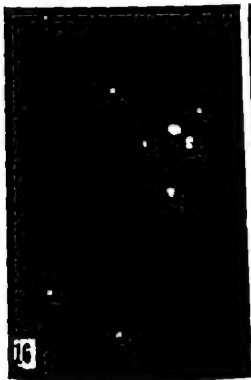
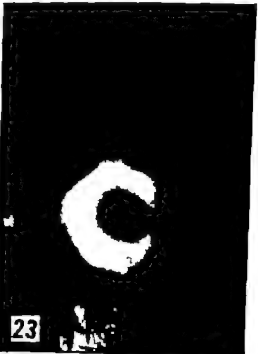
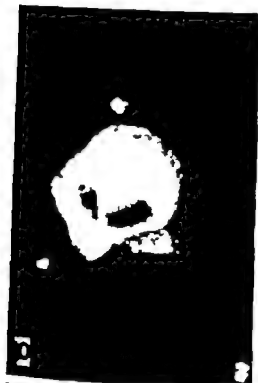


PLATE 10

EXPLANATION OF FIGURES

- 20 Impression film from a lymph node from rat given one injection of ferritin. Stained with fluorescein labeled anti-rat γ -globulin antibody. Staining of plasma cells occurs. Mag. 28,000 \times (enlarged from 1,000 \times)
- 21 From lymph node of a rat given five injections of ferritin. Paraffin section stained with anti-rat γ -globulin antibody. Staining of plasma cells occurs. Mag. 2,800 \times (enlarged from 1,000 \times)
- 22 From lymph node of a rat given twelve injections of ferritin. Frozen sections stained with ferritin followed by fluorescein labeled anti-ferritin. Staining of plasma cells containing anti-ferritin antibody occurs. Mag. 3,200 \times (enlarged from 1,000 \times)
- 23 From lymph node of rat given five injections of ferritin. Paraffin section stained with fluorescein labeled ferritin. Staining of plasma cells containing anti-ferritin antibody occurs. Mag. 3,500 \times (enlarged from 1,000 \times)



A Histochemical Study of Testosterone-induced Changes in the Submandibular and Sublingual Gland of Mice¹

JOSEPH H. KRONMAN and JOSEPH J. SPINALE
Tufts University School of Dental Medicine Boston, Massachusetts

ABSTRACT Prior studies have established definite interrelationship between the salivary glands and the endocrine system. This study was designed to histochemically characterize testosterone-induced changes in the submandibular and the sublingual glands of male and female Ajax strain mice. In addition to morphologic stains, histochemical procedures included the demonstration of tryptophan, tyrosine, and sulfhydryl groups. Alcian blue, PAS, and toluidine blue staining was also employed. The Gomori and azo dye coupling procedures were both utilized for the demonstration of alkaline phosphatase.

Sexual dimorphism in the submandibular gland of the mouse was first described by Lacazeagne (40a,b) and Fekete (41). The submandibular gland of the male was characterized by the predominance of granular tubules, while in the female these were less granular and of smaller size. Lacazeagne (40c) Chaulin-Servinière (42), Addison, Wilson and Coates (38) and others have demonstrated reversal of these structural variations in mice by castration or by administration of male or female sex hormones to the opposite sex. Shafer and Muhler (73) Cassano (58a,b) Bixler Mulder and Shafer (55) and others have reported comparable studies in the rat.

In addition to structural variations according to sex in the submandibular gland, histochemical and histochemical studies of various rodent species have confirmed these differences. Such variations have been reported for alkaline and acid phosphatase (Junqueira, 49; Junqueira, Fajer Rabinovitch and Frankenthal 48 Kronman, '63b) protease (Sreebny Meyer Bachem and Weismann '55) acidic mucopolysaccharides (Shackelford and Klapper '61) amylase (Rayneud and Rebeyrotte 49) arginase (Kochakian, Eudahl and Hall, '55) and tryptophan and tyrosine (Junqueira, 49 Kronman, '63a).

Histochemical studies of rodent salivary glands following endocrine alteration have been meager. Bixler Mulder Webster and Shafer (57) reported reduction of achar RNA in the submandibular gland of the

rat following hypophysectomy. Kronman ('63c) reported decreased protein constituents RNA, alkaline phosphatase and PAS-positive material in the rat submandibular gland after hypophysectomy.

This investigation was designed to characterize histochemical changes in the submandibular gland of male and female mice after injections of testosterone. Histochemical changes induced by hormonal alteration were compared with previously reported studies of structural changes induced by this treatment. The sublingual gland was also examined since little information regarding this gland and its relationship to the endocrine system is currently available.

MATERIALS AND METHODS

Ajax strain mice four and one-half months of age were utilized in this study. The animals were divided into six groups as follows: Group I Normal males (8 animals); Group II Normal females (8 animals); Group III Normal males injected with corn oil (8 animals); Group IV Normal females injected with corn oil (7 animals); Group V Males treated with testosterone (14 animals); Group VI Females treated with testosterone (17 animals).

All animals in Group III-VI were injected daily for 28 consecutive days. Groups III and IV received subcutaneous injections

¹This investigation was supported by U.S.P.H. research grant DE-0 643 from the National Institute of Dental Research, National Institutes of Health, Bethesda, Maryland.

of 0.1 ml of corn oil and Group V and VI received subcutaneous injections of 0.25 ml testosterone suspended in 0.1 ml of corn oil.

All animals were weighed on the first and last day of the study. On the day following the last injection, all animals were killed by decapitation. The submandibular sublingual gland complex was removed immediately and placed in neutral buffered formalin (NBF) cold acetone (4 C) or Susa fixative. After paraffin embedding the tissues were sectioned at 7 μ stained dehydrated and mounted in Permount. Those sections to be utilized for the demonstration of alkaline phosphatase however were mounted directly in glycerine jelly after staining.

Morphology was studied on NBF fixed tissues stained with hematoxylin and eosin. Azan staining of Susa-fixed material, as recommended by Jacoby and Leeson ('59) was also employed for morphologic examination particularly of the granular tubules. Tryptophan and tyrosine (NBF fixed tissues) were demonstrated by means of the techniques of Glenner and Lillie ('57-'59). Sulfhydryl groups (NBF fixed tissues) were stained by means of the DDD (2,2'-dihydroxy-6,6'-dinaphthyl disulfide) procedure described by Barnett and Sellman ('52).

Aqueous toluidine blue (0.05% pH 4.5) was used for the demonstration of RNA and metachromasia after NBF and Susa fixation. Parallel control sections were incubated for one hour at 37 C in an unbuffered ribonuclease solution (1 mg/ml) prepared with glass distilled water. The Alcian blue procedure (pH 1.8) was utilized for the demonstration of acid mucopolysaccharides (Mowry '58).

The aqueous periodic acid-Schiff (PAS) technique (NBF and acetone-fixed tissues) was employed for the demonstration of 1:2 glycol linkages (Hotchkiss 48 McManus '48). Control slides were incubated for one hour in a 1% aqueous malt diastase solution at 37 C in order to eliminate glycogen (Lillie and Greco '47).

Cold acetone-fixed tissue was utilized for the histochemical demonstration of alkaline phosphatase. The modified azo dye coupling method (Pearse '60) and the calcium cobalt metal precipitate procedure

(Gomori, '41) were both utilized in the demonstration of alkaline phosphatase. Parallel control sections were incubated in buffer without substrate.

OBSERVATIONS

All animals were healthy and active throughout the study. All animals gained weight. The following chart contains average per group (table 1). All weights were recorded in grams.

TABLE 1
Animal weights by group

Group	A wt/ animal at start	A wt/ animal at finish	A wt gain/animal
I	20.0	21.0	1.0
II	20.0	21.0	1.0
III	21.8	26.2	2.4
IV	19.0	21.0	2.0
V	22.5	25.0	2.5
VI	20.0	22.0	2.0

Submandibular gland

Examination of H & E and Azan-stained tissues in the untreated male and female mice confirmed the sexual dimorphism previously reported by others (Lacazezgne, 40a,b Fekete, '41; Causse and Lacazezgne, 42a,b). In Group I the granular tubules were larger and more numerous relative to acini than in Group II (figs. 1 and 2). No differences were observed in Groups III and IV. After testosterone injections, the granular tubules in the male mice (fig. 3) became enlarged and packed with granules. The granular tubules in the female were enlarged and more granular than in Group II (fig. 4).

Demonstration of tryptophan in the submandibular gland of untreated males and females revealed no variation in staining according to sex (fig. 5 and 6). The acini, intercalated ducts, and intralobular ducts were faintly stained. The granular tubules were strongly reactive except for faint reactivity in the basal zone. In the female, the reaction was comparable to that of the male. Since there were fewer granular tubules and in most instances they were smaller than in the male, the overall reaction did not appear to be as pronounced as in the male. The reaction in the animals

receiving corn oil (Groups III and IV) was comparable to that in the untreated controls. In testosterone treated males, the tryptophan reaction was comparable in localization and intensity to that observed in the untreated controls (fig. 7). The increased size of the granular tubules however, made the total reactivity appear greater than in the control groups. In the testosterone-treated females (Group VI) the reaction in the granular tubules was comparable to that observed in the untreated males and those males which received corn oil only (fig. 8).

Histochemical demonstration of tyrosine revealed variations according to sex in the untreated controls (Groups I and II) the reaction of the granular tubules was more pronounced in the males than in the females (figs. 9 and 10). No other staining variations between Groups I and II were noted. The reaction in Groups III and IV was comparable to that of the untreated controls. The acini were faintly reactive, the ducts were moderately and uniformly stained. In both males and females changes in reactivity following testosterone treatment were restricted to the granular tubules. Localization and intensity of the tyrosine reaction in Group V (fig. 11) was comparable to that in the normal control (fig. 9) except that since the granular tubules were quite enlarged the reactivity appeared enhanced. In Group VI (fig. 12) the enhanced reaction in the granular tubules made the reaction comparable to that observed in Group V.

The sulfhydryl reaction revealed no differences according to sex between males and females in Groups I and II. The acini, intercalated ducts and intralobular ducts were faintly and uniformly reactive. The granular tubules were faintly reactive in the basal and infranuclear regions moderately so in the remainder. No changes were noted in Groups III and IV. Alteration in localization and staining intensity in males and females which received testosterone paralleled those that were observed in these same groups after tryptophan and tyrosine staining.

Toluidine blue staining after NBF fixation produced a strong uniform, orthochromatic reaction throughout the acini and duct system of the submandibular

gland (fig. 13). After Susa fixation the ducts and tubules were not reactive but the acini were faintly stained and orthochromatic. No variation in staining intensity or localization was noted among the six groups after NBF or Susa fixation. Cytoplasmic basophilia was removed by prior incubation in ribonuclease (fig. 14).

Demonstration of acidic mucopolysaccharides after Alcian blue revealed a similar pattern and intensity in all groups regardless of fixative. The acini were faintly and uniformly stained the duct system was not reactive.

The PAS reaction (NBF) revealed no variation in reactivity between males and females in Groups I-IV (fig. 15). The acini were moderately stained. Reactivity in the intercalated ducts was strong; the intralobular ducts were negative. A faint to moderate reaction was observed in the supranuclear and apical regions of the granular tubules basal and infranuclear zones of these cells were PAS-negative. Staining in Groups III and IV was comparable to that of Groups I and II. In testosterone-injected males and females the acinar reaction (NBF) was intense (fig. 16). All other reactivity was comparable to that of Groups I-IV.

Following acetone fixation the PAS reaction was uniform and faint throughout the parenchyma of the submandibular gland. These findings were consistent in all six groups. Prior malt diastase incubation induced no change in NBF or acetone-fixed tissues.

When alkaline phosphatase was demonstrated by means of the calcium cobalt (Gomori) procedure no differences according to sex were noted in Groups I and II (figs. 17 and 18). Reactivity was strong in the connective tissue and probably the capillaries as well as the basal zone of the acinar cells. A moderate uniform cytoplasmic reaction throughout the acinar cells as well as a faintly positive nuclear reaction was also noted. Examination of Groups III and IV revealed no variation in staining from those observed in Groups I and II. Testosterone injections induced no discernible changes in Groups V and VI. Control slides incubated in buffer without substrate were negative in all animals (fig. 19).

In Group I (fig. 20) staining for alkaline phosphatase activity by means of the modified azo dye coupling revealed a moderate reaction comparable in distribution to that of the Gomori technic except that the nuclei were not stained. In Group II (fig. 21) the submandibular gland showed no activity except in blood vessels and a few acinar cells which were faintly stained in the basal region. Staining of Groups III and IV was comparable to that observed in Groups I and II. Testosterone injections induced no change in either sex (figs. 22 and 23). All parallel control slides, incubated in buffer without substrate were non-reactive.

Sublingual gland

Examination of H & E and Azan-stained sections of mouse sublingual gland revealed that its structure was "typical" of rodent sublingual glands. The structure consisted of mucous alveoli intercalated ducts and secretory "striated" ducts. Granular tubules were not present. In this study of the sublingual gland no variations either structural or histochemical, were observed between the six groups.

Reaction for tyrosine and sulphydryl, and tryptophan groups yielded similar patterns. The acini were non-reactive except for moderate staining in the basal region. The ducts were uniformly and moderately stained.

Toluidine blue staining (NBF) produced a uniform intense metachromatic alveolar reaction. The duct system was orthochromatic and strongly stained. After Susa fixation, the alveoli were moderately reactive. This latter reaction was also metachromatic; the duct system was not stained.

An intense Alcian blue reaction (NBF and Susa) was uniformly distributed throughout the alveoli; the duct system was negative.

After the PAS procedure on NBF fixed tissues (fig. 24) the alveoli were intensely and uniformly reactive; the duct system was unstained. After incubation in malt diastase prior to PAS staining (fig. 25) the alveolar reaction was nearly eliminated. When the PAS technique was employed upon acetone-fixed tissues, the alveolar reaction was faint and uniform and was un-

altered by prior treatment in malt diastase. In all six groups when the Gomori and azo-dye coupling procedures were used, the sublingual gland was alkaline phosphatase-negative except for blood vessels which were strongly positive. All control slides were negative.

DISCUSSION

The morphologic differences in the submandibular gland of male and female mice were in accord with the findings of others (Lacassagne, 40a,b; Fekete 41). The effect of testosterone upon the submandibular gland of males has also been documented (Lacassagne, 40c; Shafer and Muehler '53). Previous investigators have reported that injections of male or female hormones into the opposite sex induced reversal of male and/or "female" structure (Chaulin-Serviniere 42, Atkinson, Wilson and Coates, '59). The current investigation confirmed these findings. In both sexes the effect of testosterone administration induced comparable changes; the granular tubules were enlarged. Structural variations according to sex or experimental intervention were not observed in the sublingual gland.

Protein histochemistry of the normal submandibular gland was comparable to that reported in the mouse (Junqueira et al. 49) and other rodent species (Junqueira, 49; Kemsaku, Deguchi and Ryuchi, '62; Kronman '63b). Variations with sex in the tyrosine reaction were observed in the submandibular glands of the untreated control mice. Junqueira (49) reported such variations in the rat. Kronman ('63a) and Kronman and Charney ('65) noted comparable findings in the albino and golden hamster for both tyrosine and tryptophan. In this study of the mouse, however variations in the tryptophan reaction according to sex were not evident. It therefore appears that sex differences in protein histochemistry of the submandibular gland are species-dependent. In testosterone-injected male and female mice the apparent increase in protein reactions were probably dependent upon the enlargement of the granular tubules.

In the sublingual gland, the histochemical demonstration of tryptophan, tyrosine and sulphydryl groups revealed that the

localization and intensity of staining were comparable in all groups. Testosterone administration did not alter any of these reactions in the sublingual gland of either sex. The insensitivity of the sublingual gland to alterations in endocrine function is in accord with the view of Baker and Abrams ('35). They reported that mucous-secreting glands were not generally affected by endocrine alterations.

Since RNA is intimately related to the synthesis of secretory protein, one might expect to find variations in the ducts after toluidine blue staining because of the changes in protein histochemistry. However no such changes were observed in this study. Based upon the fact that toluidine blue staining paralleled protein alteration after hypophysectomy in the rat (Kronman, '63c) it is probable that the alteration in endocrine function induced in this investigation was not as profound as after hypophysectomy. The resulting influence upon the submandibular gland, whether directly or indirectly mediated, was, therefore probably less severe.

Distribution of the Alcian blue reaction was in accord with the findings of Shackelford and Klapper ('62). No differences in reaction according to sex or treatment were noted. This was not in accord with observations of variations in the Alcian blue reaction according to sex in the submandibular gland of male and female hamsters (Shackelford and Klapper '61; Kronman '62) and again probably reflects species variation.

Examination of tissues subjected to the PAS procedure revealed alterations in the acini of testosterone-injected males and females. It may be assumed, therefore that testosterone affects the acini as well as the tubules of the submandibular gland. Although malt diastase incubation produced no diminution of the PAS reaction in the submandibular gland decreased reactivity was noted in the acini of the sublingual gland after NBF. This was similar to the reaction in the rat sublingual gland after NBF. The faint reaction after acetone was unchanged by malt diastase. This indicates that polysaccharides were probably not as well preserved in the acetone-fixed tissues as they were after NBF fixation. It may be assumed that glycogen is

one of the major polysaccharides in the sublingual gland of the mouse.

Distribution of alkaline phosphatase activity in the submandibular gland was in accord with that reported by Gomori ('41). Utilization of the Gomori procedure in the current study produced results comparable to those reported by Junqueira and his co-workers ('49) in their study of salivary gland sexual dimorphism. The latter reported no variations in the alkaline phosphatase reaction by sex in the submandibular gland of mice. The control slides for the Gomori procedure were negative in all animals. Bourne ('43) reported a positive reaction in his control slides (incubated in buffer without substrate) of the guinea pig submandibular gland. He attributed these positive controls to the presence of preformed phosphates. However when the azo-dye coupling procedure was utilized to demonstrate alkaline phosphatase activity the reaction was greater in the submandibular gland of the male than it was in the female.

This variability in results is probably related to the fact that many investigators feel that a number of different alkaline phosphatases exist (Pearse '60). The fact that sodium-beta-glycerophosphate was the substrate used in the Gomori procedure and sodium-alpha-naphthyl phosphate was the substrate used in the azo dye coupling technic would probably account for the differences in results. It should be emphasized, however that alkaline phosphatase activity was greater in the submandibular gland of males than in females when the appropriate technic (azo dye) was used. Testosterone injections induced no changes in alkaline phosphatase activities in either sex.

Even though a salivary gland-endocrine interrelationship has been well documented, its exact mechanism is still obscure. Sreebny ('60) stated that this relationship is non-specific and that salivary gland reactions to endocrine alteration were the results of non-specific metabolism effects. Based upon this and previous studies, the author feels that Sreebny's concept is probably correct. Although endocrine alterations do change the morphology and histochemistry of the submandibular gland the nature and severity of such

changes appear to be primarily dependent upon the severity of the endocrine alteration.

The effect of hormonal therapy upon rodent salivary glands following endocrine alteration has been reported (Shafer Clark, and Muhler '56 Yoshimura, 56 Sreebny et al '57) These investigators and others have reported structural regeneration by administration of various hormones following hypophysectomy Kromman and Chauncey ('64) however have shown that reversal of morphologic changes in the granular tubules by combined injections of testosterone and thyroxine was not accompanied by restoration of a normal histochemical pattern. This tends to confirm the view that a specific hormone(s) does not restore normal salivary gland function. Future studies may establish the fact that salivary glands are sensitive to endocrine alteration and may be restored to a normal morphological and functional state only when a normal endocrine balance is re-established.

LITERATURE CITED

Atkinson, W B F Wilson and S. Coates 1959 The nature of the sexual dimorphism of the submandibular gland of the mouse. *Endocrine* 65 114-117

Jaker B L., and G. D. Abrams 1955 Growth hormone (somatotropin) and the glands of the digestive system. In *The Hypophyseal Growth Hormone Nature and Action.* (Edit by R. W Smith, Jr O. H. Gaebler and C. N. H. Long.) Chap. 8, pp. 107-122. The Blakiston Div McGraw-Hill Book Co., Inc.

Barnett, R. J. and A. M. Seligman 1959 Demonstration of protein and bound sulphydryl and disulfide groups by two new histochemical methods. *J Nat. Cancer Inst.* 13 315-318.

Blaker D., J. C. Muhler and W. G. Shafer 1953 The effect of castration, sex hormones, and desalivation on dental caries in the rat. *J Dent. Res.* 34 680-694

Blaker D., J. C. Muhler R. C. Webster and W. G. Shafer 1957 Changes in submaxillary gland ribonucleic acid following hypophysectomy thyroidectomy and various hormone treatments. *Proc. Soc. Exp Biol and Med.* 94 521-524

Bourne, G. 1943 The distribution of alkaline phosphatase in various tissues. *Quart. J. Exp. Physiol.* 33 1-7

Cassano N. A. 1956a Ghiandole salivari sottomassellari ormond. I. Effetti della castrazione, del testosterone del nor-androstendolo sui tubuli sierosi della ghiandola salivare sottomassellare del ratto. *Fol. Endocrin. Pisa, II*; 622-646.

1956b Ghiandole salivari sottomassellari ormond. II. Azione del benzoato di

-estradiolo sulla ghiandola sottomassellare del ratto. *Fol. Endocrin. Pisa, II*; 745-753.

Canat R., and A. Lacaze 1942a Rapport des formations tubuleuses et acineuses de la glande sous-maxillaire de la souris. *Compt. Rend. Soc. de Biol.* 136 413-414.

1942b Reconstruction possible de la glande sous-maxillaire de la souris. *Compt. Rend. Soc. de Biol.* 136 493.

Chaulin-Serviniere, J. 1942 Castration et glande sous-maxillaire de la souris femelle. *Compt. Rend. Soc. de Biol.* 136 335-336.

Falkow E. 1941 *Biology of the Laboratory Histology* Chap. 3, pp. 113-115. Blakiston Co Philadelphia.

Gierney G. G., and R. D. Little 1957 The histochemical demonstration of indole derivatives by the post-coupled p-dimethylamino benzoylamine reaction. *J. Histochem. Cytochem.* 5 379-394.

1959 Observations on the decarboxylation-coupling reaction for the histochemical demonstration of tyrosine. Metal chelation and furanose anilates. *J. Histochem. Cytochem.* 7 416-422.

Gomori, G. 1941 The distribution of phosphatase in normal organs and tissues. *J. Cell. and Comp. Physiol.* 17 71-83

Hutchkins R. D. 1948 A microchemical reaction resulting in the staining of polysaccharide structures in fixed tissue preparations. *Arch. Biochem.* 16 131-141

Jacoby, F. and C. R. Larson 1938 The post-natal development of the rat submandibular gland. *J. Anat., Lond* 83 291-316.

Junqueira, L. C. 1949 Estudo histológico, histoquímico bioquímico experimental da glândula submaxilar do camondongo (*Mus musculus* L.) *Arch. brasill med.* 30 381-410.

Junqueira, L. C., A. F. Jer M. Rabinowitch and L. Frankenthal 1949 Biochemical and histochemical observations on sexual dimorphism of mice. *J. Cell. and Comp. Physiol.* 34 159-159

Kensaku K., Y. Deguchi and O. Ryuchi 1952 Histochemical study of protein-bound sulphydryl and disulfide groups in normal salivary glands. *J. Dent. Res.* 41 104-111.

Kochakian, C. D. B. R. Endahl and H. D. Hall 1955 Arginase activity of the salivary glands and its inhibition by testosterone propionate. *J. Dent. Res.* 34: 790 (abstract)

Kronman, J. H. 1963 A morphological and histochemical study of hamster salivary gland development. Ph.D. dissertation Medical College of Virginia, Richmond.

1963a Hamster salivary gland sexual dimorphism. I. Protein histochemical study. *J. Dent. Res.* 42 123-127

1963b Hamster salivary gland sexual dimorphism. II. Histochemical study of acid phosphatase. *J. Dent. Res.* 42 825-830

1963c Histochemical study of hypophysectomy-induced changes in the rat submandibular and lingual glands. *Am. J. Anat.* 113: 337-346.

Kronman, J. H., and R. H. Chauncey 1964 Hormonal influences upon salivary gland histchemistry. *J. Dent. Res.* 43 820-837

- 1963 Testosterone-induced changes in salivary gland histochemistry in the female Golden Hamster. *J. Oral Ther. Pharm.*, 1: 302-303.
- Lacaze, A. 1940a. Dimorphisme sexual de la glande sous maxillaire chez la souris. *Compt. Rend. Soc. de Biol.*, 133: 160-161.
- 1940b. Mesure de l'action des hormones sexuelles sur la glande sous-maxillaire de la souris. *Compt. Rend. Soc. de Biol.*, 133: 227-228.
- 1940c. Réactions de la glande sous-maxillaire l'hormone male, chez la souris et le rat. *Compt. Rend. Soc. de Biol.*, 133: 328-340.
- Ilse, R. D. and J. Greco 1947. Malt diastase and pyruvic in place of saliv. in the identification of glycogen. *Stain Tech.*, 22: 67-70.
- Kidman, J. F. A. 1945. Histological and histochemical uses of periodic acid. *Stain Tech.*, 20: 80-108.
- Mowry R. W. 1956. Alcian blue technique for the histochemical study of acidic carbohydrates. *J. Histochem. Cytochem.*, 4: 407.
- Perse, A. G. E. 1960. *Histochemistry Theoretical and Applied*. Little Brown and Co. Boston.
- Royand, J. and P. Rebeyrolle 1949. Différence d'activité amylasique de la glande sous-maxillaire des souris mâles et des souris femelles. Fonctionnement de cette activité par les hormones androgènes. *Compt. Rend. Ac. Sc.*, 229: 84-86.
- Shackelford, J. and C. E. Klapper 1961. The influence of ovarian hormones on hamster submaxillary mucin. *Anat. Rec.*, 129: 334 (abstract).
- 1962. Structure and carbohydrate histochemistry of mammalian salivary glands. *Am. J. Anat.*, 111: 35-47.
- Shafer, W. G., and J. C. Muhler 1953. Effect of gonadectomy and sex hormones on the structure of the rat salivary glands. *J. Dent. Res.*, 32: 262-268.
- Shafer E. G. P. G. Clark and J. C. Muhler 1958. The inhibition of hypophysectomy-induced changes in the rat submaxillary glands. *Endocrin.*, 59: 516-531.
- Szebeny L. M. 1960. Study of salivary gland proteases. *Ann. N. Y. Acad. Sc.* 63: 182-186.
- Szebeny L. M., J. Meyer, E. Sackern and J. F. Weinmann 1955. Postnatal changes in proteolytic activity and in the morphology of the submaxillary gland in male and female albino rats. *Growth*, 19: 57-73.
- 1957. Restoration of enzymatic activity in the submaxillary gland of the hypophysectomized albino rat. *Endocrin.*, 60: 200-204.
- Yoshimura, F. 1956. Cytological changes in rat salivary glands following hypophysectomy and somatrophic hormone administration. *Okaj. Folia Anat. Jap.*, 30: 196-205.

PLATE 1

EXPLANATION OF FIGURES

- 1 Granular tubule in submandibular gland of untreated male mouse. Azan-stained, Susa-fixed, $\times 800$.
- 2 Submandibular gland of normal female mouse. Note that the granular tubules are smaller than in the normal male. Azan-stained, Susa-fixed, $\times 800$.
- 3 Submandibular gland of testosterone-treated male mouse. Note increased size of granular tubules. Azan-stained, Susa-fixed, $\times 800$.
- 4 Submandibular gland of testosterone-treated female mouse. Observe enlargement of granular tubules. Azan-stained, Susa-fixed, $\times 800$.



PLATE 2

EXPLANATION OF FIGURES

- 5 Tryptophan reaction in submandibular gland of untreated male mouse. NBF-fixed, $\times 400$.
- 6 Tryptophan reaction in submandibular gland of untreated female mouse. NBF-fixed, $\times 400$.
- 7 Submandibular gland of testosterone-treated male mouse stained to demonstrate tryptophan. NBF-fixed, $\times 400$.
- 8 Tryptophan reaction in submandibular gland of testosterone-treated female mouse. NBF-fixed, $\times 400$.
- 9 Tyrosine reaction in submandibular gland of untreated male mouse. NBF-fixed, $\times 400$.
- 10 Tyrosine reaction in submandibular gland of untreated female mouse. Note that reactivity is less than in the untreated male. NBF-fixed, $\times 400$.
- 11 Submandibular gland of testosterone-treated male mouse stained for tyrosine. NBF-fixed, $\times 400$.
- 12 Tyrosine reaction in submandibular gland of testosterone-treated female mouse. Note heightened reactivity as compared to the untreated female. NBF-fixed, $\times 400$.



PLATE 3

EXPLANATION OF FIGURES

- 13 Toluidine blue stain of the submandibular gland in an untreated male mouse. NBF-fixed $\times 400$.
- 14 Toluidine blue stain after prior ribonuclease incubation of the submandibular gland in an untreated male mouse. NBF-fixed, $\times 400$.
- 15 PAS reaction in submandibular gland of untreated female mouse. NBF-fixed, $\times 400$.
- 16 PAS reaction in submandibular gland of testosterone-treated female. Note enhanced acinar reaction as compared to figure 15. NBF-fixed, $\times 400$.
- 17 Alkaline phosphatase reaction, Gomori technic, in the submandibular gland of an untreated male mouse. Cold acetone-fixed, $\times 400$.
- 18 Alkaline phosphatase reaction, Gomori technic, in the submandibular gland of an untreated male mouse. Cold acetone-fixed, $\times 400$.
- 19 Alkaline phosphatase control slide for figure 18 incubated without substrate. Cold acetone-fixed, $\times 400$.

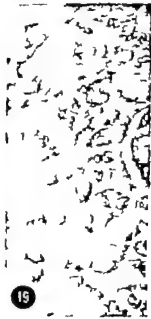
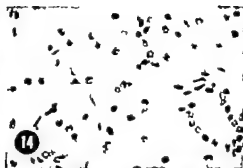
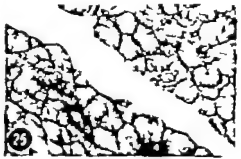
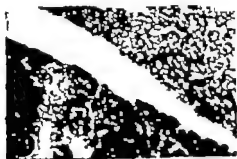
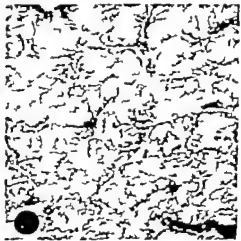
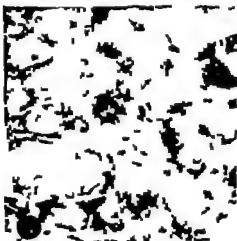
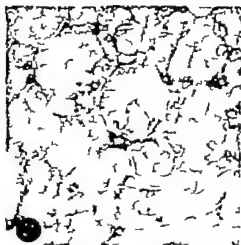


PLATE 4

EXPLANATION OF FIGURES

- 20 Alkaline phosphatase reaction, azo dye technic, in the submandibular gland of an untreated male mouse. Cold acetone-fixed, $\times 400$.
- 21 Alkaline phosphatase reaction, azo dye technic, in the submandibular gland of an untreated female mouse. Cold acetone-fixed, $\times 400$.
- 22 Submandibular gland in testosterone-treated male mouse. Alkaline phosphatase reaction, azo dye technic. Cold acetone-fixed, $\times 400$.
- 23 Submandibular gland in testosterone-treated female mouse. Alkaline phosphatase reaction, azo dye technic. Cold acetone-fixed, $\times 400$.
- 24 PAS reaction in sublingual gland of untreated male mouse. MBF fixed, $\times 200$.
- 25 PAS reaction in sublingual gland of untreated male mouse after prior malt diastase incubation. MBF-fixed, $\times 200$.



Immunohistological and Histochemical Localization of Relaxin in the Metrial Gland of the Pregnant Rat¹

G DALLENBACH-HELLWEG, J V BATTISTA AND F D DALLENBACH
Department of Pathology Dartmouth Medical School,
Hanover New Hampshire

ABSTRACT The presence of relaxin in uteri, placentae and ovaries of pregnant rats was studied immunohistologically with fluorescein labeled anti-relaxin serum and confirmed by histological and histochemical techniques.

In sections of uteri from day 12 of pregnancy stained with these antisera, the cytoplasm of the granular cells of the mesometrial decidua gave off a yellow-green fluorescence indicating antirelaxin binding. On day 15 17 and 19 the granular cells of the metrial gland and occasional lakes in near-by vascular lamina fluoresced. No other specific fluorescence was evident in the uteri or placentae. The fluorescent regions of these cells corresponded exactly with the cytoplasmic aggregates of granules in the metrial gland and mesometrial decidua. Histochemical studies of these granules which bound with antirelaxin, revealed chemical composition congruent with that known for relaxin, and with that of the relaxin-containing granules of human decidua and placental cells. The dissolution of connective tissue fibers, believed to be main function of relaxin, was observed in the last days of pregnancy within the metrial gland, especially where it borders the mesometrial decidua. These results correlate well with Schaub's discovery of collagen-degrading substance in the metrial gland. Other actions of relaxin may be explained as secondary to the primary effect of dissolution of collagen. The relaxin-containing cells in the human and in the rat differ only in their localization in the tissue which depends on their phylogenetic adaptation to different placental needs. The metrial gland cells of the pregnant rat correspond in their function to the basal trophoblastic cells of the human term placenta. The non-contracting rat has no counterpart for the endometrial granulocytes, but the granular cells in the mesometrial decidua adjacent to the site of implantation correspond to the endometrial granular cells surrounding the implantation site in the human; it is suggested their collagen dissolving action facilitates implantation.

Hisaw (26) was the first to recognize that the antepartum relaxation of the symphysis pubis of the guinea pig was under hormonal control and subsequently named the hormone causing this action relaxin. Since then by means of various bioassay techniques relaxin has been found in varying quantities in the ovaries, placenta and uterus of many species of animals (see comprehensive reviews by Hisaw and Zarrow '50 and by Steinetz et al. '59) and in the blood serum of pregnant women (Pommerenke, '34; Abramson et al., '37 Zarrow et al. '55). The demonstration of the antigenicity of relaxin (Cohen, '63 Steinetz et al. '64) indicated the fluorescent antibody technique could be used for the study of the distribution of relaxin. This procedure seemed particularly profitable since it provided great sensitivity and cellular localization. With this method relaxin has

been recently localized in the basophilic trophoblastic cells of the basal plate of the human placenta shortly before term, and in the human endometrial granulocytes during the secretory phase of the menstrual cycle (Dallenbach and Dallenbach-Hellweg, '64). As a continuation of these studies we have examined the uteri, placentae and ovaries of various mammals. This paper is a report of our studies of the localization of relaxin in the pregnant rat.

MATERIAL AND METHODS

Twenty pregnant rats of the Charles River Strain (Sprague-Dawley descendants) mated on the same day were studied by sacrificing one animal daily from the fifth day of pregnancy until they gave birth. A non-pregnant rat was

This work has been supported by the aid of United States Public Health Service grant GM 103

included for comparison. The animals were exsanguinated by aortic puncture and the ovaries, uteri and mammary glands were immediately removed. Representative specimens of each organ were quickly frozen in petroleum-ether at -70°C and then stored at -40°C until sectioned in the cryostat for immunofluorescent studies. Similar specimens of all animals were fixed in neutral 10% formalin, and in addition some in San Felices fluid, Carnoy's fixative, acetone or 4% basic lead acetate for subsequent paraffin embedding and sectioning at 5μ .

A. Immunofluorescent techniques

The techniques used were similar to those previously described (Dallenbach and Dallenbach-Hellweg, '64) and consequently need to be outlined only briefly.

The antisera to relaxin were kindly donated by Dr. B. G. Steinmetz of the Warner Lambert Research Institute. These had been prepared by injecting rabbits repeatedly at intervals of 10 days with 3.75 mg of relaxin (1000 units/mg) mixed in Freund's adjuvant. The titer of antibody was checked by the mouse inter-pubic ligament bioassay (Steinmetz et al., '64) and by the Ouchterlony agar-diffusion method (Ouchterlony '58).

The indirect fluorescent antibody technique of staining (Cooms '58) was used throughout that is after the sections had been fixed for 10 minutes, whole anti-relaxin serum was applied to them for periods of 30 minutes to six hours. The sections were then washed in buffered saline (pH 7.2) and treated with fluorescein labelled gamma globulin against rabbit gamma globulin (sheep from Baltimore Biological Laboratories and goat from Colorado Serum Company) for periods of 15 minutes to one hour.

The fixatives employed were fresh acetone, 95% alcohol and 10% neutral formalin.

The following controls were carried out to demonstrate the specificity of the staining reaction.

- a. Examination of fixed but unstained slides.
- b. Staining of sections with
 1. Rabbit anti-rat lung serum, followed by fluorescein labelled sheep

anti-rabbit gamma globulin (A) or by anti-streptococcus A serum (B) or by goat anti-rabbit gamma globulin (C).

2. Anti-relaxin serum, followed by fluorescein labelled serum B.
3. Normal rabbit serum, followed by fluorescein labeled serum A, B or C.
4. Anti-relaxin serum followed by regular (unlabelled) sheep gamma globulin against rabbit gamma globulin (blocking test) before applying fluorescein labelled sheep anti-rabbit gamma globulin.

B. Histological and histochemical techniques

Paraffin sections of all organs were stained with the following histological techniques: phloxine-tartrazine after Lendrum ('47), Masson's trichrome stain (Romels '62), azan after Heidenhain (Romels '62), azan modification after Selye and McKeown ('35), chromalum-haematoxylin-phloxine after Gomori (Humason '62), Verhoeff's elastin stain (Humason '62), Gomori's reticulum stain (Romels '62), Mallory's fibrin stain (phosphotungstic acid-haematoxylin) (Humason, '62). The histochemical reactions employed were Sudan black B (Pearse '61), PAS with and without diastase (Pearse, '61), aldehyde-fuchsin (modification by Cameron and Steele) (Humason, '62), toluidine blue (at pH 4.5 and 7.0) (Humason, '62), alcian blue (at pH 2.5) (Humason, '62), coupled tetrazolium reaction with and without benzoylation (Pearse, '61), Adams nitrite method for tryptophan (Pearse '61), Geyer's ('63) modification of the Morel-Sisley reaction for tyrosine (Pearse '61), hydroxynaphthaldehyde method for protein-bound NH-groups after Weiss et al. ('54), reaction for histidine after Bachmann and Seitz ('61), reaction for SH-groups after Barnett and Selye (Pearse, '61), Prussian blue reaction for hemoiderin (Humason '62), benzidine reaction after Lepehne for hemoglobin (Romels, '62) and determination of the isoelectric point with methylene

like at controlled pH after Pischinger (Romeis, '62)

In addition tissues hardened in the above mentioned fixatives were sectioned with the freezing microtome and compared with cryostat sections fixed (after coating) in the same solutions. Both groups were stained with all red O toluidine blue, PAS phloxine tartrazin, and the α -naphthyl acetate and naphthol-AS-acetate methods for esterase (Pearse '61)

RESULTS

A. Immunofluorescent studies

The tissues from day 12, 15 17 and 19 were studied in detail because it was noted that on these days the cells fluorescing specifically with the antirelaxin serum varied noticeably in their occurrence or distribution from the previous day

Day 12 of pregnancy In the sections treated with the antirelaxin serum and then with fluorescent antirabbit gamma globulin serum, about half of the cells in the mesometrial decidua especially those close to the ectoplacental cone and within the decidua cone contain granules with a distinct yellow-green fluorescence. Occasional other granular cells in these regions reveal a halfmoon or crescent shaped paranuclear cytoplasmic area that gives a weaker greenish fluorescence. In the metrial gland, very similar granules and cytoplasmic areas are seen in only a few of the cells. On the other hand the developing fetal placenta and the antimesometrial decidua do not show any yellow-green fluorescence specific for the binding of the labelled antiserum. There is also no yellow-green fluorescence of positive staining in the endometrium adjacent to the decidua. Only occasional pale yellow granules can be observed in a few cells in the endometrial stroma. As these are also detectable in unstained control slides they are considered to represent autofluorescence. In all the control slides the decidua and metrial gland fail to give a green or yellow-green fluorescence

Day 15 of pregnancy In the slides stained with the antirelaxin serum and then with fluorescent antirabbit gamma globulin serum, the metrial gland can be

readily recognized even under low magnification since it literally glows with fluorescein binding. At high magnification almost every cell can be seen to contain a fairly well defined yellow-green paranuclear area that is slightly larger than the nucleus and either crescent-shaped or rounded (fig. 3). In some of these fluorescent areas even more brightly stained small granules can be recognized. Yellow green fluorescent granules and lakes of fluorescent material are occasionally found in the lumina of maternal blood vessels (fig. 4) whose endothelial lining may also be diffusely fluorescent. In the regressing mesometrial decidua only a few cells with fluorescent areas can be found. The endometrium, the giant cell layer the spongiotrophoblast and the labyrinth fail to show any yellow-green fluorescence. In the connective tissues of the outer layers of the uterus close to the mesometrium groups of mast cells are evident with numerous small yellow-green fluorescing granules. After fixation in formalin, the slides stained with antirelaxin serum and then with fluorescent antirabbit gamma globulin serum fail to show any yellow-green fluorescence. In contrast, those stained after fixation in acetone give the best results. Only a slight difference in intensity of the fluorescence exists here between the slides stained for 30 minutes, for 60 minutes and for six hours.

In all the controls no specific fluorescence can be detected in the metrial gland or decidua. In the endometrial stroma occasional small cells contain golden yellow (autofluorescent) granules. The slides stained with control serum-1A disclose a yellow-green fluorescence of the peripheral cytoplasm of the giant cells likewise, the granules of the large mast cells glow brightly. The yolk sac epithelium shows a whitish-yellow autofluorescence. The slides treated with control serum-1C reveal a green fluorescence in the lining endothelial cells of all portions of the placenta. In the slides stained with the control serum-3A a yellow-green fluorescence of the apical portions of the glandular and superficial endometrial epithelium can be seen, whereas the metrial

gland and the decidua are entirely negative.

Day 17 of pregnancy Following staining with the antirelaxin serum and then with fluorescent antirabbit gamma globulin serum, the metrial gland cells contain fluorescent areas which are identical with those seen in the uterus of day 15. Their number, size and distribution also seem to be about the same, except for a perivascular accumulation of fluorescing cells in the outer myometrial portions which is not so striking in the sections from the fifteenth day. No yellow-green fluorescence can be seen in the decidual remnants or in any other structure of the placenta. The control slides give practically the same results as those from the fifteenth day.

Day 19 of pregnancy These sections when treated with the antirelaxin serum followed by the fluorescent antirabbit gamma globulin serum also reveal a very prominent yellow-green fluorescence of the granular cells of the metrial gland (fig. 5). The number of these cells is almost as large as in the metrial glands of the earlier days of pregnancy. The distribution of the cells is slightly different, however, for they are found aggregated primarily about the larger vessels of the metrial gland. Rounded fluorescent areas in the cytoplasm seem to be more numerous than those shaped like halfmoons. There is a distinct yellow-green fluorescence of the lining vascular endothelium, and occasional masses in the vascular lumen fluoresce homogeneously. No yellow-green fluorescence is observed in other parts of the uterus. In all the control slides the metrial gland fails to bind the fluorescein-labeled antirelaxin serum.

Ovary from day 19 and 20 of pregnancy A bright golden-yellow autofluorescence of groups of stromal cells is evident in all slides; these cells are histochemically identical with the fluorocytes in the human ovary (Hamperl '34). In all slides from the nineteenth and twentieth day stained with the sera 2B and 2C groups of rounded interstitial cells close to the mesovarium (mast cells) contain numerous small distinctly green fluorescent granules. The lutein cells of the corpus luteum and the granulosa cells of the smaller and

larger follicles show no fluorescence, either specific or non-specific. The slides treated with control serum 3C reveal in both ovaries a fluorescence of the capillary endothelial cells in the corpus luteum. A fluorescence clearly specific for the antirelaxin serum could not be demonstrated in the two ovaries examined.

B. Histological and histochemical findings

Since the granular cells of the metrial gland and of the mesometrial decidua at the earlier stages of pregnancy are the only cells in the uterus and placenta showing specific fluorescence with the antirelaxin serum, we limit our description to the histologic staining and histochemistry of these cells (see table 1; the results of other investigators are included).

In paraffin sections stained with phloxine-tartrazin, Masson's trichrome or chromium hematoxylin-phloxine the granules of the metrial gland cells and of the granular cells in the mesometrial decidua stain distinctly red, with azan orange-red, with PTAH clearly dark purple. They are negative (yellow) with Verhoeff's elastin stain. Generally after silver impregnation for reticulum fibers each cell is found to be enveloped by a fine reticulum network. The granules react to various histochemical tests as indicated in table 1. From these findings it can be concluded that they mainly consist of a protein (or polypeptide) containing tyrosine, tryptophan, histidine, lysine and SH-groups.

On the seventh day of pregnancy for the first time an occasional decidual cell may be found in the mesometrial decidua with one or several round intracytoplasmic granules. These granules are with striking uniformity located to one side of the nucleus. The basophilic cytoplasm of these cells suggests a high content of ribonucleic acids. By day 10 a few similar appearing cells are found in the metrial gland, but they remain much more numerous in the mesometrial decidua, particularly within the decidual cone (fig. 1). At this time they are most abundant near the ectoplacental cone where they often form a continuous boundary line at the fetal-maternal border. Here the cells contain many more granules and, in addition, peripheral cyto-

plasmic vacuoles. Many of these granular cells are binucleated and in these the granules are located between the two nuclei, whereas in the mononucleated cells most of the granules lie to one side of the nucleus. In sharp contrast to these findings, no granular cells can be detected at any time during pregnancy in the antimesometrial decidua. Especially striking is the hyperplasia and hypertrophy of the endothelial cells of the small arterioles near the implantation site.

By day 11 some of the granular cells can be seen between the trophoblast cells of the ectoplacental cone. In addition, the only trophoblastic giant cells which are located next to the antimesometrial decidua, now contain (from day 10 to 12) many distinct round granules which give the same histochemical reactions as do those of the granular cells of the mesometrial decidua already described but with one exception: they do not seem to contain histidine. They can be differentiated, however, from neighboring red blood cells or fragments of them by methods for hemoglobin and hemosiderin. They are as numerous in a cell as the granules in the decidua granular cells but slightly larger. Thereafter at the time of degeneration of the antimesometrial decidua, the granules disappear from these trophoblastic giant cells. In the metrial gland the endothelial cells lining the blood vessels proliferate and enlarge strikingly and display a distinct cytoplasmic basophilia; the contiguous basement membrane swells and stains more prominently.

As the metrial gland develops during the subsequent days of pregnancy the numerous granular cells within it often are binucleated and have abundant phloxino-phobic granules in their cytoplasm (figs. 2 & 7). In contrast, in the regressing mesometrial decidua, these granular cells gradually decrease in number. Many metrial gland cells are within the walls of the arterioles and some in close contact with the endothelium, which often in the later stages of pregnancy seems to be stretched out over granular cells bulging into the lumen (figs. 6, 7 & 8). In other vessels some of the granular cells may be seen in direct contact with the blood stream. Occasional granules accumulated within vesicles may even be

found within the vascular lumen. At the end of pregnancy (day 22 and 23) numerous granules are still demonstrable in some of the metrial gland cells that is almost exclusively about the vessels (fig. 10) in the outer portions of the gland and close to the line of placental separation (at the border of the mesometrial decidua) whereas most of the remaining cells of the metrial gland are depleted of granules and markedly vacuolated.

In frozen and cryostat sections the appearance of the granules varies depending upon the fixative used. The granules seem to be preserved best following formal, Carnoy or acetone fixation. In addition to the granules, some of the granular cells are found to contain a moderately well circumscribed rounded area adjacent to the nucleus. This area, about as large as the nucleus stains distinctly red with phloxine-tartrazin but not with PAS. In the paraffin sections these areas cannot be found, most likely being replaced by vacuoles. In the frozen sections, only the peripheral cytoplasm contains vacuoles arranged along the cell membrane like a string of pearls. In early and late stages of development of some of these granular cells the cytoplasm reveals a moderate esterase activity.

Hence these granular cells in the metrial gland and in the mesometrial decidua correspond closely in their number, time of appearance and distribution to the fluorescing cells seen only in those immunohistologic sections stained with fluorescein-labelled antirelaxin serum. This can be demonstrated especially well by using cryostat sections that have been stained with the labelled antiserum and then restaining them with phloxine-tartrazin. The fluorescent halfmoons or rounded areas in the metrial gland cells are identical with the similarly shaped conglomerates of intracytoplasmic paranuclear granules and with the rounded paranuclear areas seen in the frozen sections.

C Changes in the connective tissues of the uterus

Starting on the eleventh day of pregnancy reticulum and collagen fibers stain less intensely in the mesometrial region of the myometrium. They are also more

TABLE 1

Results of histochemical studies of the uterine gland cells of the pregnant rat

Substances detected	Results of other authors		Our results	
	Spec. granules	Cytoplasm	Spec. granules	Cytoplasm
Lipids	- (Wyslocki et al., '57)		-	-
Polysaccharides				
Glycogen		+ (Gérard, '25; Baker 48; Bridgman, 48; Padykula and Richardson '53) (+) (Wyslocki et al., '57; Bulmer and Dickson, '60)	-	(+)
Neutral MPS	+ (Ellis, '57; Wyslocki et al., '57) + or - (Bulmer and Dickson, '60)		(+)	-
Acid MPS	+ metachromasia (Wyslocki et al. 40; Ellis, '57) (+) metachromasia (Asplund et al. 40; Ellis, '57) - metachromasia (Bulmer and Dickson, '60)		- (at pH 4.5 and 7)	-
Proteins				
Total (tetrazolium)	+ (Bulmer and Dickson, '60)		+	-
SH groups	+ (Wyslocki et al., '57)		+	-
NH ₂ groups (Tyrosine)	+ (Wyslocki et al., '57)		+	-
Histidine			+	-
Tyrosine			+	-
Tryptophan			+	-
IDP	0.6-4.5 (Bulmer and Dickson, '60)		4.4	-
Enzymes				
Alkaline phosphatase		- (Pritchard, 47; Ellis, '57)		
Acid phosphatase		+ (Padykula, '58; Bulmer '64) - (Ellis, '57)		
Succinic dehydrogenase		+ (Padykula, '58)		
Esterase C		+ (Bulmer '63 and '64) (+) (Ellis, '57)		
Esterase A ₂		- (Padykula, '58)		
ATPase		+ (Padykula, '58)		
Acetylcholinesterase		+ or - (Bulmer, '63)		
β-Galactosidase		+ (Bulmer '64b)		(+)

loosely arranged than in the remaining portions of the myometrium. On the twentieth day the collagen fibers swell appear edematous, undergo dissolution and gradually disappear. A patchy loss of reticulum fibers becomes evident throughout the metrial gland. By day 22, the dissolution involves the connective tissue fibers of the entire metrial gland. At this time, the boundary between the metrial gland and the mesometrial decidua is devoid of any connective tissue fibers and consists only of an amorphous fibrinoid-like material.

DISCUSSION

The metrial gland of the rat first was described in 1891 by Duval and again in 1919 by Weill. They regarded the acidophilic, granular cells of this gland to be of connective-tissue origin. Because of the apparent secretory cycle and discharge of these granules into blood vessels Weill supposed the gland to have an endocrine function. These views were substantiated by Gérard (25) who saw these granular cells also in the mesometrial decidua. Szendi (33, 34) believed that the granules of these cells were secreted into the maternal blood and carried to the yolk sac for nutrition of the embryo. Selye and McKeown (35) and Velardo et al. (53) were able to show that a typical metrial gland developed as well beneath the decidua formed in pseudopregnant rats thereby indicating the maternal origin of the gland. Asplund et al. (40) who first precisely investigated the cells of the metrial gland found them to be most abundant from the fifteenth to the eighteenth day of pregnancy and less frequent thereafter but still evident up to the fifth day after delivery. The granules of these cells were acidophilic safraninophilic, partly metachromatic and more soluble in alkali than in acid. Their secretion into the blood was considered as probable by these authors. With progesterone treatment, Selye et al. (42) as well as Velardo et al. (53) succeeded in maintaining these cells of the metrial gland for a longer than normal period whereas administration of estrogen accelerated their regression. Baker (48) and Bridgman (48) essentially confirmed the findings of Asplund et al. Histochem-

ical results of other authors are summarized in table 1. Wislocki et al. (57) demonstrated SH and NH₂ groups in the granules of these metrial gland cells, and electron microscopically they found the granules to be surrounded by membranes. They concluded from their studies that the granules consisted of a strongly alkaline protein, rich in lysine and cystine and conjugated with a mucopolysaccharide representing a prosthetic group. They postulated that the granules could be relaxin. Previously Bridgman (48) and Velardo et al. (53) made this same assumption as did Dickson and Bulmer (61) later.

The results of our studies have shown that the fluorescein-labelled antirelaxin antibody binds to the cytoplasm of the granular cells of the metrial gland exactly where the granules are aggregated. Further evidence that the granules contain relaxin is provided by the close relationship existing between the histochemical studies of the granules of these cells (table 1) and the chemical composition of relaxin (Cohen '63). In addition the results of histochemical studies of these granular cells of the metrial gland are almost identical with those of the relaxin-containing cells in the human placenta and decidua (Dallenbach and Dallenbach-Hellweg '64). We were unable to confirm the metachromasia of these granular cells which has been reported by several authors, but we have seen metachromasia of some decidua cells (Hellweg '39) of the mesometrial decidua. The lipid granules observed in some cells of the metrial gland after the seventeenth day of pregnancy (Bridgman, 48) most likely of degenerative nature have no connection with these protein granules (Baker 48; Ellis '57). We interpret the difference in the PAS-reaction, which is negative in the human cells and weakly positive in those of the rat, as representing a species characteristic. Since all the other histochemical results of rat and human granular cells are similar this difference in PAS-reaction can be regarded as of minor importance in the overall chemical composition especially since an occasional variation in the color reaction of the granules of the metrial gland has been observed (Selye and McKeown '35; Asplund et al., 40).

Because of the morphological and histochemical results a high metabolic activity of the granular cells can be predicted. The cytoplasmic basophilia preceding the formation of granules which was first reported by Baker (48) may be interpreted as indicative of a high protein metabolism. Another sign of cellular activity is the tendency for the cells to become binucleated, a state frequently observed in endocrine cells and perhaps brought about by "reaction-amitosis" (Benninghoff '52) as the type of cellular division occurring in highly specialized cells (Peter '29). It can thus be assumed that the granules are not only stored, but also produced in the granular cells.

From our observations, we believe that cells forming the wall of the maternal blood vessels of the metrial gland may be transformed into "decidual cells" and may also become binucleated (fig. 9). This belief is analogous to Wislocki's and Streeter's ('38) and to Brettner's ('64) who observed a similar transformation in the basal decidua of the monkey and of the human placenta, with the exception that these transformed cells in the rat may in addition, contain the relaxin granules. This concept will also explain the location of the granular cells next to the endothelium which simultaneously become greatly thinned out. Apparently the granules are secreted directly into the blood stream while the cells themselves stay in place (figs. 6-7). The fluorescent lakes within occasional vessel lumina, as detectable in cryostat sections (fig. 4) may therefore be interpreted as secreted relaxin. Such a discharge of hormones into the bloodstream by perivascular cells has previously been suggested by Weill ('19). There is no proof of a holocrine secretion of these granular cells although such a process might be presumed from figure 8.

To date an exact determination of relaxin in the metrial gland has not been attempted. Zarrow ('57) suggested that relaxin could very well be present in this gland. From extracts of the metrial gland, Schaub ('64) isolated a collagen-degrading substance which, from his description is suggestive of relaxin, although the possibility was not mentioned by him. Bridgman (48) observed in the pregnant rat

a disintegration of connective tissue between the mesometrial decidua and the myometrium at the sixteenth day of pregnancy. Starting on the twelfth day Harkness and Nightingale ('62) found an increased extensibility of the collagenous fibers and a widening of the cervical canal, and both of these changes could be reproduced by the administration of relaxin. Fairstat ('63) confirmed these observations in histologic studies and showed that the collagenous fibers in the endometrium and in the metrial gland of the rat disappear after relaxin is given, as they naturally do in the later stages of pregnancy. We have made similar observations in the pregnant rat.

The collagen-degrading action of relaxin, as confirmed by histologic studies, has been known for a long time (Tahmasebi, '47; Perl and Catchpole, '49; and others). Besides its local effects, it leads to dilation of the birth canal (softening of cervix and symphysis pubis). Whether further possible actions of relaxin, especially the spontaneous inhibition of uterine motility (Krantz et al. '50; Sawyer et al. '53; Felton et al., '53) are of primary or secondary nature, or perhaps are even due to impurities, is still disputed (Kroc et al., '59; Stelcoetz et al. '59; Zarrow and Brennan, '59). The fact that Bloom et al. ('58) using preparations from metrial glands could not detect any effects upon uterine motility does not disprove the existence of relaxin in the metrial gland. Wikvist and Paul ('58) using extracts presumably containing relaxin could not demonstrate the inhibition of motility in all their animals; they were unable to explain this discrepancy. On the other hand, Smetz et al. ('57b) found that relaxin increased the effect of oxytocin on the uterus. Such results, as well as the equally contradictory results of the clinical observations reviewed and discussed by Dallenbach and Dallenbach-Hellweg, ('64) can best be explained by assuming a primary collagen-dissolving action of relaxin which may at times also help to inhibit uterine motility depending on the hormonally primed state of the uterine muscle cell. Zarrow ('57) noted that this inhibition in the presence of relaxin was most pronounced in the uterus of an estrous rat.

As soon as its main effect, the dilatation of the birth canal, has been expressed, relaxin ceases to inhibit myometrial contractions, and thereby continues to facilitate parturition.

The increase in water and glycogen of the rat uterus (Steinetz et al. '57a; Zarrow and Brennan '59) and the stimulation of decidual formation following the administration of relaxin (see Hisaw's discussion in Steinetz et al. '59 and Hisaw and Hisaw '64) have been more surely proven. The decidual regression in the rat following relaxin treatment as observed by Frieden and Velardo ('52) was not confirmed subsequently by Velardo ('58) or by Zarrow and Brennan ('59).

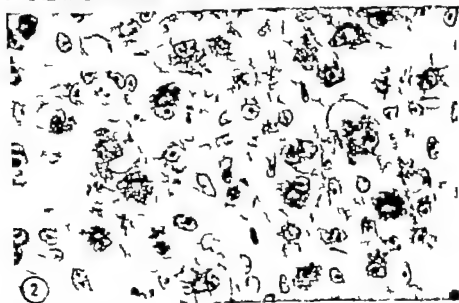
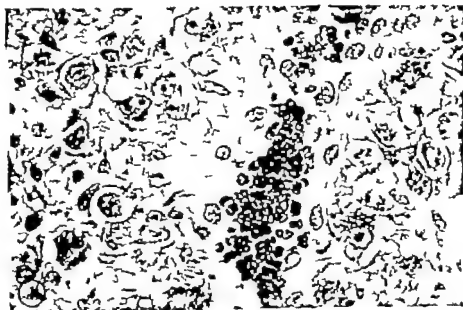
In view of the suggested high content of relaxin in the rat ovary of late pregnancy as measured by the guinea pig symphysis pubis palpation test (Steinetz et al., '59) the negative results of our immunohistological studies (failure to localize relaxin) in these ovaries remain difficult to explain. Perhaps the ovarian relaxin is not firmly bound to cellular structures and has been dissolved out in the staining procedure (Steinetz, personal communication). Before conclusions can be drawn more immunohistologic studies must be done on a larger series of ovaries. The negative results of the palpation test with extracts of rat placentae agree with the immunohistologic findings. A review of the literature indicates that extracts of the metrial gland have not yet been examined by this test.

If one compares the immunohistologic localization of relaxin in the rat with that in the human an almost complete identity of the relaxin-containing cells is evident, regarding the origin, shape, and histochemical composition of their granules. The only significant difference is their localization which can be explained by phylogenetic adaptation to specific species needs. In lower animals such as elasmobranchs and birds the ovary which is the only important organ concerned with reproduction, may contain relaxin (Steinetz et al., '59). Perhaps it facilitates ovulation. During evolutionary advancement, the ovary is found to retain fewer hormonal functions while those of

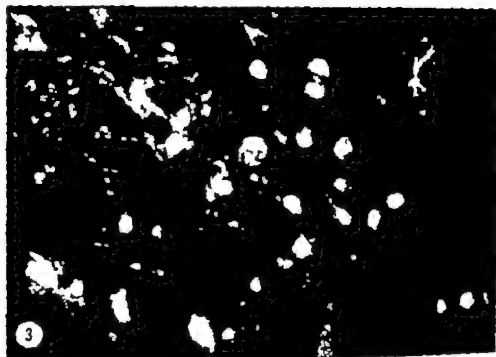
the placenta increase until it ultimately acts as an independent endocrine gland as in the human. Relaxin is produced by the human placenta (Dallenbach and Dallenbach-Hellweg, '64) and not by the ovary (Israel and Groeber '60). The rat representing an intermediate evolutionary stage with its deciduate and hemochorial placentation, reveals that part of its relaxin production is located in the uterus (the metrial gland) and part of its steroid production most likely in the placental giant cells (Deane et al. '62). In the human, two types of relaxin-containing cells may be detected: Type I, the endometrial granulocytes (Hamperl '54 Hellweg '54) which occur not only in pregnancy but also toward the end-phase of a normal menstrual cycle and Type II, the basophilic trophoblastic cells in the basal plate of the placenta at term (Dallenbach-Hellweg and Nette '63 and '64). In the rat, we can only find cells corresponding to the Type II of the human, however of maternal, not of fetal origin. Endometrial granulocytes have been detected only in animals with a cyclic menstruation (Hellweg '59). These granulocytes do not occur in non-menstruating species because they are not needed. The apparent earlier release of relaxin in the pregnant rat (during the last trimester) seems related to its remarkably shorter period of gestation as compared with that of the human in whom release occurs several days before birth (an interval of time equaling that of the rat).

Another factor to be considered is that the active participation of the maternal tissues in implantation varies from species to species. For instance in the guinea pig, the blastocyst possesses high proteolytic capacities thereby obviating maternal tissue activity on the other hand, in the rat the decidua, and not the blastocyst, shows the most proteolytic activity (Blandau 49 Starck, '52). In the rat, therefore the dissolution of the decidua can occur even in the absence of a blastocyst (Selye and McKeown, '35). This may explain the accumulation of granular cells in the mesometrial decidua to the ectoplacental cone during implantation, which is quite with the accumulation of

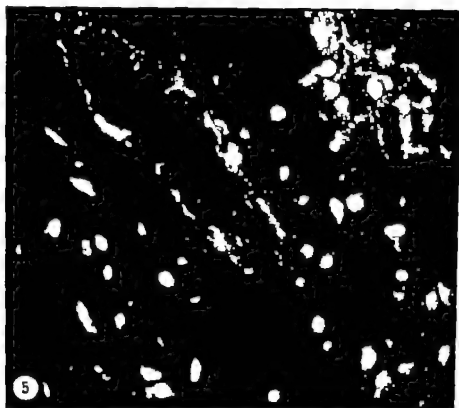
- Selye H., and T. McKernan 1935 Studies on the physiology of the maternal placenta of the rat. *Proc. Roy. Soc. of London*, 119: 1-31.
- Starck, D. 1962 Vergleichende Entwicklungsgeschichte der Wirbeltiere. *Fortschr. Zool.*, 9: 249-367.
- Steinetz, B. G., V. L. Beach, R. F. Rhye and R. L. Kroc 1957a Changes in the composition of the rat uterus following a single injection of relaxin. *Endocrinology* 61: 287-291.
- Steinetz, B. G., V. L. Beach and R. L. Kroc 1957b The influence of progesterone, relaxin and estrogen on some structural and functional changes in the preparturient mouse. *Endocrinology* 61: 271-280.
- 1959 The physiology of relaxin in laboratory animals. *Rec. Progr. Endocrin. Reprod.*, Academic Press, New York and London, pp. 389-417.
- Steinetz, B. G., V. L. Beach, L. V. Tripp and R. J. De Falco 1964 Reactions of antisera to porcine relaxin with relaxin-containing tissues of other species in vivo and in vitro. *Acta Endocrin.*, 47: 371-384.
- Szendy, B. 1933 Die Wege des Glykogens durch die hämochoriale Placenta. *Zeitschr. f. Anat. und Entwickl.-gesch.*, 101: 791-798.
- 1934 Beiträge zur Rolle der Decidua im fetalen Stoffwechsel. *Arch. f. Gynäk.*, 155: 196-216.
- Talmage, R. V. 1947 A histological study of the effects of relaxin on the symphysis pubis of the guinea pig. *J. Exp. Zool.*, 106: 281-297.
- Velardo, J. T. 1958 Inability of purified relaxin to inhibit progesterone in decidual tissue formation. *Anat. Rec.*, 130: 445-446.
- Velardo, J. T., A. B. Dawson, A. G. Olsen and F. L. Hixson 1953 Sequence of histological changes in the uterus and vagina of the rat during prolongation of pseudopregnancy associated with the presence of deciduomas. *Am. J. Anat.*, 93: 273-305.
- Weill, P. 1910 Glande myométriale endocrine dans l'utérus de la rate gestante. *C. R. Soc. Biol.*, 82: 1423-1425.
- Weiss, L. P., K. C. Tsoo and A. M. Seltman 1954 Histochemical demonstration of protein-bound amino groups. *J. Histochem. Cytochem.*, 3: 29-49.
- Wikvist, N. and K.-G. Paul 1953 Inhibition of the spontaneous uterine motility in vitro as bioassay of relaxin. *Acta Endocrin.*, 29: 135-146.
- Wislocki, G. B., G. L. Streeter 1936 On the placentation of the macaque (*Macaca mulatta*) from the time of implantation until the formation of the definite placenta. *Contr. to Embryol.*, 27: 1-66.
- Wislocki, G. B., L. P. Weiss, M. H. Burgess and R. A. Ellis 1957 The cytology histochemistry and electron microscopy of the granular cells of the metrial gland of the gravid rat. *J. of Anat.*, 91: 130-140.
- Zarrow M. X. 1957 Maternal hormones in pregnancy. In: *Gestation. Transact. of the third Conf. Princeton, 1956*, ed. by C. A. Vilez, J. Macy Foundation, New York, pp. 17-22.
- Zarrow M. X., and D. M. Brennan 1959 The action of relaxin on the uterus of the rat, mouse, and rabbit. *Ann. N. Y. Acad. Sci.*, 75: 961-990.
- Zarrow M. X., E. Holmstrom and H. Salkinick 1953 The concentration of relaxin in the blood serum and other tissues of women during pregnancy. *J. Clin. Endocrin. and Metab.*, 15: 23-27.



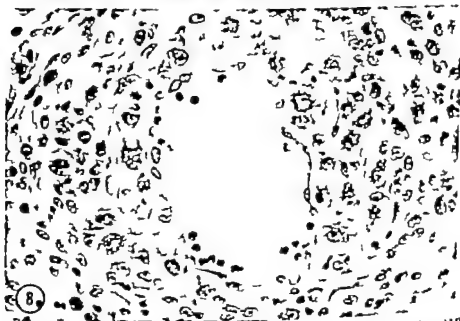
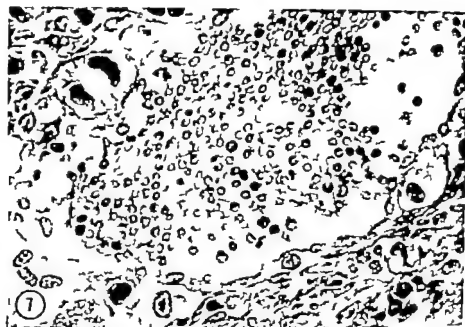
- 1 Mesometrial decidua of rat on the twelfth day of pregnancy. Many granular cells surround blood vessel near the ectoplacental cone. The cells contain prominent granules. Chromium-haematoxylin-phenol; $\times 525$.
- 2 Merial gland of rat on the fifteenth day of pregnancy with numerous granular cells. The granules are perinuclear peripherally the cytoplasm is vacuolated. Aldehyde-haem $\times 525$.



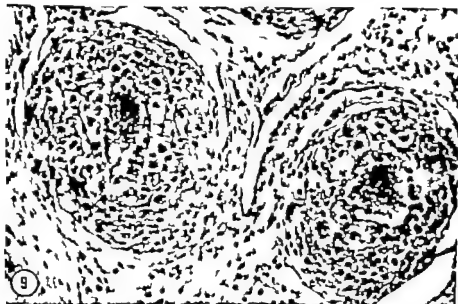
- 3 Fluorescent photomicrograph of same rat and tissue as in figure 1. Paramuclear areas of the granular cell of the uterine gland, corresponding to the aggregates of granules, fluoresce brightly after staining with fluorescein-labelled antirelaxin antiserum. Indirect technique; $\times 512$.
- 4 Fluorescent photomicrograph of same rat as in figures 1 and 3. Fluorescent areas in the lumina of blood vessels of the uterine gland after staining with fluorescein-labelled antirelaxin antiserum. Indirect technique; $\times 750$.



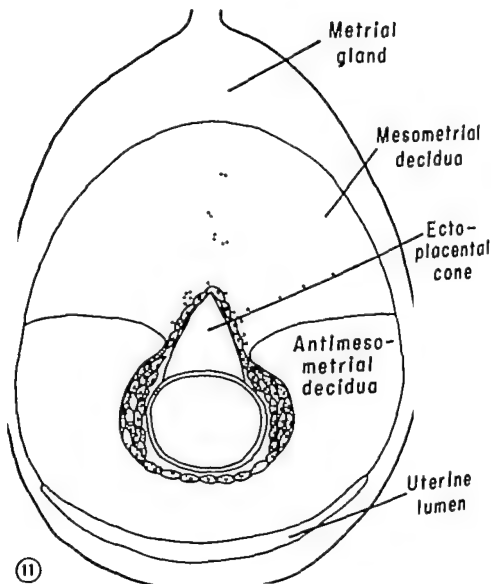
- 5 Uterine gland of rat on the nineteenth day of pregnancy. Paramuclear area of the granular cells fluoresces brightly after staining with fluorescein-labelled antirelaxin antiserum. Note faint fluorescence of ascular endothelium. Indirect technique; $\times 512$.
- 6 Uterine gland of the same rat as in Figure 5. Blood vessel surrounded by large granular cells containing prominent granules. Chromium-hematoxylin-phloxine; $\times 528$.



- 7 Metrial gland of rat on the fifteenth day of pregnancy. Mononuclear (right middle) and binuclear (upper left) granular cells lie directly beneath the thickened endothelial layer and bulge into vascular lumen. Phloxine-tartrazine; $\times 528$.
- 8 Another metrial gland of rat on the fifteenth day of pregnancy similar to figure 7 with many perivascular granular cells. Vacuoles about periphery of haem (see also fig. 7) suggest intra-vascular secretion by granular cells (? fixation artifact). Aldehyde-fuchsin; $\times 330$.



- 9 Another region of the same metrial gland as in figure 8. Cells of the vascular walls appear to be transforming into granular cells. Phloxine-tartrazine $\times 170$.
- 10 Metrial gland of rat on the twenty-second day of pregnancy. The granular cells remaining are concentrated about the vascular lumina. Masson trichrome stain; $\times 132$.



- 11 Schematic drawing of a cross section through pregnant rat uterus on the eleventh day of pregnancy. The black dots in metrial gland, mesometrial decidua and ectoplacental cone indicate the location and the frequency of granular cells at this stage. Similar granules in the cytoplasm of the trophoblastic cells surrounding the blastocyst are only seen in those cells facing the antimesometrial decidua.

Index

A

- Amputation, growth of the rat epiphyseal cartilage plate following partial 221
- Androgen administration and thyroidectomy on the cytology of the pituitary gland of the five-striped palm squirrel, *Famambalus pennanti* (Wroughton) effects of gonadectomy 353
- Antibody distribution in the rat lymph node after primary and secondary responses and after prolonged stimulation, antigen (ferritin) and 385
- Antigen (ferritin) and antibody distribution in the rat lymph node after primary and secondary responses and after prolonged stimulation 385
- Arteries in man patterns of origin and distribution of the major bronchial 19

B

- BATTISTA, J. V. See Dallenbach-Hellweg, G. RICHETTA, LUISA, AND LEOPOLDO MONTES. Secretory epithelium of the large axillary sweat glands. A cytochemical and electron microscopic study 433
- BOWATTECHUK, F. Study of calcification of mammalian cartilage in norm and pathology by stain historadiography the 257
- Bone implants, connective tissue response to altered collagen and 151
- Brain of ferritin injected into cerebrospinal fluid compartments. II. Parenchymal distribution, the 193
- Brain regions rich in monoamine terminals, fluorescence and electromicroscopic study on certain 33
- BROTHMAN, MILTON W. Distribution within the brain of ferritin injected into cerebrospinal fluid compartments. II. Parenchymal distribution the 193
- Bronchial arteries in man, patterns of origin and distribution of the major 19
- Bronchial glands on the cytology and cytochemistry of the opossum's 311
- BULGAK, RUTH ELLEN. Fine structure of the glomerular nephron of the toadfish, *Opsanus beta* the 171
- BUTENGER, IRVAN KAMILL SEVRI MUTLU AND FRANK A. PIPP. Antigen (ferritin) and antibody distribution in the rat lymph node (see primary and secondary responses and after prolonged stimulation 385

C

- Calcification of mammalian cartilage in norm and pathology by stain historadiography the 257

- Cartilage in norm and pathology by stain historadiography the study of calcification of mammalian 257
- Cell granules before and after secretory stimulation, morphologic heterogeneity of mouse pancreas 385
- Cells, the transverse tubular system in mammalian myocardial 1
- Collagen and bone implants, connective tissue responses to altered 151
- Comparison of the incisor teeth of intact hypophysectomized and thyroparathyroidectomized rats, a 159
- Compartments. II. Parenchymal distribution, the distribution within the brain of ferritin injected into cerebrospinal fluid 193
- Connective tissue response to altered collagen and bone implants 151
- Cytochemistry of the opossum bronchial glands, on the cytology and 311
- Cytology and cytochemistry of the opossum bronchial glands, on the 311
- Cytology and histochemistry of the pituitary gland of the five-striped palm squirrel, *F. famambalus pennanti* (Wroughton) 339

D

- DALLENBACH, F. D. See Dallenbach-Hellweg, G. 433
- DALLENBACH-HELLWEG, G., J. V. B. BATTISTA AND F. D. DALLENBACH. Immunohistological and histochemical localization of relaxin in the uterine gland of the pregnant rat 433
- DRAME, HELEN WENZELWE, AND SARAH WENZELMANN. Electron microscopic observations on the postnatal differentiation of the seminal vesicle epithelium of the laboratory mouse 91
- DRAHVAL, GURMEET K., AND M. R. N. PRASAD. Cytology and histochemistry of the pituitary gland of the five-striped palm squirrel, *Famambalus pennanti* (Wroughton) 339
- DRAHVAL, GURMEET K., AND M. R. N. PRASAD. Effects of gonadectomy and androgen administration and thyroidectomy on the cytology of the pituitary gland of the five-striped palm squirrel, *Famambalus pennanti* (Wroughton) 233
- Distribution within the brain of ferritin injected into cerebrospinal fluid compartments. II. Parenchymal distribution, the 193
- DUFFY, P. E., AND MENEVYK, M. Electron microscopic observations of neurosecretory granules, nerve and glial fibers and blood vessels in the median eminence of the rabbit 251

E

- Effects of gonadectomy androgen administration and thyroidectomy on the cytology of the pituitary gland of the five-striped palm squirrel, *Famambulus pennanti* (Wroughton) 353
- Electron microscopic observations of neurosecretory granules, nerve and glial fibers, and blood vessels in the median eminence of the rabbit 251
- Electron microscopic observations on the postnatal differentiation of the seminal vesicle epithelium of the laboratory mouse 81
- Electronmicroscopic study on certain brain regions rich in monoamine terminals a fluorescence and 33
- Eminence of the rabbit, electron microscopic observations of neurosecretory granules, nerve and glial fibers, and blood vessels in the median 251
- Enamel, phase microscopic observations of rat incisor 233
- Epithelium of the large axillary sweat glands, secretory A cytochemical and electron microscopic study 1
- Epithelium of the laboratory mouse, electron microscopic observations on the postnatal differentiation of the seminal vesicle 91
- Epithelium of the rat esophagus, mitosis and differentiation in the stratified squamous 73
- Esophagus mitosis and differentiation in the stratified squamous epithelium of the rat 73

F

- Ferritin injected into cerebrospinal fluid compartments. II. Parenchymal distribution: the distribution within the brain of 190
- Fibers, and blood vessels in the median eminence of the rabbit, electron microscopic observations of neurosecretory granules nerve and glial 251
- Fine structure of the glomerular nephron of the toadfish, *Opsanus tau* the 171
- Fluorescence and electronmicroscopic study on certain brain regions rich in monoamine terminals, 33
- FRIEND, DANIEL E AND MICHAEL J MURRAY Osmium impregnation of the Golgi apparatus 135
- FURK, KJELL, THOMAS HÖRNFELT AND OVE NILSSON A fluorescence and electronmicroscopic study on certain brain regions rich in monoamine terminals 33

G

- GAVIN J B A comparison of the incisor teeth of intact, hypophysectomized and thyroparathyroidectomized rats 159
- Gland of the five-striped palm squirrel, *Famambulus pennanti* (Wroughton) effects of gonadectomy androgen administration and thyroidectomy on the cytology of the pituitary 353

- Glands, on the cytology and cytochemistry of the opossum's bronchial 353
- Glands, secretory epithelium of the large axillary sweat. A cytochemical and electron microscopic study 251
- Golgi apparatus, osmium impregnation of the 81
- Gonadectomy androgen administration and thyroidectomy on the cytology of the pituitary gland of the five-striped palm squirrel *Famambulus pennanti* (Wroughton) 33
- Effects of 251
- Granules, nerve and glial fibers, and blood vessel in the median eminence of the rabbit, electron microscopic observations of neurosecretory 81
- Growth of the rat epiphyseal cartilage plate following partial amputation 33

H

- Heterogeneity of mouse parathyroid cell granule before and after secretory stimulation morphologic 1
- Histochemical localization of relaxin in the metrial gland of the pregnant rat, histomorphological and 91
- Histochemical study of testosterone-induced changes in the submandibular and sublingual gland of mice, 73
- Histochemistry of the pituitary gland of the five-striped palm squirrel, *Famambulus pennanti* (Wroughton) cytology and 73
- Histodiography the study of calcification of mammalian cartilage in norm and pathology by tann 190
- HÖRNFELT THOMAS. See FURK, KJELL

I

- Immunohistological and histochemical localization of relaxin in the metrial gland of the pregnant rat 171
- Impregnation of the Golgi apparatus, osmium 33
- IRVING, J T AND S A. MCELROY. Connective tissue responses to altered collagen and bone implants 135

K

- KRONMAN JOSEPH H AND JOSEPH J SPINALE A histochemical study of testosterone-induced changes in the submandibular and sublingual gland of mice 33

L

- LEWIS, C. P. See Marques Pereira, J P
- LEWIS AVIRILL A. Patterns of origin and distribution of the major bronchial arteries in man 353

M

- Mammalian myocardial cells, the transverse tubular system in 1
- See, patterns of origin and distribution of the major bronchial arteries in 19
- MARCOYA-PICCOLI, J. P., AND C. P. LEBLOUM. Mitosis and differentiation in the stratified squamous epithelium of the rat esophagus 73
- MARTIN, M. See Duffy P. E.
- Metrial gland of the pregnant rat, immunohistological and histochemical localization of relaxin in the 433
- Mice, histochemical study of testosterone-induced changes in the submandibular and sublingual gland of 417
- MILLER, S. A. See Irving, J. T.
- Mitosis and differentiation in the stratified squamous epithelium of the rat esophagus locomotor terminals, fluorescence and electronmicroscopic study on certain brain regions rich in 151
- MURRAY LEOPOLDO F. See Blemppica, Lois
- Moose loose electron microscopic observations on the postnatal differentiation of the seminal vesicle epithelium of the laboratory mouse peneth cell granules before and after secretory stimulation, morphologic heterogeneity of 365
- Morphologic heterogeneity of mouse peneth cell granules before and after secretory stimulation 365
- MURRAY MICHAEL J. See Friend, Daniel S.
- MUTLU KAMILE SEVGI. See Buyukozur Ihan

N

- Nephron of the toadfish, *Opsanus tau*, the fine structure of the glomerular 171
- NILSSON OVE. See Fuxe Kjell
- Norm and pathology by stain historadiography the study of calcification of mammalian cartilage in 287
- NOVEMACHER, RUDOLPH F. See Simmons, David J.

O

- Observations of neurosecretory granules, nerve and glial fibers, and blood vessels in the median eminence of the rabbit, electron microscopic 251
- Observations of rat incisor enamel, phase microscopic 233
- On the cytology and cytochemistry of the opossum bronchial glands 311
- Opossum bronchial glands, on the cytology and cytochemistry of the 311
- Opsanus tau* the fine structure of the glomerular nephron of the toadfish, 171
- Osmium impregnation of the Golgi apparatus 133

P

- Pathology by stain historadiography the study of calcification of mammalian cartilage in norm and 287
- Patterns of origin and distribution of the major bronchial arteries in man 19
- PERE, FRANK A. See Buyukozur Ihan
- Phase microscopic observations of rat incisor enamel 233
- Pituitary gland of the five-striped palm squirrel, *Parasubulbus parvulus* (Wroughton) cytology and histochemistry of the 339
- Plate following partial amputation, growth of the rat epiphyseal cartilage 221
- Postnatal differentiation of the seminal vesicle epithelium of the laboratory mouse, electron microscopic observations on the 91
- PRASAN, M. R. N. See Dhallwal, Gurmeet K.

R

- Rabbit, electron microscopic observations of neurosecretory granules nerve and glial fibers, and blood vessels in the median eminence of the 251
- Rat epiphyseal cartilage plate following partial amputation, growth of the 221
- Rat esophagus, mitosis and differentiation in the stratified squamous epithelium of the 73
- Rat, immunohistological and histochemical localization of relaxin in the metrial gland of the pregnant 433
- Rat, lymph node after primary and secondary responses and after prolonged stimulation, antigen (ferritin) and antibody distribution in the 385
- Rats, comparison of the incisor teeth of intact, hypophysectomized and thyroparathyroidectomized 189
- Relaxin in the metrial gland of the pregnant rat, immunohistological and histochemical localization of 433
- Responses and after prolonged stimulation, antigen (ferritin) and antibody distribution in the rat lymph node after primary and secondary 385
- Responses to altered collagen and bone implants, connective tissue 151

S

- Seminal vesicle epithelium of the laboratory mouse electron microscopic observations on the postnatal differentiation of the 91
- SIMMONS DAVID J. AND RUDOLPH F. NOVEMACHER. Growth of the rat epiphyseal cartilage plate following partial amputation 221
- SIMPSON F. O. The transverse tubular system in mammalian myocardial cells 1

- SHOKIN, SERGEY PETRIMOVICH. On the cytology and cytochemistry of the opossum bronchial glands 311
- SPWALE, JOSEPH J. See Kronman, Joseph H.
- Squamous epithelium of the rat esophagus: mitosis and differentiation in the stratified Squirrel, *Famemulus pennsylvanicus* (Wroughton) cytology and histochemistry of the pituitary gland of the five-striped palm Squirrel, *Famemulus pennsylvanicus* (Wroughton) effects of gonadectomy androgen administration and thyroidectomy on the cytology of the pituitary gland of the five-striped palm 417
- STALEY, MARY W. AND JERRY S. TAHER. Morphologic heterogeneity of mouse parathyroid cell granules before and after secretory stimulation 73
- Stimulation, morphologic heterogeneity of mouse parathyroid cell granules before and after secretory 339
- Study of calcification of mammalian cartilage in norm and pathology by stain historadiography the 353
- Study of testosterone-induced changes in the submandibular and sublingual gland of mice, histochemical 171
- Sublingual gland of mice, a histochemical study of testosterone-induced changes in the submandibular and 1
- Submandibular and sublingual gland of mice, histochemical study of testosterone-induced changes in the 265
- Sweat glands, secretory epithelium of the large axillary A cytochemical and electron microscopic study 365

T

- Tissue responses to altered collagen and bone implants, connective 131
- Teeth of intact, hypophysectomized and thyroparathyroidectomized rats, a comparison of the tector 159
- Thyroidectomy on the cytology of the pituitary gland of the five-striped palm squirrel *Famemulus pennsylvanicus* (Wroughton) effects of gonadectomy androgen administration and 353
- Toadfish, *Opsanus tau*, the fine structure of the glomerular nephron of the Transverse tubular system in mammalian myocardial cells, the 1
- TAHER, JERRY S. See Staley Mary W. 265
- Tubular system in mammalian myocardial cells the transverse 1

V

- Vessels in the median eminence of the rabbit, electron microscopic observations of neurosecretory granules, nerve and glial fibers, and blood 331

W

- WEINER, DENNIS. Phase microscopic observations of rat lactotrophic gland 333
- WURZELMAN, SARAH. See Deane Helen 91
- WUNDERLICH 1

